UNIVERSITY OF OKLAHOMA

GRADUATE COLLEGE

TOWARDS ENHANCING RESILIENCE AND ACCURACY OF AI MODELS AND WIRELESS NETWORKS UNDER REAL-WORLD CHALLENGES

A DISSERTATION

SUBMITTED TO THE GRADUATE FACULTY

in partial fulfillment of the requirements for the

Degree of

DOCTOR OF PHILOSOPHY IN ELECTRICAL AND COMPUTER ENGINEERING

BY

WASEEM RAZA
Norman, Oklahoma
2025

Downloaded from SHAREOK. Persistent Handle URL: https://hdl.handle.net/11244/341635

TOWARDS ENHANCING RESILIENCE AND ACCURACY OF AI MODELS AND WIRELESS NETWORKS UNDER REAL-WORLD CHALLENGES

A DISSERTATION APPROVED FOR THE
SCHOOL OF ELECTRICAL AND COMPUTER ENGINEERING

BY THE COMMITTEE CONSISTING OF

Dr. Ali Imran, Chair

Dr. James J. Sluss, Jr.

Dr. Samuel Cheng

Dr. Timothy G. Ford

© Copyright by Waseem Raza 2025
All Rights Reserved.

Acknowledgments

I am deeply grateful to Dr. Ali Imran, my supervisor, whose exceptional guidance and mentorship have been crucial in completing this dissertation. I will forever be indebted to Dr. Ali Imran for instilling in me the qualities of a diligent researcher and providing invaluable advice on excelling in both personal and professional aspects of life. I would also like to express my most profound appreciation to Dr. Sabit Ekin for his support and encouragement throughout this journey. His guidance has been instrumental in shaping my academic path. Additionally, I am grateful to Dr. Fahd Khan, Dr. Usama Masood, and Dr. Haneya Qureshi for providing me with the opportunity to benefit from their knowledge and expertise. I would also like to thank the committee members, Dr. James J. Sluss, Dr. Timothy G. Ford, and Dr. Samuel Cheng, for their valuable contributions. I would also like to express my sincere appreciation to Denise Davis and Krista Pettersen for their exceptional support and assistance in handling all administrative tasks during my study at OU-Tulsa.

I am also immensely grateful to my family, who have been with me through all the highs and lows of this challenging journey. The contributions of my parents, Ami and Baba, are truly invaluable. Their prayers and constant encouragement have played a pivotal role in my success. I want to extend my heartfelt thanks to my wife, Mehreen Shah, for her unwavering support, patience, and unwavering belief in me. Her presence has been a consistent source of strength and motivation. I extend my sincere gratitude to my friends and colleagues, Dr. Sajid Masood, Dr. Marvin, Dr. Aneeqa, and Dr. Umar bin Farooq, at the AI4Networks Research Center. Their steadfast support and assistance have been invaluable during my academic journey. Finally, I dedicate this dissertation to my beloved daughter, Zahaa. Born during the demanding period of my PhD, her arrival brought immense joy and renewed purpose, serving as a constant reminder of the beautiful future I am working towards. Her innocence and boundless energy were a source of profound inspiration, and her very existence provided the deepest motivation to persevere and complete this significant academic milestone.

Table of Contents

1 Introduction 1
1.1 Background and Motivation 1
1.2 Research Objectives 4
1.3 Problem Statements 6
1.4 Proposed Solutions 8
1.5 Current and Planned Publications 11
1.6 Structure of the Dissertation 15

2 AI based Resilience Enhancement for Emerging Networks 17
2.1 Introduction 17
2.1.1 Background 18
2.1.2 Related Work 20
2.1.3 Challenges and Motivation 27
2.1.4 Proposed Contributions 28
2.1.5 Chapter Organization and Notation 30
2.2 System Model, and Proposed Outage Management Framework . . . 32
2.2.1 System Model and Preliminaries 32
2.2.2 Proposed Outage Management Framework 35
2.3 Proposed Solution - Part 1: Outage Detection and Localization . . 38
2.3.1 Anomaly Detection Schemes 39
2.3.2 Machine Learning methods for Cell Outage Detection 40
2.4 Proposed Solution - Part 2: Outage Compensation Approaches . . . 42
2.4.1 RL Overview and Preparation for Compensation 44
2.4.2 SARL-AC: Single-Agent RL with Actor-Critic 49
2.4.3 MARL-AC: Multi-Agent RL with Actor-Critic 58
2.5 Simulation Setup & Performance Evaluation 61
2.5.1 Simulation Setup 62
2.5.2 Outage Detection Results 63
2.5.3 Outage Compensation Results 67

2.5.4 Time Complexity Comparison 76
2.5.5 Advantages and Limitations of the Proposed Schemes 78
2.6 Conclusion and Transition to Next Chapter 83

3 AI Methods for Network Resilience against Positioning Errors . 85
3.1 Introduction 85
3.1.1 Background and Motivation 86
3.1.2 Importance of Accurate Positioning in UUDNs 87
3.1.3 Challenges in User-Centric Ultra-Dense Networks 87
3.1.4 Existing Works and Research Gap 88
3.1.5 Key Contributions of This Chapter 90
3.1.6 Organization of the Chapter 92
3.2 System Model & Synthetic Data Generation 93
3.2.1 Network Architecture and Channel Model 93
3.2.2 Network Parameters and Performance Indicator 99
3.2.3 Synthetic Data Generation for COPs Combinations 101
3.2.4 Positioning Error Impact Modeling 102
3.3 Proposed Error Compensation Approaches 104
3.3.1 P1: Time-Series Forecasting for Error Impact Minimization . 104
3.3.2 P2: Data-Driven Optimization and Error Compensation . . 109
3.3.3 Comparison with Baseline Approaches 114
3.4 Simulation Setup & Performance Evaluation 116
3.4.1 Simulation Parameters and Setup 116
3.4.2 Error Characterization and Alleviation Results 117
3.4.3 DD-OEC Framework Evaluation 121
3.5 Conclusion and Transition to Next Chapter 126

4 ML Models Resilience to Data Scarcity in Wireless Networks . 129
4.1 Introduction 129
4.1.1 Related Work 131
4.1.2 Problem Statement and Motivation 136
4.1.3 Contribution Summarized 137

4.2 System Model and Propagation Modeling 140
4.2.1 System Model for Propagation Data Collection 140
4.2.2 Data Driven Propagation Modeling 142
4.3 Proposed Domain Informed Weight Transfer GAN for Data Generation 143
4.3.1 Overview of the Proposed Framework 144
4.3.2 M1: Proposed Domain Informed Weight Transfer based GAN 145
4.3.3 M2: Synthetic Data Generation & Evaluation Module 150
4.3.4 M3: Propagation Model Training & Inference Module 151
4.4 Simulation Setup & Performance Evaluation 153
4.4.1 Experimental Setup and Baseline Schemes 153
4.4.2 Ablation Study: Impact of Weight Transfer GAN 155
4.4.3 Comparison with Generative Models in Data-Scarce Regimes 156
4.4.4 Performance Variation with GAN Training Data Size 158
4.4.5 ML Applicability: Model Prediction Performance 162
4.5 Conclusion and Transition to Next Chapter 165

5 Enhancing AI Model Resilience to Distribution Shifts 167
5.1 Introduction 167
5.1.1 Related Work 169
5.1.2 Problem Statement and Motivation 174
5.1.3 Contribution Summarized 175
5.2 Data Collection and Framework 178
5.2.1 Proposed Resilient Propagation Modeling Framework 178
5.2.2 Propagation Related Data Collection (M1 in Fig. 1) 179
5.3 Resilience Analysis: Model Performance against Varying Test Data Distributions 182
5.3.1 ML-based Propagation Model Training (M2 in Fig. 1) 182
5.3.2 Model Evaluation against Test Data Scenarios with Varying JS Similarity (M3 in Fig. 1) 185
5.4 Resilience Enhancement: Data Augmentation and Attention through Segmentation Approach 188
5.4.1 Synthetic Data Generation Approach (M4 in Fig. 1) 188

5.4.2 AtS: Attention through Segmentation Enhanced Training for the Machine Learning Models (M5 in Fig. 1) 193
5.5 Simulation Setup & Performance Evaluation 197
5.5.1 Experimental Setup 197
5.5.2 Evaluation of GANs: Data Quality and Convergence 199
5.5.3 Evaluation of Proposed AtS Methodology 202
5.5.4 Evaluation of AtS Complexity and Convergence 207
5.6 Conclusion and Transition to Next Chapter 210

6 Conclusion and Future Research Directions 212
6.1 Contributions and Conclusions of Each Chapter 212
6.2 Implications for Emerging Wireless Networks 214
6.3 Future Research Directions 215

Funding Acknowledgement 218

References 219

List of Figures

2.1 Proposed framework for machine learning based outage detection and the actor-critic reinforcement learning based outage compensation. . 31

2.2 Deep neural network architecture for actor-critic reinforcement learning based outage compensation. 43

2.3 Confusion matrices comparing the proposed Impv-XGBoost and baseline classifiers for outage detection. 58

2.4 Performance improvements of the proposed scheme over baseline schemes for Matthews correlation with respect to increasing shadowing. 62

2.5 Matthews correlation coefficient versus user device density for outage detection algorithms. 63

2.6 Convergence behavior under varying shadowing and user density for outage detection algorithms. 65

2.7 SARL rewards accumulation for various combinations of rewards based on arithmetic mean, geometric mean, and Jain's fairness index. 66

2.8 Average reference signal received power variations of outage users (oUEs) for various combinations of rewards based on arithmetic mean, geometric mean, and Jain's fairness index. 67

2.9 Average reference signal received power variations of served users (sUEs) for various combinations of rewards based on arithmetic mean, geometric mean, and Jain's fairness index. 69

2.10 Single-agent reinforcement learning rewards accumulation under different combinations of reward criteria. 70

2.11 Outage user device signal strength variations across reward schemes. 71

2.12 Outage user device signal strength variations across reward schemes. 73

2.13 Training process of multi-agent actor-critic reinforcement learning agents under different reward weight configurations. 75

2.14 Reference signal received power variations of outage user equipment under multi-agent training. 76

2.15 Reference signal received power variations of served user equipment under multi-agent training. 77

2.16 Cumulative distribution of reference signal received power for outage user equipment under multi-agent training. 78

2.17 Cumulative distribution of reference signal received power for served user equipment under multi-agent training. 79

3.1 Modeling of user-centric positioning errors in ultra-dense networks. 94
3.2 Impact of user positioning errors on received signal strength. 95
3.3 Comparing ideal vs. erroneous RSRP across combinations of user and base station errors. 102
3.4 Framework for error impact characterization and minimization in ultra-dense networks. 105
3.5 The Data-Driven Optimization and Error Compensation Modeling framework, employing the historical database for error impact characterization and residual learning for error impact compensation . . 109
3.6 Error trends in the reference signal received power with respect to user and base station positioning inaccuracies. 115
3.7 Error trends in area spectral efficiency due to positioning inaccuracies. 116
3.8 Error trends in energy efficiency under different positioning inaccuracies. 118
3.9 Percentage decrease and recovery of key performance indicators for the considered techniques. 120
3.10 Training and forecasting errors for comparative model evaluation. . 121
3.11 Convergence behavior of simulated annealing under baseline and proposed optimization. 122
3.12 Convergence behavior of genetic algorithm under baseline and proposed optimization. 124
3.13 Comparative iterations required for baseline and proposed optimization schemes. 126

4.1 Framework overview for Domain Informed GAN-based model augmentation 143
4.2 M2 module for synthetic data generation and evaluation 144
4.3 M3 module for propagation model training and benchmarking . . . 146
4.4 This equation depicts the comprehensive analytical equation derived from integrating the (4.4) and (4.5) into (4.1). 149
4.5 Performance Comparison of WTGAN with Tabular GANs (Tabular Variational Autoencoder, Conditional Tabular Generative Adversarial Network (CTGAN)) under Varying Data Regimes 157
4.6 Column Shape metric across baseline and WTGAN variants 159
4.7 Column Pair Trends metric across baseline and WTGAN variants . 161
4.8 Comparison for the *baseline* (NAugm, CTGAN, Gaussian copula) and *proposed* (PS: WTGAN) schemes for the root mean square error metric against increasing augmented data size. 163

4.9 Comparison for the *baseline* (NAugm, CTGAN, Gaussian copula) and *proposed* (PS: WTGAN) schemes for the adjusted R^2 square metric against increasing augmented data size. 164

5.1 The proposed framework for model resilience analysis, and enhancement through data augmentation and proposed attention through segmentation approach. 177

5.2 Shap summary plot for the impact of relevant features on models output to determine the important features of propagation data . . 183

5.3 A tripartite plot to depict the histograms of the top three important features determined in Shap summary plot 185

5.4 Evaluating model performance across test scenarios with varying similarity to training data. 186

5.5 Multi-stage GAN-based synthetic data generation using weight transfer 187

5.6 Comparison of synthetic data generation for Legacy GAN and proposed Multistage GAN on different SDMetrics. 198

5.7 Convergence iteration and inference time for Legacy and Multistage GAN across key features 200

5.8 Root mean square error performance of baseline and AtS models for Distance feature across different test set similarity levels 202

5.9 Root mean square error performance of baseline and AtS models for Indoor Path feature across test similarity levels 203

5.10 Root mean square error performance of baseline and AtS models for Base Station Azimuth feature across similarity bins 204

5.11 Root mean square error trends for baseline and AtS models under low and high similarity cases for Distance feature 206

5.12 Comparing model complexity and training iterations across AtS schemes for Distance, Indoor Path, and Base Station Azimuth features . . . 208

List of Tables

2.1 Simulation parameters for macro and micro base stations, including user density and propagation conditions. 61

2.2 Training and testing time comparison for outage detection and compensation schemes. 81

3.1 Performance of the automated machine learning based model fitting module for regression models. 110

3.2 Simulation parameters utilized to generate the UER-KPI and COP-KPI databases under different error and network configurations. . . 114

3.3 Time series forecasting parameters for SARIMA and MLP-REG models. 118

3.4 Performance comparison of proposed DD-OEC and baseline optimization schemes. 126

4.1 Simulation and propagation model parameters used in simulations . 152

4.2 Ablation study on evaluating the impact of domain-informed weight transfer effects in GAN training 155

5.1 Comparison between original and generated data parameters for the number and proportions of low frequency bins. 192

5.2 Network simulation parameters with their values. 195

List of Abbreviations

3GPP	3rd Generation Partnership Project
5G	Fifth Generation
6G	Sixth Generation
AC	Actor Critic
AI	Artificial Intelligence
AtS	Attention-through-Segmentation
AUROC	Area Under the Region Of Convergence Curve
COP	Configuration and Optimization Parameter
CTGAN	Conditional Tabular Generative Adversarial Network
DQN	Deep Q-Networks
DTs	Digital Twins
GAN	Generative Adversarial Network
GC	Gaussian Copula
GM	Geometric Mean
JFI	Jain's Fairness Index
JS	Jensen–Shannon
KNN	K-Nearest Neighbors
KPIs	Key Performance Indicators
KSC	Kolmogorov-Smirnov Complement
LigthGBM	Light Gradient-Boosting Machine
MARL-AC	Multi-Agent Actor-Critic Reinforcement Learning
MCC	Mathews Correlation Coefficients
MDT	Minimizing Drive Test
MLP	Multi-Layer Perceptron
OC-SVM	One-Class Support Vector Machine
RL	Reinforcement Learning
RMSE	Root Mean Squared Error
RSRP	Reference Signal Received Power
RSRQ	Reference Signal Received Quality
SARIMA	Seasonal Auto-Regressive Integrated Moving Average
SARL-AC	Single-Agent Actor-Critic Reinforcement Learning
SHAP	SHapley Additive exPlanations
SINR	Signal to Interference plus Noise Ratio
UE	User Equipment
UER	Underlaying Error Radius
WTGAN	Weight Transfer Generative Adversarial Network
XGBoost	eXtreme Gradient Boosting

Abstract

The rapid evolution of wireless networks toward ultra-dense, user-centric, and AI- and machine learning-based architectures introduces unprecedented challenges in ensuring reliable, efficient, and resilient network operation. Key obstacles towards these networks include (1) frequent occurrences of the outages and inadequacy of traditional methods to handle extensive volume especially in dense deployments and high shadowing scenarios, (2) performance degradation and subsequent adverse affect on optimization methods due to positioning errors in users and remote radio heads, and (3) the lack of resilience of the traditional machine learning based solutions against the scarcity and distribution shift of high-quality data required for effective machine learning modeling. These issues undermine the effectiveness of traditional management and modeling approaches, which are often incapable of handling the complexity, heterogeneity, and real-world uncertainties of next-generation networks.

This dissertation systematically addresses these challenges through data-driven frameworks that leverage advanced artificial intelligence and domain-informed machine learning. First, we propose a robust, automated two-tier outage management solution for dense cellular networks. An enhanced XGBoost-based detection model achieves superior accuracy in scenarios with high shadowing and sparse data. At the same time, an actor-critic reinforcement learning compensation strategy ensures fair and efficient service restoration for both outage-affected and already-served users.

Next, we tackle the adverse impact of positioning errors in user-centric ultra-dense networks, which can severely degrade area spectral efficiency and energy efficiency by misguiding service zone formation and user association. To mitigate this, we introduce a data-driven optimization and error compensation framework that combines residual learning, automated machine learning, and multi-objective optimization. Our results show that the data-driven optimization and error compensation

approach recovers up to 23% of performance lost due to localization errors, outperforming baseline methods. Complementary time-series forecasting techniques, including seasonal auto-regressive integrated moving average (SARIMA) and multilayer perceptron regression, further enable dynamic compensation for the degradation of key performance indicators, with SARIMA achieving the highest prediction accuracy.

Addressing the pervasive challenge of data scarcity in wireless propagation modeling, we develop a domain-informed generative adversarial network framework. By integrating analytical propagation equations into the training of generative adversarial networks, the proposed method generates high-fidelity synthetic data even under extreme data limitations. Experimental evaluations demonstrate up to 50% improvement in data quality metrics and a 48% reduction in root mean square error for downstream machine learning tasks compared to conventional augmentation techniques, establishing a new benchmark for data-driven modeling in data-scarce scenarios. Finally, to enhance model robustness against distribution shifts and support resilient digital twin applications, we introduce a multistage framework combining conditional tabular generative adversarial network-based data augmentation with attention-through-segmentation training. This approach accelerates the convergence of generative adversarial networks by up to 35%, while attention-through-segmentation reduces the root mean square error by up to 67% and improves generalization across diverse and dynamic wireless environments.

Collectively, the methodologies developed in this dissertation advance the state of the art in artificial intelligence-powered wireless network management and modeling. By addressing outage resilience, positioning error compensation, and robust propagation modeling under data scarcity and distribution shifts, this work lays a solid foundation for the next generation of intelligent, self-sustaining wireless networks that can meet the demands and uncertainties of future networks.

CHAPTER 1

Introduction

The transition toward Artificial Intelligence (AI) enabled, ultra-dense, and user-centric wireless networks is reshaping the foundations of network management and modeling. As Fifth Generation (5G) technologies reach maturity and the road-map toward Sixth Generation (6G) systems becomes more defined, future wireless infrastructures are expected to handle unprecedented levels of complexity, heterogeneity, and dynamic adaptation. Traditional methodologies, centered on manual configuration, rule-based automation, or legacy zero-touch automation, are increasingly unsuitable for managing the scale, diversity, and real-time responsiveness required by next-generation deployments. This dissertation addresses these emerging challenges through a unified, data-driven framework that leverages AI and domain-informed machine learning to improve the resilience, adaptability, and accuracy of wireless network operations and modeling.

1.1 Background and Motivation

The accelerating shift toward intelligent, resilient, and user-centric wireless systems is fundamentally transforming the design and operation of communication networks [1]. Modern networks are expected to support highly dynamic, data-intensive applications such as augmented reality [1], connected autonomous vehicles, and mission-critical services [2], each requiring stringent guarantees on latency, reliability, and scalability [3]. These expectations are driving the development of heterogeneous architectures that integrate massive device deployments [4], non-terrestrial components, and highly variable propagation environments [5]. Consequently, con-

ventional network planning and optimization strategies, typically reliant on static modeling and manual intervention, are proving increasingly insufficient [6, 7].

To respond to this evolving landscape, both industry and academia are converging on a new paradigm marked by intelligent automation [8], real-time self-adaptation, and semantic-aware service orchestration [9]. This shift supports the adoption of zero-touch automation, a significant evolution beyond legacy self-organizing network frameworks [10]. In this context, tasks such as configuration, optimization, and fault recovery are autonomously managed by AI-enabled agents [11]. In this context, zero-touch automation capabilities become essential for ensuring operational resilience, particularly for mitigating outages, minimizing interference, and preserving service continuity. However, conventional alarm-triggered or rule-based systems fall short in managing complex, multi-fault scenarios, especially within ultra-dense deployments [12, 13].

Meanwhile, the emergence of user-centric architectures, including ultra-dense networks, reconfigurable intelligent surfaces, and distributed base station infrastructures, has redefined the spatial and contextual dynamics of wireless service delivery [14]. Rather than relying on fixed cell boundaries, these architectures enable the formation of dynamic service zones based on user context and spatial awareness [15]. However, their effectiveness is tightly coupled with the accuracy of relevant nodes, such as the user equipment and base stations, an assumption often violated in practice due to global positioning error, signal blockages, and latency in position estimation [16, 17]. Such uncertainties propagate downstream, leading to suboptimal decisions in user association, power control, and coverage planning [18]. These limitations necessitate the design of AI models that can function reliably under incomplete or noisy input conditions [19].

Another major frontier in the evolution of AI-native wireless systems is the development of accurate and generalizable propagation models [20]. The rise of digital

twins and AI-augmented simulators has underscored the importance of data-driven channel modeling approaches that can capture fine-grained environmental and user-specific variations [21]. Traditional modeling techniques, whether empirical, deterministic, or stochastic, have laid foundational ground but lack the flexibility and adaptability needed for emerging use cases [22]. Machine learning-based alternatives have been proposed to address this gap [23, 24]. Yet, their effectiveness is often undermined by challenges such as limited real-world data availability, class imbalance, and distributional shifts over time, regions, and technologies [25–27].

These challenges are particularly pronounced in wireless datasets dominated by tabular formats, where generative models such as Generative Adversarial Network (GAN) face inherent limitations due to the absence of spatial structure or contextual redundancy, advantages typically exploited in domains like vision or speech [28, 29]. Moreover, standard generative adversarial networks often suffer from instability, mode collapse, and degraded performance when trained on sparse or imbalanced datasets. To address these limitations, recent research has turned toward domain-informed generative modeling, where prior knowledge is explicitly embedded in the training process to improve convergence, stability, and generalization under data-scarce conditions [30, 31].

To advance the resiliency and accuracy of wireless modeling in the abovementioned contexts, this dissertation proposes a framework pipeline spanning four dimensions: (i) intelligent outage detection and compensation via optimized eXtreme Gradient Boosting (XGBoost) and Reinforcement Learning (RL); (ii) robust positioning error characterization, and data driven optimization of Key Performance Indicators (KPIs) through residual error modeling; (iii) synthetic data generation in low-data regimes using domain-informed generative adversarial networks; and (iv) segmentation-based attention mechanisms for enhanced generalization and improved performance under the distribution shifts in data driven propagation mod-

eling. These contributions not only have technical merit but also serve as strategic responses to the pressing needs of future artificial intelligence-native networks.

1.2 Research Objectives

This dissertation seeks to advance the resilience, adaptability, and accuracy of artificial intelligence-powered wireless network modeling under real-world constraints. The research is structured around the following objectives, aligned with a key technical challenge and motivated by the pressing needs of modern and future network environments:

1. **Obj. 1: Develop a robust framework for outage detection in ultra-dense wireless networks.** This objective aims to design an intelligent detection mechanism capable of accurately identifying cell outages even in scenarios affected by signal shadowing, limited reporting data, and dynamic network topologies. The proposed framework emphasizes learning from noisy and imbalanced data while preserving reliability in harsh propagation conditions.

2. **Obj. 2: Design fairness-aware and scalable reinforcement learning strategies for outage compensation.** This objective addresses the need for intelligent compensation mechanisms that not only restore service to affected users but also preserve fairness for previously connected users. The solution emphasizes adaptive parameter tuning, fairness-guided policy learning, and scalable architectures that can handle and compensate for multiple simultaneous failures.

3. **Obj. 3: Quantify and mitigate the impact of localization uncertainty in user-centric wireless network architectures.** This objective aims to explore the sensitivity of service zone formation and resource allocation processes to the errors in user and base-station position estimates in user-centric

ultra-dense networks. It further seeks to develop data-driven techniques that can model the impact of these errors on key performance indicators and compensation mechanisms to recover the fall in these performance indicators.

4. **Obj. 4: Enable error-resilient wireless resource configuration using automated learning pipelines under uncertain location inputs.** Building upon the previous objective, this goal focuses on exploring data-driven configuration parameter optimization under realistic positioning error conditions, as characterized in the last objective. For this purpose, we aim to utilize historical data, residual error learning, and an automated machine learning framework to describe the error impact on multi-objective optimization problems in user-centric networks, and employ heuristic techniques to solve these optimization problems.

5. **Obj. 5: Develop domain-informed generative models to infuse the knowledge for propagation modeling in data-scarce conditions.** This objective focuses on integrating classical wireless propagation models into deep generative architectures to support prediction in severely low-data environments. We aim to guide the generator's learning process using structural constraints derived from analytical models such as path loss and shadowing laws, thereby enhancing the semantic validity and interpretability of the synthetic data generated.

6. **Obj. 6: Design a weight-transfer-based generative learning pipeline to accelerate training and improve sample quality under extreme data scarcity.** Building upon the incorporation of domain knowledge, this objective targets the development of a weight transfer generative adversarial network, where the generator is initialized using a deep neural network trained on analytically generated data. The aim is to stabilize and accelerate the convergence of generative adversarial networks while preserving physical

realism in the output, thereby addressing the instability of training generative adversarial networks on tabular and small-sample wireless datasets.

7. **Obj. 7: Investigate the robustness of wireless learning models to dataset imbalance and deployment-induced distribution shifts.** This objective involves systematically analyzing the vulnerability of trained models to data heterogeneity and regional deployment shifts in propagation characteristics. We aim to quantify the fragility of conventional neural architectures and propose robustness-aware evaluation frameworks that reflect real-world performance degradation and resilience under unseen data distributions.

8. **Obj. 8: Improve model generalization in skewed wireless data using segment-aware attention and ensemble learning.** To address poor performance in underrepresented or skewed conditions, this objective introduces an attention-over-segments strategy. The goal is to partition the training data based on behavioral feature distributions and train localized models, which are later combined using a lightweight attention mechanism. This promotes adaptive generalization across diverse operating environments and improves learning fidelity in edge cases.

1.3 Problem Statements

The evolution of wireless networks into ultra-dense, user-centric, and AI-based infrastructures introduces a wide range of modeling and optimization challenges. These challenges are intensified by the inherent uncertainty in real-world environments, limitations in data availability, and the need for automation at scale. This dissertation investigates the following core technical problems:

- **PS1 – Failures of Conventional Outage Detection Methods in High Shadowing and Sparse Data Conditions:** In dense wireless deployments,

timely and accurate detection of cell outages is critical for network resilience. Outage detection methods rely on data from important performance measures. Still, disparities in this data due to sparse deployment, high showing, and delays result in missed or delayed outage identification, which in turn prolongs service disruptions and undermines network resilience.

- **PS2 – Lack of the Fairness-Aware Outage Compensation in Reinforcement Learning based Approaches:** Current reinforcement learning frameworks for outage compensation often prioritize the rapid compensation of outage users but overlook fairness constraints across both already served and affected users. This leads to unstable service delivery, degraded quality for non-outage users, and inequitable resource allocation, especially during multi-cell failures.

- **PS3 – Mis-configurations Stemming from Localization Inaccuracy in User-Centric Architectures:** Dynamic service zone formation depends on the precise localization of both users and infrastructure. However, global positioning system noise, latency, and environmental interference frequently cause misalignment between intended and actual coverage zones. These errors result in inefficient configurations and suboptimal network performance.

- **PS4 – Inadequate Compensation Mechanisms for Localization-Induced Key Performance Indicator Degradation:** Conventional configuration techniques do not account for residual errors caused by uncertain location inputs. As a result, adaptive policies become rigid or fail to compensate for performance losses, especially when real-time corrections are not feasible or training data lacks diversity in localization conditions.

- **PS5 – Limited Generalization of Propagation Models Under Distribution Shifts:** Machine learning-based propagation models often overfit to the training distribution and fail when deployed in previously unseen or

evolving environments. These distribution shifts may stem from changes in urban morphology, frequency bands, or environmental dynamics, which can compromise the reliability of prediction frameworks.

- **PS6 – Data Imbalance and Under-representation of Edge Scenarios in the Datasets:** Public and industrial datasets used for propagation modeling tend to be skewed toward urban and well-instrumented regions. This bias hinders the effectiveness of models when applied to rural, sparse, or dynamic topologies, where rare yet critical patterns are essential for robustness.

- **PS7 – Instability of Generative Models on Tabular and Sparse Wireless Data:** Classical generative adversarial networks assume continuous, dense, and high-dimensional inputs. However, wireless data is often tabular, low-volume, and sparse, making generative adversarial network training unstable and resulting in the generation of poor-quality synthetic data for downstream applications.

- **PS8 – Absence of Domain Knowledge Integration in Generative Modeling Pipelines:** Most generative adversarial networks used in wireless modeling overlook analytical knowledge of propagation phenomena such as path loss, shadowing models, or domain-specific constraints. This leads to low-fidelity generation, weak interpretability, and missed opportunities to encode meaningful priors in data-scarce regimes.

1.4 Proposed Solutions

This dissertation introduces a unified suite of solutions that enhance the resiliency, fairness, and generalization capabilities of artificial intelligence-driven wireless network modeling under real-world constraints. The proposed contributions span four core themes: outage detection and compensation, localization-aware configuration,

robust propagation modeling, and data augmentation through domain-informed generative modeling. The principal solutions are summarized below:

1. **Joint AI-Driven Framework for Outage Detection and Fair Compensation:** We propose an integrated solution for cell outage management that unifies supervised outage detection and fairness-aware compensation. Enhanced XGBoost classifiers with imbalance-handling mechanisms are utilized for detection, while actor-critic reinforcement learning policies are employed to restore connectivity and maintain service fairness dynamically.

2. **Multi-Agent Reinforcement Learning for Scalable Recovery:** To address multi-cell failure scenarios, we design a cooperative Multi-Agent Actor-Critic Reinforcement Learning (MARL-AC) scheme with a centralized critic. This enables decentralized agents to optimize compensation actions under coordinated reward structures jointly, improving recovery performance in ultra-dense deployments.

3. **Localization-Aware Performance Degradation Modeling and Compensation:** We quantify the impact of user and infrastructure positioning errors in user-centric architectures. Time-series forecasting models (e.g., Seasonal Auto-Regressive Integrated Moving Average (SARIMA), Multi-Layer Perceptron (MLP)) are used to predict deviations in key performance indicators and guide proactive adjustments to control parameters in the face of global positioning uncertainty.

4. **Automated Machine Learning based Residual Learning for Resilient Configuration:** We develop a robust, automated machine learning pipeline that learns to identify residual errors between ideal and noisy localization conditions. These residuals are embedded in a multi-objective optimization loop to dynamically tune wireless configuration parameters, ensuring robustness

against location-induced errors.

5. **Attention-through-Segmentation (AtS) for the Robust Propagation Modeling:** To address the challenges of generalization in propagation modeling, we introduce a segmentation-based attention mechanism. The dataset is partitioned into segments based on feature space characteristics, and local models are trained per segment, enhancing resilience to data imbalance and distribution shift.

6. **Domain-Informed Generative Modeling using Weight Transfer Generative Adversarial Network (WTGAN):** We design a two-stage WTGAN framework for augmenting wireless propagation data. A deep neural network is first trained on pseudo-random, analytically generated data with embedded domain constraints. The learned weights are then transferred to initialize the generative adversarial network generator, thereby accelerating convergence and enhancing the physical realism of the synthetic data.

7. **Validation-Aware Training and Quality-Guided Early Stopping:** A quality-driven training strategy is integrated into the weight transfer generative adversarial network, where intermediate synthetic samples are evaluated using statistical fidelity metrics to trigger early stopping. This ensures that the generated samples retain their column-wise structure and inter-feature relationships, which are critical for downstream tasks.

8. **Resilience Evaluation through Distribution Shift and Data Scarcity Analyses:** We conduct extensive sensitivity analyses to evaluate the robustness of the proposed propagation modeling pipeline under various scenarios, including spatial distribution shifts, data removal, and sparsity conditions. These results demonstrate the system's ability to sustain performance with up to 40% of data removed or replaced.

9. **Analytical-Guided Data Augmentation for Minority Classes:** To support underrepresented scenarios (e.g., NLoS conditions or rural terrains), analytical propagation models are leveraged to guide the generation of minority-specific synthetic data. This improves the performance of learning models in skewed and edge deployment settings.

10. **Generalizable Artificial Intelligence-based Approach for Resilient Wireless Systems:** Collectively, the developed techniques form a modular and extensible blueprint for building artificial intelligence native wireless systems. By integrating expert knowledge, learning resilience, and fairness principles, the proposed framework contributes to the broader goal of zero-touch automation in innovative, data-constrained environments.

1.5 Current and Planned Publications

Academic Awards: **Peer-Reviewed Journal Articles:**

J1. **Waseem Raza**, Muhammad Umar Bin Farooq, Aneeqa Ijaz, Marvin Manalastas, and Ali Imran, "AI-Powered Resilience: A Dual-Approach for Outage Management in Dense Cellular Networks," *Computer Communications*, Volume 236, 2025, Article 108129, ISSN 0140-3664.

J2. **Waseem Raza**, Muhammad Umar Bin Farooq, Haneya Naeem Qureshi, and Ali Imran "Resilience by Design: Innovative Machine Learning Strategies for Robust Propagation Modeling in Wireless Networks," submitted in *IEEE Transaction on Network Science and Engineering* [**In 2nd Revision**].

J3. **Waseem Raza**, Syed Basit Ali Zaidi, Muhammad Umar Bin Farooq, and Ali Imran, "Domain-Informed Generative Methods for Advancing Wireless

Propagation Modeling in Data-Scarce Scenarios," 2nd revision submitted in *IEEE Access*.

J4. **Waseem Raza**, Ethan Abele, John OHara, Behnaz Sadr, Peter LoPresti, Ali Imran, Wooyeol Choi, Ickhyun Song, Serhat Altunc, Obadiah Kegege, Sabit Ekin, "Toward a Hybrid RF/Optical Lunar Communication System (LunarComm)," in *IEEE Network*, vol. 36, no. 6, pp. 76-83, November/December 2022, doi: 10.1109/MNET.103.2100419.

J5. Aneeqa Ijaz, **Waseem Raza**, Hasan Farooq, Marvin Manalastas and Ali Imran, "An AI-Enabled Framework to Defend Ingenious MDT-Based Attacks on the Emerging zero-touch Cellular Networks," in *IEEE Network*, vol. 38, no. 1, pp. 228-237, Jan. 2024. .

J6. Usama Masood, **Waseem Raza**, Fahd Ahmed Khan, and Ali Imran "BOOSTER: A Novel Deep Transfer Learning Framework for Modeling Network Behavior using Sparse Data," 2nd revision submitted in *IEEE TNSE*, 2024. **(equal contributing author)**

J7. Usama Masood, **Waseem Raza**, Fahd Ahmed Khan, and Ali Imran "STORM: Predicting Transfer Learning Gains with Domain-Aware Spatio-Temporal Similarity," 1st revision submitted in *IEEE TCCN*, 2024. **(equal contributing author)**

J8. Muhammad Umar Bin Farooq, Marvin Manalastas, **Waseem Raza**, Syed Muhammad Asad Zaidi, Ali Rizwan, Adnan Abu-Dayya, and Ali Imran "A Data-Driven Self-Optimization Solution for Inter-Frequency Mobility Parameters in Emerging Networks," in *IEEE Transactions on Cognitive Communications and Networking*, vol. 8, no. 2, pp. 570-583, June 2022, doi: 10.1109/TCCN.2022.3152510.

J9. Syed Basit Ali Zaidi, Haneya Naeem Qureshi, **Waseem Raza**, Muhammad

Ali Imran, Shuja Ansari, and Ali Imran, "IINN: Innately Intelligent Neural Networks for Applications in Wireless Networks and Beyond," To be submitted in *IEEE Transactions on Machine Learning*.

J10. Mehreen Shah, Haneya Naeem Qureshi, **Waseem Raza**, Ali Rizwan, and Ali Imran, "AI-Enabled Dietary Habit Monitoring in Free Life using Smartwatch" in *IEEE Transaction on Human Machine Systems*, (in **2nd revision**).

Peer-Reviewed Conference Papers:

C1. **Waseem Raza**, Syed Basit Ali Zaidi, Muhammad Umar Bin Farooq, Haneya Naeem Qureshi and Ali Imran, "Refining Wireless Propagation Models using Domain-Informed GANs amid Data Scarcity," *2024 IEEE 100th Vehicular Technology Conference (VTC2024-Fall)*, Washington, DC, USA, 2024, pp. 1-6.

C2. **Waseem Raza**, Fahd Ahmed Khan, Haneya Naeem Qureshi, Usama Masood and Ali Imran, "An AI-Driven Framework for Enhancing Resilience in Propagation Models to Enable Digital Twin," *2024 IEEE 35th International Symposium on Personal, Indoor and Mobile Radio Communications (PIMRC)*, Valencia, Spain, 2024, pp. 1-6.

C3. **Waseem Raza**, Muhammad Umar Bin Farooq, Aneeqa Ijaz and Ali Imran, "Data-Driven Intelligent Outage Management for High Shadowing Environments in 5G&B Networks," *2024 International Conference on Smart Applications, Communications and Networking (SmartNets)*, Harrisonburg, VA, USA, 2024, pp. 1-6.

C4. **Waseem Raza**, Fahd Ahmed Khan, Muhammad Umar Bin Farooq, Sabit Ekin and Ali Imran, "Positioning Error Impact Compensation through Data-Driven Optimization in User-Centric Networks," *GLOBECOM 2023 - 2023*

IEEE Global Communications Conference, Kuala Lumpur, Malaysia, 2023, pp. 3928-3933.

C5. **Waseem Raza**, Umair Sajid Hashmi, Ali Imran, and Sabit Ekin, "Towards Positioning Error Impact Characterization and Minimization in User-Centric RAN," *2022 IEEE Wireless Communications and Networking Conference (WCNC)*, Austin, TX, USA, 2022, pp. 734-739.

C6. Syed Basit Ali Zaidi, **Waseem Raza**, Haneya Naeem Qureshi, Muhammad Ali Imran, Ali Imran and Shuja Ansari, "A Domain-Aware Framework for Interpretable and Resilient Propagation Models: Enabling Digital Twins for Wireless Networks," *2024 IEEE 99th Vehicular Technology Conference (VTC2024-Spring)*, Singapore, Singapore, 2024, pp. 1-6.

C7. Syed Basit Ali Zaidi, **Waseem Raza**, Muhammad Umar Bin Farooq, Ali Imran, Muhammad Ali Imran, and Shuja Ansari, "A Novel Innately-Intelligent Transfer Learning Framework for Wireless Networks & Beyond," invited paper accepted in *IEEE International Symposium on Personal, Indoor and Mobile Radio Communications (PIMRC)*, 2025.

C8. Marvin Manalastas, Muhammad Umar Bin Farooq, Syed Muhammad Asad Zaidi, Aneeqa Ijaz, **Waseem Raza**, and Ali Imran "Machine Learning-Based Handover Failure Prediction Model for Handover Success Rate Improvement in 5G," *2023 IEEE 20th Consumer Communications & Networking Conference (CCNC)*, Las Vegas, NV, USA, 2023, pp. 684-685.

C9. Muhammad Umar Bin Farooq, Marvin Manalastas, **Waseem Raza**, Aneeqa Ijaz, Syed Muhammad Asad Zaidi, Adnan Abu-Dayya and Ali Imran, "Data Driven Optimization of Inter-Frequency Mobility Parameters for Emerging Multi-band Networks," *GLOBECOM 2020 - 2020 IEEE Global Communications Conference*, Taipei, Taiwan, 2020, pp. 1-6.

1.6 Structure of the Dissertation

This dissertation is structured into five core chapters, each targeting a key research challenge related to building resilient and accurate wireless network models under real-world constraints. The progression of chapters reflects the evolution from foundational fault management in cellular systems to advanced data-driven modeling strategies that tackle distribution shifts and data scarcity.

Chapter 2 focuses on resilience in self-organizing networks by addressing the dual problems of cell outage detection and compensation. By proposing a unified, artificial intelligence-powered framework based on enhanced XGBoost and actor-critic reinforcement learning, this chapter lays the groundwork for intelligent and fair outage management, particularly in the context of ultra-dense fifth-generation networks.

Chapter 3 transitions toward the user-centric network paradigm, where the accuracy of location information plays a critical role in optimizing network performance. This chapter examines the adverse effects of user and base station positioning errors in user-centric ultra-dense networks. It proposes a data-driven framework that leverages time-series forecasting and automated machine learning-based optimization to mitigate the resulting performance degradation. It highlights the importance of modeling uncertainty in next-generation networks and compensating for its effects using intelligent inference.

In Chapter 4, the dissertation addresses the fundamental issue of data scarcity in wireless network modeling, especially for tabular data where standard augmentation techniques often fall short. This chapter presents the weight transfer generative adversarial network framework, which leverages domain-informed initialization to overcome the data bottleneck. By synthesizing realistic and high-quality data from limited samples, the weight transfer generative adversarial network architecture

demonstrates how domain knowledge can be effectively integrated into generative processes to support robust propagation modeling.

Chapter 5 extends the scope to modeling accuracy, particularly under distribution shifts between training and testing environments. Recognizing the challenges posed by real-world heterogeneity in data distributions, this chapter proposes a robust and scalable framework that integrates conditional generative adversarial network-based data augmentation with attention-driven segmentation. The approach enhances model robustness across diverse propagation scenarios, contributing to the development of resilient artificial intelligence models for dynamic wireless environments.

Finally, Chapter 6 summarizes the core findings of this dissertation and reflects on their broader significance. It outlines key insights gained through the integration of machine learning, domain knowledge, and advanced modeling strategies, and concludes with a discussion of future research directions aimed at expanding the scalability and applicability of the proposed techniques across broader wireless communication scenarios.

Together, these chapters contribute a cohesive body of work that systematically addresses the challenges of ensuring reliability and accuracy in wireless networks through data-driven and AI-enhanced solutions. The dissertation offers not only novel methodologies but also practical pathways for deploying artificial intelligence in increasingly complex, dynamic, and data-constrained real-world wireless systems.

CHAPTER 2

AI based Resilience Enhancement for Emerging Networks

As future wireless networks evolve toward greater density and complexity, ensuring resilient and autonomous fault management becomes increasingly vital. Cell outages, whether caused by hardware failures or software anomalies, pose a significant threat to uninterrupted service delivery. Traditional network management approaches are inadequate for these dynamic environments. This chapter proposes a unified, artificial intelligence-based framework for cell outage management that integrates intelligent detection and adaptive compensation. By combining ensemble learning for failure identification with actor-critic reinforcement learning for real-time recovery, the framework supports scalable, fair, and responsive operation in next-generation networks.

2.1 Introduction

The increasing densification of base stations, proliferation of connected devices, and diversity of service demands have made network fault management more complex than ever before. In ultra-dense deployments, even a single cell outage can lead to significant service degradation, particularly when faults go undetected or are compensated ineffectively. Conventional methods are often fragmented, treating detection and recovery as separate tasks, and rely on static rules or manual intervention, which limits their responsiveness and scalability. To address these challenges, we develop an artificial intelligence-based framework that automates both the detection of outages and the compensation process. Our approach utilizes a tailored ensemble learning method for early and accurate fault identification, and

an actor-critic reinforcement learning strategy to adjust network parameters for adaptive recovery. The framework is designed to ensure fairness, robustness, and coordination in the face of multiple concurrent failures. The following sections provide background on network fault management, examine related work, and present the design and evaluation of our proposed solution.

2.1.1 Background

With the exponential growth of data-driven applications and gigabit wireless connectivity, cellular networks have become increasingly complex across successive generations. This rising complexity stems from the introduction of new technologies, the growing number of adjustable network parameters, and the substantial increase in heterogeneous base station deployments [6]. The implications of these complex combinations are intricate network operations that make manual network management very expensive and tedious, necessitating a paradigm shift to address these pressing challenges. Therefore, self-organizing networks standardized by the Third Generation Partnership Project [7] promote the use of intelligent and autonomous systems throughout the network life cycle: self-configuration during deployment, self-optimization during operation, and zero-touch automation during maintenance [10]. In particular, the zero-touch automation functionality of self-organizing networks aims to detect faults in network operations and trigger the compensation mechanisms to resolve these faults, referring to these processes as cell outage detection and compensation, respectively [12].

Traditional self-healing capabilities, such as software updates, network monitoring, and hardware enhancements, have been employed in legacy systems like 3G and 4G [11]. However, these manual methods are not scalable and fail to address the real-time challenges that future networks will pose. For instance, “sleeping cells” a type of network outage caused by hardware or software failure, are difficult to

detect even with self-healing support when operating and maintenance alarms are unavailable [32]. Additionally, the 5G ecosystem and beyond is defined by its highly heterogeneous network architecture, increased operational complexity, and the massive growth in connected devices serving a wide range of applications [33]. These complexities exacerbate the limitations of current self-healing schemes, reducing their effectiveness in 5G and beyond networks. A key feature of these networks is the massive growth in data-driven services and software-defined networking, which inherently relies on data to operate [13]. This widespread data-based approach provides the opportunity to employ data-driven machine learning methods for self-healing functionalities [32]. Therefore, the integration of AI in outage detection and compensation offers a promising solution.

The limitations of current zero-touch automation solutions necessitate the use of advanced analytics to enable closed-loop automation in zero-touch automation networks. In response to these challenges, AI-driven techniques for automating outage detection and implementing compensation mechanisms have gained significant traction in recent years [13]. AI-based outage detection methods commonly rely on Minimizing Drive Test (MDT) data. These approaches aim to detect abnormal reports from User Equipment (UE) within the coverage area of the affected base station. Since minimization of drive test data is tagged with the location of the user equipment, it can be used to detect outages and localize base stations from the outage, which is crucial for triggering and running compensation mechanisms. Whereas AI-based outage compensation solutions are also gaining traction, as discussed in and referenced therein [34].

In general, outage compensation solutions leverage reinforcement learning techniques to dynamically adjust network parameters such as transmission power and antenna tilt, optimizing coverage for affected users [35]. However, conventional reinforcement learning methods, particularly value-based approaches like Deep Q-

Networks (DQN), struggle in non-stationary environments due to their reliance on experience replay, which can introduce outdated decisions when applied to dynamically evolving networks. Actor-critic methods provide a more robust alternative by continuously learning policies and value functions in real-time, enabling them to adapt effectively to changing network conditions. This adaptability is particularly critical in outage compensation scenarios, where network states fluctuate rapidly, requiring a method that optimally balances coverage restoration and interference mitigation. Given these advantages, this work employs an actor-critic-based reinforcement learning approach to address the challenges of outage compensation in dynamic wireless networks.

2.1.2 Related Work

Effective management of cell outages, encompassing both detection and compensation, is essential for maintaining the reliability and quality of wireless communication networks, particularly as these networks transition into next-generation emerging networks [35]. As network deployments become more complex with higher user densities and diverse service requirements, the need for automated, efficient, and scalable solutions grows [36]. Traditional approaches to outage management rely heavily on rule-based or manual methods, which are time-consuming and lack the adaptability needed for dynamic environments [37]. To address these limitations, the research community has developed a variety of approaches, ranging from traditional methods to AI-driven techniques. We have organized the literature based on the key focus of the work, i.e., (1) detection only, (2) compensation only, and (3) integrated approaches, highlighting their respective strengths and limitations.

Cell Outage Detection Only

Traditional non artificial intelligence based outage detection solutions, while abundant [38–40], require highly trained domain experts to manually parse data logs for detecting abnormal behavior. This manual process is inefficient and time-consuming, making it unsuitable for modern networks' dynamic and dense environments. Therefore, to incorporate the much-needed automation and increase efficiency in future networks, the research community has increasingly turned to artificial intelligence-based cell outage detection solutions [41, 42]. The motivation for using artificial intelligence in cell outage detection lies in its ability to automate complex tasks, reduce human intervention, and enhance detection accuracy. Artificial intelligence-based outage solutions offer promising advancements by leveraging machine learning and deep learning techniques to analyze large volumes of network data, identify patterns, and detect anomalies [43–45]. This review discusses notable outage detection methods, categorizing them by their primary approach, and highlights both their advantages and limitations in addressing key challenges [46, 47].

Building on the need for automation in outage detection, several studies have focused on unsupervised learning techniques for detecting anomalies in network performance data. The work in [42] explored artificial neural networks optimized by differential evolution for outage detection, but concerns remain regarding the robustness of these models under varying network conditions. Authors in [41] introduced methods such as local outlier factor, One-Class Support Vector Machine (OC-SVM), and K-Nearest Neighbors (KNN) to analyze the minimization of drive test data for anomaly detection. The work in [43] applied these techniques to handle large datasets, consisting of Reference Signal Received Power (RSRP) and Reference Signal Received Quality (RSRQ) values, demonstrating scalability in dense and time-varying environments. Building on these efforts, Ping et. al, [44] developed a deep convolutional Actor Critic (AC) to manage data imbalance and avoid reliance

on user location data, thereby further improving anomaly detection without the need for labeled data. While these unsupervised methods provide scalability, they often struggle in highly dynamic networks. This limitation affects their ability to precisely detect nuanced outage patterns, such as partial or intermittent outages.

Some works have combined supervised and unsupervised techniques to improve accuracy and handle data imbalance [45–47]. Usama et al. [45] employed a deep learning approach with autoencoders for outage detection, demonstrating improved accuracy compared to baseline methods. However, its performance is constrained by the scarcity of training data, a common issue in small-cell environments. The work in [46] utilizes generative adversarial networks combined with Adaboost to synthesize minority class data and improve classification in imbalanced datasets. Additionally, sparse autoencoders, paired with techniques such as synthetic minority over-sampling, have been used to detect anomalies in wireless networks [47]. While these hybrid models achieve high classification accuracy, particularly under imbalanced data conditions, they struggle to capture the full variability of real-time network dynamics. Moreover, their reliance on data synthesis and static models limits their adaptability in fast-changing environments. It makes them less robust in handling complex outage scenarios, such as partial outages or high shadowing. Addressing these limitations requires solutions that not only improve detection robustness under diverse conditions but also adapt in real-time to evolving network scenarios—challenges we address with our proposed improved XGBoost model for outage detection.

Cell Outage Compensation Only

Cell outage compensation mechanisms are essential to mitigate the effects of base station outages and maintain service continuity [48]. Over the years, various compensation strategies have been proposed, ranging from traditional power control

methods to advanced machine learning and reinforcement learning approaches. Traditional cell outage compensation methods adjust transmission power and antenna tilt in neighboring cells to extend coverage to outage areas, offering computational efficiency and suitability for applications in early networks [48, 49]. In [48], authors show that adjusting reference signal power by a centralized system can restore service to most of the affected users. Similarly, power tuning has been effective in balancing coverage and interference across various network densities [49]. Genetic algorithms have also optimized parameters like downlink power and antenna tilt for faster compensation in zero-touch automation networks. However, they perform best in static environments. In addition, automatic pilot power control [50] and dynamic clustering [51] improve compensation by autonomously adjusting signal strength and resources based on user distribution. However, these methods focus on static adjustments and lack flexibility in dynamic, heterogeneous networks.

Machine learning has significantly enhanced cell outage compensation strategies by enabling more adaptive and optimized responses to outages. For instance, deep neural networks have been used in non-orthogonal multiple access networks to optimize user association and power allocation, maintaining service quality while maximizing spectral efficiency [52]. While these methods improve resource management, they often prioritize throughput over critical factors, such as user fairness and dynamic load balancing. A hybrid approach that combines fuzzy logic with machine learning offers more flexibility, dynamically selecting compensation strategies based on the specific type of service degradation. This model improves network resilience by addressing issues such as coverage gaps and load imbalances, although it increases computational demands and requires careful tuning for stability in varying conditions [53]. Despite the scalability and flexibility of these methods, they still face challenges in real-time coordination, computational demands, and equitable restoration of services in heterogeneous networks.

Reinforcement learning has emerged as a powerful tool for real-time, adaptive optimization of network parameters in cell outage compensation. In dynamic environments, reinforcement learning models excel where traditional methods struggle. Q-learning, for example, has been applied to adjust antenna tilt and transmission power in self-organizing networks, reducing coverage gaps and restoring service efficiently [54]. More advanced techniques, such as the actor-critic model, further enhance adaptability by learning optimal adjustments from real-time network interactions, enabling faster responses in zero-touch automation networks [55]. However, these single-agent models may struggle to scale in ultra-dense networks. To address scalability challenges, deep reinforcement learning has been applied to complex networks, such as 5G ultra-dense environments. A deep reinforcement learning-based mechanism uses distributed clustering and deep Q-networks to adjust base station transmission power, optimizing service recovery [56]. While effective in managing dense networks, deep reinforcement learning relies heavily on clustering and power adjustments, which limits its flexibility in more dynamic scenarios, such as high user mobility or interference. In massive Internet of Things environments, deep reinforcement learning has been used to optimize antenna tilt and power control, demonstrating efficiency in managing large numbers of connected devices [57]. These methods perform well but require substantial computational resources and extensive training, which may hinder real-time scalability. In the following section, we discuss studies that have considered both detection and compensation together.

Cell Outage Detection and Compensation Combined

While cell outage detection and compensation have been widely studied, many existing approaches treat these tasks as separate processes, limiting their overall effectiveness. Early compensation strategies relied on static parameter tuning, such as heuristic-based adjustments of transmission power and antenna tilt, but lacked

adaptability in dynamic network conditions [58, 59]. More advanced solutions incorporated AI-driven optimization techniques; however, many relied on predefined, rule-based models that struggle with real-time adaptation. To address these challenges, learning-based approaches have been proposed, where reinforcement learning enables autonomous decision-making under changing network conditions. However, not all reinforcement learning methods are equally suited for outage compensation. Traditional value-based methods, such as deep Q networks, have been explored in prior works [60], but they face key limitations in non-stationary environments. DQN's reliance on experience replay can lead to outdated learning, and its discrete action space makes it challenging to optimize parameters like transmission power and antenna tilt effectively [56]. In contrast, actor-critic methods dynamically update both policy and value functions in real-time, making them better suited for environments where continuous adaptation is essential. Given the fluctuating nature of outage scenarios, our work leverages the actor-critic framework to enhance compensation efficiency and network resilience.

Early approaches to detecting and compensating for outages in cellular networks relied on basic machine learning and optimization techniques, though they often struggled to adapt to dynamic environments. For instance, [58] proposed a two-tier network solution that used a classification algorithm for anomaly detection and a Lagrange optimization algorithm to adjust transmission power for compensation. However, the static nature of spectrum allocation limited its effectiveness as network conditions changed. Similarly, [59] developed a model that combined machine learning with drive test data for autonomous outage detection, while a fuzzy logic-based reinforcement learning algorithm handled compensation by optimizing antenna tilt and transmission power. These methods, though foundational, lacked the flexibility needed to handle rapidly evolving network conditions.

As networks grew denser and more heterogeneous, more specialized machine learn-

ing techniques became necessary to meet the increased demands of real-time adaptability and resource management. In this context, [35] introduced a machine learning-based approach for heterogeneous networks, employing k-nearest neighbors and local outlier factor for outage detection, paired with an actor-critic reinforcement learning model for compensation. While this approach demonstrated improved adaptability compared to traditional heuristic-based compensation methods, its reliance on periodic signal strength updates resulted in higher computational overhead and limited scalability. Our work builds upon the concept of reinforcement learning-based compensation by leveraging actor-critic methods in a structured framework that effectively adapts to real-time changes in network conditions. Furthermore, pre-configured data reduced its responsiveness in dynamic environments. Similarly, [36] applied a support vector data description algorithm for anomaly detection in ultra-dense networks, combined with a resource allocation model for load balancing. Despite its effectiveness, the need for manual parameter tuning hampered its operational efficiency in real-time, fast-changing conditions.

More advanced approaches have recently been developed to address the growing complexity of emerging wireless networks. For example, [61] integrated big data and pre-coding techniques to enhance zero-touch automation capabilities, utilizing real-time machine learning models to classify cell statuses and initiate compensation actions. However, reliance on big data posed scalability challenges for smaller networks. In a similar effort, [62] proposed a location-aware framework combining network performance metrics and location data to optimize compensation in ultra-dense environments. While feature engineering reduced data complexity, the computational demands of processing location data still limited scalability. Finally, [63] introduced a reinforcement learning-based coordination method for 5G networks, dynamically managing self-configuration, optimization, and healing. Though more adaptable, the computational intensity of reinforcement learning presents a significant challenge for real-time network management. While these advanced methods

offer effective solutions for complex network environments, their high computational requirements hinder scalability and real-time performance.

2.1.3 Challenges and Motivation

The literature reveals several persistent challenges in outage management for emerging wireless networks, particularly in the areas of detection and compensation. Existing AI-based cell outage detection methods often struggle with high shadowing conditions and sparse training data, leading to unreliable performance. Additionally, treating detection and compensation as separate processes overlooks the opportunity to leverage synergies that could enhance overall network efficiency. Most existing work that considers both detection and compensation assumes single base station failure, neglecting the possibility of multiple base station failures and the corresponding compensation strategies required in such scenarios. Moreover, current compensation schemes fail to address two critical aspects of fairness. First, fairness among affected users (outage users or oUEs) is often overlooked, resulting in compensation actions that disproportionately benefit some users while leaving others with sub-optimal service quality. Second, fairness for users already served by the compensating base stations (served users or sUEs) is equally essential; compensation measures should not degrade the service quality for these users. Addressing both dimensions of fairness is crucial in achieving an effective and equitable recovery during outage scenarios.

Given the increasing complexity of modern networks, particularly with the rise of ultra-dense deployments, a more integrated and scalable solution is required. *To the best of our knowledge, no existing framework fully integrates both detection and compensation processes while simultaneously addressing the challenges of shadowing, data sparsity in detection, and managing both single and multiple base station failures, along with fairness in reinforcement learning-based compensation strate-*

gies. This gap in the literature motivates our work to provide a comprehensive solution that bridges these critical divides.

Building on previous work in cell outage management, our research addresses critical limitations by proposing an innovative, integrated framework that unifies both detection and compensation processes. We enhance detection robustness in high-shadowing environments through an improved XGBoost model and ensure fairness in the reinforcement learning process by incorporating Jain's Fairness Index (JFI) and the Geometric Mean (GM) of signal strength, thereby providing equitable service quality for all users. To achieve adaptive and scalable compensation, our framework employs an actor-critic reinforcement learning approach, which is particularly well-suited for dynamic, non-stationary network environments where predefined models and static value functions struggle to generalize effectively. Additionally, multi-agent reinforcement learning enables efficient management of multiple base station outages, offering scalability to meet the challenges of ultra-dense network environments.

2.1.4 Proposed Contributions

Our research advances outage detection and compensation approaches as two modules of the outage management framework, as shown in Fig. 2.1. The proposed detection approach excels at detecting outages in heavily shadowed scenarios with limited data, whereas the compensation strategy, through actor-critic reinforcement learning, refines the transmit power and antenna tilt for adjacent base stations, thus better serving the affected users.

The key contributions of this study are summarized here.

1. **Comprehensive Outage Management Framework:** We present a novel two-phase outage management framework that integrates the processes of out-

age detection and compensation. The framework addresses the distinct processes of detection and compensation, allowing for more efficient handling of outages in high-shadowing network environments. This integrated approach ensures that outages are managed seamlessly and in real-time, enhancing network resilience.

2. **Enhanced Outage Detection with Impv-XGBoost:** For outage detection, we employ the XGBoost scheme with a predetermined *scale-pos-weight* hyperparameter to effectively distinguish between outage and normal classes. This scheme, termed Impv-XGBoost, outperforms the other baseline schemes under various shadowing and minimization conditions for drive test data sparsity. The chosen *scale-pos-weight* optimizes the model for better outage detection accuracy by balancing the distribution of classes. This approach has demonstrated superior detection performance in high-shadow environments and with sparse data.

3. **Novel Actor-Critic RL based Compensation Method:** We introduce the Single-Agent Actor-Critic Reinforcement Learning (SARL-AC) approach for the outage compensation. This method improves the RSRP of users affected by BS outages (oUEs) by dynamically adjusting the antenna tilt and transmission power of nearby compensating Base Stations (cBSs). The SARL-AC algorithm optimizes oUEs coverage while ensuring the quality of service of the users already served by cBS (sUEs) is not compromised. The feedback and reward calculation mechanism incorporates the RSRP distribution of both oUEs and sUEs to balance the compensation process.

4. **Sophisticated Reward Mechanism for Reinforcement Learning:** The reward mechanism for the SARL-AC framework is refined with the use of Jain's fairness index and the geometric mean of the RSRP. The JFI-based reward component ensures fairness among users, accelerating convergence time

during training. However, the GM-based reward stabilizes fluctuations in the compensation process, resulting in a smoother and more reliable improvement in network performance. Integrating these fairness-driven metrics into the reinforcement learning process is an innovative contribution that distinguishes this work from previous RL-based compensation schemes.

5. **Multi-agent Reinforcement Learning for Multiple BS Failures:** To handle the failures of multiple base station, we have extended the single-agent approach to incorporate the MARL-AC method. This method employs decentralized actors and a common critic in a cooperative-competitive reinforcement learning environment to compensate for distinct groups of users. Agents cooperate to achieve individual goals and are penalized for conflicts, ensuring the effective and scalable management of multiple base station failures.

These contributions collectively address the limitations of current zero-touch automation techniques in 5G&B networks, providing a robust and scalable framework for enhanced outage management. By integrating advanced AI-driven solutions, this dissertation advances the state-of-the-art in network resiliency and accuracy, ensuring continuous and reliable service in increasingly complex and dynamic wireless environments.

2.1.5 Chapter Organization and Notation

The remainder of this chapter is organized as follows. Section 2.2 introduces the system model and the proposed outage management framework. It presents the network architecture, challenges in dense cellular networks—including interference management, dynamic channel variations, fairness, and scalability—and outlines MDT-based outage detection and reinforcement learning-based compensation strategies. Section 2.3 focuses on the first part of the proposed solution, detail-

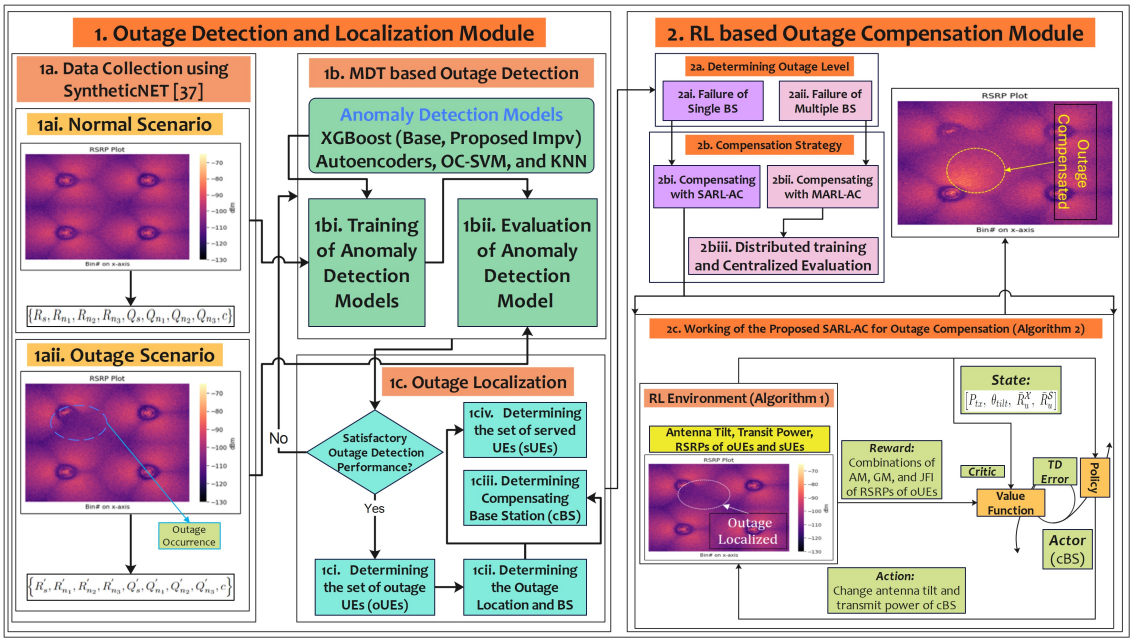


Fig. 2.1: An overview of the proposed *Outage Detection and Compensation* framework, consisting of two primary modules: (1) *Outage Detection and Localization Module*, which leverages MDT data and anomaly detection techniques to detect and localize outages, and (2) *Reinforcement Learning-based Outage Compensation Module*, which dynamically adjusts network parameters via SARL-AC to restore service coverage.

ing various machine learning-based anomaly detection methods, such as OC-SVM, autoencoders, k-nearest neighbors, and XGBoost. The section further describes data preparation, model training, and performance evaluation metrics. Section 2.4 discusses reinforcement learning-based outage compensation, covering single-agent and Multi-agent actor-critic (SARL-AC and MARL-AC) approaches. It explains the formulation of RL-based compensation models, training methodologies, and optimization techniques. Section 2.5 presents the simulation setup and performance evaluation. This includes outage detection and compensation results, complexity comparisons, and empirical performance metrics. A discussion on the advantages and limitations of the proposed schemes is also included. Finally, Section 2.6 concludes the chapter by summarizing key findings, outlining open research challenges, and highlighting directions for future work.

2.2 System Model, and Proposed Outage Management Framework

This section provides an overview of the network architecture and the key challenges associated with outage management in dense cellular networks. We first describe the system model, outlining the deployment of network elements and the related constraints. Next, we discuss the challenges in ultra-dense networks, including interference trade-offs, dynamic variations, and scalability concerns. Finally, we introduce the proposed outage management framework, detailing the methodologies for outage detection, localization, and compensation. This framework leverages MDT-based data collection and reinforcement learning techniques to enhance network resilience and adaptability.

2.2.1 System Model and Preliminaries

This work simulates a 3rd Generation Partnership Project (3GPP) compliant wireless network representing a dense urban environment. This network features a two-tier heterogeneous structure, with macrocells providing broad coverage and microcells addressing areas of high user density and traffic hotspots. The network simulation utilizes the 3GPP system-level simulator, SyntheticNET, to generate realistic drive test data minimization [64]. The macro base stations are strategically placed in a regular grid pattern to ensure comprehensive coverage across the network area. This deterministic placement of macro base stations helps to provide uniform coverage and manage interference effectively. Conversely, the micro base stations are randomly deployed, following a uniform distribution to simulate realistic scenarios of traffic hotspots and high-density areas within the macro cell coverage [65]. Users are randomly deployed across the network area, following a

Poisson distribution, which reflects the stochastic nature of user distribution in urban environments [66]. Each user connects to the base station that offers the highest reference signal received power.

We employ a two-slope path loss model for the propagation model, which accurately reflects the signal attenuation over distance [67]. The model differentiates between distances below and above a threshold d_{th}, providing more precise calculations for near- and far-field conditions [67]. The path loss is calculated as follows,

$$PL_{\mathrm{D}}(d) \quad = \quad \begin{cases} F(1m) + 10p_1 \log_{10}(d), & d \leq d_{\mathrm{th}}, \\ F(1m) + 10\left(p_1 \log_{10}(d_{\mathrm{th}}) + p_2 \log_{10}(\frac{d}{d_{\mathrm{th}}})\right), & d > d_{\mathrm{th}}, \end{cases} \tag{2.1}$$

where F(1m) represents the free space path loss at 1 meter, p_1 and p_2 are the path loss exponents for distances below and above d_{th}, respectively [68]. The path loss calculations also include a Gaussian distributed shadowing component to account for signal variations due to obstacles and environmental factors [69]. Shadowing is modeled by dividing its standard deviation into global and local components, which simulate the variability in different network regions and better reflect real-world scenarios [68].

In this system, slow fading, comprising path loss and shadowing, is modeled explicitly, given its significant impact on long-term network performance [40]. The MDT data applies Layer 3 filtering to mitigate short-term variations such as fast fading [70]. This results in more stable indicators, such as RSRP and RSRQ, which are used to focus on long-term behaviors. Although fast fading is not explicitly modeled in our simulations, we acknowledge its importance and plan to incorporate its direct modeling in future work to enhance the robustness of our approach [70]. The RSRQ is a key performance indicator that measures the quality of the received signal, taking into account both signal strength and interference. RSRQ is math-

ematically defined as the ratio of RSRP to the received signal strength indicator, which includes both the power of the carrier signal and the power of interference and noise across the bandwidth. By incorporating RSRQ into the cell outage detection algorithm, our system is capable of detecting outages even in congested or interference-heavy environments, ensuring more robust detection.

An outage event in our system occurs when a base station is unable to provide adequate service to its connected user equipment. This failure can occur due to hardware malfunctions, severe interference, signal fading, or a significant reduction in signal strength [71]. An outage is explicitly identified for practical implementation when the reference signal received power falls below a threshold, typically ranging from -120 to -140 dBm, within the coverage area of base stations. It is important to note that outages may also arise from various other factors, such as environmental signal fading, interference from other devices, physical obstructions, or hardware issues [72]. The primary effect of these failures is a substantial and often prolonged drop in the received power of the reference signal, degrading the quality of service for users. In the context of machine learning-based outage detection and compensation, it is common practice, as highlighted in [40,45], to simulate outage events by deactivating a base station (i.e., setting its transmit power to zero) and observing the significant impact on RSRP and other key performance indicators such as RSRQ and signal to interference plus noise ratio for the users served by that base station.

We adopt an orthogonal frequency division multiple access frequency reuse scheme with a reuse factor of 1. This implies that the same frequency bands are reused in adjacent cells, maximizing spectral efficiency [52]. However, advanced interference management techniques are required to maintain signal quality and network performance [73]. This multiple access method, with a reuse factor of 1, is commonly used in modern cellular networks, including 4G and 5G, to optimize available band-

width by dividing the spectrum into multiple orthogonal subcarriers, allowing the simultaneous transmission of various signals without interference.

Our network model reflects the core characteristics of dense cellular networks by incorporating both macrocells and a high density of microcells. This architecture significantly increases the number of base stations per unit area, enhancing the network's capacity and coverage, particularly in urban environments where high traffic demands are prevalent [74]. The increased density of users in the simulation further emulates realistic high-density scenarios, resulting in a higher volume of MDT data points and reflecting the intensified network load typical of dense networks [36]. While this high-density deployment improves coverage and capacity, it also introduces key challenges, such as increased interference, dynamic channel variations, and complex resource allocation trade-offs. These challenges must be carefully addressed to ensure effective outage detection and compensation, as discussed in the next subsection.

2.2.2 Proposed Outage Management Framework

The proposed outage management framework consists of two primary modules: ***Outage Detection and Localization*** and ***Reinforcement Learning-based Outage Compensation***, as shown in Fig. 2.1. These modules collaborate to efficiently detect outages, localize the affected areas, and compensate for service loss by adjusting the parameters of nearby base stations. Integrating machine learning and reinforcement learning in this framework ensures scalability and adaptability in dynamic network environments. The first module comprises three blocks: *Data Collection* for both normal and outage scenarios, *MDT-based Outage Detection*, and *Outage Localization*. To explain the working flow of these blocks and the processes involved in each, we have employed a hierarchical numbering system, as shown in Fig. 2.1, and discussed here.

MDT Data Collection

The framework begins with minimization of drive test data collection, where user equipment reports critical network measurements, including RSRP, RSRQ, and channel quality indicators, to the central base station as outlined by the 3GPP standard in [75]. These measurements are captured for both the serving and neighboring base stations, stored in the trace collection entity, and can be used for various self-organizing functions such as mobility optimization, load balancing, and machine learning-based outage detection [34]. The data is aggregated into a feature vector involving RSRP R, RSRQ Q and channel quality indicator c,

$$\mathbf{V} = \{R_s, R_{n_1}, R_{n_2}, R_{n_3}, Q_s, Q_{n_1}, Q_{n_2}, Q_{n_3}, c\}\,, \tag{2.2}$$

where s refers to the serving base station, and n_i refers to the neighboring base stations ranked by signal strength. The MDT data generated from the *normal scenario* is used to train the anomaly detection models listed in the **MDT based Outage Detection** block. The heatmap in the *Outage Scenario* shows the occurrence of an outage simulated by turning off one base station. This occurrence of the outage is manifested by a changed MDT data vector corresponding to the user whose associated base station has gone through the outage. Similarly to (2.2), the MDT data vector for the outage instance is

$$\mathbf{V}^{'} = \left\{R_s^{'}, R_{n_1}^{'}, R_{n_2}^{'}, R_{n_3}^{'}, Q_s^{'}, Q_{n_1}^{'}, Q_{n_2}^{'}, Q_{n_3}^{'}, c\right\}. \tag{2.3}$$

The MDT database aggregates all feature vectors in both typical and outage scenarios, incorporating user locations and their respective base station IDs, which can be used to accurately determine the outage location, as outlined in Section 2.5.1.

MDT based Outage Detection and Localization

Once the MDT data is gathered from both normal and outage scenarios in the **(1a)** block, outage detection and localization are carried out in **(1b)** and **(1c)** blocks, respectively, as shown in Fig. 2.1. Specifically, in **MDT based Outage Detection** block, various anomaly detection models such as the XGBoost and its improved variant, autoencoders, OV-SVM, and KNNs are trained on the normal data as depicted by *1bi* process in Fig. 2.1. To detect outages, mixed MDT data, which includes both outage and normal instances, is fed into these anomaly detection models. These models flag data instances showing significant deviations from normal scenarios as outages, as depicted by the *1bii* process in Fig. 2.1. Once an outage event is detected, the framework proceeds to **(1c)** block for the outage localization. The outage localization block identifies (i) the set of affected users, termed as the (outage UEs), (ii) the geographical location of the outage using localization information provided by the users during MDT reporting, (iii) compensating base station based on the location of the outage found in (iii), and (iv) set of the users already served by the compensating base station (served UEs). The information in this block is used in Module 2 to determine whether single or multiple base stations fail to select the appropriate compensation strategy.

Reinforcement Learning-based Outage Compensation

Once the outage localization is complete, the **Reinforcement Learning-based Outage Compensation** module is utilized, where, in **(2a)**, the extent of the outage is evaluated, determining whether it involves a single or multiple base station failures as shown in Fig. 2.1. Based on this evaluation, the framework selects the appropriate strategy in **(2b)**: single-agent reinforcement learning actor-critic for single base station failure or multi-agent reinforcement learning actor-critic for multiple base station failures. The RL-based compensation algorithm is triggered

to dynamically adjust the antenna tilt and transmission power of neighboring base stations. This reinforcement learning model is typically managed within the core network, using systems such as the network operation and maintenance system or the management data analytics function in 5G networks. The RL algorithm relies on user feedback, with the reward mechanism driven by improvements in KPIs, such as the RSRP, RSRQ, and Signal to Interference plus Noise Ratio (SINR).

In **(2c)**, the selected reinforcement learning agents adjust key parameters, such as antenna tilt and transmission power, of the compensating base station to restore coverage for the affected users. The compensation process employs a reward mechanism that incorporates performance metrics, including the arithmetic mean, geometric mean, and Jain's fairness index, to ensure both efficient service restoration and fairness across all users. This method guarantees that service quality for already-served users is maintained while effectively compensating for the outage. This integrated framework combines anomaly detection, outage localization, and reinforcement learning-based compensation to provide a comprehensive and scalable solution for managing network outages.

2.3 Proposed Solution - Part 1: Outage Detection and Localization

The growing complexity of modern cellular networks calls for advanced solutions that can dynamically manage network operations. AI plays a crucial role by optimizing network parameters in real-time and minimizing the need for manual interventions. This section focuses on the detection component of our framework, employing both traditional unsupervised methods and advanced AI techniques to effectively identify outages.

2.3.1 Anomaly Detection Schemes

We first discuss the overview of the conventional unsupervised outage detection schemes, namely one-class support vector machine and autoencoder. Subsequently, we delve into the supervised K-nearest neighbor and improved XGboost (Impv-XGBoost) based outage detection, which exhibits good performance with limited training data and reduced training time. As highlighted earlier, AI-based approaches offer the automation and efficiency necessary for effective outage management in 5G and beyond networks.

One-Class Support Vector Machine

OC-SVM is a popular anomaly detection technique suited for identifying outages in cellular networks by learning patterns from normal network behavior [41]. Unlike the standard support vector machine, which classifies between two or more classes, OC-SVM is trained exclusively on normal data. It constructs a boundary around this normal data to distinguish it from any abnormal (outage) data. This makes it effective in identifying anomalies, such as outages that deviate from expected behavior.

Autoencoder (AE)

An autoencoder is a type of neural network designed to learn compressed representations of data by encoding input data into a lower-dimensional space and then reconstructing it back [44]. The model is trained on normal data, where it minimizes reconstruction error, the difference between the input and output data [76]. During inference, the autoencoder detects anomalies (outages) when the reconstruction error is significantly higher, as the model struggles to accurately reconstruct abnormal data that deviates from its learned normal patterns [76].

K-Nearest Neighbor (KNN)

The K-nearest neighbor is a simple yet effective classification method often employed when there is limited prior knowledge about the data distribution, particularly in outage detection problems. It measures the dissimilarity between a test instance and its nearest neighbors using a distance metric, typically Euclidean distance [77]. The algorithm selects the closest K neighbors and assigns the test instance the majority class label among these neighbors. In cases where the data is imbalanced or skewed, a weighted classification method is used to give more importance to the nearest neighbors in the voting process [78].

Extreme Gradient Boosting (XGBoost, Impv-XGBoost)

Extreme gradient boosting is a tree-based ensemble learning method [79] known for its computational efficiency and ability to avoid overfitting. XGBoost is efficient for supervised classification (binary) problems due to its robustness to overfitting, suitability to parallelization, and relatively short training time. However, XGBoost does not natively support unsupervised classification [79]; therefore, we adopt a slight modification in it, termed Impv-XGBoost, which uses the output of an autoencoder to compute the *scale-pos-weight* parameter of this model. This parameter inputs the prior knowledge about the distribution of normal and outage instances in the dataset. It enables the model to better differentiate between normal and outage conditions in an unsupervised setting [78].

2.3.2 Machine Learning methods for Cell Outage Detection

This section details the training and evaluation processes of machine learning models, OC-SVM, AE, KNN, and Impv-XGBoost, used for cell outage detection. These models are trained and tested using the minimization of drive test data, which con-

tains key measurements like RSRP and RSRQ from user equipment. The models can identify anomalies that indicate potential outages by analyzing these metrics.

Data Preparation and Preprocessing

The MDT data collected from users includes critical measurements such as RSRP, RSRQ, and users' locations, providing a comprehensive snapshot of network coverage [34]. These features make the minimization of drive test data invaluable for detecting network outages. To ensure model resilience to outliers, the feature vectors of each MDT instance are transformed using the robust scaler technique [75], which involves subtracting the median and dividing by the inter-quartile range. This ensures the model's performance remains stable, even in the presence of outliers, a common issue in real-world network data.

Training and Evaluation for OC-SVM and AE

One-class support vector machine and autoencoder models are trained using normal minimization of drive test data, allowing them to learn the underlying patterns of a fault-free network [76]. The OC-SVM model is trained to establish a decision boundary that encloses normal data points with minimal error. Once trained, the model evaluates new data by checking if it falls within this boundary. Data points falling outside are flagged as anomalies, which indicate potential outages [41]. The autoencoder learns a compact representation of normal data during training by minimizing the reconstruction error. The key difference from OC-SVM is that the autoencoder focuses on learning to accurately recreate input data, and during inference, it flags outlier data based on high reconstruction errors [44]. This approach exploits the model's inability to accurately reconstruct abnormal data (outage data). For both models, evaluation is performed using mixed data that contains both normal and outage instances [76]. The effectiveness of each model is

assessed by its ability to correctly classify normal and outage data, with a one-class support vector machine based on decision boundary violations and an autoencoder based on high reconstruction error thresholds.

Training and Evaluation for KNN and XGBoost

The KNN and Impv-XGBoost models are trained using both normal and outage data [77]. This combined dataset enables these models to effectively distinguish between normal and anomalous conditions. KNN is trained with labeled MDT data that includes normal and simulated outage scenarios [77]. The model classifies data points based on their similarity to the labeled training examples, using the nearest neighbors to determine the label of a new data point. XGBoost, an enhanced version of XGBoost, is trained on a combined dataset of normal and simulated outage data [78]. The model employs gradient boosting to build an ensemble of decision trees, iteratively improving classification accuracy by minimizing errors on both normal and outage data. For the Impv-XGBoost scheme, we utilize the autoencoder's output to compute the *scale-pos-weight* parameter, thereby optimizing the model for improved outage detection accuracy in an unsupervised environment [78].

2.4 Proposed Solution - Part 2: Outage Compensation Approaches

While accurate detection and localization of outages are essential, an effective outage management framework must also include a robust compensation mechanism [10]. This mechanism must restore the coverage for the affected users to normal service without disrupting overall network operations. We propose a solution that utilizes a compensating base station and a reinforcement learning technique

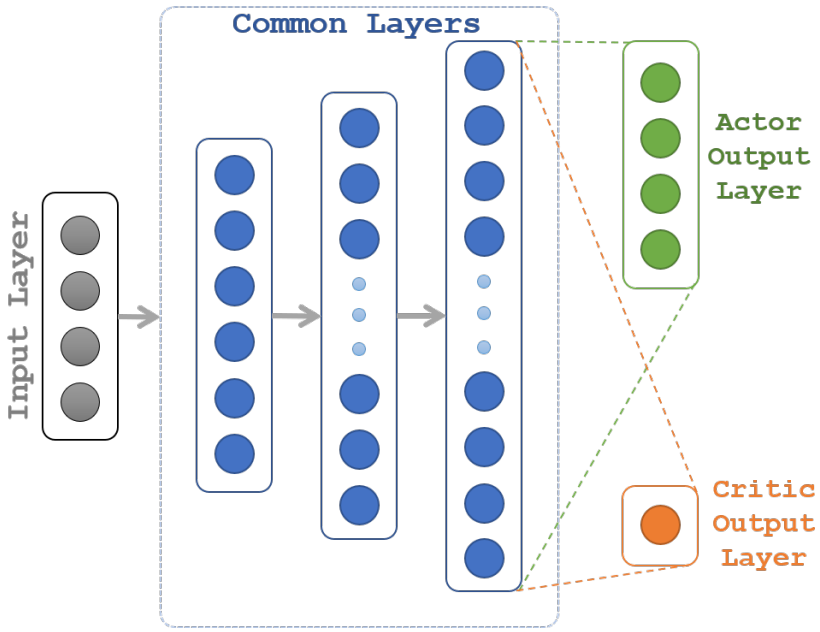


Fig. 2.2: Deep neural network with common hidden layers, and actor and critic output layers, for actor-critic reinforcement learning based cell outage compensation.

to adjust the antenna tilt and transmit power, thereby enhancing service for users affected by outages. Adjusting the tilt angle plays a critical role in optimizing coverage, mitigating interference, and dynamically adapting to real-time network conditions [71]. It should be noted that our primary objective is to restore adequate signal coverage to the affected users (oUEs). Therefore, we use RSRP as the key metric during this phase, as it directly reflects the signal power received by the users, which is crucial for restoring basic connectivity after an outage. While RSRQ is vital for managing interference during detection, RSRP is better suited for compensation because it focuses on signal coverage restoration, which is the immediate concern following a base station outage. Further, to address scenarios with the outages of multiple base stations, we extend this solution to a multi-agent reinforcement learning framework, where multiple compensating base station agents collaborate to restore service to affected users [72]. Before detailing the reinforcement learning approach, we outline the process for selecting compensating base stations and categorizing users, along with the fundamental concepts of reinforcement learning, to provide a clear understanding of the solution.

2.4.1 RL Overview and Preparation for Compensation

Reinforcement learning is central to our outage compensation approach, which addresses two primary components: problem formulation and agent training. Problem formulation involves defining critical elements of reinforcement learning, such as the agent (the compensating base station), environment (the cellular network), states, actions, rewards, and policies [60]. These elements, illustrated in Fig. 2.1 and outlined in Algorithm 1, govern the interaction between the reinforcement learning agent and the network [57]. The second focus of reinforcement learning is the techniques used to train the compensating base station, enabling it to make decisions that maximize network performance by restoring affected user equipment to normal service conditions.

Reinforcement Learning Basics

In our framework, the RL agent represents the compensating base station, whose role is to interact with the network environment by adjusting key parameters, such as transmit power and antenna tilt, to restore service to affected users. Mathematically, a reinforcement learning problem can be formulated using the concept of the Markov decision process, which is described by a 5-tuple as $D = [\mathcal{S},\ \mathcal{A},\ P(s|s,a),\ r,\ \gamma]$, where $\mathcal{S} = \{s_1, s_2, ..., s_k\}$ is the set of states, $\mathcal{A} = \{a_1, a_2, ..., a_n\}$ is the set of actions, which each agent can choose from and transitions from one state to another [57]. $P(s_j^{t+1}|s_i^t, a_l)$, where $a_l \in \mathcal{A}$ and s_i & $s_j \in \mathcal{S}$, represents the probability of transition from state s_i in the time slot t to s_j in the time slot $t+1$ while taking action a_l. For every action taken by the agent, the environment provides feedback in the form of an immediate reward, $r(s,a)$. The mapping of each state s to the probabilities of selecting every action a is termed the *policy* $\pi(s) = a$, which can be a deterministic function or a stochastic approximation. It

provides guidelines on how to take optimal action in a certain state with the goal of maximizing the long-term total reward. γ is the discount factor that accounts for the importance of future rewards.

In reinforcement learning, the effectiveness of an agent being in a certain state is determined by its *state value function*, which measures the expected future rewards the agent will receive by following a certain policy π in a given state. This is formally expressed as,

$$\mathcal{V}^{\pi}(s) = \mathbb{E}\left\{\sum_{t=0}^{\infty} \gamma^t \times r(s_t, \pi(s)) | s_t = s\right\}, \tag{2.4}$$

where γ is the discount factor that controls the balance between immediate and future rewards, and $\mathbb{E}$ denotes the expectation operator. A higher γ prioritizes long-term rewards, while a lower value gives more weight to immediate gains.

Dynamic programming can calculate the optimal policy in simple, well-modeled environments where the environment's dynamics (i.e., the state transition probabilities) are known and understood. However, real-world wireless environments are complex and highly dynamic, making it impractical to model them explicitly [56]. Therefore, we employ model-free RL techniques, which learn the optimal policy and value functions from interaction with the environment rather than relying on predefined models [80]. To find the optimal state value function and policy, we use deep RL, where neural networks approximate both the value function and the policy, allowing the agent to learn directly from raw environmental feedback [60]. The optimal value function and policy are defined as,

$$\mathcal{V}^{*}(s) = \max_{\pi} \mathcal{V}^{\pi}(s) \quad \text{and} \quad \pi^{*} = \arg\max_{\pi} \mathcal{V}^{\pi}(s), \tag{2.5}$$

where π^{*} represents the policy that maximizes the future rewards. To solve for the optimal policy and value function, reinforcement learning algorithms can be

categorized into two main types: policy-based and value-based methods. In policy-based methods, the agent directly learns the policy by optimizing its parameters to maximize long-term rewards. These methods are well-suited for problems with continuous action spaces, but can suffer from higher variance and may converge to sub-optimal solutions [57]. In contrast, value-based methods, such as Q-learning, estimate the value of each state-action pair and choose actions based on these estimates [60]. While effective for problems with discrete actions, these methods can become unstable and computationally complex in large environments. Combining the strengths of both approaches, the actor-critic method, a hybrid of policy-based and value-based methods, is employed in our work. This method uses two neural networks: the actor, which learns the policy, and the critic, which estimates the value function to guide the actor's decisions [57]. This combination improves convergence stability and is particularly well-suited for continuous and complex environments, such as compensating for the base station outages.

Motivation for Adopting the Actor-Critic RL Approach

The actor-critic RL approach was chosen over other methods, such as deep Q-networks, due to its unique suitability for the requirements of dynamic wireless networks. Wireless networks are characterized by non-stationary environments with rapidly changing interference patterns, user mobility, and variable traffic loads. In such scenarios, actor-critic methods excel due to their ability to learn policies and value functions simultaneously through real-time interactions with the environment. This eliminates the need for experience replay, which is often problematic in non-stationary settings where stored experiences quickly become outdated.

Unlike deep Q-networks, which rely on stored experiences to approximate action values, actor-critic methods continuously update both the policy and value functions using real-time feedback. This ensures that the learned policy remains aligned

with the most recent network conditions, making it more effective for dynamic cellular environments where past experiences may quickly become irrelevant. Moreover, DQN operates in a discrete action space, which can be restrictive for tasks such as antenna tilt and transmission power adjustments that benefit from continuous decision-making. Actor-critic methods naturally handle such continuous control problems, improving the adaptability of the compensation mechanism. Additionally, actor-critic methods support multi-agent extensions, enabling decentralized agents to collaborate under a centralized critic for global optimization. This scalability is essential for managing cooperative outage compensation scenarios, where multiple base stations must coordinate their actions without direct communication. In contrast, DQN-based multi-agent implementations require more complex coordination mechanisms and face stability challenges in dynamic environments.

Actor-critic also enhances exploration in environments with sparse rewards by leveraging stochastic policies, allowing the reinforcement learning agent to discover effective actions more efficiently than DQN. This balance between exploration and exploitation ensures that fairness and signal quality can be simultaneously optimized across all users, even under challenging conditions. Finally, the computational efficiency of actor-critic makes it better suited for real-world applications. Unlike DQN, which requires significant memory and computational resources to maintain replay buffers, the actor-critic updates its actor and critic networks using real-time feedback, thereby reducing overhead while maintaining stability.

While deep Q-networks remain a viable RL method, the choice of actor-critic aligns with the specific needs of this study. The ability of AC methods to balance coverage recovery and fairness makes them particularly well-suited for dense cellular networks, where maintaining quality for both outage-affected and already-served users is crucial. Unlike value-based approaches that struggle with evolving interference conditions, AC dynamically refines compensation actions based on real-time

feedback, ensuring that adjustments to transmission power and antenna tilt do not inadvertently degrade service for nearby users. These properties make AC a robust and scalable solution for managing outage recovery in high-density environments.

Determining BS and Categorizing UEs for Compensation

Minimization of drive test reports plays a vital role not only in accurately detecting outages but also in determining the most appropriate compensating base station for out-of-service users. Since MDT reports include the location of users, they can be used to localize the region affected by the outage. The second-best serving base station is identified as the potential cBS for each UE in this region. In the case of single-agent RL, this cBS is selected as the one reported by most out-of-service users. The selected cBS is trained using SARL with the temporal difference method, adjusting its antenna tilt and transmit power to expand coverage toward the oUEs. During this process, two distinct sets of users are considered:

- **Outage UEs (oUEs):** UEs previously served by the base station experiencing the outage.
- **Served UEs (sUEs):** UEs already connected to the cBS before the compensation process.

These two sets of users, i.e., oUEs and sUEs, can be combined into a single set called combined UEs (cUEs), denoted as $\mathcal{C}_u = \mathcal{O}_u \cup \mathcal{S}_u$. In the training of reinforcement learning agents, two cases arise depending on the focus of compensation:

- **Case 1 (oUEs-based training):** In this case, the RL agent focuses solely on improving the RSRP of the out-of-service UEs without considering the needs of the users already connected to the compensating base station.

- **Case 2 (cUEs-based training):** In this case, the reinforcement learning agent aims to optimize the service for both the oUEs and sUEs, ensuring that both groups are accounted for in the compensation process.

2.4.2 SARL-AC: Single-Agent RL with Actor-Critic

The SARL-AC framework represents a key contribution of this work, designed to address single base station failures in dynamic cellular networks. By leveraging the actor-critic approach, SARL-AC optimizes parameters such as antenna tilt and transmission power to compensate for outage-affected users effectively. This foundational framework demonstrates the applicability of reinforcement learning for outage management, serving as the basis for the extended multi-agent approach, which is discussed in Section IV-C.

SARL-AC Problem Formulation and State Space Analysis

Key components of the reinforcement learning environment for the outage compensation problem are outlined below, which remain consistent across different training scenarios.

State: The state of the proposed reinforcement learning solution is represented as a 4-tuple:

$$S = \left[P_{tx},\ \theta_{tilt},\ \bar{R}_u^{\mathcal{X}},\ \bar{R}_u^{\mathcal{S}}\right], \tag{2.6}$$

where each component captures critical network parameters:

- **Downlink Transmission Power (P_{tx}):** Represents the transmit power of the base station, ranging from 0 to 43 dBm with a granularity of 0.5. This is crucial for balancing coverage region and interference in the network.

Algorithm 1: The SARL-AC Environment

Class *Class*

Def `_init_` (A)**:**

$A.p^{txp}_{ini-min}$, $A.p^{txp}_{ini-max}$, $A.\theta^{ant}_{ini-min}$, $A.\theta^{ant}_{ini-max}$, $A.a^{act}_{ini}$ ***Initialize all parameters***

return A

Def `Reset` $(A,\ \mathcal{X}_{ues},\ \mathcal{S}_{ues})$**:**

$A.p^{txp}_{ini} = \text{rand}\left(p^{txp}_{ini-min},\ p^{txp}_{ini-max},\ 1\right)$

$A.\theta^{tilt}_{ini} = \text{rand}\left(\theta^{tilt}_{ini-min},\ \theta^{tilt}_{ini-max},\ 1\right)$

$A.\bar{R}_x = mean\left(\texttt{comp_RSRP}\left(A, \mathcal{X}_{ues}\right)\right)$

$A.\bar{R}_s = mean\left(\texttt{comp_RSRP}\left(A, \mathcal{S}_{ues}\right)\right)$

$A.S = \left[A.p^{txp}_{ini},\ A.\theta^{tilt}_{ini},\ A.\bar{R}_x,\ A.\bar{R}_s\right]$ ***state***

return $A.S$ ***return the new state***

Def `Step` $\left(A,\ r^R_A,\ r^R_G,\ r^R_J\right)$**:**

$A.p^{txp}_{cur} = A.S[0]$ ***current tx power***

$A.\theta^{tilt}_{cur} = A.S[1]$ ***current antenna tilt***

$A.\bar{R}_x = mean\left(\texttt{comp_RSRP}\left(A, \mathcal{X}_{ues}\right)\right)$

$A.\bar{R}_s = mean\left(\texttt{comp_RSRP}\left(A, \mathcal{S}_{ues}\right)\right)$

Find, $\bar{R}^{\mathcal{X}_u}_{dba}$, (2.10) ***parameters before action***

$A.S =$`Take_action` $(A,\ \mathcal{X}_{ues},\ \mathcal{S}_{ues})$

$A.p^{txp}_{cur} = A.S[0]$ ***current tx power***

$A.\theta^{tilt}_{cur} = A.S[1]$ ***current antenna power***

$A.\bar{R}_x = mean\left(\texttt{comp_RSRP}\left(A, \mathcal{X}_{ues}\right)\right)$

$A.\bar{R}_s = mean\left(\texttt{comp_RSRP}\left(A, \mathcal{S}_{ues}\right)\right)$

Find, $\bar{R}^{\mathcal{X}_u}_{daa}$, (2.11) ***parameters after action***

Assign a reward following (2.7), (2.8), & (2.12)

$A.r$ using (2.13) ***total reward***

return $A.S$, $A.r$, $A.d$

Def `Take_action` (A)**:**

if $A.action == 0$ **then**

$A.S[0] += 0.5$ ***Increase transmit power***

end

if $A.action == 1$ **then**

$A.S[0] -= 0.5$ ***Decrease transmit power***

end

if $A.action == 2$ **then**

$A.S[1] += 0.5$ ***Increase antenna tilt***

end

if $A.action == 3$ **then**

$A.S[1] -= 0.5$ ***Decrease antenna tilt***

end

return $A.S$

Def `Seed` (A)**:**

$A.seed$ ***seeding to same random start***

return $A.seed$

- **Antenna Tilt (θ_{tilt}):** Defines the directional coverage of the base station's signal, ranging from 0° to 15° with a granularity of 0.5°. Adjusting this parameter allows the base station to optimize its coverage area dynamically.

- **Mean RSRP of Users ($\bar{R}_u^{\mathcal{X}}$):** Denotes the average reference signal received power for users ($\mathcal{X}$) under consideration depending on the training cases, i.e., Case 1 (oUEs-based training) or Case 2 (cUEs-based training). Here, $\mathcal{X}$ serves as a placeholder and can represent either outage-affected users (oUEs) in oUEs-based training or combined users (cUEs = oUEs + sUEs) in cUEs-based training. This metric provides critical feedback on the quality of service experienced by users impacted by different compensation actions.

- **Mean RSRP of Served Users ($\bar{R}_u^{\mathcal{S}}$):** This parameter represents the average RSRP for the users (sUEs) already served by the base station. Maintaining this metric ensures fairness and prevents service degradation for existing users during the compensation process.

By integrating these parameters into the state space, the SARL-AC framework effectively captures the trade-offs between fairness, coverage, and interference mitigation. The state space supports two distinct training scenarios: (1) **oUEs-based training**, where the focus is on recovering outage-affected users, and (2) **cUEs-based training**, where both outage-affected and already-served users are considered.

It is observed from the performance evaluation and analysis that oUEs-based training effectively recovers outage-affected users but may lead to service degradation for already-served users due to increased interference. Conversely, cUEs-based training ensures fairness by optimizing service for both user groups, achieving better overall network performance. The inclusion of parameters like $\bar{R}_u^{\mathcal{S}}$ allows the RL agent to address this trade-off dynamically. Fig. 5c illustrates the role of these state space

components in guiding the RL agent's actions and their contribution to achieving the study's objectives.

Action: An agent can take four actions: the increment of antenna tilt and transmit power and the decrement of the antenna tilt and transmit power. Every action corresponds to a transition in the state space.

Reward: The reward of the learning algorithm is based on the mean RSRP improvements and fairness among users regarding their respective RSRP values, as discussed in the following subsections.

SARL-AC Rewards

A detailed description of reinforcement learning rewards is explained here.

Arithmetic mean of RSRP: Let the arithmetic mean of RSRP of xUEs before and after action are represented by the $\bar{R}_{ba}^{\mathcal{X}_u}$ and $\bar{R}_{aa}^{\mathcal{X}_u}$, respectively, and the mean target RSRP $\bar{R}_{tg}^{\mathcal{X}_u}$. Next, the absolute difference of the RSRP values from the target before and after the actions is given as $\bar{R}_{dba}^{\mathcal{X}_u} = |\bar{R}_{ba}^{\mathcal{X}_u} - \bar{R}_{tg}^{\mathcal{X}_u}|$ and $\bar{R}_{daa}^{\mathcal{X}_u} = |\bar{R}_{aa}^{\mathcal{X}_u} - \bar{R}_{tg}^{\mathcal{X}_u}|$, respectively. The RSRP-based reward is incremented by a constant r_A if the difference between the current and target RSRP decreases after an action, following the condition,

$$r_A^R = \begin{cases} r_A, & \bar{R}_{daa}^{\mathcal{X}_u} < \bar{R}_{dba}^{\mathcal{X}_u}, \\ 0 & \text{otherwise.} \end{cases} \tag{2.7}$$

Enhancement in the rewards by Geometric Mean of the RSRP: The geometric mean of a set of values can be interpreted as the measure of randomness which is less prone to outliers. A higher geometric mean corresponds to more similarity between values. The geometric mean of the RSRP of the xUEs before and

after actions are shown by the $\tilde{R}_{ba}^{\mathcal{X}_u}$ and $\tilde{R}_{aa}^{\mathcal{X}_u}$ respectively, and reward is incremented by a fixed value of r_G by,

$$r_G^R = \begin{cases} r_G, & \tilde{R}_{aa}^{\mathcal{X}_u} > \tilde{R}_{ba}^{\mathcal{X}_u}, \\ 0 & \text{otherwise.} \end{cases} \tag{2.8}$$

Enhancement in the rewards by Jean's Fairness Index of the RSRP: In contrast to the previous metrics, which use an individual value, i.e., arithmetic or geometric mean of the RSRPs to determine the reward process, the Jean's fairness index based reward of the RSRP values of every user in the normal case as the target parameter and achieved RSRP values in the reinforcement learning process. Jean's fairness index is a bounded, continuous function that measures fairness in any process involving resource allocation. For a given vector of values of a certain parameter $\mathbf{x} \in \mathbb{R}_+^N$ and its optimum values in the ideal/normal situation in $\mathbf{y} \in \mathbb{R}_+^N$, the Jean's fairness index J is given as [81],

$$\text{JFI}(\mathbf{x},\ \mathbf{y}) = \frac{\left(\sum_{i=1}^{N} \frac{x_i}{y_i}\right)^2}{N \sum_{i=1}^{N} \left(\frac{x_i}{y_i}\right)^2} \text{ where } x_i \in \mathbf{x} \ \&\ y_i \in \mathbf{y}. \tag{2.9}$$

To use Jean's fairness index for the reward process, we need to have normal RSRP values, which were, in the case of non-outage, of xUEs calculated in milliwatts given in the vector $\mathbf{v}_{nor}^{\mathcal{X}_u}$. The measured RSRPs of the xUEs before and after each action are given in $\mathbf{v}_{ba}^{\mathcal{X}_u}$ and $\mathbf{v}_{aa}^{\mathcal{X}_u}$, respectively. Jean's fairness index value before and after actions is calculated as follows,

$$J_{ba}^{\mathcal{X}_u} = \text{JFI}\left(\mathbf{v}_{ba}^{\mathcal{X}_u},\ \mathbf{v}_{nor}^{\mathcal{X}_u}\right), \tag{2.10}$$

$$J_{aa}^{\mathcal{X}_u} = \text{JFI}\left(\mathbf{v}_{aa}^{\mathcal{X}_u},\ \mathbf{v}_{nor}^{\mathcal{X}_u}\right), \tag{2.11}$$

respectively. This function ranges in the interval $\left[\frac{1}{N},\ 1\right]$, with $\frac{1}{N}$ corresponding to the smallest possible value and 1 corresponding to the largest possible value of the fairness index. The JFI-based reward is also increased by r_J,

$$r_J^A = \begin{cases} r_J, & J_{aa}^{\mathcal{X}_u} > J_{ba}^{\mathcal{X}_u}, \\ 0 & \text{otherwise.} \end{cases} \tag{2.12}$$

Total reward in an RL training step is the sum of all these with the flexibility to include or exclude using binary variables,

$$r_T = b_A\, r_A^R + b_G\, r_G^R + b_J\, r_J^R. \tag{2.13}$$

By incorporating rewards based on Jain's fairness index and the geometric mean of RSRP, we ensure that these adjustments provide equitable service quality to all users, enhancing overall network performance and resilience.

Actor and Critic Parameter Updates

The actor and critic in the proposed actor-critic framework share a common neural network architecture, where the input state is processed through shared hidden layers, and separate output layers are used for the actor and critic components. This design allows the network to extract common features relevant to both policy optimization (actor) and value estimation (critic). The actor output generates a probability distribution over actions, representing the policy $\pi(a|s;\theta)$, while the critic output estimates the value function $V(s;\theta)$, where θ represents the shared network parameters.

Parameter Updates: The parameter updates for the actor and critic are based on the temporal difference error, which measures the discrepancy between the pre-

dicted value and the observed return:

$$\delta_t = r_t + \gamma V(s_{t+1}; \theta) - V(s_t; \theta), \tag{2.14}$$

where r_t is the immediate reward, and γ is the discount factor.

Critic Update: The critic minimizes the mean squared error of the temporal difference error to improve the value function approximation:

$$\theta \leftarrow \theta - \alpha_c \nabla_\theta \delta_t^2, \tag{2.15}$$

where α_c is the learning rate for the critic update.

Actor Update: The actor adjusts its policy using the policy gradient method, which maximizes the expected cumulative reward:

$$\nabla_\theta J = \mathbb{E}\left[\delta_t \nabla_\theta \log \pi(a|s; \theta)\right]. \tag{2.16}$$

The actor's parameters are updated as:

$$\theta \leftarrow \theta + \alpha_a \nabla_\theta J, \tag{2.17}$$

where α_a is the learning rate for the actor update.

Collaborative Training Process: The shared architecture ensures that the feature extraction layers are trained dynamically to serve both the actor and critic objectives, allowing efficient use of network parameters. The centralized critic evaluates joint actions and states, providing consistent feedback that guides the actor's updates. This collaborative training process enhances stability and convergence, particularly in dynamic and non-stationary environments, such as dense cellular networks. Fig. 2.2 illustrates the shared architecture, and Algorithm 2 outlines the

Algorithm 2: The SARL-AC Training Process

Input: *model*

while $\epsilon_c \leq \epsilon_{max}$ *and not* $target_achieved$ **do**

- $A.S = RL_Net_Env.Reset\left(A.a_{ini}^{act},\ \mathcal{X}_{ues},\ \mathcal{S}_{ues}\right)$
- $act_prb_hst = []; crt_val_hst = []; rwrds_hst = []$
- $R_\epsilon = 0$ ***episode reward***
- $R_r = 0$ ***running reward***
- **foreach** t_s *in* $\mathcal{T}_\epsilon^{max}$ **do**
  - $act_prb,\ crt_val = model(A.S)$
  - $A.S,\ A.r,\ A.d = RL_Net_Env.Step\left(A.a_{ini}^{act},\ r_A^R,\ r_G^R,\ r_J^R\right)$
  - $act_prb_hst.append(act_prb)$
  - $crt_val_hst.append(crt_val)$
  - $rwrds_hst.append(A.r)$
  - $R_\epsilon = R_\epsilon + A.r$
  - $A.p_{cur}^{tilt} = A.S[0]$ ***current tx power***
  - $A.\theta_{cur}^{tilt} = A.S[1]$ ***current antenna tilt***
  - $A.\bar{R}_o = mean\left(\texttt{comp_RSRP}\left(A,\ \mathcal{O}_{ues}\right)\right)$
  - $A.\bar{R}_s = mean\left(\texttt{comp_RSRP}\left(A,\ \mathcal{S}_{ues}\right)\right)$
  - $A.S[2] = A.\bar{R}_o$
  - $A.S[3] = A.\bar{R}_s$
  - $R_{d-ret} = 0$ ***discounted return***
  - **foreach** r *in* $rwrds_hst$ **do**
    - $R_{d-ret} = r + \gamma\, R_{d-ret}$
  - $hst = zip(act_prb_hst,\ crt_val_hst,\ R_{d-ret})$
  - **foreach** $log_p,\ val,\ ret$ *in* hst **do**
    - $d = ret - val$
    - $\mathcal{L}_{act}.append(-log_p \times d)$ ***actor loss***
    - $\mathcal{L}_{crt}.append(\mathcal{L}_{hub}(val, ret))$ ***critic loss***
  - $\mathcal{L}_{cmb} = \mathcal{L}_{act} + \mathcal{L}_{crt}$
  - $g = tape.grad(\mathcal{L}_{cmb}, model.train_var)$
  - $optm.apply_grad(zip(g, model.train_var))$
- $hst.clear.(act_prb, crt_val, rwrds)$

training process in detail.

SARL-AC Problem Solution

The working of the SARL-AC model is detailed in Algorithm 2, while the environment in which the agent is trained is defined in Algorithm 1. The environment class consists of four different functions. It is clear from Algorithm 2 that the training process is based on episodes, where agents take steps in each episode to meet

the predefined target regarding improving RSRP for oUEs. The running episode terminates if the target is achieved at any step, and training proceeds to the next episode. Further, the RL-based compensation algorithm is implemented in a 3GPP-compliant SyntheticNET simulator, where we have defined the reinforcement learning environment and observed the real-time impact of adjustments to antenna tilt and power on network performance measured as user RSRP. While the real-world implementation of this algorithm would require more complex interaction between the core network, base stations, and users, the simulation-based approach provides sufficient proof of concept for the scope of this study.

In our proposed SARL-AC model, we utilize a neural network with shared layers for both the actor and critic network operations (Fig. 2.2). The network architecture comprises an input layer, three shared hidden layers, and two separate output layers connected to the last shared hidden layer. The input layer takes in the network state vector, and the actor output layer produces the action probabilities, while the critic output layer generates the value estimate. During training, the actor network learns to maximize the overall reward by selecting actions that lead to the highest expected returns. The critic network evaluates these actions by learning the value of each state-action pair, thus guiding the actor to make better decisions. The reward structure, as discussed, is designed to encourage actions that improve the RSRP for users.

The training process involves the following steps:

- **Actor-Critic Training:** The actor network's output probabilities are used to sample actions, which are then executed in the environment. The resulting state transition and reward are observed.
- **Reward Calculation:** Rewards are discounted and summed to calculate the total expected return.

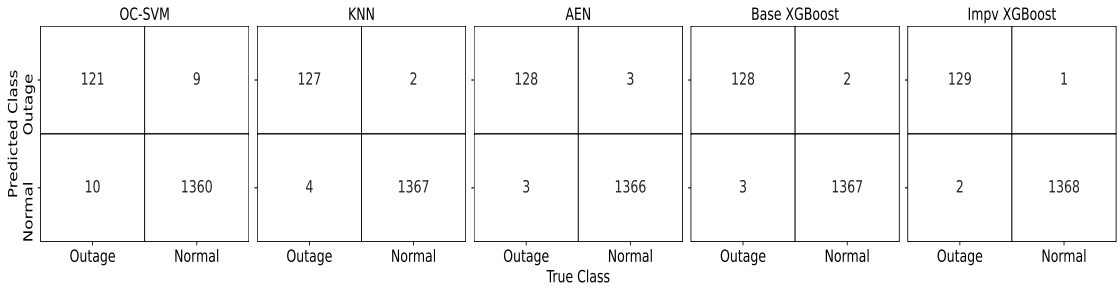


Fig. 2.3: Confusion matrices comparing outage detection performance of the proposed Impv-XGBoost with baseline classifiers (OC-SVM, KNN, Autoencoder, and XGBoost) under 4 dB shadowing with 300 user devices per square kilometer.

- **Loss Computation:** The actor's loss is computed using the negative logarithmic probabilities of the selected actions, weighted by the advantage (difference between actual and estimated returns). The critic's loss is calculated using the Huber loss, which measures the error between the estimated value and the actual return.

- **Back-Propagation:** The losses from both the actor and critic networks are summed and back-propagated through the shared layers to update the network weights.

The performance of the SARL-AC model, including its ability to enhance the RSRP of oUEs and the network's overall performance, will be discussed in Section 2.5.3. In the subsequent section, we will address the issue of multiple BS failures and the implementation of multi-agent reinforcement learning schemes to handle such scenarios effectively.

2.4.3 MARL-AC: Multi-Agent RL with Actor-Critic

After discussing single-agent RL, this section elaborates on the multi-agent RL with an actor-critic method, focusing on the motivation for its usage, the working principle, and the modifications adopted from SARL-AC for the training process.

Motivation for using MARL-AC

Single-agent reinforcement learning approaches are inadequate to address the potential for multiple base station failures in real networks, particularly when these base stations are spatially far apart [82]. Therefore, we employ multi-agent actor-critic reinforcement learning, where multiple cBSs cooperate and compete to bring a group of users back into coverage without disrupting network operations or degrading user quality of experience [82].

Traditional reinforcement learning approaches, such as policy gradient and Q-learning, are unsuitable for multi-agent environments due to their non-stationary behavior from an individual agent's perspective, where policies continuously change during learning [83]. Hence, experience replay, crucial for deep Q-learning, cannot be straightforwardly realized. Similarly, policy-gradient methods face coordination challenges among multiple agents and suffer from high variance issues. Thus, extending actor-critic methods to multi-agent scenarios, following specific rules for agent-environment interactions, is essential for robust learning and coordination [84].

MARL-AC Working Principle and Training

Despite differences in agent interactions, MARL shares many working principles with SARL. Specifically, the environment description algorithm remains consistent, with each agent acting independently on its distinct users (both sUEs and oUEs categories) [85]. Our approach involves distributed training and centralized evaluation for multiple cBSs, where direct communication between actors is not possible [83]. In addition, the environment considered in MARL is similar to the cooperative navigation discussed in [84], where N agents cooperate to achieve a set of goals N. Agents observe relative positions and infer goals, with communication occur-

ring solely through the critic's evaluation of actions, shared among all agents [84]. Specifically, in a typical training instance, each base station only has information of its state, so its actor is trained based on its own information to take action. The actions of all cBSs are combined in a single input vector and fed into the critic network, which is trained to evaluate every agent's action [84]. The learning process evolves so that all actors stick to the best actions and pull the corresponding users out of the coverage. The typical critic ensures that the respective actors should stop when the target is achieved and not extend their coverage to the neighboring base stations' coverage area [85].

Similar to the SARL approach, the training of each agent can be reduced to oUEs alone or oUEs and sUEs combined. Similarly, the primary form of the reward process is based on the arithmetic mean of RSRP only; however, the combinations of both the JFI and the geometric mean of RSRP are implemented to ensure fairness among all users and fastness in convergence. Also, the centralized controller ensures that all agents follow the same training approach and reward process. It will be discussed further in the results discussion section 2.5.3, we implement cUEs-based training for every agent to ensure that outage compensation does not disturb the coverage to sUEs, and a combination of JFI and GM-based rewards so that convergence to target RSRP is accelerated and random fluctuations in mean RSRP are reduced.

MARL-AC builds upon the SARL-AC framework by enabling decentralized cooperation among multiple cBSs. In this framework, each cBS acts as an independent agent that dynamically adjusts its parameters (e.g., antenna tilt and transmission power) to optimize coverage for outage-affected users while minimizing interference to neighboring cells. The cooperative-competitive nature of MARL-AC introduces versatility and scalability, making it particularly effective in scenarios involving overlapping outage regions or densely deployed networks. Each agent learns to bal-

Table 2.1: Simulation parameters defining the macro and micro base station setup, user density range, transmit power, shadowing conditions, and base station heights.

System Parameters	Value
Number of macro Base Stations	9
Number of micro Base Stations	15
Number of sectors per macro base station	3
Number of Users	$2500 - 15000$
Operating frequency of macro Base Stations	2100 MHz
Operating frequency of micro Base Stations	2500 MHz
Bandwidth of macro Base Stations	15 MHz
Bandwidth of micro Base Stations	20 MHz
Transmit power of macro Base Station	43 dBm
Transmit power of micro Base Station	20 dBm
Standard deviation of shadowing	$0 - 12$ dB
Base stations height	30 m
Small Base stations height	10 m

ance local objectives (e.g., coverage enhancement for nearby users) with global goals (e.g., fairness and overall network stability). The results presented in Section V-C-3 demonstrate the efficacy of MARL-AC in managing complex outage scenarios, validating its role as a scalable extension to the single-agent framework.

2.5 Simulation Setup & Performance Evaluation

In this section, we evaluate the performance of the proposed detection and compensation solutions. Our evaluation methodology assesses the outage detection and compensation mechanisms under various network conditions using a 3GPP-compliant wireless network simulated in SyntheticNET. First, the simulation setup is discussed, and subsequently, the performance of the outage detection schemes is analyzed under various network conditions, including increased shadowing and user density. Then, we discuss the progress of the compensation approaches under

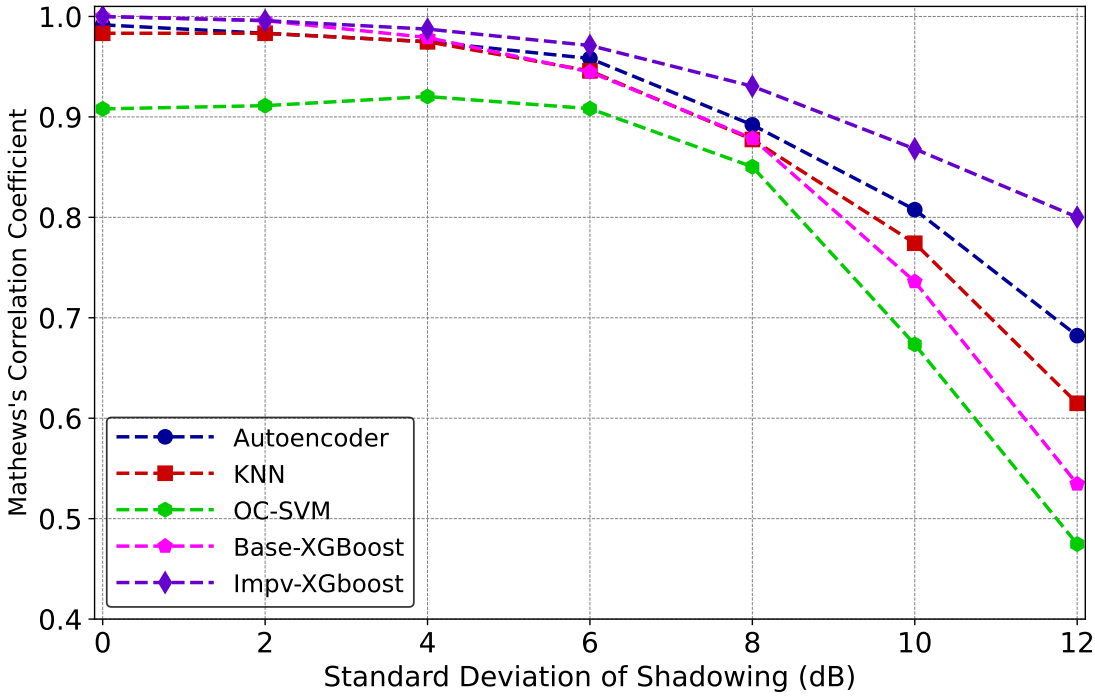


Fig. 2.4: Performance improvements of the proposed scheme over baseline schemes for Matthews correlation with respect to increasing shadowing standard deviations.

the SARL scheme, using different cases of agent training and reward combinations. Then, we compare the results of the multi-agent actor-critic RL solution, where three agents cooperate and compete to compensate for multiple BS outage scenarios. In all these outage compensation comparisons, we focus on observing the oUEs RSRP improvements and the impact of RL training on the sUEs coverage. The simulation setup for our system is explained in the following subsection.

2.5.1 Simulation Setup

A 3GPP compliant long-term evolution simulator [64] generates MDT data instances in a square network area of $5Km \times 5Km$. The users are evenly distributed and served by 9 macrocells and 16 micro-cells. For the outage scenario, the transmit power is set to 0 dBm, and MDT reports are generated from all users. The non-outage scenario is also simulated, and the users' association with base stations

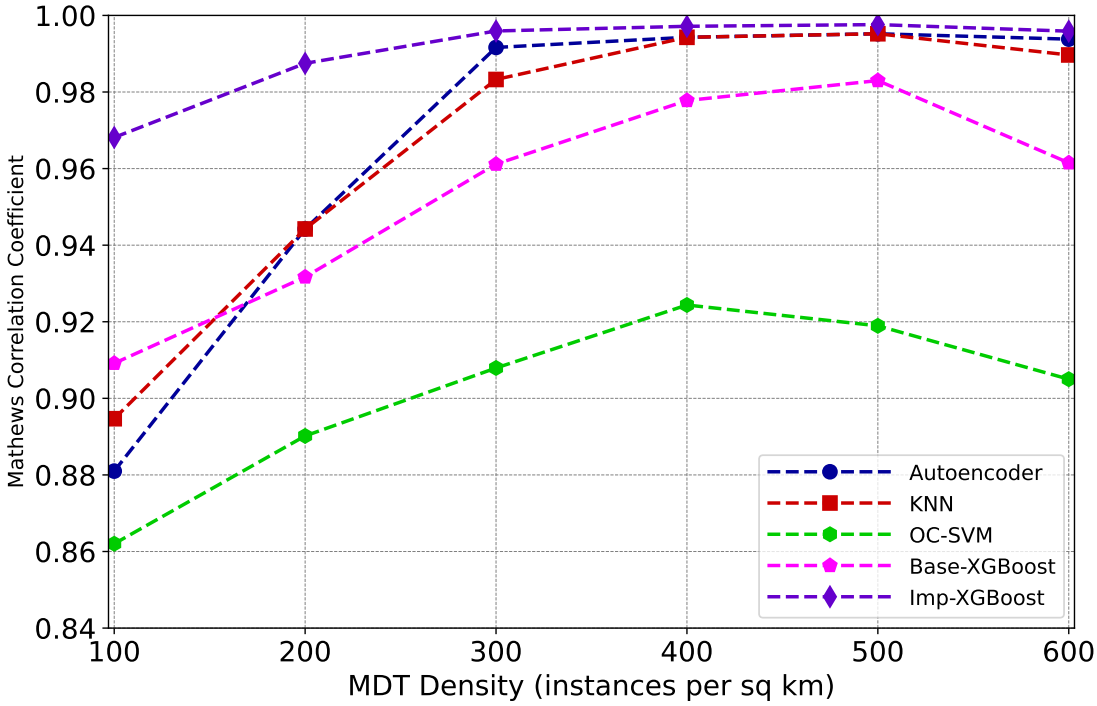


Fig. 2.5: Matthews correlation coefficient plotted against user device density for the proposed and baseline schemes. The proposed Impv-XGBoost maintains higher accuracy and scalability even in lower network and data density.

is retained. The simulation parameters provided in Table 2.1 are selected based on empirical studies for urban and suburban environments [86], 3GPP industry standards [75], and experimental tuning [87]. Also, to simulate a dense network environment, we increase the number of users, as indicated by the rising minimization of drive test density values depicted on the x-axis of Fig. 2.5. This setup ensures that our network model can address the high traffic loads and performance requirements characteristic of dense cellular networks.

2.5.2 Outage Detection Results

We compare the cell outage detection schemes using confusion matrices, the Area Under the Region Of Convergence Curve (AUROC), and the Mathews Correlation Coefficients (MCC). MCC evaluates the comparison schemes to vary the shadowing

and density of the minimization of drive test data.

Performance Evaluation Metrics

Before delving into the details of the performance evaluation for the detection and compensation schemes, we summarize the performance evaluation metrics for both of these approaches.

- **Confusion Matrix:** The confusion matrix is a table that summarizes the performance of a classification model by displaying the counts of true positives (t_p), false positives (f_p), true negatives (t_n), and false negatives (f_n). The confusion matrix allows us to understand the distribution of classification errors and assess the reliability of our detection algorithm.

- **Area Under the Receiver Operating Characteristic Curve (AUROC):** AUROC is a performance measurement for classification problems at various threshold settings. The ROC curve is created by plotting the true positive rate against the false positive rate. AUROC provides a single measure of the overall performance of the detection algorithm, with values closer to 1 indicating better performance.

- **Matthews Correlation Coefficient:** The Matthews correlation coefficient measures the quality of binary classifications. It considers true positives, false positives, true negatives, and false negatives, providing a balanced measure even if the classes are of very different sizes. MCC values remain unchanged even if the depiction of the outage event is flipped by one or vice versa.

$$MCC = \frac{(t_p \times\ t_n) - (f_p \times\ f_n)}{\sqrt{(t_p + f_p)(t_p + f_n)(t_n + f_p)(t_n + f_n)}} \tag{2.18}$$

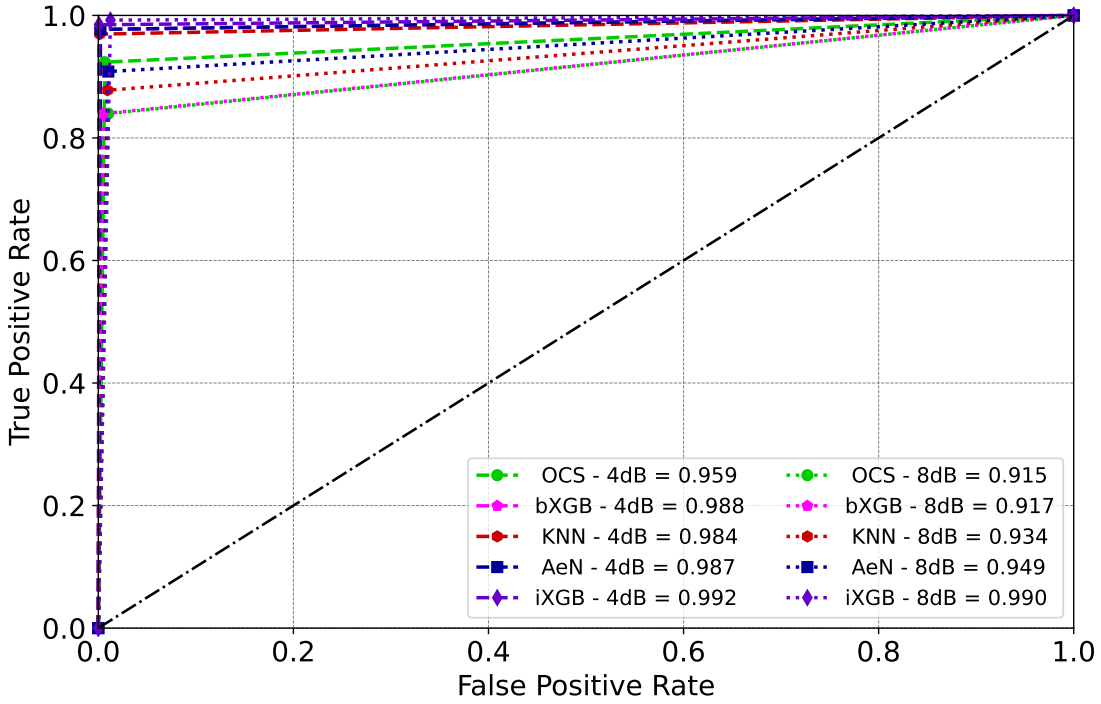


Fig. 2.6: Convergence behavior of outage detection algorithms under different combinations of shadowing and user densities.

Performance Evaluation as the Confusion Metrics

The confusion matrices for cell outage detection schemes at a 4 dB shadowing level and a user density of 300 users/sq km, depicted in Fig. 2.3, reveal varying performance levels. Impv-XGBoost leads by misclassifying only 2 outages and one normal instance. Although OC-SVM is the least effective, it misclassifies 19 instances, showcasing acceptable performance. This comparison, especially with the shadowing in Fig. 2.4, underscores the Impv-XGBoost's superior capability to handle shadowing effects efficiently.

Performance Comparison against Varying Shadowing

The performance of outage detection schemes in low shadow environments is generally satisfactory due to clear differences between the normal and outage MDT val-

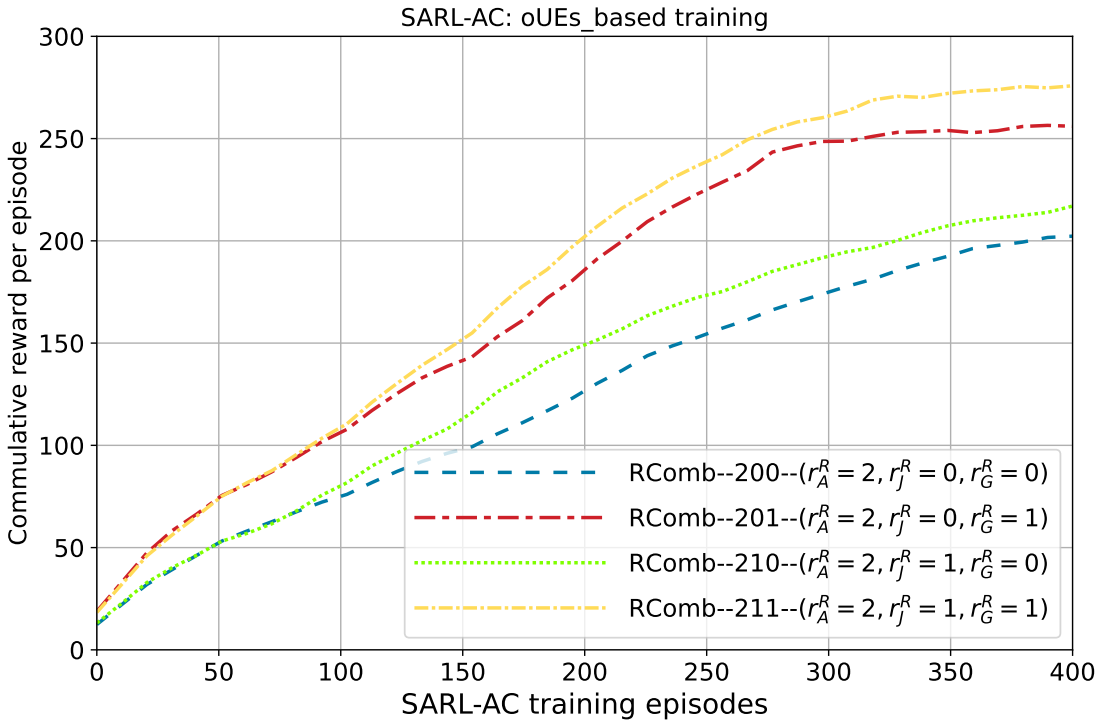


Fig. 2.7: Comparison of cumulative rewards achieved by single-agent reinforcement learning across combinations of reward schemes utilizing arithmetic mean, geometric mean, and Jain's fairness index.

ues. However, distinguishing between these conditions becomes challenging in areas of high shadow, such as metropolitan and urban regions. As shadowing increases, as shown in Fig. 2.4, the performance of all schemes declines; however, the resilience of Impv-XGBoost, followed by KNN and Autoencoder, against higher shadowing levels is notable. This resilience highlights the need for robust COD solutions, with Impv-XGBoost emerging as the optimal choice for high-shadow conditions due to its reduced training requirements, discussed in Section 2.5.4.

Performance Comparison against Varying Data Density

Additionally, the impact of the minimization of drive test data density on detection performance is analyzed in Fig. 2.5. An increase in MDT reports enhances the performance of all schemes, with neural networks, such as Autoencoder, benefiting significantly from the availability of ample data. KNN and Impv-XGBoost also im-

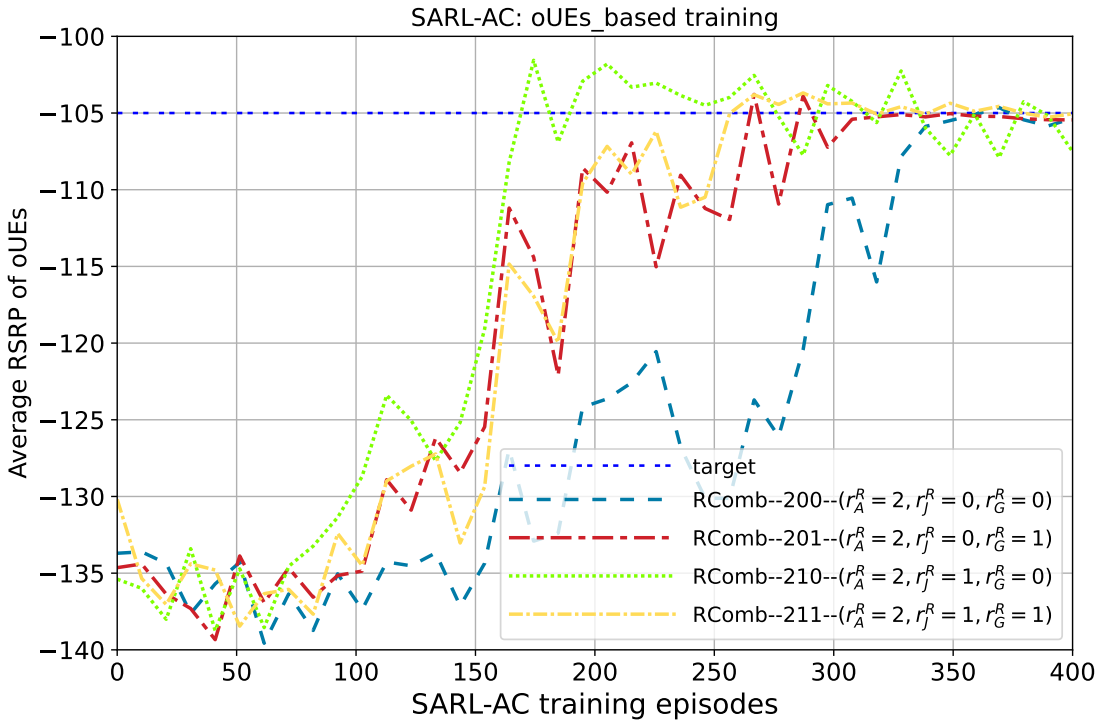


Fig. 2.8: Average RSRP variations for outage users across different reward combinations leveraging arithmetic mean, geometric mean, and Jain's fairness index.

prove, yet their performance plateaus, remaining lower than that of Impv-XGBoost. Interestingly, the performance of OC-SVM and Base-XGBoost peaks before declining, with a greater minimization of drive test data. These observations confirm the effectiveness of Impv-XGBoost in minimizing drive test data across varying shadowing and densities. The efficacy of outage detection schemes is further validated by the AUROC curves in Fig. 2.6 for different shadowing and minimization of drive test data conditions, where Impv-XGBoost consistently outperforms the others. The next section addresses the performance of the proposed outage compensation solutions.

2.5.3 Outage Compensation Results

In this section, we discuss the progress of the outage compensation solutions, specifically the SARL-AC and MARL-AC algorithms.

Compensation performance using SARL-AC and oUEs-based training

The results of the compensation approach with oUEs-based training are shown in Fig. 2.7, Fig. 2.8, and Fig. 2.9. The labels in each figure represent the combination of rewards in terms of the arithmetic mean (r_A^R), JFI (r_J^R), and GM (r_G^R). For example, the combination "210" means $r_A^R = 2$, $r_J^R = 1$ and $r_G^R = 0$, indicating JFI-assisted training. Fig. 2.7 shows the cumulative rewards for all combinations (4) with oUEs-based training, while Figs. 2.8 and 2.9 present the effects of these combinations on the mean RSRP of oUEs and sUEs, respectively. The performance of the compensation approach is evaluated in terms of cumulative rewards per episode of the underlying reinforcement learning approach and the average RSRP of respective users, as depicted on the y-axis of Figs. 2.7 to 2.15. Another aspect to note in the performance is the impact of reward combinations on the agent's learning in terms of convergence to the target RSRP (horizontal blue dashed line) and random fluctuations before and after convergence.

Analysis of various combinations of rewards in oUEs-based training reveals that without any assistance in terms of Jain's fairness index or GM (Rewards-200), the mean RSRP values exhibit random fluctuations and a longer convergence time. Additionally, this combination yields the lowest cumulative reward during training. This suggests that the reward process should include a fairness mechanism, such as the RSRP, GM (Rewards-201), to ensure that the overall mean values stick to the target after convergence. The outage compensation with JFI-based reward is shown with Rewards-210, which accelerates the convergence process but cannot reduce random fluctuations. Finally, the combination of Jain's fairness index and GM-based rewards (Rewards-211) balances convergence time and minimization of post-convergence fluctuations. Similar trends are observed for the average RSRP of sUEs; however, they fall short of their respective target because the cBS parameter training process is based only on oUEs.

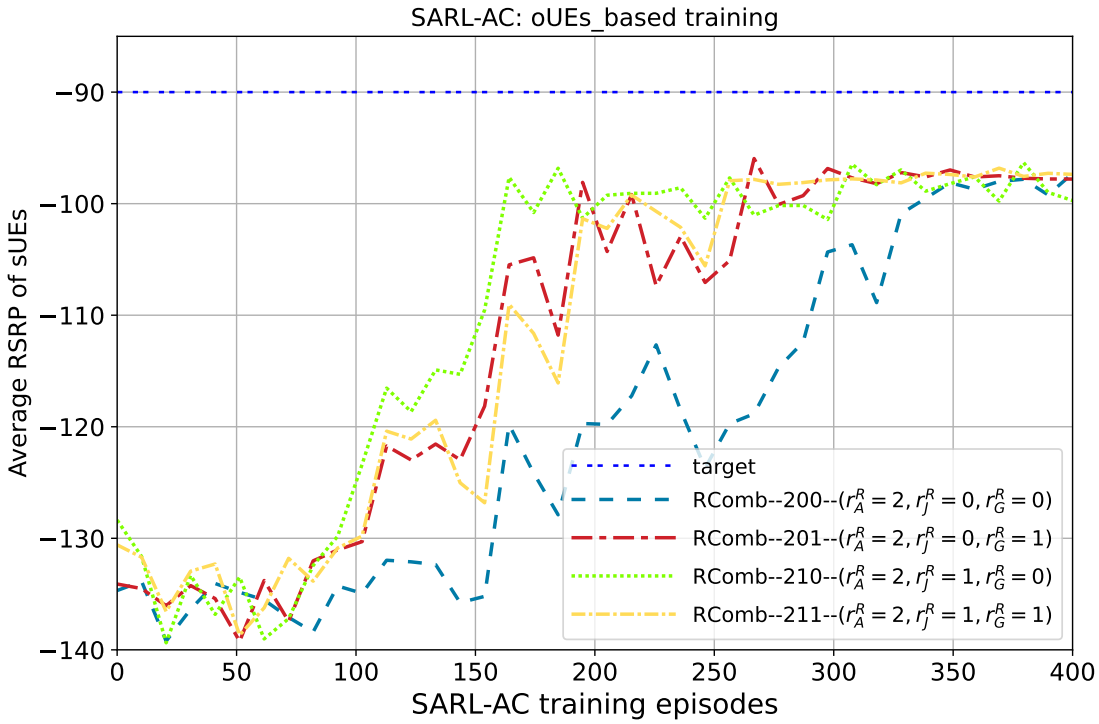


Fig. 2.9: Average RSRP variations for served users under various reward formulations utilizing arithmetic mean, geometric mean, and Jain's fairness index.

Compensation using SARL-AC cUEs-based training

The outage compensation progress with training based on cUEs (oUEs + sUEs) is given in Fig. 2.10, Fig. 2.11, and Fig. 2.12. Similarly to the previous case, here the cumulative rewards in all combinations of 4 are shown in Fig. 2.10 while their effects on the mean RSRP of oUEs and sUEs are shown in Fig. 2.11 and Fig. 2.12, respectively. These results show that cUEs-based training enables the agent to learn the best combinations of transmit power and antenna tilt values to ensure that not only are the oUEs compensated, but also that the reduction of the RSRP values of the sUEs is prevented. Furthermore, the results of different reward combinations are consistent with those discussed above in the oUEs-based training process. Therefore, it can be deduced from these results that cUEs-based training with a combination of a reward process using a deep actor-critic network can enable the compensation process that exhibits significant improvements in terms of RSRP

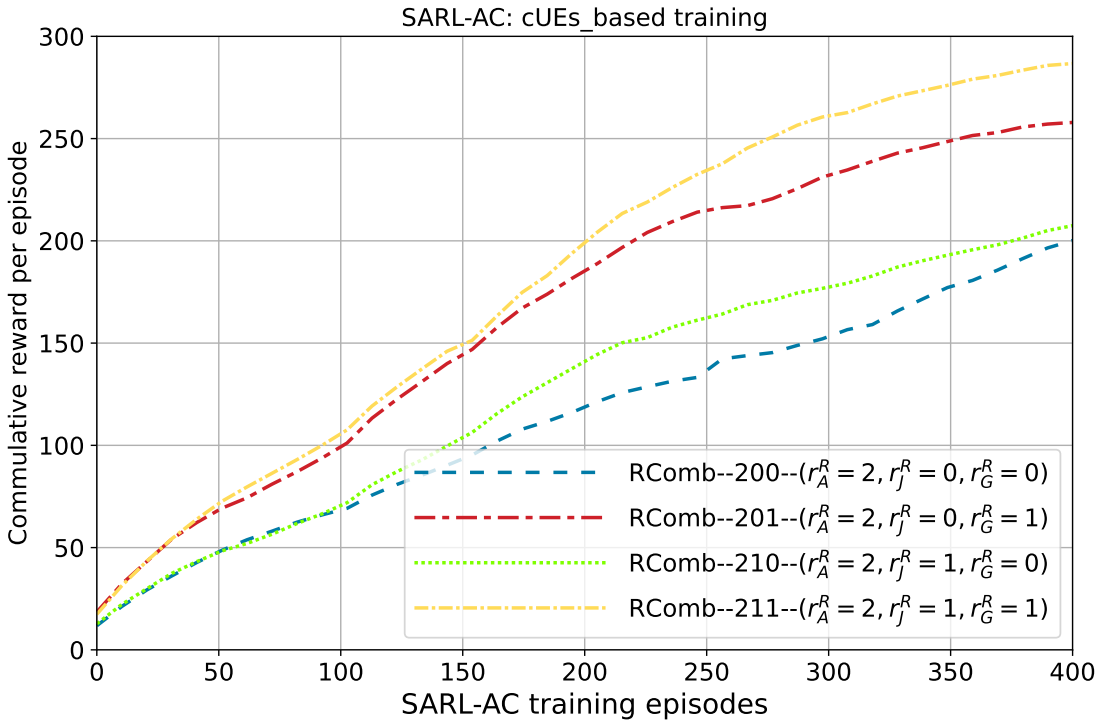


Fig. 2.10: Training of single-agent reinforcement learning rewards under different combinations of arithmetic mean, geometric mean, and Jain's fairness index.

of oUEs and a notable decrease in random fluctuations in their average values without causing any major drop in coverage of the sUEs.

The cumulative reward trends observed in Fig. 2.7 and Fig. 2.10 highlight key differences in the reinforcement learning training process based on the user sets considered. In Fig. 2.7, the RL training focuses exclusively on oUEs. The reward function components, arithmetic mean, geometric mean, and Jain's fairness index, are applied to this smaller, more homogeneous user set. The RL agent's objective is singular: to maximize coverage for oUEs by improving their RSRP. This focused scope simplifies the optimization process, enabling faster convergence to a stable policy. As a result, cumulative rewards stabilize within 400 training episodes. In Fig. 2.10, the RL training process includes both oUEs and already-served users, collectively referred to as cUEs. The reward function components (AM, GM, JFI) are now applied to this broader, more diverse user set. This introduces trade-offs

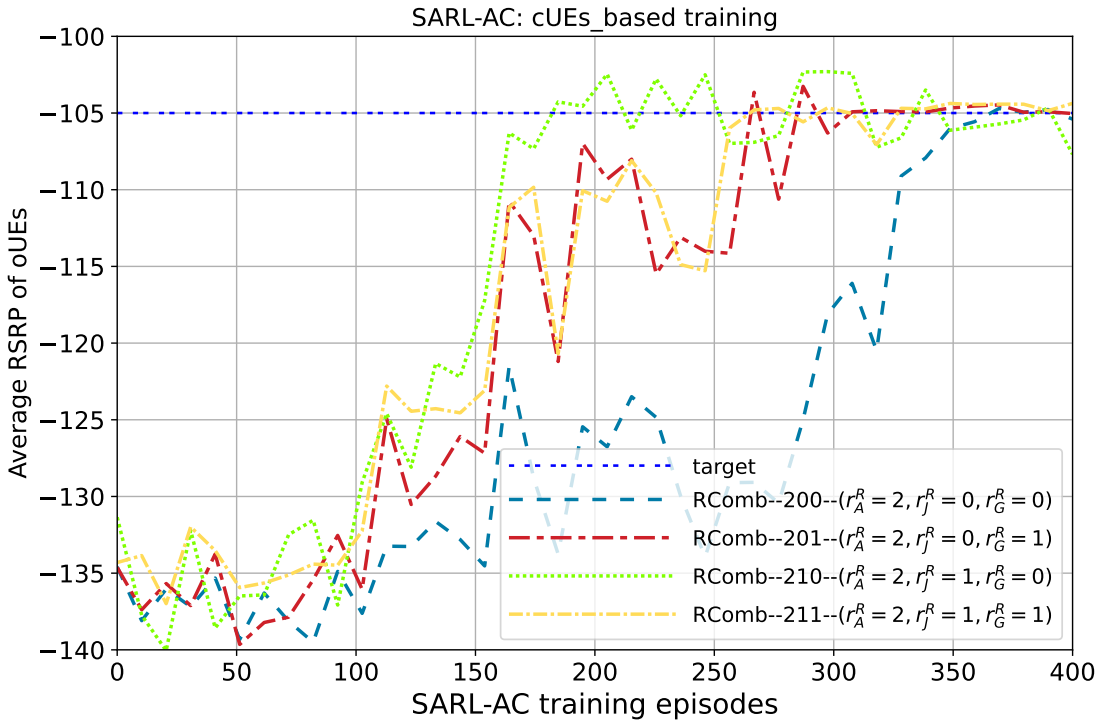


Fig. 2.11: Average RSRP variations for outage users under various reward formulations utilizing arithmetic mean, geometric mean, and Jain's fairness index.

between competing objectives: (1) the AM term seeks to improve the overall average RSRP for both oUEs and sUEs, (2) the GM and JFI terms promote fairness across all users, requiring the RL agent to balance signal quality between oUEs and sUEs.

These trade-offs make the optimization process more complex, requiring additional iterations to refine the policy. The gradual accumulation of rewards in Fig. 2.10 reflects this iterative balancing, as the RL agent adjusts its actions to improve coverage for oUEs without compromising fairness for sUEs. While cumulative rewards appear to grow continuously within the observed episodes, extending the training beyond 400 episodes would likely reveal clearer stabilization, similar to the pattern in Fig. 2.7. These trends align with the real-world challenges of dynamic cellular networks, where optimization must account for diverse and competing objectives to ensure balanced performance across user groups.

Using these results as the fundamental insight into the training process, we resort to the cUEs-based training with both GM and JFI-induced reward processes in the MARL-AC-based compensation process. The ability of the actor-critic framework to balance fairness and coverage in real-time is particularly beneficial in dense cellular environments, where excessive power adjustments can exacerbate inter-cell interference. Unlike static optimization techniques, AC-based compensation dynamically adjusts network parameters in response to real-time network conditions, ensuring that outage recovery does not degrade service quality for users who are already being served. These trends confirm that the AC-RL framework provides a scalable and fair solution for outage compensation in high-density deployments.

Compensation using MARL-AC cUEs-based training

The MARL-AC results are as follows: Three base stations face outage situations and are compensated by three cooperating base stations. The aim is to provide RSRP mean oUEs and sUEs closer to their respective targets. Outage users are divided equally among the compensating base stations based on proximity. The best possible compensating base station serves each outage user. Each cBS has its own set of sUEs, which, along with its assigned oUEs, form the set of cUEs. Each cBS uses its set of cUEs, JFI, and GM-assisted rewards for training. The training of each actor is decentralized, with three separate actor networks and one common critic network. The results of the MARL-AC using JFI and GM-based fairness approaches are shown in Fig. 2.13, Fig. 2.14, and Fig. 2.15. The training process, measured in terms of the rewards of the three agents that work together to bring all oUEs out of outage, is shown in Fig. 2.13. The impacts on RSRP of oUEs and sUEs are shown in Fig. 2.14 and Fig. 2.15, respectively. As shown in the figure, the distributed actors and the centralized critic approach aim to bring all compensating base stations to a common target, increasing the mean RSRPs of the respective users. The learning

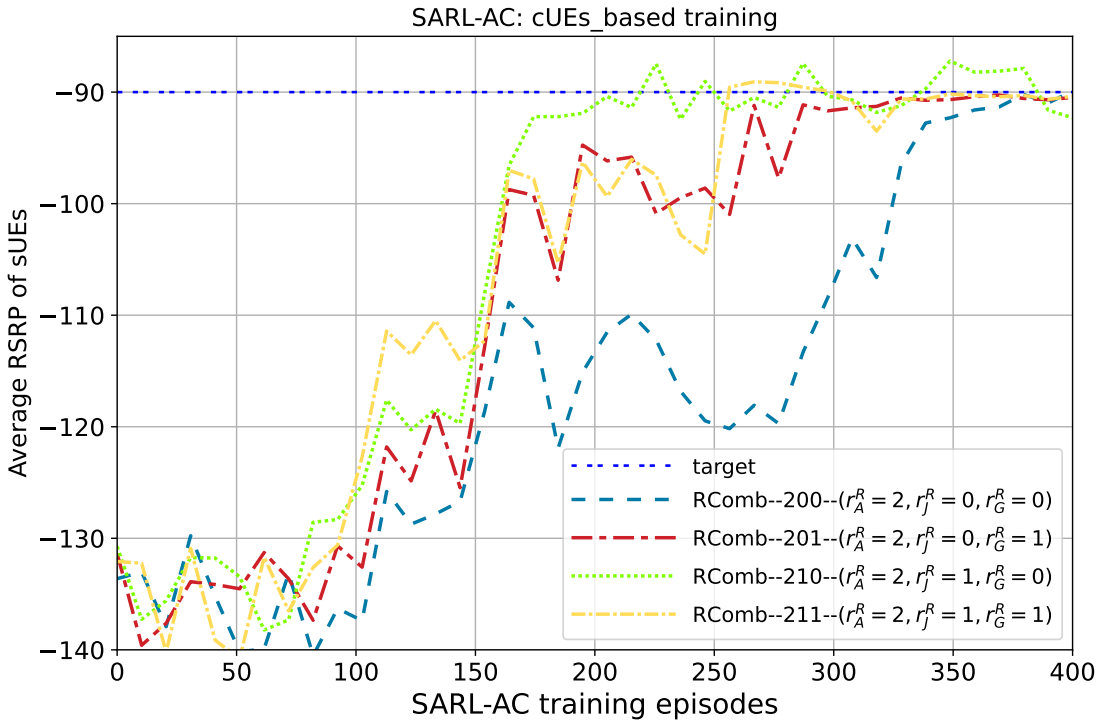


Fig. 2.12: Average RSRP variations for served users under various reward formulations utilizing arithmetic mean, geometric mean, and Jain's fairness index.

curve of each agent is different due to their actor network, but the common critic network balances out the differences in RSRPs. The fluctuating trends observed in Fig. 2.14 and Fig. 2.15 are characteristic of the cooperative-competitive dynamics in the MARL-AC framework, where multiple compensating base stations act as independent agents. These trends arise due to several factors:

1. **Exploration-Exploitation Trade-Off:** Each agent balances exploration and exploitation during training, which introduces variability as agents refine their policies.

2. **Multi-Agent Dynamics:** Agents independently optimize their local policies for their assigned users (cUEs = oUEs + sUEs) but are collectively evaluated by a centralized critic. These interactions occasionally lead to temporary trade-offs, such as when an action by one agent impacts the performance of others.

3. **Dynamic Network Environment:** Variations in user distributions, interference patterns, and target RSRPs require continuous policy adjustments, contributing to the observed fluctuations.

4. **Reward Function Complexity:** The inclusion of arithmetic mean, geometric mean, and Jain's fairness index in the reward function introduces competing objectives, requiring iterative refinement of agent policies.

Despite these fluctuations, the overall trends in Fig. 2.13, Fig. 2.14, and Fig. 2.15 indicate convergence, with cumulative rewards increasing steadily across episodes. The results demonstrate the MARL-AC framework's ability to effectively coordinate multi-agent policies, striking a balance between coverage and fairness in dynamic outage scenarios. In multi-agent environments, the need for adaptive and decentralized coordination further reinforces the selection of the actor-critic framework. By dynamically refining policies for each compensating base station while maintaining global stability through a centralized critic, MARL-AC effectively manages outage compensation across distributed agents. This scalability and adaptability are crucial advantages over alternative RL approaches.

Compensation Performance as Empirical CDFs

We discuss the compensation results in terms of the empirical cumulative distribution function of the normal and outage values of the RSRP. From these results, we compare the proposed SARL-AC with the autonomic particle swarm optimization algorithm to generate the compensation solution and the genetic algorithm schemes for both training approaches, as shown in Fig. 2.16 and Fig. 2.16. These results demonstrate the distribution of RSRP among oUEs and cUEs before and after compensation, providing insight into the proposed SARL-AC approach's ability to serve all oUEs affected by an outage.

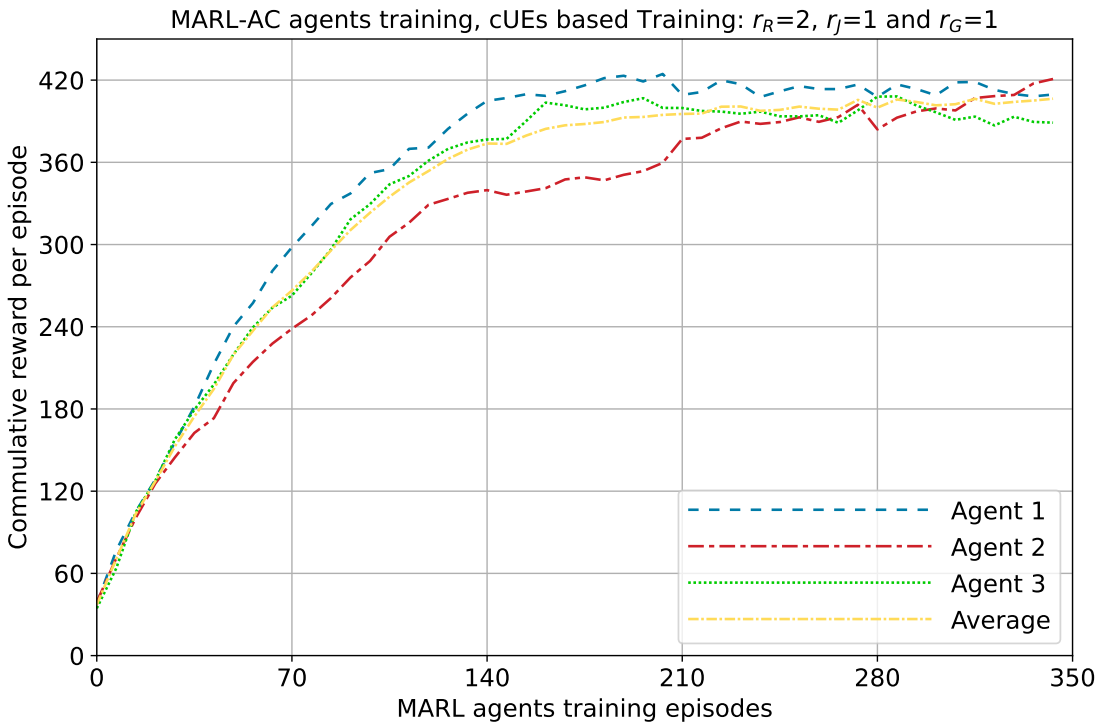


Fig. 2.13: Training process of multi-agent actor-critic reinforcement learning agents under different weight configurations ($r_R = 2$, $r_J = 1$, $r_G = 1$), demonstrating cumulative rewards per episode across all agents and their average.

Fig. 2.16 shows the cumulative distribution functions with oUEs-based training. The outage curve represents the range of RSRP values that cannot support users with acceptable quality of service. At the same time, the normal case is the original distribution of users before the outage, which should be met with an ideal compensation scenario. The results show that the proposed approach fairly compensates for the oUEs but cannot fully restore the normal case. However, the RSRP distribution of the compensation from the proposed scheme is higher than the autonomic particle swarm optimization algorithm and genetic algorithm schemes. It has less deviation due to the applied fairness approaches. Furthermore, in Fig. 2.16, similar compensation results are shown for cUEs-based training. The cUEs-based approach enhances the oUEs' coverage while retaining the sUEs' coverage, as confirmed by the cumulative distribution function curves of the SARL-AC. While heuristic methods provide effective parameter tuning, their static nature limits adaptability in rapidly

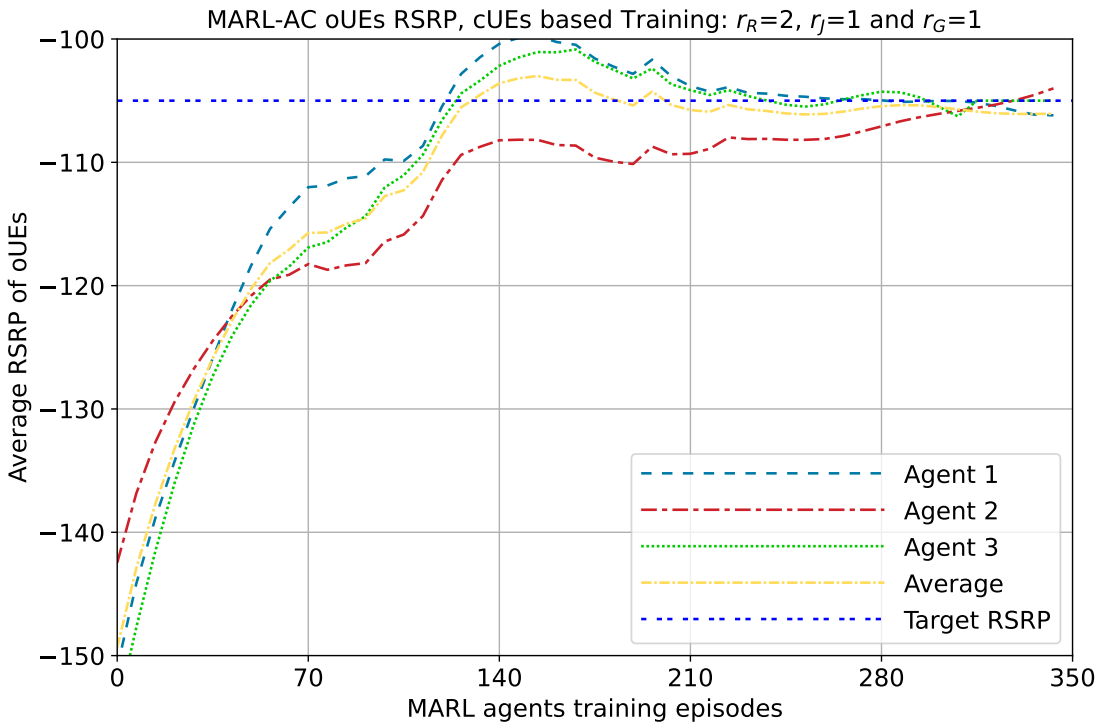


Fig. 2.14: The RSRP variations of outage users under multi-agent actor-critic reinforcement learning training with reward settings $r_R = 2$, $r_J = 1$, and $r_G = 1$.

evolving network conditions. The results demonstrate that reinforcement learning, particularly actor-critic-based compensation, provides a more responsive solution by continuously adjusting actions based on real-time feedback, thereby ensuring improved service recovery without requiring excessive manual tuning.

2.5.4 Time Complexity Comparison

In this sub-section, we discuss the comparison of the detection and compensation approaches in terms of training and prediction time, as given in Table 2.2. The time required for training the autoencoder-based detection is much longer than other schemes, despite its robustness to higher shadowing (Section 2.5.2). This, along with the high training data requirement, undermines its use as a first-choice detection approach. An unusual aspect is that the training time for KNN is less than the testing time, which is inherent in the KNN algorithm's operation. The time

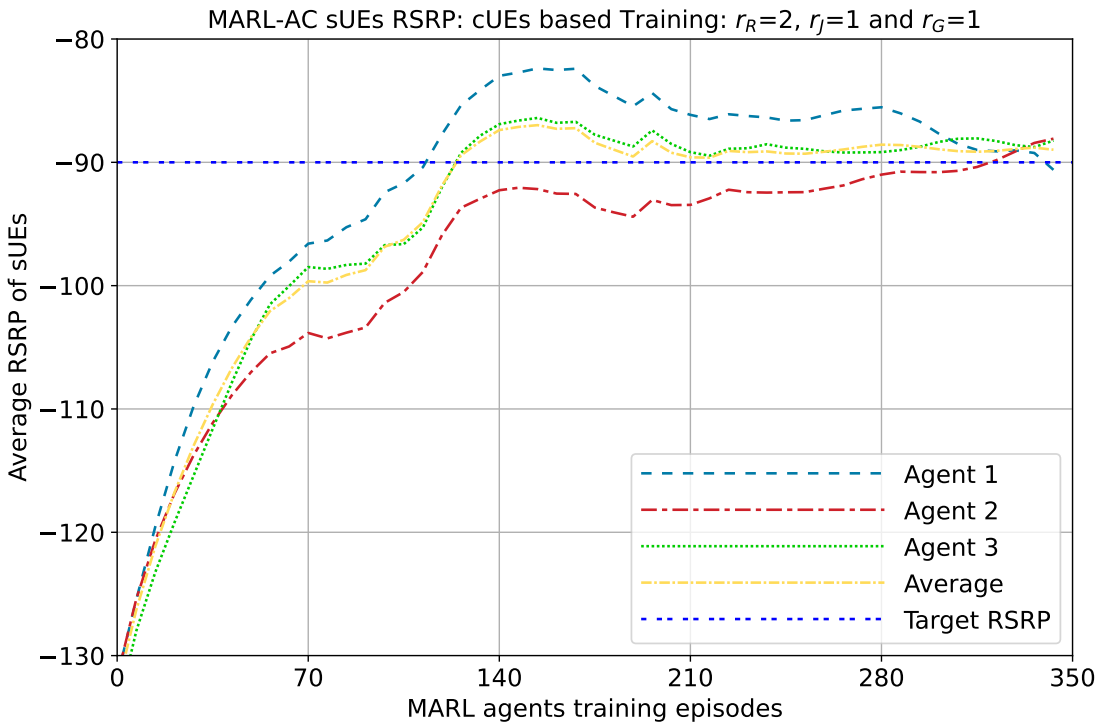


Fig. 2.15: The RSRP variations of served users under multi-agent actor-critic reinforcement learning training with reward settings $r_R = 2$, $r_J = 1$, and $r_G = 1$.

taken by Base-XGBoost is minimum among all the compared schemes, while OC-SVM also takes significantly less time. However, the performance of both schemes degrades with higher shadowing scenarios. The proposed Impv-XGBoost scheme requires about an order of magnitude longer training time than OC-SVM and Base-XGBoost, and similar to KNN, but significantly less than the autoencoder scheme.

A time complexity comparison is also presented for our proposed outage compensation cases. The time required to compensate for the cUEs-based solution is approximately twice that required in the oUEs-based training for each reward combination. The reward combination of 201, invoked by the geometric mean, requires the maximum time in both oUEs-based and cUEs-based training. The JFI-based reward shown by 210 reduces the training time, getting the minimum values in both training cases. The joint work of JFI and geometric mean again requires more training time. With a similar reward combination of 211, the time required for cUEs-based

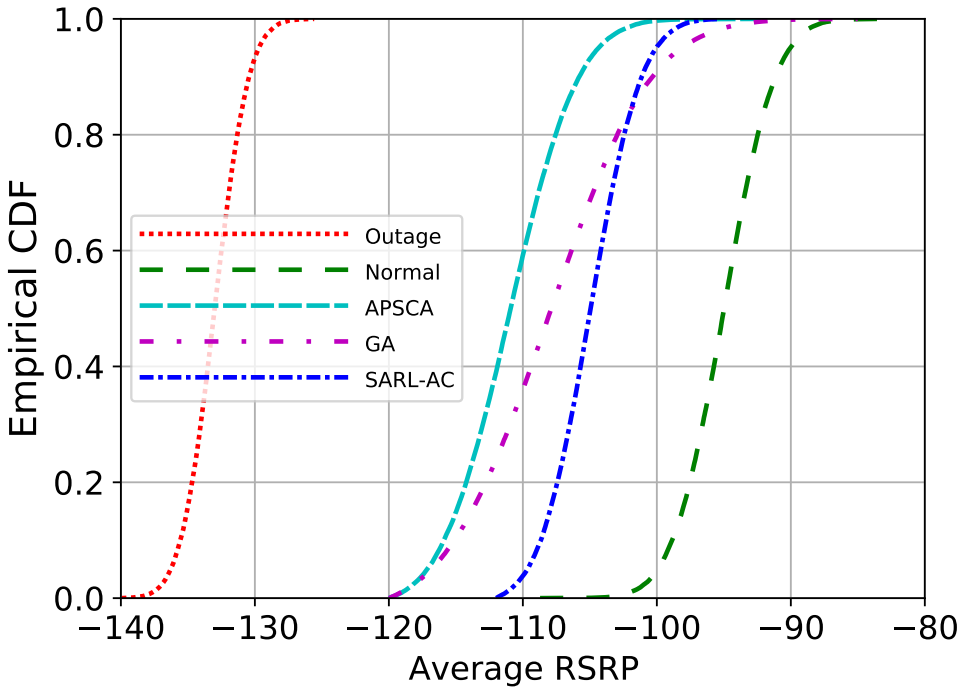


Fig. 2.16: Cumulative distribution of the reference signal received power for the outage users under multi-agent actor-critic reinforcement learning training.

training in MARL-AC is shown in the last row of Table 2.2. It should be noted that although multiple agents will work simultaneously in a real network, in simulation settings, our 3 agents' computations are performed in sequence. Hence, this time of 314.7749 seconds is the total time taken by all three agents to get trained on the cUEs, with a common critic. The MARL-based solution would compensate for multiple base station outages much earlier than the SARL counterparts.

2.5.5 Advantages and Limitations of the Proposed Schemes

The proposed schemes for outage detection and compensation offer several significant advantages, as well as some limitations. Therefore, in this section, we discuss some of the important advantages and disadvantages of the proposed scheme. Also, we discuss the potential impact of the advantages and possible mitigation approaches for the limitations.

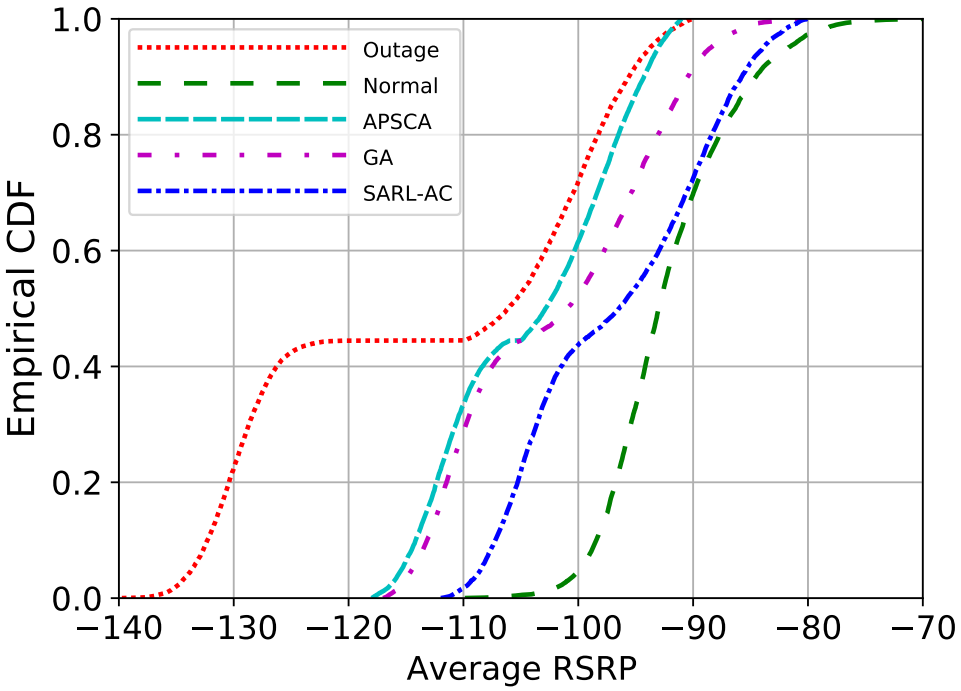


Fig. 2.17: Cumulative distribution of reference signal received power for served user equipment under multi-agent actor-critic reinforcement learning training.

Advantages of the Proposed Scheme

The benefits of the proposed approach, outlined below, demonstrate the effectiveness and innovation in managing network outages in dense heterogeneous networks [58].

- **Integrated Outage Detection and Compensation Framework:** Our approach integrates detection and compensation into a cohesive framework, which enhances the overall efficiency and responsiveness of the network by ensuring that both detection and compensation processes work seamlessly together. By addressing outages promptly and efficiently, the framework improves the reliability of the network, reducing downtime and maintaining service quality for users.

- **Robustness to High Shadowing and Sparse Data:** The use of an en-

hanced XGBoost model (Impv-XGBoost) for the cell outage detection provides robustness against high shadowing environments and sparse data conditions, which ensures accurate detection in challenging conditions where traditional methods may falter. The ability to accurately detect outages in challenging environments enhances the overall reliability of the network and improves user satisfaction.

- **Fairness and Rapid Convergence for the Cell Outage Compensation:** Our cell outage compensation approach incorporates a sophisticated reward mechanism that includes the arithmetic mean, geometric mean, and Jain's fairness index. This mechanism ensures fair resource allocation and rapid convergence of the learning process. By promoting fairness among users and ensuring quick adaptation to network changes, the proposed scheme enhances the user experience and maintains high levels of service quality.

- **Handling Multiple Base Station Failures:** The proposed framework employs multi-agent reinforcement learning by adopting the decentralized actors and a common critic to effectively handle the multiple base station failures. This approach balances cooperation and competition among agents to optimize network performance. The ability to manage multiple failures concurrently ensures that the network remains stable and operational, even in the face of significant disruptions.

Disadvantages of the Proposed Scheme

While the proposed scheme offers numerous advantages, it is important to acknowledge certain limitations. These challenges are inherent to the complexity and innovation of the approach [10]. We summarize the disadvantages and propose mitigation strategies that might be adopted in future works:

Table 2.2: Training and testing time comparison for different outage detection algorithms (OC-SVM, AE, KNN, Base-XGBoost, Impv-XGBoost) and compensation schemes (SARL-oUEs, SARL-cUEs, MARL-cUEs) with reward variations.

Simulation Type	**Detection Scheme**	**Training Time (s)**	**Testing Time (s)**
Detection	OC-SVM	0.0089	0.0039
	AE	57.3	0.072
	KNN	0.0108	0.0466
	Base-XGBoost	0.0015	0.0014
	Impv-XGBoost	0.0194	0.0197
Compensation	**Compensation Scheme**	**Rewards (A, J, G)**	**Compensation Time (s)**
	SARL-oUEs-based	200	112.3894
		201	114.2807
		210	104.4338
		211	105.6720
	SARL-cUEs-based	200	229.1495
		201	238.5766
		210	182.0938
		211	192.1008
	MARL-cUEs-based	211	314.7749

- **Computational Complexity:** The integrated framework and advanced machine learning models increase the computational complexity of the system. This complexity may require more powerful hardware and longer processing times, which could be a limitation in resource-constrained environments. To address this, optimization techniques and hardware accelerators can be employed to enhance processing efficiency. Additionally, techniques such as model pruning, quantization, and efficient neural network architectures (e.g., MobileNets) can reduce the computational load. Future work will explore these optimization strategies in more detail to ensure the framework can be

efficiently deployed in various environments.

- **Data Dependency:** The effectiveness of the proposed scheme relies on the availability of high-quality minimization of the drive test data for training and evaluation. In environments where data collection is limited or challenging, the performance of the scheme may be affected. Data augmentation techniques and transfer learning can be employed to enhance the robustness of models in data-scarce scenarios. By augmenting existing data with synthetic samples or leveraging pre-trained models on related tasks, the need for extensive data collection can be minimized. Future research will focus on developing robust data augmentation and transfer learning methods to enhance model performance in data-limited settings.

- **Implementation Complexity:** Implementing the proposed scheme in real-world networks involves significant complexity, including integration with existing network management systems and ensuring compatibility with diverse hardware and software environments. To address this issue, a phased implementation approach, starting with pilot projects and incremental integration, can help manage complexity and ensure smooth deployment. Initial pilot studies can provide valuable insights into potential integration challenges, allowing for iterative improvements. Future work will aim to develop detailed implementation guidelines and best practices to facilitate the smoother integration of these systems into operational networks.

While the identified disadvantages highlight some of the challenges associated with the proposed scheme, they also provide opportunities for future research and development. Addressing these challenges is beyond the current scope of this paper, but they represent important areas for future exploration. By acknowledging these limitations and proposing mitigation strategies, we demonstrate a comprehensive

understanding of the potential hurdles and a commitment to enhancing the practicality and effectiveness of our approach in future studies.

2.6 Conclusion and Transition to Next Chapter

In this chapter, we presented a robust AI-driven framework for cell outage management in emerging wireless networks. The proposed solution comprises two core components: an enhanced artificial intelligence-based cell outage detection scheme and a reinforcement learning-based compensation strategy. The detection component leverages an optimized XGBoost algorithm, termed Impv-XGBoost, which is fine-tuned for high-shadowing and sparse-data conditions commonly encountered in real-world deployments. This enhancement improves classification accuracy while reducing training complexity, enabling more reliable detection of outage events.

For outage compensation, we employed actor-critic reinforcement learning strategies in both single-agent and multi-agent settings to address single and multiple base station failures, respectively. The reward structure integrates the geometric mean and Jain's fairness index of the reference signal received power values for both outage-affected users and served users, ensuring fairness and performance stability. The geometric mean promotes reward smoothness during learning, while the fairness index accelerates convergence and enhances equitable resource distribution. We also investigated hybrid reward formulations incorporating arithmetic mean components to balance learning responsiveness with stability.

The analysis and evaluations in this chapter assume that the minimization of drive test data and user positions is accurately reported, a simplification that may not hold in real-world networks. In practice, minimization of drive test reports and user positioning is prone to errors due to signal fluctuations, sensor inaccuracies, and environmental variability. These errors can lead to suboptimal compensation

decisions, increased interference, and a reduction in overall network resilience. The implications are particularly severe in emerging user-centric architectures, where accurate localization of users and base stations is foundational to effective operation.

Motivated by these challenges, the next chapter shifts focus toward quantifying and mitigating the effects of user and base station positioning inaccuracies. It examines how such inaccuracies impact key performance indicators and proposes a data-driven framework to reduce performance loss through time-series forecasting and residual modeling. This progression builds upon the resiliency theme introduced here, extending it to consider real-world imperfections in network observability and control.

CHAPTER 3

AI Methods for Network Resilience against Positioning Errors

This chapter investigates the impact of positioning errors in user-centric ultra-dense networks and presents data-driven methodologies to mitigate their effects. The proposed approaches leverage machine learning-based optimization techniques, including residual learning and time-series forecasting, to enhance network resilience against localization inaccuracies. Through systematic analysis and simulations, we demonstrate how intelligent compensation techniques can significantly improve network performance under uncertain positioning conditions.

3.1 Introduction

Wireless and mobile networks operate at a massive scale, providing connectivity to millions of users. To ensure an optimal user experience, networks must be designed with a user-centric focus, not only in terms of marketing strategies but also in their fundamental architectural design [14]. user-centric ultra-dense networks evolve from ultra-dense networks by shifting from a base station centric model to a flexible, adaptive service provisioning paradigm. This transition eliminates cell-edge users and dynamically forms service zones based on real-time user distribution [88].

The effectiveness of user-centric ultra-dense networks depends on the accurate positioning of user equipment and data-base-stations to dynamically allocate resources and form Szones. However, practical deployments suffer from positioning inaccuracies due to errors in the global positioning systems, signal propagation distortions,

and sensor noise. These errors distort the association of the user to the data-base-station, increase interference, and degrade key network performance indicators such as area spectral efficiency and energy efficiency [89]. The ability to compensate for these inaccuracies is critical to maintaining optimal network performance.

3.1.1 Background and Motivation

The concept of user-centric ultra-dense networks builds upon the centralized radio access network architecture, where a central controller dynamically activates remote radio heads to serve users [88]. Unlike macro-cellular networks, where base stations serve predefined geographic regions, user-centric ultra-dense networks optimize service delivery in real time based on user location. This flexibility leads to significant gains in spectral efficiency, energy efficiency, and quality of service [15].

However, user-centric ultra-dense networks assume that the central controller has precise knowledge of user and data-base-station locations to form non-overlapping Szones and activate the most suitable data-base-station. In reality, every positioning technique, including global positioning systems and network-based localization, introduces inaccuracies [16, 17]. Even minor deviations in location data lead to erroneous data-base-station activations, inefficient power allocation, and increased interference.

The growing complexity of network configurations further compounds the challenge. With the proliferation of AI-driven network management, data-driven approaches are being employed to predict faults, model user mobility, and optimize resource allocation [19,90]. While most artificial intelligence applications have been focused on base-station-centric networks, user-centric ultra-dense networks introduce additional challenges, as erroneous positioning can misguide AI-based decision-making [91].

3.1.2 Importance of Accurate Positioning in UUDNs

In the context of user-centric ultra-dense networks, accurate location information is paramount. The user-centric architecture with flexible service zones is gaining recognition due to its promising benefits, such as lower interference, improved area spectral efficiency, and better quality of experience by eliminating cell-edge users [15, 92]. These benefits are realized by serving users within non-overlapping, flexible service zones tailored to their specific service requirements. The Szone of a user-centric ultra-dense network and the activation of a serving data-base-station are controlled by a central controller, which requires accurate user equipment and data-base-station location information for efficient network operation and resource allocation.

While accurate location information is also necessary for BS-centric networks in tasks involving network automation and zero-touch automation, its importance increases in user-centric ultra-dense networks. Even a slight error in the position of the user or the data-base-station can result in scheduling users that are close to each other or activating data-base-stations that are far from the users. Both scenarios can lead to high interference, which can have a detrimental impact on network performance. Therefore, in real-world user-centric ultra-dense networks, where the central controller may not have access to error-free locations of all users and data-base-stations, the use of artificial intelligence and machine learning techniques to compensate for imperfect location information is essential for its data-driven operations [93, 94].

3.1.3 Challenges in User-Centric Ultra-Dense Networks

Positioning inaccuracies introduce several fundamental challenges in user-centric ultra-dense networks. One key issue is Szone formation, where the central con-

troller determines the optimal Szone radius (R_s) for each active user, ensuring non-overlapping service regions [88]. However, errors in reported user locations can lead to unintended Szone overlap, causing interference, or undersized Szones, leading to coverage gaps. Another major challenge is the association of the user with the data-base-station. Ideally, each user should be assigned to the closest and most suitable data-base-station. However, positioning errors often result in users being associated with a suboptimal data-base-station, increasing path loss, reducing signal quality, and degrading network throughput [94]. Interference management becomes increasingly complex under localization inaccuracies. Misalignment of service zones due to erroneous user and data-base-station positions increases inter-cell interference, reducing spectral efficiency [95]. Traditional interference mitigation strategies rely on accurate user positions, rendering them ineffective in the presence of significant positioning errors. Finally, network energy efficiency is directly affected by erroneous positioning. When incorrect association of user to data-base-station leads to unnecessary data-base-station activations, the network wastes transmit power, reducing energy efficiency [96]. Without error compensation, user-centric ultra-dense networks operate at suboptimal configurations, resulting in increased power consumption and failing to meet spectral efficiency targets.

3.1.4 Existing Works and Research Gap

The characterization of the impact of positioning errors in traditional base-station-centric networks has been conducted in several studies. The authors in [16] analyze how errors in user positions affect cell-edge reliability and coverage probability under different environmental conditions. This work was extended in [17] to incorporate the effects of base station positioning errors, demonstrating the degradation of coverage estimation when geographical inaccuracies are present. Similarly, [95] investigates how erroneous positioning affects signal-to-interference ratio, revealing

that higher base station density exacerbates the degradation in the area spectral efficiency. The authors in [18] examine the relationship between positioning error and quantization loss in coverage estimation, showing that an optimal bin width can mitigate their combined effects.

While these studies provide a solid foundation for understanding localization inaccuracies in traditional networks, they assume fixed service areas and do not account for the dynamic service zones of user-centric ultra-dense networks. Existing user-centric ultra-dense network-focused works [15, 97] demonstrate the benefits of user-centric architectures but assume perfect location knowledge for the user and data-base-station. This assumption does not hold in practical deployments, where errors in the global positioning system, sensor noise, and propagation uncertainties introduce significant localization inaccuracies.

Artificial intelligence and machine learning based approaches have been proposed for network optimization in various contexts, including predictive mobility management [90], data-driven fault diagnosis [19], and network resource allocation [91]. Some studies apply AI techniques in user-centric network settings. For example, K-way clustering is utilized in [93] to optimize code-book allocation, minimizing interference while maximizing throughput. In [98], a deep residual learning model is used for cooperative beamforming in user-centric networks, while [94] explores machine learning based interference approximation for spectrum sensing. However, these works focus on resource allocation and network configuration rather than compensating for localization errors.

Thus, while several efforts have characterized positioning errors and introduced AI-driven optimizations, a significant gap remains in developing a unified, data-driven framework that jointly models positioning errors and compensates for their impact on network performance. This chapter addresses this gap by integrating machine learning-based residual learning, time-series forecasting, and optimization-

based compensation strategies.

3.1.5 Key Contributions of This Chapter

The increasing reliance on user-centric, AI-driven wireless architectures demands robust mechanisms to compensate for real-world localization inaccuracies. This chapter presents a comprehensive framework for mitigating the impact of positioning errors in user-centric ultra-dense networks, integrating data-driven modeling, machine learning-based residual learning, and time-series forecasting to enhance network resilience against localization uncertainties. By systematically addressing performance degradation, resource misallocation, and interference management, this work extends both analytical and AI-based network optimization approaches to improve spectral and energy efficiency in user-centric deployments.

The main contributions of this chapter are as follows:

- **A Unified Data-Driven Framework for Positioning Error Compensation:** This work introduces a comprehensive framework that integrates multiple artificial intelligence driven approaches to mitigate the impact of positioning errors in user-centric ultra-dense networks. The proposed solution systematically combines synthetic data generation, time-series forecasting, and machine learning-based optimization to develop a unified methodology for minimizing performance degradation. By addressing both the direct and residual impacts of positioning errors, this framework enables user-centric ultra-dense networks to function efficiently despite localization uncertainties.

- **Simulation-Based Characterization of Positioning Errors in UUDNs:** A 3GPP-compliant 5G system-level simulator is used to model user-centric ultra-dense networks under both ideal and erroneous positioning conditions [16]. The simulations generate two types of databases by capturing relationships

between (1) Underlaying Error Radius (UER) and (2) Configuration and Optimization Parameter (COP)s as inputs and the key performance indicators as the outputs. The characterization quantifies how increasing localization errors affect overall network performance, providing valuable insights for compensation strategies.

- **Time-Series Forecasting for Positioning Error Compensation:** To anticipate and mitigate the adverse effects of positioning inaccuracies, a forecasting-based approach is developed, leveraging seasonal auto-regressive integrated moving average-based statistical modeling and MLP regression to predict key performance indicator variations under different levels of localization error [99]. This predictive capability enables real-time network adaptation, ensuring robust user-centric ultra-dense network operation despite inaccurate user equipment and data-base-station location data.

- **Proposed Data-Driven Optimization and Error Compensation (DD-OEC) Framework:** A novel automated machine learning based model is developed to learn the residual error between ideal and erroneous network configurations. The framework refines network parameter selection by leveraging historical error-free configurations, enabling compensatory adjustments to transmit power, Szone radius, and data-base-station density. By integrating machine learning based residual learning with multi-objective optimization techniques, the framework dynamically compensates for positioning errors to restore optimal performance.

- **Comparative Performance Evaluation with Baseline Approaches:** The proposed data-driven optimization and error compensation framework is extensively evaluated against baseline error-agnostic optimization schemes. Simulation results demonstrate that the framework significantly improves the area spectral efficiency and energy efficiency, reducing the performance degra-

dation caused by localization inaccuracies by up to 23% compared to conventional approaches. The findings establish the necessity of incorporating error-aware optimization strategies in real-world user-centric ultra-dense deployments.

- **Broader Impact and Future Implications:** Beyond addressing positioning errors in user-centric ultra-dense networks, the proposed framework contributes to the broader field of AI-driven wireless network optimization. The methodologies developed in this work can be extended to other dynamic network challenges, such as mobility-aware resource allocation, zero-touch automation network architectures, and interference-aware scheduling. The integration of machine learning and data-driven models with traditional network optimization frameworks sets the foundation for future advancements in intelligent, resilient, and adaptive wireless networks.

3.1.6 Organization of the Chapter

The remainder of this chapter is structured as follows. Section 3.2 introduces the system model and synthetic data generation framework, covering network architecture, user and data-base-station distribution, service zone formation, and channel modeling. It also defines the configuration optimization parameters and key performance indicators. Also, details the synthetic data generation methodology, including the creation of UER-KPI and COP-KPI databases. The section further discusses how positioning errors influence network performance and explains the motivation behind error modeling. The proposed approaches for error compensation are discussed in Section 3.3. It covers time-series forecasting for error minimization, including seasonal auto-regressive integrated moving average-based prediction and multi-layer perceptron regression for the recovery of key performance indicators. Additionally, a data-driven optimization and error compensation framework

is introduced, integrating automated machine learning based residual error learning and multi-objective optimization. Section 3.4 presents the simulation setup and performance evaluation. The effectiveness of machine learning based compensation techniques is analyzed, along with a comparative study of seasonal auto-regressive integrated moving average and multi-layer perceptron models. The section also evaluates optimization frameworks such as simulated annealing and genetic algorithms. Finally, Section 3.5 summarizes key findings, identifies open research challenges, and transitions to the next chapter.

3.2 System Model & Synthetic Data Generation

This section presents the system model used for user-centric ultra-dense networks, including network architecture, channel modeling, and the interplay between configuration and optimization parameters and key performance indicators. Additionally, we describe the methodology for generating synthetic data, which serves as the foundation for modeling positioning errors and performance analysis.

3.2.1 Network Architecture and Channel Model

The user-centric ultra-dense network model considered in this work consists of a dense deployment of data-base-stations and user equipment within a given network area. Unlike conventional base-station-centric architectures, the user-centric ultra-dense network employs a flexible Szone-based approach, where resource allocation dynamically adapts to user distribution and traffic demand. The spatial placement of users and base stations is modeled as a stationary Poisson point process, ensuring a stochastic representation of their locations. The densities of data-base-stations and users are denoted by λ_{DBS} and λ_{UE}, respectively. The network assumes an ultra-dense deployment scenario, where the data-base-station density is compara-

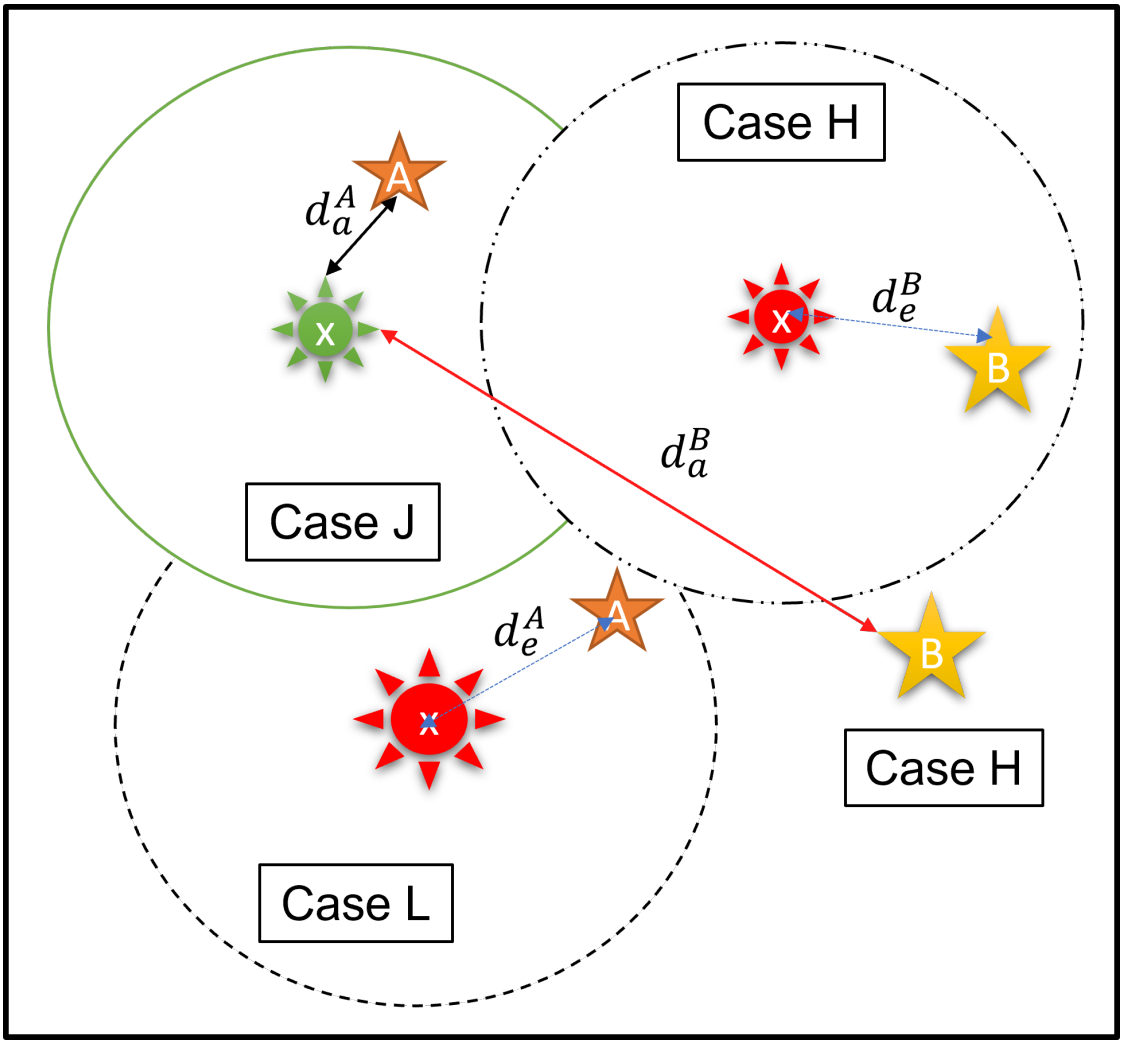


Fig. 3.1: Modeling the positioning errors experienced by devices in user-centric ultra-dense networks depicting different scenarios across typical operating cases.

ble to or higher than the user density. A macro base station acts as the central controller, coordinating network resource allocation, scheduling users, and dynamically adjusting service zone parameters to optimize system performance.

User and DBS Distribution

User-centric ultra-dense network follows an independent stationary Poisson point process for the spatial distribution of users and database stations. Given the density parameters λ_{UE} and λ_{DBS}, the users and data-base-stations are randomly distributed across the network area. The average number of users within the network can be

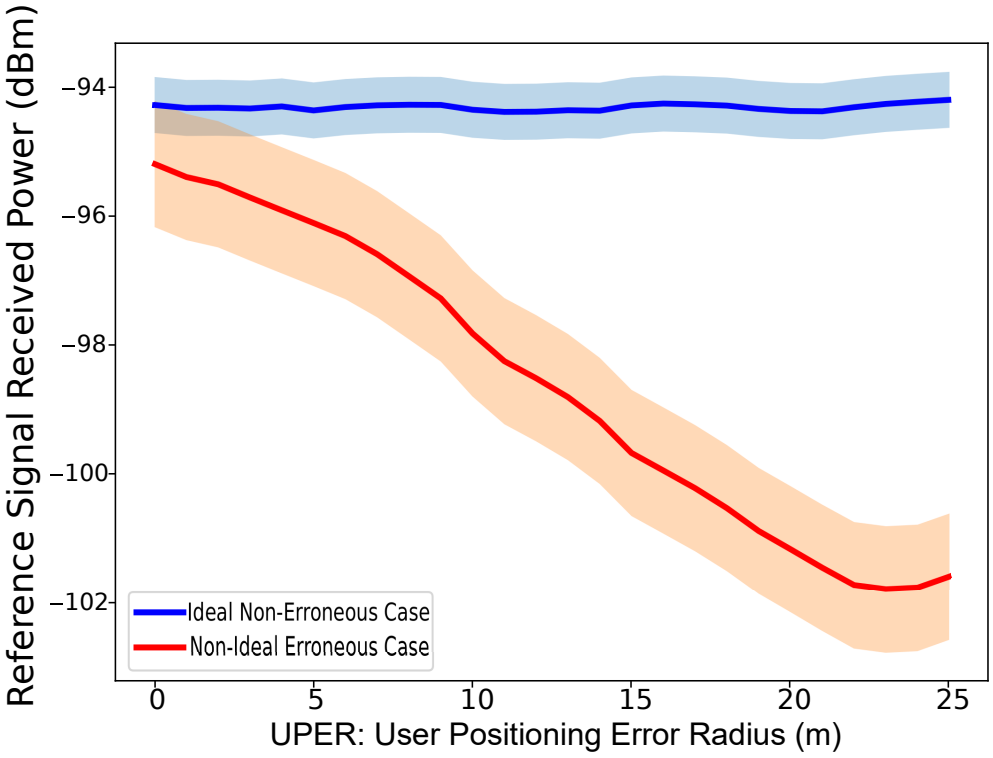


Fig. 3.2: RSRP decrease against user positioning error radius, depicting its negative impact on an important key performance indicator under consideration.

characterized by $\lambda_{\text{UE}}A$, where A represents the total coverage area.

To model scheduled users, we utilize the Matern hard core type II thinning process, which ensures that users are served within non-overlapping service zones. This thinning process refines the initial random user distribution to select a subset of scheduled users per transmission time interval, where each scheduled user forms the center of its respective Szone. The Szone radius, denoted by R_{sz}, defines the coverage of each data-base-station. The number of data-base-stations in a given Szone is characterized by its density and the Lebesgue measure of a circular disc with radius R_{sz}, given as $\lambda_{\text{DBS}}\pi R_{\text{sz}}^2$.

Each data-base-station is equipped with a single omnidirectional antenna and transmits with a fixed power level P_t, which the central controller controls. The data-base-station serving a given user is selected based on the highest reference signal

received power within a Szone of the user. If multiple data-base-stations fall within R_{sz} of a user, the data-base-station with the best channel conditions is assigned to serve that user.

Service Zone Formation and Scheduling

A fundamental feature of UUDNs is the formation of virtual, non-overlapping Szones around the scheduled users. The central controller ensures that the minimum distance between two scheduled users is at least $2R_{\text{sz}}$, preventing inter-Szone interference. If two users are found to be closer than this threshold, they are scheduled in separate transmission time intervals based on a priority-based scheduling algorithm.

The scheduling process follows a dynamic time-division multiple access approach, where each user is assigned a transmission slot within its transmission time interval. The priority assignment for users is based on multiple factors, including traffic demand, quality of service requirements, and network load conditions. If a user does not have a data-base-stations within its designated Szone, the network can dynamically adjust and increase R_{sz} to accommodate disadvantaged users, ensuring seamless connectivity.

After scheduling, the data-base-station activation is determined by selecting the highest reference signal received signal data-base-station within the Szone of each scheduled UE. The system operates under an interference-limited regime, where the impact of thermal noise is negligible compared to inter-cell interference. This scheduling and activation mechanism ensures optimal resource utilization while mitigating interference effects.

Channel Model

The wireless channel between a user and its associated data-base-station is modeled as a combination of large-scale path loss and small-scale fading effects. The signal power attenuation is governed by a two-slope path loss model with log-normal shadowing, which accurately captures propagation characteristics in ultra-dense environments.

The path loss for a given user to data-base-station link at distance d is expressed as:

$$PL(d) = PL_0 + 10\alpha \log_{10}(d) + X_\sigma, \tag{3.1}$$

where:

- PL_0 is the reference path loss at a distance of 1 meter,
- α is the path loss exponent, which varies based on the propagation environment,
- d is the distance between the user and the serving data-base-station,
- X_σ represents log-normal shadowing with standard deviation σ.

For small-scale fading, we assume Rayleigh fading with an exponentially distributed amplitude. The received signal power at the user is given by:

$$P_r = P_t G_t G_r |h|^2 d^{-\alpha}, \tag{3.2}$$

where:

- P_t is the transmit power of the data-base-station,
- G_t and G_r are the antenna gains of the transmitter and receiver, respectively,

- h is the complex fading coefficient, following a Rayleigh distribution.

A key aspect of this study is the incorporation of positioning errors in the channel model. In practical deployments, the estimated positions of users and data-base-stations often deviate from their actual locations due to inaccuracies from the global positioning system, localization algorithm errors, and environmental obstructions [17]. To model these inaccuracies, we define an underlying error radius, which represents the difference between the actual and estimated positions of users and data-base-stations.

Each user and data-base-station is assumed to be randomly located within a circular region of radius r_{err} around its estimated position. This deviation introduces discrepancies in:

- User to data-base-station association, leading to suboptimal link selection,
- Path loss and interference estimation, affecting network-wide resource allocation,
- Szone formation, resulting in potential overlapping service zones and scheduling conflicts.

For every scheduled user to data-base-station pair, the corresponding key performance indicators (area spectral efficiency, energy efficiency, and interference metrics) are computed based on the actual channel conditions while maintaining a database of error-influenced channel realizations. This database serves as a foundation for further data-driven error compensation mechanisms, which are explored in later sections.

3.2.2 Network Parameters and Performance Indicator

In user-centric ultra-dense networks, network performance is influenced by several system-level parameters that require careful tuning to optimize spectral and energy efficiency. These parameters, known as configuration optimization parameters, determine how network resources are allocated and how different performance metrics are affected. The relationship between configuration parameters and key performance indicators is fundamental to optimizing network operations.

Configuration Optimization Parameters

The primary configuration parameters in user-centric ultra-dense networks include:

- ***DBS Density (λ_{DBS}):*** The density of data-base-stations directly impacts network spectral efficiency and interference levels. A higher λ_{DBS} leads to reduced user to data-base-station distances, potentially enhancing signal quality but increasing inter-cell interference.

- ***Service Zone Radius (R_{sz}):*** The radius of a Szone defines the area within which a DBS can serve a user. A larger R_{sz} allows a user to connect with more data-base-stations, increasing connectivity options but potentially leading to overlapping Szones, which degrade spectral efficiency.

- ***Transmit Power (P_t):*** The transmission power of data-base-stations determines signal strength and coverage. Increasing P_t improves link quality but raises interference and power consumption.

- ***Threshold Parameters:*** The system employs reference signal received power and signal-to-interference ratio thresholds to regulate coverage probability and spectral efficiency. These thresholds influence the user to data-

base-station association, determining whether a data-base-station can reliably serve a user.

The values of these configuration and optimization parameters must be carefully optimized to achieve an optimal balance between spectral efficiency, energy efficiency, and interference mitigation.

Key Performance Indicators

The performance of user-centric ultra-dense networks is evaluated using multiple key performance indicators. The most critical key performance indicators considered in this work are:

- ***Area Spectral Efficiency:*** The performance indicator quantifies spectral resource utilization efficiency by measuring the number of bits transmitted per unit bandwidth per unit area. It is mathematically defined as:

$$\theta_{\mathrm{SE}} = \frac{1}{A} \sum_{\forall x \in \mathbb{U}} \log_2(1 + \gamma_x), \tag{3.3}$$

  where $\mathbb{U}$ represents the set of served users in the network, A denotes the network area, and γ_x is the SINR of user x. Area spectral efficiency provides a direct measure of the network's spectral efficiency, which is impacted by data-base-station density, Szone size, and interference conditions.

- ***Network Energy Efficiency:*** This key performance indicator represents the amount of data transmitted per unit of energy consumed, reflecting the network's power efficiency. It is expressed as:

$$\eta_{\mathrm{EE}} = \frac{A}{P_T} \theta_{\mathrm{SE}}, \tag{3.4}$$

where P_T is the total power consumption of all data-base-stations in the network, and θ_{SE} is the area spectral efficiency. This metric is crucial in ultra-dense deployments where power efficiency must be optimized to sustain long-term network operation.

By analyzing the relationship between configuration and optimization parameters and key performance indicators, the system can be optimized to maximize area spectral efficiency and energy efficiency while minimizing interference and power wastage.

3.2.3 Synthetic Data Generation for COPs Combinations

To comprehensively evaluate the impact of positioning errors and system configurations on user-centric ultra-dense networks, a systematic synthetic data generation process is employed. This process utilizes SyntheticNET, a 3GPP-compliant system-level simulator designed to facilitate AI-driven network modeling and optimization. The simulator generates two primary datasets: the UER-KPI database and the COP-KPI database, each serving distinct purposes. Positioning errors pose fundamental challenges in user-centric ultra-dense networks, impacting scheduling, resource allocation, and overall network efficiency. Since these errors cannot be eliminated in real-world deployments, it is essential to develop an analytical or data-driven framework to quantify their impact and formulate compensation strategies.

The COP-KPI database is generated by systematically varying configuration and optimization parameter values while keeping other network parameters fixed. This database offers insight into how various configurations impact area spectral efficiency, energy efficiency, and other key network performance metrics. For each configuration, network deployment and scheduling are executed over a predefined transmission time interval horizon. The simulator logs the key performance indicator values for every transmission time interval, forming a comprehensive dataset

for performance evaluation. The aforementioned configuration parameters, DBS density, Szone radius, and transmit power, are varied to generate the COP-KPI database. The generated data is utilized for network optimization, enabling the system to identify configurations that maximize performance in terms of key performance indicators.

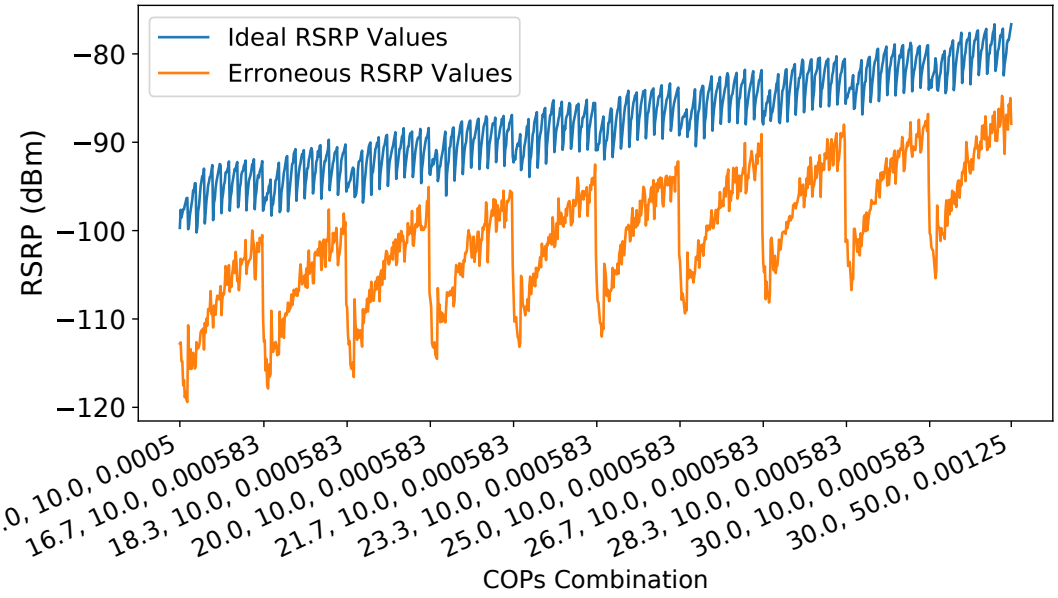


Fig. 3.3: Comparison of reference signal received power under ideal and erroneous scenarios across different combinations of user positioning and base station errors.

3.2.4 Positioning Error Impact Modeling

Positioning errors pose fundamental challenges in user-centric ultra-dense networks, impacting scheduling, resource allocation, and overall network efficiency. Since these errors cannot be completely eliminated in real-world deployments, it is essential to develop an analytical framework to quantify their impact and formulate compensation strategies.

Motivation for the Error Modeling

The central controller of a user-centric ultra-dense network relies on the estimated positions of users and data-base-stations to allocate resources effectively. However, real-world positioning estimates contain inherent inaccuracies due to global positioning errors, sensor noise, and environmental factors. These inaccuracies impact various network operations, including scheduling and Szone formation.

For example, when positioning errors cause users to be scheduled too closely together, the expected inter-Szone separation of $2R_{\mathrm{sz}}$ may not be maintained, leading to unintended interference. Similarly, errors in data-base-station positions may cause the activation of a data-base-station outside its intended service zone, reducing received signal strength and increasing interference to nearby users. Without an error compensation mechanism, such discrepancies degrade key performance indicators, necessitating an error-aware optimization framework.

Database Aided Error Modeling

To systematically analyze and mitigate the impact of positioning errors, a database-aided modeling approach is employed. The framework consists of three primary steps: first, empirical positioning error statistics are collected from real-world datasets to establish a representative error distribution. Second, the error distributions are applied to simulated user-centric ultra-dense networks, introducing controlled deviations in user and data-base-station positions. Third, variations in key performance indicators due to these errors are measured and stored in an error-aware database.

This modeling framework enables the classification of positioning errors into distinct regimes. In the low-error regime, association of the user to the data-base-station remains unchanged, but network resources are allocated based on incorrect distance estimates. In contrast, in the high-error regime, mis-positioning leads to inaccurate

positioning of the user with respect to the data-base-station, significantly degrading the signal to the inference network and network performance. The database-driven analysis enables the development of predictive models and AI-based compensation techniques to dynamically adjust network configurations in response to localization inaccuracies.

3.3 Proposed Error Compensation Approaches

To address the impact of positioning errors in user-centric ultra-dense networks, this section presents two complementary approaches for mitigating performance degradation: time-series forecasting for modeling key performance indicator trends and a data-driven optimization and error compensation framework. The proposed methods aim to enhance key performance indicators, including area spectral efficiency and network energy efficiency, by leveraging synthetic data generation, machine learning-based residual learning, and multi-objective optimization techniques.

3.3.1 P1: Time-Series Forecasting for Error Impact Minimization

Time-series forecasting is employed as a fundamental technique to predict variations in key performance indicators resulting from positioning errors. Given the seasonal nature of network performance variations and the observed trends in key performance indicator degradation, a forecasting-based model can extrapolate key performance indicator values and recommend optimal configuration adjustments to mitigate performance loss.

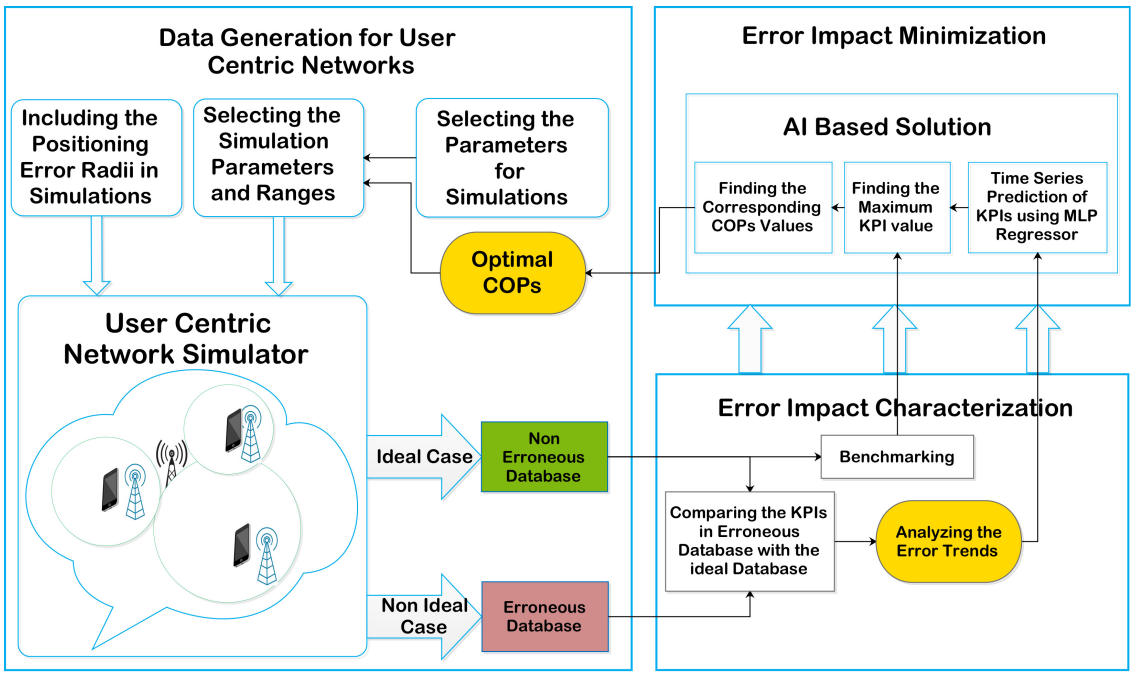


Fig. 3.4: Framework for characterizing and mitigating the impact of positioning errors in user-centric ultra-dense networks, integrating the data-driven models to quantify the impact of errors on key performance indicators and optimizing deployment parameters to minimize these effects using predictive and heuristic strategies.

Overview of the Proposed Framework: Time Series Based Modeling

The proposed framework for time series-based modeling is designed to mitigate the impact of positioning errors in user-centric ultra-dense networks. The framework consists of three major components: data generation for user-centric networks, error impact characterization, and AI-based error impact minimization, as illustrated in Fig. 3.4.

Data Generation for User-Centric Networks: The first stage of the framework involves synthetic data generation using a 3GPP-compliant user-centric ultra-dense network simulator, which models real-world network conditions with and without positioning errors. The simulator takes several configuration optimization parameters as input, including transmit power, service zone radius, and data-base-station density, along with additional simulation parameters such as bin size, net-

work area, and transmission time interval duration.

To systematically assess the impact of positioning errors, the simulator can include or exclude error radii in the user and data-base-station positions. This results in two distinct datasets: an ideal (non-erroneous) database, where users and data-base-stations are assumed to be accurately positioned, and a non-ideal (erroneous) database, where positioning errors distort network configurations. These databases serve as the foundation for subsequent performance evaluation and optimization.

Error Impact Characterization: Once the synthetic data is generated, the second stage of the framework performs error impact characterization by benchmarking the network key performance indicators obtained from the erroneous database against those in the ideal database. This comparison helps quantify the degradation in key performance indicators, including area spectral efficiency, network energy efficiency, reference signal received power, and coverage probability.

A crucial step in this process is analyzing error trends, which reveal systematic patterns in key performance indicator degradation due to positioning inaccuracies. Understanding these trends is essential for developing predictive models that can recommend configuration adjustments to counteract the effects of localization errors.

AI-Based Error Impact Minimization: The third and final stage of the framework focuses on AI-based error minimization, leveraging machine learning techniques to forecast variations in key performance indicators and recommend optimal configuration and optimization parameter values. The error compensation process follows a structured approach:

1. ***Time-Series Prediction Using Multi-Layer Perceptron Regression:*** A multi-layer perceptron regressor is trained on the erroneous database to

learn the relationship between positioning errors and key performance indicator degradation. The model predicts future key performance indicator values by capturing the underlying temporal trends in the data.

2. ***Finding the Maximum Key Performance Indicator Value:*** Based on the forecasted trends, the framework identifies the achievable upper bound for key performance indicator recovery, ensuring that network performance is restored as closely as possible to the ideal conditions.

3. ***Deriving Optimal Configuration and Optimization Parameter Values:*** The predicted key performance indicator trends are used to compute the optimal configuration parameter settings required to mitigate positioning error effects. The framework searches for the configuration and optimization parameter values that align with the maximum achievable key performance indicator, ensuring efficient resource allocation despite localization inaccuracies.

By integrating data-driven insights, predictive modeling, and optimization techniques, the proposed framework systematically compensates for performance degradation caused by positioning errors. The results demonstrate that time-series forecasting provides an effective mechanism for preemptively adjusting network configurations, ensuring improved spectral and energy efficiency in real-world user-centric ultra-dense network deployments.

SARIMA-Based Error Prediction

The seasonal auto-regressive integrated moving average model is employed as a time series forecasting technique due to its suitability for handling periodic patterns in network key performance indicators. SARIMA effectively captures the temporal variations in area spectral efficiency and energy efficiency, modeling their seasonal

fluctuations over multiple time steps. The model is trained on an indexed subset of the database, referred to as DB-08, containing observed key performance indicator values across different configuration and optimization parameter settings.

To evaluate its effectiveness, SARIMA is applied to predict the key performance indicator values for an extended database, DB-09, which includes additional configuration and optimization parameter combinations not present in DB-08. The predicted key performance indicator values are then compared against the actual values recorded in DB-09, allowing an assessment of forecasting accuracy. The results indicate that SARIMA can accurately approximate the optimal trends in key performance indicators, providing a reliable mechanism for recommending configuration adjustments.

Multi-layer Perceptron Regressor for the Recovery of KPIs

In addition to SARIMA, a multi-layer perceptron regressor is utilized to model the key performance indicator trends under varying positioning error conditions. The multi-layer perceptron regressor, a type of artificial neural network, is trained on DB-08 and applied to predict the key performance indicator values for DB-09. The predicted values are validated by comparing them with the ground truth values, measuring the forecasting error.

For the case of received signal reference power, an illustrative example shows that positioning errors significantly reduce RSRP values. However, by leveraging SARIMA and multi-layer perceptron regression, the framework can identify new configurations and optimization parameter combinations that yield improved key performance indicator values despite localization inaccuracies. The forecast key performance indicator values guide the selection of updated configuration and optimization parameter settings that restore network performance to near-ideal conditions.

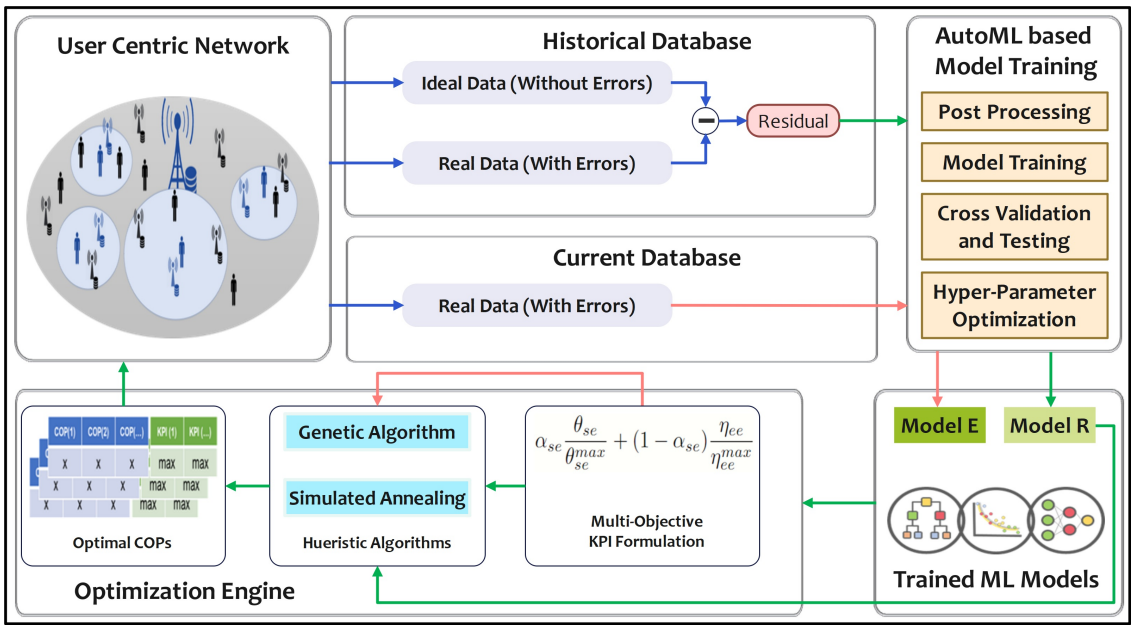


Fig. 3.5: The Data-Driven Optimization and Error Compensation Modeling framework, for user-centric ultra-dense networks. This framework utilizes a historical database for error impact characterization and residual learning to compensate for its impact, as manifested in the multi-objective optimization of key performance indicators using two heuristic algorithms: the genetic algorithm and simulated annealing.

3.3.2 P2: Data-Driven Optimization and Error Compensation

While time series forecasting offers an effective solution for estimating key performance indicator trends, a more robust approach is needed to optimize network configurations in the presence of positioning errors. The DD-OEC framework integrates machine learning-based residual learning with multi-objective optimization to maximize both area spectral efficiency and energy efficiency simultaneously.

Overview of the Proposed DD-OEC Framework:

The Data-Driven optimization and error compensation framework is designed to mitigate the impact of positioning errors in user-centric ultra-dense networks by integrating machine learning based residual learning with heuristic multi-objective

optimization techniques. As illustrated in Fig. 3.5, the framework consists of multiple interconnected components, including historical and current databases, an AutoML-based model training module, trained machine learning models, and an optimization engine. These components work in synergy to estimate optimal configuration optimization parameters that maximize key performance indicators such as area spectral efficiency and network energy efficiency.

Historical and Current Databases: The framework relies on two distinct data sources: a historical database containing ideal network data (without errors) and a current database containing real network data (with errors). The historical database consists of key performance indicator measurements collected under ideal conditions, where user and data-base-station positions are assumed to be perfectly known. Conversely, the current database is generated under real-world conditions, incorporating positioning errors that degrade network performance.

To quantify the discrepancy between these two datasets, the framework computes a residual error, which represents the deviation between the ideal and erroneous key performance indicator values. This residual is a crucial component in learning the impact of positioning errors and guiding the optimization process.

Table 3.1: Performance evaluation of the automated machine learning based model fitting module using a range of Regression models including Gradient Boosting (GBR), Light GBM (LGR), Random Forest (RFR), CatBoost (CBR), and AdaBoost (ABR), highlighting their comparative RMSE results for the studied KPIs.

	AutoML Model Name			**RMSE Performance**		
Case Flag	**1st Model**	**2nd Model**	**3rd Model**	**1st Model**	**2nd Model**	**3rd Model**
ASE Model-E	GBR	LGR	RFR	3.71E-5	3.78E-5	3.99E-5
EE Model-E	GBR	LGR	CBR	2.02E-5	2.06E-5	2.14E-5
ASE Model-R	ABR	LGR	CBR	1.02E-5	2.17E-5	2.34E-5
EE Model-R	LGR	ABR	CBR	2.17E-5	2.46E-5	2.12E-5

AutoML-Based Model Training and Residual Learning: To enhance the optimization process, the framework employs an AutoML-based model training module that automates feature selection, hyperparameter tuning, cross-validation, and performance evaluation. This module trains two machine learning models:

- Model E: Learns the relationship between configuration and optimization parameters and key performance indicators using the erroneous (real) database.
- Model R: Captures the residual error between the ideal and erroneous key performance indicators, enabling compensation for positioning inaccuracies.

By incorporating residual learning, the framework refines key performance indicator predictions, reducing the adverse effects of localization errors and improving network performance estimation.

Multi-Objective Optimization Engine: Once the machine learning models are trained, their outputs feed into the optimization engine, which employs a multi-objective key performance indicator formulation to determine optimal configuration and optimization parameter values. The objective function is formulated as:

$$f_{\text{obj}}(\theta_{\text{SE}}, \eta_{\text{EE}}) = \alpha_{\text{SE}} \frac{\theta_{\text{SE}}}{\theta_{\text{SE}}^{\max}} + (1 - \alpha_{\text{SE}}) \frac{\eta_{\text{EE}}}{\eta_{\text{EE}}^{\max}}, \tag{3.5}$$

where α_{SE} and $(1 - \alpha_{\text{SE}})$ control the trade-off between area spectral efficiency and energy efficiency. The optimization engine utilizes two heuristic algorithms, genetic algorithm and simulated annealing, to efficiently search the solution space and identify optimal network configurations.

Integration and Output of the Framework: The trained machine learning models interact with the optimization engine, guiding the search for error-compensated

configuration and optimization parameter values. The optimization results are validated against key performance indicator benchmarks to ensure that performance gains are achieved. The final output of the framework consists of a set of optimal configurations and optimization parameter values, which are used to adjust network configurations and enhance performance under real-world deployment conditions.

By integrating historical data analysis, residual learning, machine learning, and heuristic optimization, the DD-OEC framework systematically addresses the challenges posed by positioning errors, significantly improving network adaptability and performance in user-centric ultra-dense networks.

Multi-Objective Optimization Problem Formulation and Algorithm

Given the trade-off between area spectral efficiency and energy efficiency, the optimization objective function is formulated as a weighted sum of the normalized key performance indicator values:

$$f_{\text{obj}}(\theta_{\text{SE}}, \eta_{\text{EE}}) = \alpha_{\text{SE}} \frac{\theta_{\text{SE}}}{\theta_{\text{SE}}^{\max}} + (1 - \alpha_{\text{SE}}) \frac{\eta_{\text{EE}}}{\eta_{\text{EE}}^{\max}}, \tag{3.6}$$

where α_{SE} and $(1 - \alpha_{\text{SE}})$ represent the weight factors for area spectral efficiency and energy efficiency, respectively. The optimization problem aims to maximize f_{obj} while satisfying the constraints on data-base-station density, service zone radius, and transmit power:

$$\begin{aligned} \max_{\lambda_{\text{DBS}}, R_{\text{sz}}, P_{\text{tx}}} \quad & f_{\text{obj}}(\theta_{\text{SE}}, \eta_{\text{EE}}), \\ \text{s.t.} \quad & 0 \leq \lambda_{\text{DBS}}^{\min} \leq \lambda_{\text{DBS}} \leq \lambda_{\text{DBS}}^{\max}, \\ & 0 \leq R_{\text{sz}}^{\min} \leq R_{\text{sz}} \leq R_{\text{sz}}^{\max}, \\ & 0 \leq P_{\text{tx}}^{\min} \leq P_{\text{tx}} \leq P_{\text{tx}}^{\max}. \end{aligned} \tag{3.7}$$

Given the non-convex nature of this optimization problem, heuristic algorithms such as simulated annealing and genetic algorithms are employed to effectively explore the solution space.

Automated Machine Learning for Residual Error Learning

To improve optimization accuracy, the DD-OEC framework incorporates residual learning using AutoML techniques. Two machine learning models are trained: Model-E, which learns the relationship between configuration and optimization parameters and key performance indicators based on erroneous data, and Model-R, which captures the residual error between the ideal and erroneous cases. The combined outputs of these models enhance the optimization engine, enabling it to generate error-compensated configuration and optimization parameter recommendations.

Model-E is trained on real-time erroneous data, whereas Model-R utilizes historical ideal data to learn the discrepancy caused by positioning errors. By leveraging residual learning, the framework effectively mitigates inaccuracies in key performance indicator estimation, leading to improved network performance.

Multi-Objective Optimization with configuration parameters

The final stage of the DD-OEC framework involves executing multi-objective optimization using simulated annealing and a genetic algorithm. Simulated annealing employs an adaptive temperature schedule that dynamically adjusts the cooling rate, ensuring efficient exploration of the solution space. A genetic algorithm, on the other hand, applies evolutionary principles, such as mutation and crossover, to iteratively refine configuration and optimization parameter selections.

By integrating machine learning-based residual learning with heuristic optimization, the DD-OEC framework effectively compensates for positioning errors, leading to

Table 3.2: Simulation setup and configuration parameters to generate the UER-KPI and COP-KPI datasets, including network deployment settings, error characteristics, and algorithm-specific parameters for SA and GA for heuristic optimization.

Parameter Name	**Parameter Type**	**UER-KPI Scenario**	**COP-KPI Scenario**
User Density (λ_{ue})	NOP	0.0005	
DBS Density (λ_{dbs})	COP	0.0005	0.0005 - 0.0125
Transmit Power (P_{tx})	COP	20 dBm	15 - 30 dBm
Szone Radius (R_{sz})	COP	25 m	10 - 50 m
UPER (User Positioning Error Radius)	EMP	0 – 25 m	15 m
DPER (Data-Base-Station Positioning Error Radius)	EMP	0 – 25 m	15 m
Positioning Error Distribution	EMP	Uniform	
Shadowing Standard Deviation	NOP	4	
UEs and DBS Deployment	NOP	Poisson Point Process	
Network Area	NOP	1 km^2	1 km^2
Bin Size	NOP	10	
Simulation Time for Simulated Annealing	NOP	100 cycles	
Error Radii	EMP	15 m	
Population Size	NOP	24	
Initial Temperature	NOP	250	
Simulated Annealing δ	NOP	0.0001	
Cooling Rate (σ)	NOP	0.01	

substantial improvements in both area spectral efficiency and energy efficiency.

3.3.3 Comparison with Baseline Approaches

The effectiveness of the proposed methods is evaluated against baseline approaches that do not incorporate error compensation. Conventional machine learning based optimizers, which do not consider positioning errors, exhibit degraded performance due to inaccuracies in user and data-base-station locations. In contrast, the DD-

OEC framework significantly reduces key performance indicator degradation by adapting to real-time error conditions.

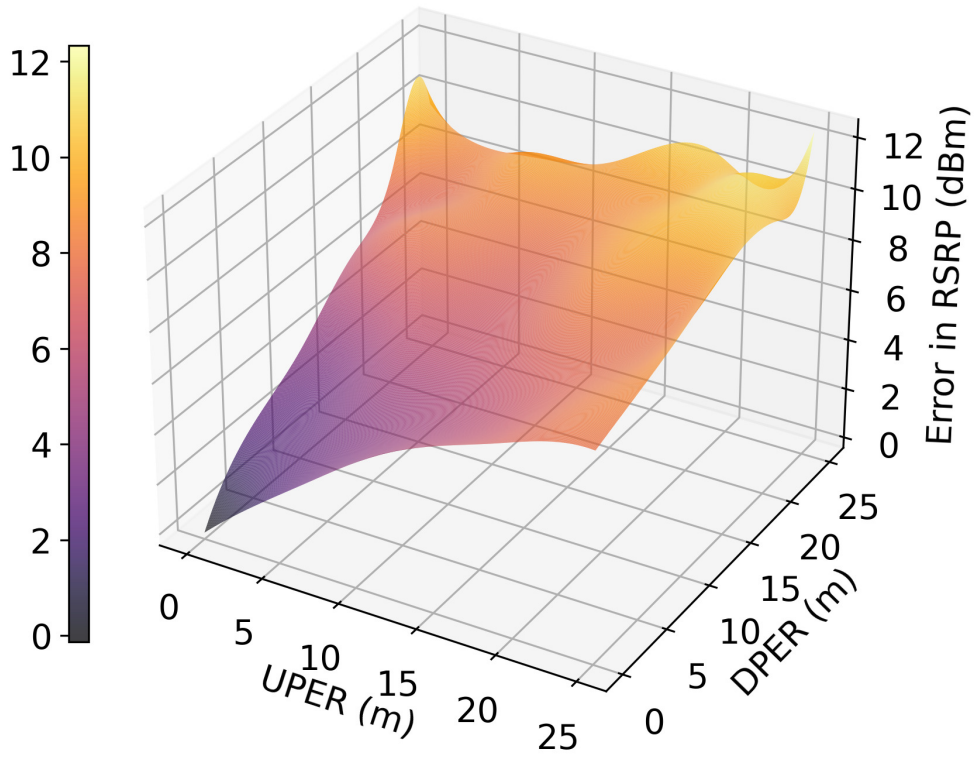


Fig. 3.6: Error trends in reference signal received power under increasing user and base-station positioning inaccuracies. The surface illustrates how spatial errors jointly degrade signal strength in ultra-dense deployments.

Simulation results demonstrate that the proposed framework achieves up to 23% improvement in area spectral efficiency and energy efficiency compared to baseline models. These findings underscore the importance of incorporating error-aware optimization techniques in user-centric ultra-dense networks, thereby ensuring reliable network performance under realistic deployment conditions.

3.4 Simulation Setup & Performance Evaluation

This section presents the simulation methodology used to evaluate the impact of positioning errors in user-centric networks and the effectiveness of the proposed data-driven compensation techniques. The experiments utilize synthetic data generation and 3GPP-compliant system-level simulations to model network behavior under varying configurations.

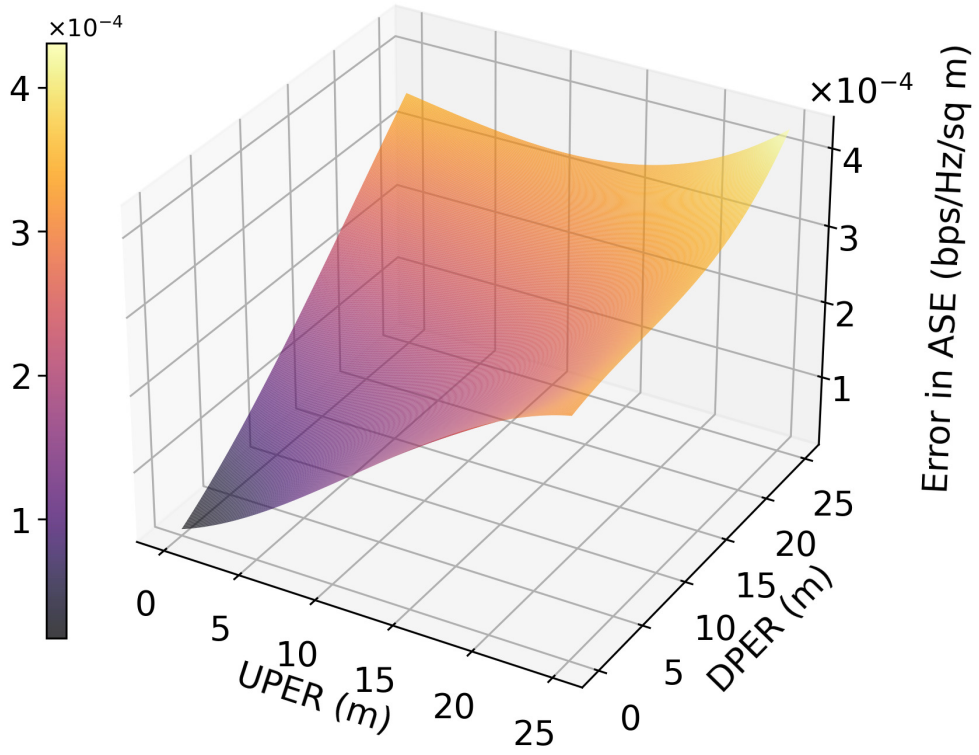


Fig. 3.7: Error trends in area spectral efficiency with respect to user and base-station positioning errors. The figure shows the impact of spatial deviations on overall spectral efficiency across dense network configurations.

3.4.1 Simulation Parameters and Setup

The simulation setup consists of a network deployed over a 1 km^2 area, where user equipments and data-base-station are distributed according to a stationary Poisson

point process. The key simulation parameters are provided in Table 3.2, detailing the network conditions for both the error characterization (UER-KPI scenario) and optimization-based compensation (COP-KPI scenario). The DBS density is varied between 0.0005 and 0.0125 per square meter in the COP-KPI scenario to analyze its impact on performance, while in the UER-KPI scenario, it remains fixed. The transmit power is also adjusted between 15 dBm and 30 dBm to study its effect on network key performance indicators. Similarly, the service zone radius is varied between 10 m and 50 m in the optimization scenario to assess its influence on spectral and energy efficiency.

The positioning error distribution follows a uniform model, with user and data-base-station positioning error radii ranging from 0 m (ideal case) to 25 m. The impact of these errors is analyzed by comparing the degraded key performance indicators against their ideal values in error-free conditions. The simulations incorporate shadowing effects with a standard deviation of 4 dB to reflect realistic propagation conditions. The evaluation is conducted over 100 Monte Carlo iterations, ensuring statistical robustness. A bin size of 10 is used for data aggregation, and the population size for optimization is set to 24. Additionally, simulated annealing parameters, including an initial temperature of 250 and cooling factors of 0.0001 and 0.01, are used to ensure effective convergence of the optimization algorithms.

3.4.2 Error Characterization and Alleviation Results

In this subsection, we discuss the error characterization and alleviation results by first examining the impact of errors in user and data-base-station positions on network key performance indicators, and then highlighting the performance of various time series prediction models in recovering the decline in these performance indicators.

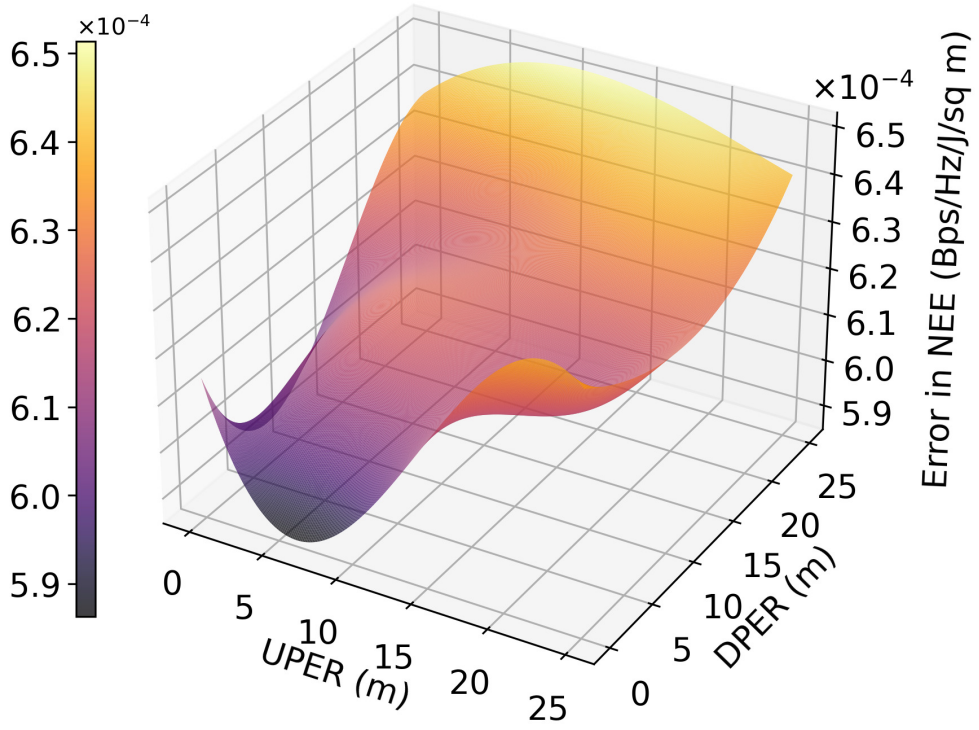


Fig. 3.8: Error trends in network energy efficiency under user and base-station positioning inaccuracies. The results reveal the compounded effect of spatial errors on energy performance, emphasizing the need for robust compensation.

Impact of Positioning Errors on Network Key Performance Indicators

The results of the error impact characterization on the understudy's key performance indicators are discussed here. The fall in RSRP, area spectral efficiency,

Table 3.3: Model configurations for SARIMA and MLP-REG used in forecasting RSRP, ASE, and NEE, to outline seasonal and non-seasonal SARIMA parameters, and MLP-REG specifications including solver and activation function for each KPI.

SARIMA Model Parameters			**MLP-REG Parameters**	
	Trend Elements (p, d, q)	**Seasonal Elements (P, D, Q, m)**	**Model Specs (l, n)**	**Solver and Activation Functions**
RSRP	(1, 1, 1)	(1, 1, 1, 64)	(5, 20)	(lbfgs, relu)
ASE	(1, 1, 1)	(1, 0, 1, 64)	(10, 50)	(adam, relu)
NEE	(1, 1, 1)	(1, 0, 0, 64)	(10, 50)	(lbfgs, tanh)

and energy efficiency with respect to the user positioning error radius and data-base-station positioning error radius is shown in Fig. 3.6, Fig. 3.7, and Fig. 3.8, respectively. For this analysis, we assume the fixed Szone radius of 50 m, transmit power of 20 dBm, and users and data-base-station densities of 0.0005 Km^{-2}. Both of the abovementioned errors vary from a minimum value of 0, referring to the ideal condition, to the maximum value of 25 m (half of the sZone radius). The figure contains errors in the reference signal received power, area spectral efficiency, and energy efficiency values, which are computed by differing from the ideal values due to user and DBS positioning error radii. The general trend in all these results suggests that as positioning errors increase, the fall in each key performance indicator increases. However, the specific fluctuations are idiosyncratic to the respective key performance indicator's inherent nature and to the fact that these trends are averaged over all users and transmission time intervals. An important observation to note is that the effect of error in one parameter is more pronounced, while the error in the other one is lower. Specifically, the RSRP results indicate that both positioning errors harm the reference signal received power. However, the impact of reference signal received power on the error in reference signal received power is significant when the data-base-station error is low, because the uncertainty in database-station position in this situation can lead to cases where even erroneous data-base-stations are located closer to the users, which contributes to reference signal received power improvement.

Performance of SARIMA against MLP-REG to Recover KPIs

As discussed in Section 3.3.1, for all the key performance indicators, we employ MLP-REG and SARIMA models for the time series forecasting with relevant parameters, selected after extensive search are listed in Table 3.3 and results for models' errors and performance is shown in Fig. 3.10. The percentage of each key

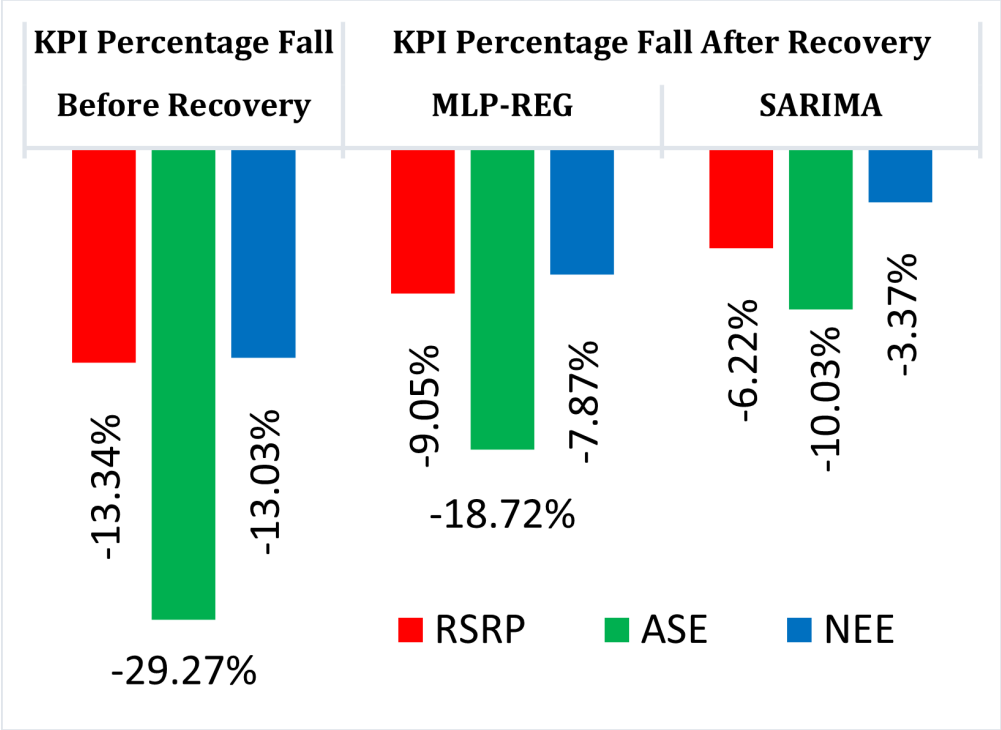


Fig. 3.9: Percentage reduction and subsequent recovery in KPIs using different recovery techniques, showing that SARIMA and MLP-REG methods reduce the impact of positioning errors on signal and network efficiency to varying extents.

performance indicator's fall and recovery, as compared to the models, is depicted in Fig. 3.9. Although the fall in RSRP is visualized in Fig. 3.3, the left three bars show the decline in all key performance indicators, averaged over transmission time intervals. To illustrate the impact of compensation, the percentage change in key performance indicators after recovery, as indicated by the respective time series schemes, is plotted. These results indicate that, in the given network settings. However, a significant portion of the key performance indicator can be recovered by adopting the configuration and optimization parameter values; the non-erroneous case cannot be achieved due to a sufficiently high error radius. Comparing the SARIMA and MLP-REG progress, it is evident that the former models outperform the latter for all key performance indicators due to their natural tendency to learn the seasonal patterns in the database. It is corroborated by the training and forecasting errors of all key performance indicators, where the SARIMA model

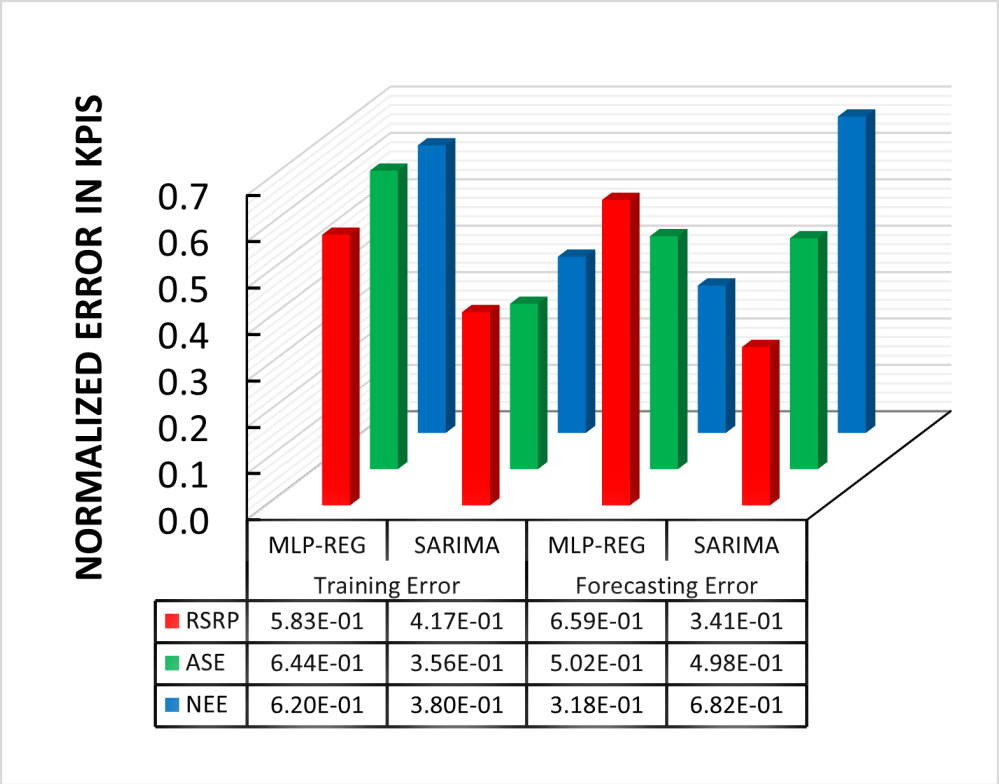


Fig. 3.10: Normalized training and forecasting errors for RSRP, ASE, and NEE using MLP-REG and SARIMA. The comparison reflects the predictive accuracy and generalization capability of each model across network performance indicators.

achieves better performance in all comparisons except the energy efficiency forecasting. The training and forecasting errors are independently normalized between the two comparison schemes to better visualize their performance.

3.4.3 DD-OEC Framework Evaluation

The performance of the proposed DD-OEC framework is analyzed through numerical simulations. To illustrate the benefit of learning the residual and performing error compensation, the performance of the DD-OEC framework is compared with that of a *baseline* optimization framework, which does not process the residual and optimizes based solely on the model trained on erroneous data. The performance is evaluated in terms of the achieved objective function values, key performance indicator values, and the corresponding configuration and optimization parameter

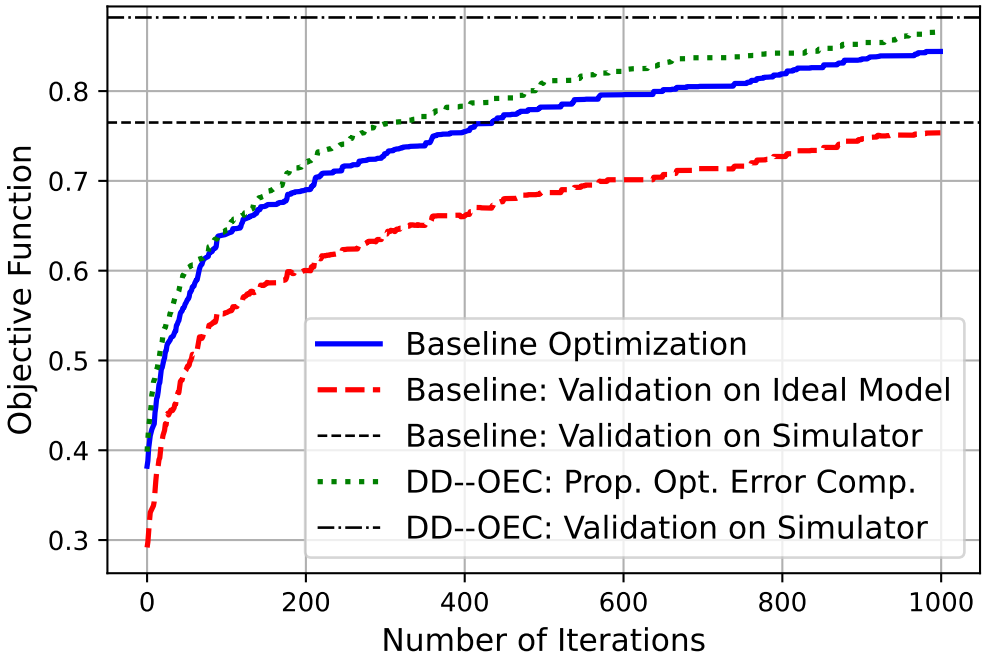


Fig. 3.11: Convergence behavior of simulated annealing under baseline and DD-OEC optimization schemes, comparing the improvement in objective function and demonstrating better convergence using error compensation.

combinations. Additionally, the number of iterations required for convergence is also evaluated. We simulate the user-centric network over a geographic area of 1 km by 1 km. The values of the relevant parameters for network simulation and data generation are given in Table 3.2. For data generation, 10 equally spaced values are taken within the ranges specified in Table 3.2, for each configuration and optimization parameter parameter. Moreover, as there are three configuration and optimization parameters, the length of both erroneous and ideal databases becomes 1000. Finally, the parameters δ and σ describe the initial temperature and the rate of cooling for simulated annealing.

Convergence of Simulated Annealing and Genetic Algorithm

The convergence performance of simulated annealing and genetic algorithm for both DD-OEC and baseline schemes is shown in Fig. 3.11 and Fig. 3.12, respectively.

These performance curves are obtained after averaging the converged objective function values from 1000 Monte Carlo trials. The configuration and optimization parameters obtained after algorithm convergence are validated on the simulator by giving the converged configuration and optimization parameters as input to the simulator and using the resulting key performance indicators to evaluate the objective function in (3.7). Additionally, the converged configuration and optimization parameters are validated using a machine learning-based model of the simulator, trained on ideal (error-free) COP-KPI combinations. These validated values are plotted as horizontal lines and represent the maximum values after convergence. Moreover, the configuration and optimization parameters obtained through the baseline scheme are also validated in each iteration using the ideal model.

It can be observed from Fig. 3.11 and Fig. 3.12 that even though the baseline scheme improves the objective function value with erroneous data (see blue curve) when these configuration and optimization parameters are validated using the ideal model (red curve) or the simulator, the objective function value is much lower. This indicates that with erroneous data, the configuration and optimization parameters obtained after optimization are highly sub-optimal for the actual network. On the contrary, the configuration and optimization parameters obtained via the DD-OEC scheme achieve the maximum value of the objective function when validated using the simulator. These results indicate that the DD-OEC mechanism is necessary for achieving a close-to-optimal COP combination, resulting in a better network operating point.

Moreover, it can be observed that the convergence of the genetic algorithm differs from simulated annealing convergence and is able to converge earlier. Simulated annealing exhibits a rising trend due to the high degree of variability in its convergence path across each run. In contrast, the convergence path of the genetic algorithm is relatively less variable across multiple runs. Furthermore, as a genetic

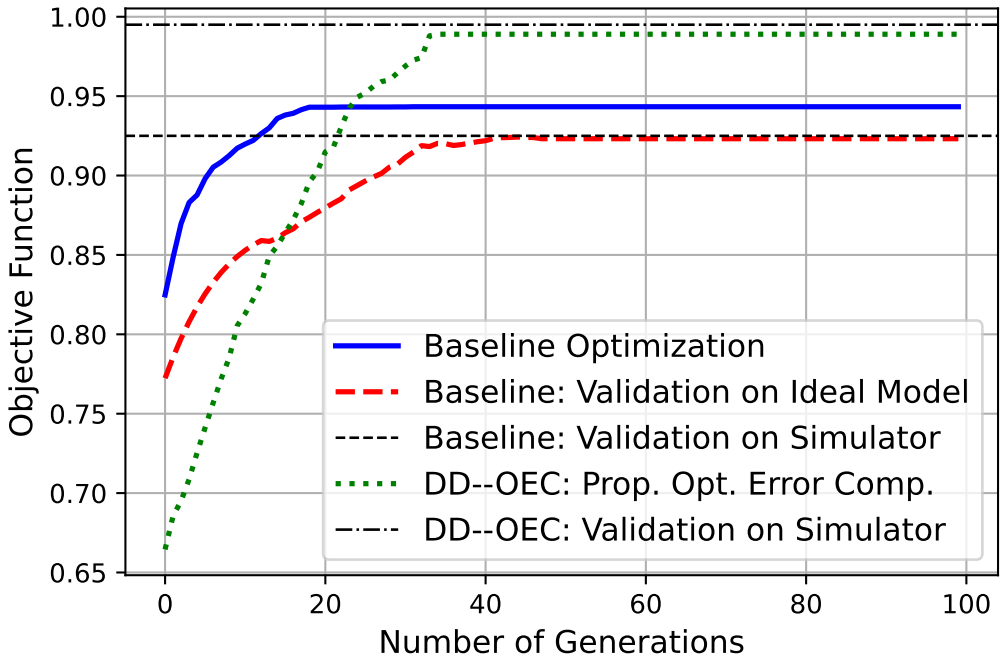


Fig. 3.12: Convergence performance of genetic algorithm under baseline and DD-OEC optimization strategies, showing faster and higher objective values with the proposed error-compensated approach.

algorithm is a population-based algorithm, which remains fixed in each run, its initialization is not as random as that of simulated annealing, and it reaches the optimum solution in relatively less time. Additionally, the number of generations or iterations required to reach the optimal solution varies across different runs of the same algorithm. Hence, to provide more insights, we plot these results using box plots in Fig. 3.13. An important observation to note here is that the number of required iterations in the DD-OEC scheme is slightly higher than in the baseline scheme because the DD-OEC scheme needs to combine the effects of both *Model-E* and *Model-R*; hence, it takes more time to converge.

Comparison of DD-OEC with Baseline Optimization

The simulation results with different values of α_{se} and $1 - \alpha_{se}$ are summarized and compared in Table 3.4. For both the baseline and proposed DD-OEC schemes, the

achieved objective function value along with the corresponding energy efficiency and area spectral efficiency values and the respective configuration and optimization parameter values, indicated by the triplet [λ_{dbs}, R_{sz}, P_{tx}], are also shown in Table 3.4. It is worth noting that, for both simulated annealing and genetic algorithms, the objective function value achieved for the baseline scheme is lower than that for the DD-OEC scheme. When the baseline configuration and optimization parameters are validated using the simulator, the objective function value is lowered further, highlighting the sub-optimality of the solution. On the contrary, when the optimized configuration and optimization parameters from the DD-OEC framework are validated on the simulator, the utility degradation is minimal. Compared to the baseline scheme, it is noted that the simulated annealing scheme yields a gain of up to 15%, while the genetic algorithm scheme achieves a gain of up to 23%. This highlights the need for the DD-OEC scheme and validates its effectiveness in counteracting the impact of errors.

Furthermore, it can be noted that the optimized configuration and optimization parameters for different cases converge to lower values of λ_{dbs} and R_{sz} and medium values for the transmit power. This is because, for the lower Szone sizes, relatively more users are scheduled, which increases the area spectral efficiency. A lower Szone radius increases interference; however, this consequence is avoided by reducing the transmit power. The lower value of the data-base-station density is due to the limited user density, and this lower data-base-station density is sufficient to serve the limited user density. Comparing the different values of α_{se}, it can be noted that the maximum objective function value is obtained when both area spectral efficiency and energy efficiency are given equal weight, as both components are normalized. Finally, comparing genetic algorithms and simulated annealing reveals that the former, with its population-based solution-finding approach, can efficiently reach convergence, and the converged objective function values are also higher. Hence, for this problem, a genetic algorithm is the better choice.

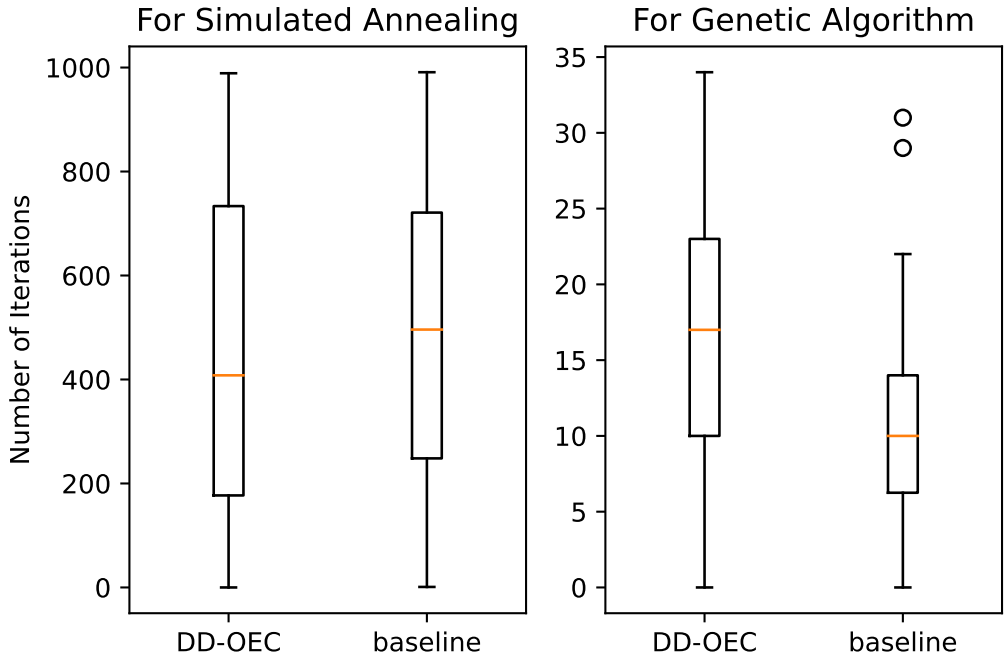


Fig. 3.13: Boxplot comparison of convergence iterations for simulated annealing and genetic algorithm using baseline and DD-OEC optimization. The results demonstrate improved efficiency and reduced iteration counts with the proposed scheme.

Table 3.4: Comparative evaluation of the proposed DD-OEC framework against baseline simulated annealing and genetic algorithm optimizations, presenting the objective scores, validated results, COP combinations, and execution times across multiple weight scenarios.

Opt. Alg. Name	Weight Case $(\alpha_{se}, 1-\alpha_{se})$	Baseline Optimization		COPs Validation on Simulator	DD-OEC Optimization		COPs Validation on Simulator	Exec. Time (s)
		Objective Function	Opt. COP Comb. $[\lambda_{dbs}, R_{sz}, P_{tx}]$		Objective Function	Opt. COP Comb. $[\lambda_{dbs}, R_{sz}, P_{tx}]$		
SA	(0.25, 0.75)	0.82=(0.21+0.61)	[5.17E-4, 13.33, 24.41]	0.77=(0.22+0.55)	0.85=(0.23+0.62)	[5.79E-4, 10.95, 18.34]	0.84=(0.23+0.61)	433
	(0.50, 0.50)	0.86=(0.45+0.41)	[5.74E-4, 11.62, 17.64]	0.78=(0.44+0.34)	0.87=(0.45+0.42)	[6.24E-4, 10.05, 20.64]	0.87=(0.45+0.42)	406
	(0.75, 0.25)	0.84=(0.61+0.23)	[5.16E-4, 12.94, 23.31]	0.79=(0.61+0.18)	0.92=(0.72+0.20)	[5.68E-4, 10.70, 16.35]	0.91=(0.71+0.20)	443
GA	(0.25, 0.75)	0.88=(0.19+0.69)	[5.05E-4, 12.26, 17.23]	0.72=(0.16+0.56)	0.89=(0.18+0.71)	[5.89E-4, 11.23, 20.36]	0.89=(0.18+0.71)	313
	(0.50, 0.50)	0.94=(0.46+0.48)	[5.50E-4, 11.63, 15.25]	0.92=(0.48+0.44)	0.98=(0.49+0.49)	[5.35E-4, 10.16, 15.00]	0.96=(0.49+0.47)	306
	(0.75, 0.25)	0.88=(0.69+0.19)	[5.20E-4, 13.24, 23.31]	0.81=(0.62+0.19)	0.87=(0.72+0.15)	[5.75E-4, 11.07, 18.85]	0.86=(0.72+0.14)	316

3.5 Conclusion and Transition to Next Chapter

This chapter examined the adverse impact of positioning inaccuracies in user-centric ultra-dense networks, where real-time resource allocation and dynamic service zone

formation are critically dependent on accurate localization of user equipment and data-base-stations. Through detailed simulation-based modeling and database-aided analysis, we demonstrated how even moderate localization errors can substantially degrade area spectral efficiency and network energy efficiency by misguiding user association, interfering with interference management, and triggering sub-optimal DBS activation.

To counteract these challenges, we introduced two complementary approaches. The first leverages time-series forecasting techniques, specifically seasonal auto-regressive integrated moving average and multi-layer perceptron Regression, to model and predict key performance indicator trends under varying levels of positioning error. These models offer predictive insights that enable the network controller to adjust configuration parameters proactively, mitigating performance degradation.

The second and more robust solution is the data-driven optimization and error compensation framework, which integrates historical error-free and erroneous datasets to learn residual trends. This automated machine learning-enhanced system utilizes residual modeling in conjunction with multi-objective optimization, employing genetic algorithms and simulated annealing, to recommend configuration parameters that restore degraded key performance indicators. Empirical evaluations confirm that the data-driven optimization and error compensation framework recovers up to 23% of performance loss in the presence of significant positioning error, outperforming conventional optimization methods that ignore spatial inaccuracies.

While the proposed solutions improve resilience against spatial uncertainty, another pressing issue in wireless network modeling is the scarcity of high-quality data, especially for training data-hungry machine learning models used in propagation prediction. The next chapter addresses this by proposing a domain-informed generative adversarial network framework that integrates expert knowledge with limited

real data to enable reliable and efficient propagation modeling under data-scarce conditions. This transition continues our broader theme of enhancing resilience in wireless systems through principled, artificial intelligence-driven methodologies.

CHAPTER 4

ML Models Resilience to Data Scarcity in Wireless Networks

This chapter addresses the challenge of data scarcity in wireless propagation modeling by introducing domain-informed generative methods. Traditional data-driven models often struggle when working with limited or imbalanced datasets, leading to reduced accuracy and generalization. To overcome this, we propose a framework that integrates analytical domain knowledge with Generative Adversarial Networks (GANs), enabling the creation of high-quality synthetic data even in data-scarce scenarios. The chapter details the design of a weight transfer generative adversarial network approach, where domain knowledge is embedded into the generative process to improve data fidelity and model robustness. We systematically evaluate the proposed method against conventional augmentation techniques, demonstrating its effectiveness in enhancing the performance of machine learning models for wireless propagation tasks. The insights presented here lay the groundwork for resilient and data-efficient modeling in next-generation wireless networks.

4.1 Introduction

The rapid evolution of wireless communication systems demands innovative solutions to address growing complexities in network design, optimization, and management [23]. A cornerstone of this endeavor is propagation modeling, which predicts essential metrics such as signal strength, coverage, and interference [100,101]. These models play a pivotal role in tasks ranging from planning and deployment to ensuring the reliability and scalability of next-generation networks. With the rise of

advanced technologies and dynamic network environments, there is a pressing need for propagation models that are not only accurate but also computationally efficient and adaptable to diverse scenarios [102, 103].

Traditional propagation models, broadly categorized as empirical, deterministic, and stochastic, have historically been an important design consideration in all generations of wireless networks [22]. Empirical models, such as the COST-Hata model, rely on measurements and statistical analysis, offering simplicity but limited generalizability [104]. Deterministic models, including ray tracing techniques, achieve high accuracy by incorporating detailed physical and environmental characteristics but are computationally intensive [105]. Stochastic models employ probabilistic distributions to balance computational efficiency with flexibility, yet they often lack the realism required for complex scenarios [22, 103]. These limitations have driven the exploration of data-driven approaches that leverage advanced machine learning techniques to overcome the constraints of traditional methods [106].

Data-driven propagation modeling introduces the ability to learn intricate and nonlinear relationships from large datasets, combining realism, completeness, and computational efficiency [23]. Machine learning techniques, such as deep neural networks, have been applied to learn the relationship between various geographic and network features and predict propagation metrics, including path loss and reference signal-to-noise ratio. In contrast, feature selection methods have been used to enhance interpretability and optimize resource usage [22,24]. Generative models, such as generative adversarial networks, further extend the capabilities of data-driven methods by generating synthetic data to augment scarce datasets [107]. Despite their promise, these approaches face significant challenges, including data quality sensitivity, instability in the training process, and the computational burden of handling high-dimensional inputs [23]. Addressing these challenges is essential for the practical adoption of data-driven methods in real-world wireless network scenarios.

One of the most critical challenges in leveraging data-driven approaches is the issue of data scarcity [28]. Data collection in wireless networks is often constrained by high costs, geographic imbalances, and the dynamic nature of network environments [102]. This scarcity leads to skewed datasets, biased models, and limited generalizability. Data augmentation, particularly through generative techniques, offers a promising avenue for mitigating these issues. However, existing generative methods require significant amounts of data for practical training, and otherwise often fail to capture domain-specific nuances critical for propagation modeling, underscoring the need for innovative approaches.

This work explores the integration of domain knowledge into data-driven propagation modeling to address the limitations of traditional and existing data-driven techniques. By leveraging analytical insights derived from the technical report guidelines of the third-generation partnership project [30], we propose a novel generative framework that enhances model performance under extreme data scarcity. This approach bridges the gap between domain knowledge and advanced machine learning methodologies, paving the way for more accurate and generalizable propagation models in next-generation wireless networks.

4.1.1 Related Work

Propagation modeling is the cornerstone of wireless network design and optimization, enabling accurate predictions of signal strength, coverage, interference, and reliability [100, 101]. At its core, propagation modeling involves understanding how electromagnetic waves travel through complex environments, influenced by phenomena such as reflection, diffraction, and scattering [108, 109]. These models play a vital role in various tasks, including network planning and performance evaluation, particularly in dynamic scenarios where geographic and environmental factors influence signal behavior.

Traditional Propagation Models

Traditionally, propagation models are categorized as empirical, deterministic, or stochastic [22]. Empirical models, such as the Okumura-Hata model, rely on real-world measurements and statistical analysis to provide quick estimates of signal attenuation but often lack accuracy in heterogeneous environments [110]. Deterministic models, including ray-tracing techniques, use physical laws and environmental geometry to simulate wave propagation in high detail but at a significant computational cost [108, 111]. Stochastic models employ probabilistic distributions to capture channel variability, making them suitable for scenarios involving high mobility or fluctuating conditions [104]. Although these models are helpful, their reliance on simplified assumptions limits their ability to capture the complex, nonlinear dynamics of modern wireless environments [112].

Machine Learning based Propagation Models

Machine learning has emerged as a powerful alternative to traditional propagation models, and is capable of learning complex, nonlinear patterns in propagation dynamics [23, 106]. By leveraging large datasets and advanced algorithms, machine learning based methods enhance prediction accuracy, computational efficiency, and adaptability to diverse environments.

Deep neural networks and support vector machines have demonstrated superior accuracy in modeling signal propagation, enabling real-time predictions and scenario simulations [102, 113]. Advanced frameworks such as bi-directional long short-term memory and convolutional encoder–decoder networks have further improved prediction capabilities in complex settings by integrating big data and physics-based features [106, 114]. However, these methods often rely heavily on large-scale datasets, which limits their applicability in data-scarce scenarios.

Machine learning models that incorporate geographical and engineered features have also improved propagation accuracy. For example, models that leverage terrain and environmental data enhance interpretability and performance across diverse environments [115]. Hybrid approaches that combine machine learning predicted clutter losses with classical physics-based methods demonstrate strong generalization capabilities [116]. Nevertheless, maintaining the accuracy under highly dynamic or sparse data conditions remains a challenge.

Efforts to reduce computational complexity and training time have resulted in models such as the Light Gradient-Boosting Machine (LigthGBM), which achieve significant accuracy gains while reducing prediction time [22]. Similarly, three-dimensional machine learning propagation models trained with smart predictors offer computational efficiency while minimizing the reliance on ray tracing [24]. Despite these advancements, machine learning models often require sufficiently rich datasets for practical training, which poses a critical limitation in real-world applications.

Most machine learning-based propagation models assume the availability of abundant data and struggle in scenarios with sparse or imbalanced data. This limitation underscores the necessity for advanced data augmentation techniques, such as generative adversarial networks, to generate high-quality data. Integrating domain knowledge into the training of generative adversarial networks is a promising direction for enhancing machine learning performance under such conditions, and this is the focus of this work.

Data Augmentation Approaches in Propagation Modeling

Data augmentation is a crucial strategy for increasing the diversity and quantity of training data in machine learning. Non generative techniques, such as geometric transformations in computer vision [117, 118], synonym replacement in natural

language processing [119], and noise injection in signal processing [120, 121], are computationally efficient but often rely heavily on domain-specific knowledge and high-quality datasets. These methods also struggle to capture the intricate relationships and variability found in complex tabular datasets, such as those used in wireless networks.

Generative adversarial network-based approaches have emerged as powerful tools for addressing these limitations in wireless networks and propagation modeling. By generating synthetic data that reflects real-world channel conditions, generative adversarial networks enable advanced modeling and improved performance across various applications. For instance, generative adversarial networks have been used to autonomously model wireless channels by training on raw measurement data, reducing reliance on domain expertise and simplifying the modeling process [122]. Extensions of these methods incorporate advanced architectures, such as gated recurrent units and long short-term memory, to predict and synthesize channel characteristics for the future sixth-generation communications networks, demonstrating improved accuracy and computational efficiency compared with traditional models [123, 124].

Specific users of generative adversarial networks include air-to-ground communication and intelligent reflecting surface-aided systems. Conditional generative adversarial networks have been used to model air-to-ground channels and predict parameters such as path gain and Doppler frequency based on location and velocity [125]. Similarly, generative adversarial networks applied to intelligent reflecting surface systems have significantly enhanced channel estimation accuracy compared with conventional methods [126, 127]. Generative adversarial networks have also been utilized for predicting network traffic and estimating path loss. For example, the path-loss generative adversarial network, referred to as the path loss generative adversarial network, generates maps from satellite images, providing a computa-

tionally efficient alternative to ray tracing [128]. These applications demonstrate the versatility of generative adversarial networks in addressing diverse challenges in wireless network modeling.

Despite these advancements, most generative adversarial network-based methods focus on image-based datasets or require extensive, high-quality data, thereby limiting their effectiveness for tabular datasets in propagation modeling. This study addresses these gaps by proposing a domain-informed generative adversarial network framework tailored for tabular data under data-scarce conditions, enhancing synthetic data quality and bridging the gap between analytical models and machine learning techniques.

Domain Knowledge Integration in DNNs and GANs

Integrating domain knowledge into deep neural networks and generative adversarial networks has proven effective in enhancing model performance, interpretability, and robustness, particularly in data-limited scenarios. By embedding domain-specific principles, these methods reduce reliance on extensive datasets while ensuring consistency with known system dynamics. For deep neural networks, logical and numerical constraints have been employed to improve interpretability and reliability across applications. Dash et al. [129] highlighted the role of such constraints, whereas authors in [130] demonstrated their effectiveness in optimizing ultra-reliable communications for sixth-generation networks. In generative adversarial networks, domain knowledge integration focuses on improving the fidelity of synthetic data. Methods such as monotonicity constraints [131] and sensitivity-based learning have shown improvements in generalization and data quality. Self-organizing neural networks combined with reinforcement learning further enhance learning efficiency [132].

Despite these advancements, domain-informed generative adversarial networks for tabular data, particularly in wireless propagation modeling, remain under-explored.

Addressing this gap requires leveraging domain-specific insights to effectively train generative adversarial networks under conditions of sparse data. This study builds on these concepts by integrating analytical propagation models into the training of generative adversarial networks, paving the way for the generation of high-quality synthetic data tailored to the requirements of propagation modeling.

4.1.2 Problem Statement and Motivation

Data-driven machine learning-based propagation modeling relies on diverse network and environmental parameters represented in tabular data formats. Unlike image data, which benefits from spatial correlations, tabular datasets present unique challenges owing to their mix of discrete and continuous variables and the lack of contextual structure. Moreover, the scarcity of high-quality, labeled tabular data in real-world scenarios further complicates the extraction of meaningful patterns, making the practical training of models difficult. Generative adversarial networks have emerged as powerful tools for synthetic data generation, but their practical training requires substantial amounts of data that is often unmet in tabular data scenarios. This creates a paradoxical situation where data scarcity hinders the training of generative adversarial networks. In contrast, the absence of a well-trained generative adversarial network prevents the generation of synthetic data to mitigate the scarcity. This vicious cycle underscores the need for innovative adaptations to generative adversarial network architectures and training processes to fully harness their potential in data-scarce environments. This study focuses on addressing the following key challenges:

- **Integration of Domain Knowledge:** How can the domain knowledge from analytical propagation models be effectively incorporated into generative adversarial network training to generate high-quality synthetic data under scarce data conditions?

- **Performance under Extreme Data Scarcity:** How can data-driven propagation models perform reliably in scenarios with insufficient data to train machine learning models to learn complex propagation relationships?

This aims to address these questions by proposing a novel framework that integrates domain knowledge into the training of generative adversarial networks, thereby enabling the generation of synthetic data for improved propagation modeling performance. Building on the preliminary findings published in VTC-Fall 2024 [31], this study expands the scope of analysis and provides an in-depth evaluation under diverse conditions.

4.1.3 Contribution Summarized

The key contributions of this work are summarized below:

1. **A Comprehensive Framework to Tackle Data Scarcity in Propagation Modeling:** We address the critical challenge of data scarcity in wireless network modeling by proposing a novel weight transfer generative adversarial network framework. Our framework integrates domain knowledge into machine learning pipelines, enabling the generation of high-quality synthetic data with minimal training datasets. As illustrated in Fig. 5.1, the framework consists of three interconnected modules: propagation modeling (M1), synthetic data generation and evaluation (M2), and machine learning applicability analysis (M3). This end-to-end solution ensures enhanced data quality and robust applicability of machine learning for wireless network tasks.

2. **Weight Transfer for Efficient GAN Training:** We propose a two-stage GAN-based approach with weight transfer to overcome data scarcity challenges in propagation modeling. In the first stage, the **Generator Network**

(G1) is trained on deterministic pseudo-random data generated from an analytical propagation model, which encodes domain knowledge into its weights. These pre-trained weights are then transferred to the **Generator Network (G2)** in the second stage, which is fine-tuned using real datasets within the generative adversarial network framework. This weight transfer mechanism provides G2 with a solid understanding of propagation characteristics, reduces data requirements, and accelerates the convergence of the generative adversarial network, ensuring that domain-specific insights are incorporated into the training process.

3. **Pseudo-Random Data Generation:** We formulate a domain-specific analytical propagation modeling equation that incorporates Line-of-Sight (LoS) and non-LoS (NLoS) components, 3D antenna parameters, and key wireless channel features, as detailed in Section 4.3.2. This equation generates pseudo-random propagation data, which is then used to train a deep neural network to capture the relationship between environmental features and signal strength, reference signal received power. The trained neural networks served as the first stage of our weight transfer generative adversarial network framework, providing a robust initialization for training generative adversarial networks.

4. **Quality-Driven Synthetic Data Generation:** To ensure high fidelity, synthetic data generation in Module M2 employs a quality-driven training mechanism. Synthetic data is iteratively validated using quality metrics, with early stopping determined by the synthetic data's adherence to the statistical and structural properties of the original data. This method ensures consistent data quality, achieving an average improvement of about 16% & 12% in column shape, and 24% & 50% in column pair trends metrics compared to the baselines, Conditional Tabular Generative Adversarial Network (CTGAN) and Gaussian Copula (GC), respectively.

5. **Machine Learning Applicability Analysis:** To assess and validate the utility of the proposed weight transfer GAN-generated data, we conducted machine learning applicability experiments in M3. Regression models trained on our hybrid augmented datasets consistently outperformed those trained on CTGAN and GC data across all data sizes. Specifically, for the Root Mean Squared Error (RMSE), the weight transfer generative adversarial network achieved an average improvement of 48.6% over Gaussian copula, and 37.4% over conditional tabular GAN. Similarly, for the Adjusted R^2 metric, WTGAN showed an average improvement of 54.8% over Gaussian copula, and 10.1% over conditional tabular generative adversarial network. These results highlight the robustness and effectiveness of our proposed approach for improving machine learning performance in wireless propagation modeling.

6. **Broader Impact:** This study leverages domain knowledge and machine learning to provide a scalable framework for data-scarce environments. By enhancing the quality of synthetic data and improving the applicability of machine learning, the proposed approach offers a robust solution for wireless network modeling. It lays the groundwork for its extension to other domain-specific applications.

The remainder of this chapter is organized as follows. Section 4.2 discusses the foundational aspects of the proposed framework, including the system model for propagation modeling, data preprocessing, and machine learning-based modeling. Key steps such as feature extraction from base station, geographic, and user equipment data are also highlighted. Section 4.3 introduces the proposed Domain-Informed WTGAN-based Synthetic Data Generation Framework, detailing its three modules: knowledge extraction and GAN training, synthetic data generation and validation, and propagation model training and inference. In Section 5.5.1, we describe the experimental setup, outline baseline schemes such as CTGAN and GC, and evaluate

the framework's performance using metrics like Column Shape and Column Pair Trends. The applicability of augmented datasets is analyzed through regression-based evaluations. Finally, Section 4.5 summarizes the contributions and highlights potential future research directions, focusing on overcoming data scarcity in wireless network modeling.

4.2 System Model and Propagation Modeling

The proposed framework is grounded in data-driven propagation modeling, which necessitates a systematic approach to data collection and processing, as well as the application of machine learning techniques. This section provides a brief description of (1) the system model for data collection, detailing how relevant data is obtained and preprocessed for propagation modeling, and (2) data-driven machine learning-based propagation modeling.

4.2.1 System Model for Propagation Data Collection

The system model plays a crucial role in establishing a comprehensive framework for propagation modeling. The system model outlines the setup for network deployment, simulation parameters, and data collection methodologies employed to gather relevant data for propagation modeling. The proposed framework utilizes a 3GPP-compliant fifth-generation cellular system, which is deployed using the Atoll radio network planning and optimization tool. This tool is instrumental in creating a realistic network topology, simulating various network conditions, and generating the datasets required for modeling. Atoll's capabilities include sophisticated ray-tracing techniques that accurately model the physical propagation environment, taking into account factors such as antenna heights, directional antenna patterns, ground and building heights, and land-use maps. This level of detail is crucial for

capturing the real-world complexities of signal propagation [22].

Synthetic Data Collection:

This process involves gathering data essential for propagation modeling [24], and includes the following steps:

- **Base station information** includes the parameters such as antenna height, azimuth, tilt angles, and transmit power, etc., which describe the network configuration.
- **Geographic information** includes digital models of terrain, building heights, and land use to capture the terrain and structures of the propagation environment.
- **User equipment measurements** include the signal strength, location, and timestamps obtained through drive tests and crowd-sourcing applications.

Data Preprocessing:

Ensuring the quality and usability of the collected data is a critical step [22]. It involves:

- **Data cleaning** focuses on detecting and removing anomalies and incomplete traces to maintain uniformity.
- **Data gridding** aims to aggregate and average the signal measurements into spatial bins (e.g., 10m x 10m) to reduce noise and variability [24].

Feature Engineering:

Feature engineering is a crucial component of the proposed framework for propagation modeling, leveraging domain knowledge to create features that accurately

characterize the propagation environment and enhance the predictive accuracy of machine learning models.

- **Propagation distance** is the horizontal distance between the user and its serving base station, capturing the signal attenuation over distance.
- **Angular separations** include both horizontal and vertical angles relative to the base station antenna boresight, capturing the impact of antenna directions.
- **Line-of-Sight (LoS)** is a binary feature indicating whether a user is in the LoS or non-LoS region of a base station. [24].
- **Building penetration** is the building counts penetrated by a signal path, and is relevant in urban environments.
- **Indoor/Outdoor distances** are the lengths of the signal path traversing indoor and outdoor areas [22].

These features, combined with additional features such as clutter types and diffraction points, form a rich dataset for machine learning-based propagation modeling.

4.2.2 Data Driven Propagation Modeling

Machine learning-based propagation modeling predicts key signal parameters, such as path loss or received signal reference power, using the feature set described in Section 4.2.1. These features serve as predictors, whereas the target variable, typically RSRP or path loss, reflects the received signal strength, a critical metric for evaluating network performance. Regression models are predominantly used for this purpose owing to the continuous nature of the target variable. Models, such as neural networks, establish a mapping between input features and the target variable

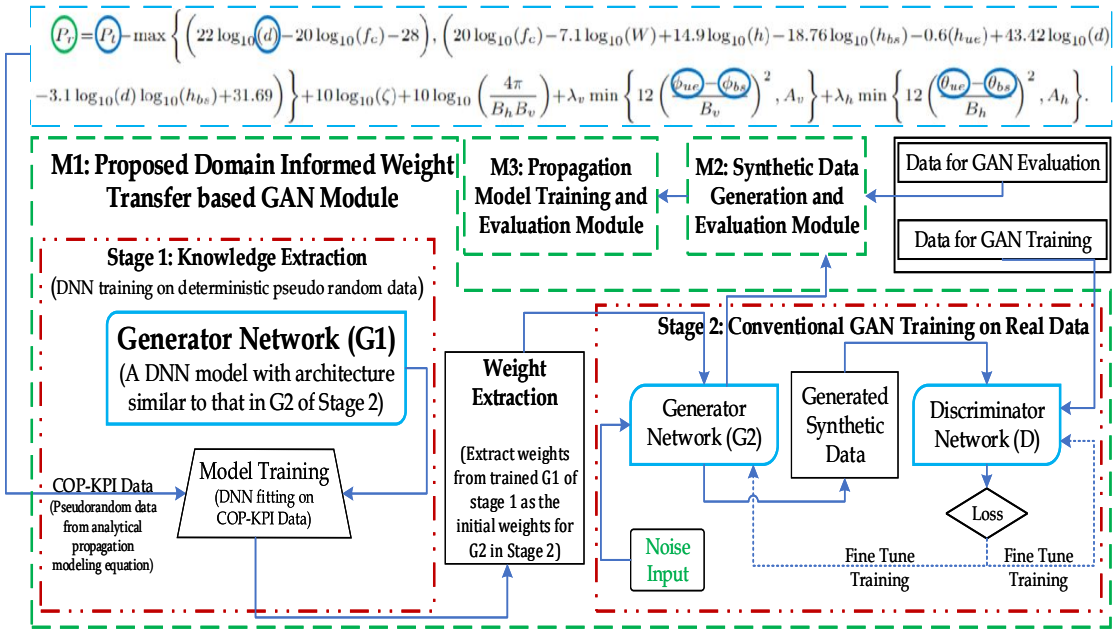


Fig. 4.1: An overview of the proposed framework for generative adversarial network-based propagation model augmentation in data-scarce scenarios. The framework is organized into three core modules: M1 handles knowledge extraction and domain-informed training of generative adversarial networks using weight transfer; M2 is responsible for generating and evaluating synthetic data; and M3 covers regression model training and benchmarking using both original and augmented data.

by minimizing error metrics, such as the root mean square error. This approach is effective for capturing complex, nonlinear relationships in diverse environments and accommodating variations in terrain and clutter types. A key challenge in machine learning based propagation modeling is data scarcity, which can hinder model generalization and reliability. Addressing this issue requires strategies to augment the training datasets and improve the model performance, as discussed in the subsequent sections.

4.3 Proposed Domain Informed Weight Transfer GAN for Data Generation

In this section, we discuss the proposed framework, which employs a domain-informed approach for weight transfer GAN-based synthetic data generation. We

first present a brief overview of the entire framework, and then delve into the details of its modules.

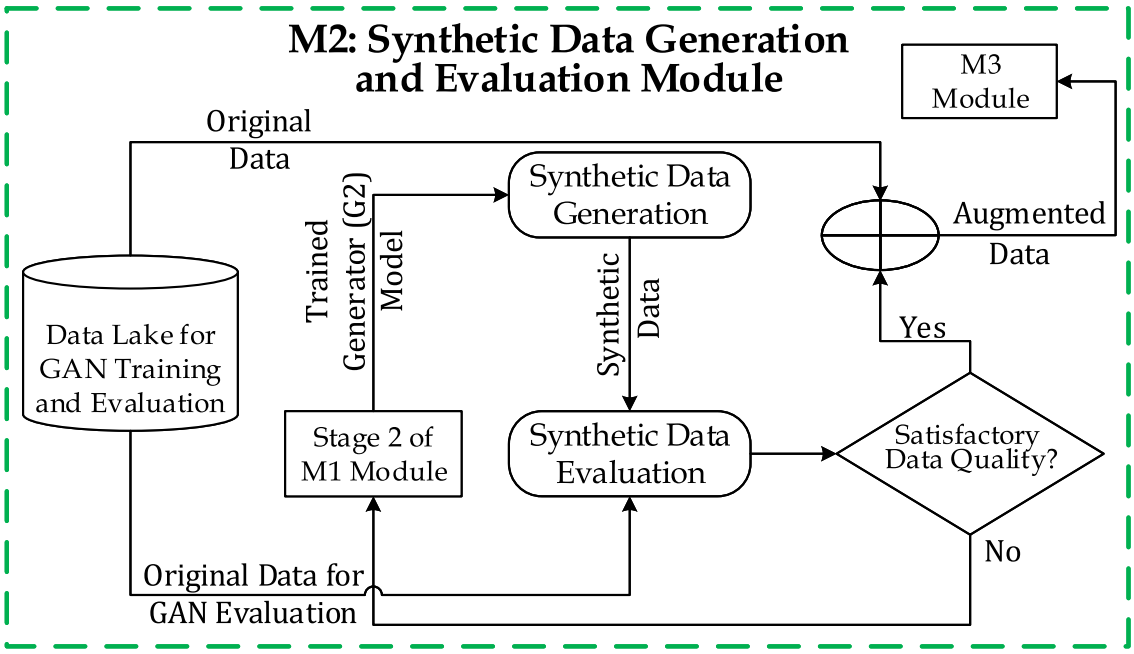


Fig. 4.2: Details of the M2 module of the proposed framework, responsible for generating synthetic data using the trained generator (G2) and evaluating its quality against the original data. Data augmentation proceeds only if the synthetic data meets specified evaluation thresholds; otherwise, the process is iteratively refined.

4.3.1 Overview of the Proposed Framework

The proposed framework is designed to address the challenge of training reliable propagation models under data scarcity by leveraging synthetic data augmentation guided by domain knowledge. As illustrated across Figs. 4.1–4.3, the framework consists of three interlinked modules that collectively enable efficient training, data enrichment, and predictive modeling under sparse conditions.

The first module (Fig. 4.1) focuses on domain-informed generative modeling using a two-stage GAN training strategy. In Stage 1, a generator network (G1) is trained using deterministic pseudo-random data generated from analytical propagation equations. This stage encodes domain-specific knowledge into the G1 model,

particularly in environments where collecting real-world measurements is impractical or limited. The trained weights from G1 are then extracted and used to initialize a second generator network (G2) in Stage 2. G2 undergoes conventional generative adversarial network training on limited real datasets, aided by a discriminator network (D) to refine the synthetic data quality. This weight transfer mechanism promotes faster convergence and improved generalization, especially when training data is sparse.

Module 2 (Fig. 4.2) handles the generation and evaluation of synthetic data. The generator model (G2), trained in Module 1, is used to synthesize new data samples, which are evaluated based on predefined statistical quality metrics. Only synthetic data that passes these quality checks is selected for augmentation. The approved samples are then combined with the original dataset to form a higher-quality, more diverse training corpus. This iterative evaluation loop ensures that only data with meaningful statistical fidelity is propagated to the learning stages.

In Module 3 (Fig. 4.3), the augmented data is used to train and test regression models for wireless propagation modeling. Two parallel training streams are executed: one on the original dataset (Model A) and the other on the augmented dataset (Model B). Both undergo the same preprocessing steps and are subsequently benchmarked to evaluate prediction performance. The comparison between these models highlights the impact of synthetic data augmentation on prediction accuracy, generalization, and model robustness.

4.3.2 M1: Proposed Domain Informed Weight Transfer based GAN

The first important module of this framework focuses on the proposed domain-informed weight transfer-based generative adversarial network, where knowledge

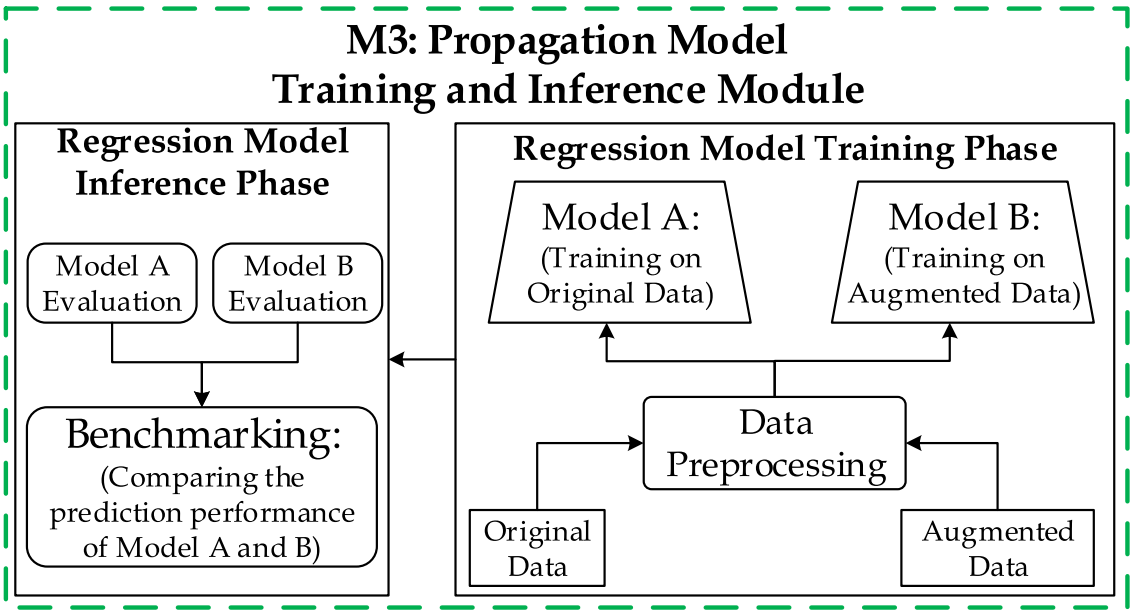


Fig. 4.3: Details of the M3 module of the proposed framework, which involves training regression models on both original and augmented datasets (Model A and Model B, respectively), followed by inference and performance benchmarking to assess the utility of generative adversarial network-based data augmentation.

is extracted from a pseudo-random analytical equation. The formulation of the propagation modeling equation used in knowledge extraction is discussed below.

Analytical Propagation Modeling Equation Formulation to get the Domain Knowledge

In this study, it is essential to establish a connection between the inputs and outputs when formulating an analytical equation, considering different characteristics and the target variable. By leveraging expertise in the field, we pinpoint critical features that accurately capture the physical and geometric attributes of the signal propagation environment.

The proposed methodology is exemplified by focusing on the fundamental coverage metric, reference signal received power. When the RSRP is employed, it is possible to derive other key performance indicators, such as the SINR or channel capacity. Consequently, for a specific location between the base station and user, the equation

for calculating the received power RSRP of a user can be expressed as follows,

$$P_r[\text{dBm}] = P_t - PL + G - L + X, \tag{4.1}$$

where, P_t is the power transmitted by the BS. In this context, PL stands for path loss, G represents antenna gain, L indicates attenuation from obstacles such as buildings and trees, and X covers additional losses from the BS cable and equipment. According to 3GPP TR 36.873 Release 12 [30], the path loss model, PL, for the LoS and non-LoS scenarios in a 3D UMa setting can be described as a function of frequency, f_c, distance, d, BS height, h_{bs}, UE height, h_{ut}, building height, h, and street width W. The path loss is calculated as $PL[dB] = \max(PL_{LoS}, PL_{NLoS})$, which indicates that it represents the maximum path loss in both the LoS and NLoS scenarios. Moreover, these path-loss models specified in the standard are valid for frequency ranges from 2 GHz to 6 GHz, considering variations in antenna heights,

$$PL_{LoS}(d, f_c) = 22.0 \log_{10}(d) + 28.0 + 20 \log_{10}(f_c). \tag{4.2}$$

This part of the analytical formula calculates the path loss for a direct connection between the user and the base station that serves it. In this context, the constant $c = 3.0 \times 10^8$ m/s represents the speed of propagation in vacuum,

$$\begin{aligned} PL_{3D-UMa-NLoS} = 161.04 - 7.1 \log_{10}(W) + 7.5 \log_{10}(h) - \left(24.37 - 3.7 \left(\frac{h}{h_{bs}}\right)^2\right) \log_{10}(h_{bs}) \\ + 20 \log_{10}(f_c) + (43.42 - 3.1 \log_{10}(h_{bs})) \\ (\log_{10}(d) - 3) - \left(3.2 (\log_{10}(17.625))^2 - 4.97\right) - 0.6(h_{ut} - 1.5). \end{aligned} \tag{4.3}$$

This part of the analytical equation describes signal attenuation in an NLoS setting, illustrating a scenario in which there is no direct transmission path between the UE and its serving BS. According to the recommendation of 3GPP [30], the antenna

gain G in (4.1) is defined as the product of the maximum antenna gain, G_{max} and the antenna attenuation, A_{att}, expressed as $G = G_{max} \cdot A_{att}$. The value of G_{max} depends on the efficiency of the antenna ζ, as well as the horizontal and vertical beamwidths B_h and B_v, and is associated with the directivity of the antenna,

$$G_{\max}\left(B_h, B_v, \zeta\right) = \zeta D = \zeta \frac{4\pi}{B_h B_v}. \tag{4.4}$$

The value of A_{att} is estimated following the 3GPP guideline,

$$A_{att}\left(B_h, B_v, \phi_u, \phi_{tilt}, \theta_u, \theta_{azi}, \lambda_h, \lambda_v, A_h, A_v\right)[\mathrm{dB}] = \\ \lambda_v \min[12(\frac{\phi_u - \phi_{tilt}}{B_v})^2, A_v] + \lambda_h \min[12(\frac{\theta_u - \theta_{azi}}{B_h})^2, A_h]. \tag{4.5}$$

The azimuth angles for the base station and user equipment are denoted by θ_u and θ_{azi}, respectively. Furthermore, the tilt angles for the base station and user equipment are as ϕ_u and ϕ_{tilt}, respectively. The weighting factors for both directions of the beam pattern are given by λ_h and λ_v, respectively. In addition, the maximum horizontal and vertical attenuations for the sides and back of the bore-sight are indicated by A_h and A_v, respectively. Therefore, the comprehensive analytical formula for calculating the coverage of the RSRP for a user, incorporating various configuration parameters, is expressed in (4.6). Initially defining RSRP, (4.1) is now formulated as a function of different COPs, as elaborated in (4.6). Acting as a basic, crude analytical expression, (4.6) encompasses intricate interconnections within the wireless system.

Knowledge Extraction and GAN Training on Real Data

Module 1, encompasses two crucial stages aimed at extracting knowledge and training the generative adversarial networks for synthetic data generation.

$$P_r(d, f_c, W, h, h_{ut}, h_{bs}, B_h, B_v, \phi_{ue}, \phi_{bs}, \theta_{ue}, \theta_{bs}, \lambda_h, \lambda_v, A_h, A_v) = P_t -$$
$$\max[(22\log_{10}(d) - 20\log_{10}(f_c) - 28),$$
$$(20\log_{10}(f_c) - 7.1\log_{10}(W) + 14.9\log_{10}(h) - 18.76\log_{10}(h_{bs}) - 0.6(h_{ut})$$
$$- 3.1\log_{10}(d)\log_{10}(h_{bs}) + 43.42\log_{10}(d) + 31.69)] + 10\log_{10}(\zeta) +$$
$$10\log_{10}(\frac{4\pi}{B_h B_v}) + \lambda_v \min[12(\frac{\phi_{ue} - \phi_{bs}}{B_v})^2, A_v] + \lambda_h \min[12(\frac{\theta_{ue} - \theta_{bs}}{B_h})^2, A_h]. \quad (4.6)$$

Fig. 4.4: This equation depicts the comprehensive analytical equation derived from integrating the (4.4) and (4.5) into (4.1).

- **Stage 1: Knowledge Extraction by DNN Training:** In initial stage, the objective is to train a **Generator Network (G1)** using deterministic pseudo-random data derived from the COP-KPI datasets. This stage is critical for capturing the underlying patterns in the data. The **Generator Network (G1)** is designed with a layer structure similar to the subsequent **Generator Network (G2)** to facilitate seamless weight transfer. The training process involves fitting a deep neural network model to the COP-KPI datasets, which serve as a proxy for real-world propagation modeling data. By training G1 on this deterministic data, the model learns the essential features and patterns that are encoded into the network's weights. Once the training is complete, the trained weights from G1 are extracted and preserved for use in the next stage. This knowledge extraction process ensures that the foundational patterns and features identified by G1 are effectively transferred to G2, thereby setting the stage for improved generation of synthetic data.

- **Stage 2: Conventional GAN Training on Real Data:** Stage 2 builds on the knowledge extracted in Stage 1 by utilizing the trained weights from G1 to initialize the **Generator Network (G2)**. This stage involves a conventional generative adversarial network setup in which G2 generates synthetic data while a **Discriminator Network (D)** evaluates its quality. The process begins with G2 generating synthetic data from the noise input, which is then

fed into the discriminator network. The discriminator distinguishes between the real and synthetic data and provides feedback to G2. Both the generator and discriminator networks undergo fine-tuning using a real dataset, allowing the generative adversarial network to iteratively improve the quality of the synthetic data generated by G2. The fine-tuning process ensures that G2 can produce high-fidelity synthetic data that closely mimics real-world data distributions. This stage not only enhances the quality of synthetic data but also leverages the domain-specific knowledge encoded in the weights transferred from G1, resulting in more accurate and reliable data generation.

Improved Validation

To enhance the training process of the generative adversarial network for tabular data, we incorporated a quality-check mechanism into its training setup. In this approach, after each iteration, synthetic data is generated by the trained generative adversarial network and evaluated against a set of high-quality, real data. Unlike conventional deep neural network training, where the loss function guides early stopping, the losses of the generator and discriminator in the generative adversarial network do not follow a consistent trend. This quality-based validation process adds an additional layer of assurance, ensuring the generation of high-fidelity synthetic data. Furthermore, the generative adversarial network training continues based on the trends observed in the quality of the generated data, irrespective of the individual loss trends, until the quality metrics plateau, indicating convergence.

4.3.3 M2: Synthetic Data Generation & Evaluation Module

Following the completion of GAN training in Module 1, Module 2 (illustrated in Fig. 4.2) focuses on generating synthetic data using the trained Generator Network (G2) and evaluating its quality. G2, initialized with weights transferred from the

analytically informed G1, receives noise input and produces synthetic data samples intended to replicate the distributional characteristics of real-world propagation measurements.

Once generated, the synthetic data undergoes a rigorous evaluation phase using statistical metrics such as marginal distribution alignment (e.g., KS complement) and pairwise correlation similarity. These metrics evaluate how effectively the synthetic data replicates the structural and statistical properties of the original dataset. Only data that meets predefined quality thresholds is considered acceptable for augmentation. If the synthetic samples fail to meet these standards, the generation-evaluation process can be repeated with refined GAN configurations or re-initialized inputs.

When the synthetic data is deemed satisfactory, it is combined with the original dataset to form an augmented training set. This enriched dataset aims to improve the diversity and completeness of training samples, especially in scenarios where collecting large-scale measurements is impractical or costly. The augmented dataset is subsequently passed to Module 3 for downstream learning tasks.

4.3.4 M3: Propagation Model Training & Inference Module

As shown in Fig. 4.3, Module 3 is dedicated to evaluating the impact of synthetic data augmentation on model training and generalization. This module comprises two stages: the regression model training phase and the inference phase. In the training phase, two parallel learning streams are established. The first stream trains a model solely on the original dataset, serving as a baseline. The second stream trains an identical model architecture on the augmented dataset that combines original and high-fidelity synthetic data from Module 2. Before training, both datasets are passed through the same preprocessing pipeline to ensure consistency in format and feature normalization.

Once trained, both models are evaluated using a standardized test set that includes diverse propagation conditions. The inference phase aims to benchmark their generalization performance, particularly under conditions not seen during training. Performance is assessed in terms of metrics such as root mean squared error and adjusted R^2, allowing for quantitative comparison between models trained with and without synthetic data augmentation. This dual-stream approach not only enables a fair performance comparison but also illustrates the practical utility of domain-informed synthetic augmentation in improving the robustness and predictive accuracy of data-driven propagation models.

Table 4.1: Simulation parameters defining the propagation environment, including power, frequency, antenna settings, and spatial factors affecting signal behavior in ultra-dense wireless scenarios.

Parameter Name	**Symbol**	**Value**
Transmit Power	P_t	$[10, \quad 43]$ dBW
Distance (3D)	d_{3D}	$[10 - 2000]$ m
Carrier Frequency	f_c	2.4 GHz
Bandwidth	W	20
Height	h	30
Base Station Tilt Angle	$\phi_{\text{bs_tilt}}$	$[0, \quad 6^o]$
User Equipment Tilt Angle	$\phi_{\text{ue_tilt}}$	$[-86, \quad -9^o]$
Base Station Azimuth Angle	$\theta_{\text{bs_azim}}$	$[40, \quad -320^o]$
User Equipment Azimuth Angle	$\theta_{\text{ue_azim}}$	$[0, \quad -360^o]$
Vertical Wavelength factor	λ_v	1
Horizontal Wavelength factor	λ_h	1
Antenna Gain (Horizontal)	A_h	30 dB
Antenna Gain (Vertical)	A_v	30 dB
Beamwidth (Horizontal)	B_h	65^o
Beamwidth (Vertical)	B_v	65^o
Base Station Height	h_{bs}	30
User Equipment Height	h_{ue}	3
Path Loss	L	0
Path Loss Exponent	X	50
Shadowing Factor	ζ	0.7

4.4 Simulation Setup & Performance Evaluation

In this section, we discuss the simulation setup and the performance of the proposed framework. We first discuss the details of the experimental setup and baseline schemes.

4.4.1 Experimental Setup and Baseline Schemes

Experimental Setup

The experimental setup is designed to evaluate the effectiveness of the proposed propagation modeling framework using a detailed simulation environment created using Atoll software. The Atoll is a comprehensive radio network planning and optimization tool that enables the simulation of complex network environments with high precision. The simulation encompasses a geographic area of 1000 $m \times 1000$ m, which is served by 10 macrocells. This setup aims to replicate a realistic urban network scenario by capturing the essential characteristics of a densely populated wireless environment. The simulation parameters governing this setup are detailed in Table 4.1, which provides a comprehensive overview of the network configuration and conditions used in the experiments.

To systematically analyze the radio signal propagation within this area, the geographic region is segmented into discrete spatial bins. Within each bin, the RSRP values are calculated for multiple users. The RSRP value for each bin is determined by averaging the RSRP values of all the users located within that bin, thereby providing a robust measure of the signal strength distribution across the simulation area. A total of $1,000$ users are distributed across the simulation area, following a Poisson distribution. This distribution pattern is chosen to realistically model the random nature of user locations in an urban environment. The dataset generated

from this simulation comprises $5,000$ instances, which are divided into subsets of varying sizes for training the GANs and for testing purposes.

For the purpose of GAN training, subsets of the dataset are used to train the models to generate synthetic data that closely mimics the real-world data. To assess the quality of the synthetic data generated by the GANs, a portion of the dataset, approximately 2500 instances, is kept aside for testing. This testing dataset is used to evaluate the quality of GAN data generation and to benchmark the performance of the machine learning model in both the baseline and proposed schemes. The evaluation process involves comparing the performance of machine learning models trained on the augmented dataset (the original dataset plus GAN-generated data) against models trained on the original dataset alone. This comparative analysis helps in understanding the impact of data augmentation on model accuracy and robustness. Therefore, the experimental setup provides a controlled environment for rigorously testing and validating the proposed propagation modeling framework, ensuring its applicability and effectiveness in real-world scenarios.

Baseline Schemes

In order to compare and evaluate the data generation performance of the proposed

- **Gaussian copula:** The Gaussian copula method is a statistical technique for data synthesis that captures and replicates the complex correlations between variables in a dataset. It first identifies the individual probability distributions of each column, standardizing them into normal distributions through an inverse cumulative distribution function transformation. Next, it learns inter-variable correlations to construct a copula model, which encapsulates these relationships. Synthetic data is then sampled from this model, preserving the original dataset's correlation structure while offering computational efficiency.

- **Conditional Tabular Generative Adversarial Network (CTGAN):** CTGAN is a GAN-based framework designed for synthesizing tabular data, excelling in handling non-Gaussian and multimodal distributions. It incorporates a conditional generator and a training-by-sampling mechanism to balance discrete column representation, ensuring authenticity in conditional distributions. Continuous variables are modeled using a variational Gaussian mixture model to effectively capture distribution modes, while discrete columns are balanced through a specialized sampling strategy. Architecturally, CTGAN employs densely connected layers in its generator and discriminator, enabling the creation of high-fidelity synthetic data that addresses the complexities and imbalances typical of real-world datasets.

Table 4.2: Ablation analysis comparing WTGAN with CTGAN (no weight transfer), highlighting improvements in fidelity (KS complement), correlation, and regression accuracy on synthetic data.

Metric	**CTGAN (no WT)**	**WTGAN**	**% Improvement**
KS Complement (↑)	0.784	0.847	+8.0%
Pearson Correlation (↑)	0.874	0.912	+4.3%
RMSE (↓)	6.49	5.70	+12.2%
Adjusted R^2 (↑)	0.82	0.86	+4.9%

4.4.2 Ablation Study: Impact of Weight Transfer GAN

To investigate the impact of weight transfer in the proposed domain-informed generative adversarial framework, we perform an ablation study by comparing two configurations. In the first configuration, the second-stage generator is initialized using the learned weights from a deep neural network trained on analytically generated pseudo-random data for propagation. In the second configuration, the same generator is initialized randomly, without prior knowledge, while maintaining the network architecture and training pipeline. This controlled setup allows us to isolate and assess the specific influence of the weight transfer mechanism.

The results of this comparative analysis, summarized in Table 4.2, reveal consistent improvements across all evaluation metrics when domain-informed weight transfer is applied. In particular, the Kolmogorov-Smirnov Complement (KSC) a measure of the similarity between the original and synthetic data distributions shows an improvement of approximately 8%. The Pearson correlation coefficient also exhibits a noticeable gain, reflecting stronger linear dependence between absolute and generated values. Additionally, the root mean square error between the predicted and actual values is significantly reduced, indicating enhanced fidelity of the generated data. Finally, the adjusted coefficient of determination also improves, suggesting that the augmented data contribute positively to the predictive capacity of the downstream model.

These results demonstrate the effectiveness of initializing the generator with domain-aligned weights. The observed gains underscore how incorporating prior domain knowledge into the early stages of training can enhance convergence, improve data quality, and support better downstream performance in regression tasks. This highlights the importance of the proposed weight transfer strategy as a key component of the overall framework.

4.4.3 Comparison with Generative Models in Data-Scarce Regimes

To evaluate the practical utility of the proposed framework, we compare its performance with that of two widely recognized generative models for tabular data synthesis: the conditional tabular generative adversarial network and the tabular variational autoencoder. These models have been extensively adopted in recent studies for generating realistic synthetic data in various domains, including healthcare, finance, and telecommunications. However, they are fundamentally data-driven and do not incorporate domain knowledge, which can be a critical limitation

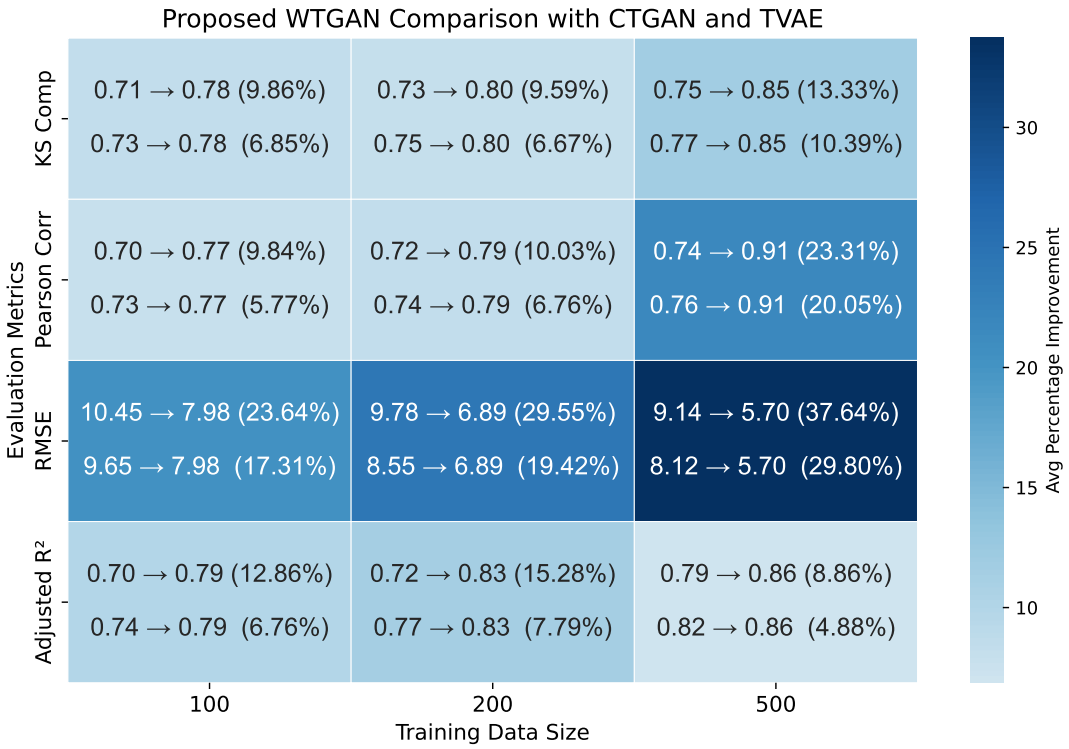


Fig. 4.5: Performance comparison of WTGAN against CTGAN and TVAE across low, medium, and high data regimes, showing consistent gains of WTGAN in KS complement, Pearson correlation, RMSE, and adjusted R^2, under data scarcity.

in scenarios with sparse or noisy datasets.

In contrast, the proposed approach incorporates domain knowledge through a weight transfer mechanism, where initial representations learned from analytically derived propagation data guide the generative training process. This mechanism is particularly advantageous when real-world data is limited, as it provides a strong inductive bias aligned with the underlying physical principles of wireless propagation.

Figure 4.5 illustrates the comparative performance of the proposed approach across multiple training data regimes, ranging from 100 to 500 samples, using four evaluation metrics that assess both the realism and predictive quality of the generated data. These metrics include the Kolmogorov-Smirnov complement for column-wise distribution alignment, Pearson correlation for pairwise relationships, root mean squared error for predictive fidelity, and the adjusted coefficient of determination

to evaluate regression performance.

Several notable trends emerge from this comparison. First, under extremely low data conditions (e.g., 100 samples), the proposed method demonstrates substantial improvements across all metrics. For example, the root mean squared error in the predictive task is reduced by nearly 38% compared to baseline methods, reflecting a significantly closer match to the target data distribution. Similarly, gains in correlation-based metrics, such as Pearson correlation, exceed 20% in some cases, indicating a more faithful preservation of inter-variable dependencies.

Second, while the performance gap narrows with larger training datasets (e.g., 500 samples), the proposed framework consistently maintains a lead over both baseline models. This sustained advantage confirms the effectiveness of the domain-informed initialization not only in low-data regimes but also in moderate ones. Importantly, the improvement is not limited to statistical alignment but extends to downstream regression performance, where improvements in the adjusted coefficient of determination reinforce the utility of synthetic data in practical predictive modeling.

4.4.4 Performance Variation with GAN Training Data Size

In this section, we evaluate the performance of various generative models in generating synthetic data to model the wireless propagation. The assessment focuses on key metrics that measure the fidelity and quality of the artificial data in comparison to the original dataset. By analyzing these metrics, we aim to understand the effectiveness of the proposed WTGAN models in capturing the complex relationships inherent in the data and compare their performance with that of baseline models, such as the Gaussian copula and CTGAN. The following subsections detail the evaluation of the column shape metric and the column pair trend, providing insights into the strengths and limitations of each approach.

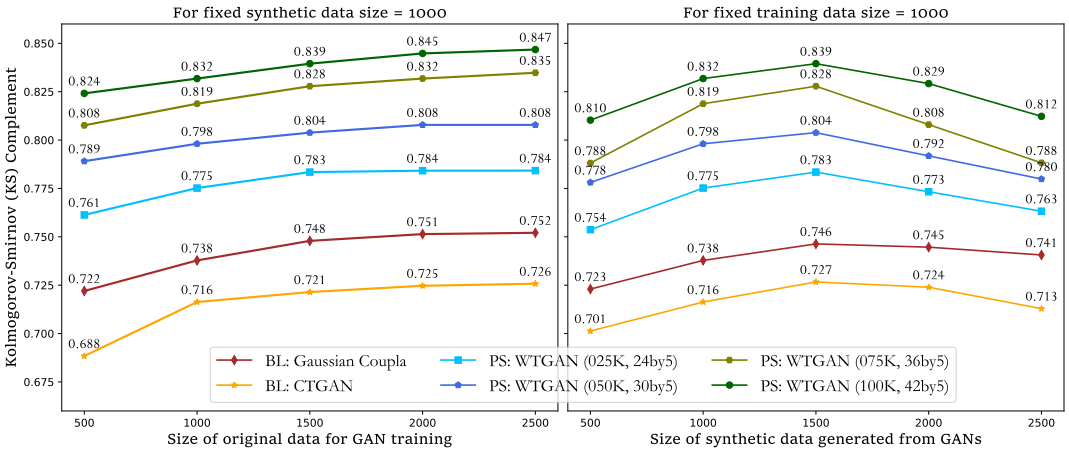


Fig. 4.6: Comparing the Column Shape metric of the baseline (Gaussian Copula, CTGAN) and different variants of the proposed WTGAN scheme, against different data sizes for (a) GAN training and (b) synthetic data generation.

Column Shape Metric

Figure 4.6 presents a detailed comparison of the Column Shape metric, evaluated using the KS complement, which quantifies the similarity between the distributions of original and synthetic data columns. This metric serves as a strong indicator of how well a generative model captures the underlying statistical properties of individual features in the dataset.

The left plot in Figure 4.6 investigates how the size of training data influences the fidelity of generated synthetic samples, while keeping the synthetic data size fixed at 1000 samples. As the training data increases from 500 to 2500 samples, all models exhibit a gradual improvement in the KS complement metric, although the rate of progress and overall performance vary. Baseline models, including the Gaussian copula and CTGAN, show only modest gains, reaching a plateau beyond 2000 samples. By contrast, the proposed weight transfer-based generative models show consistent improvements with increased training data. Notably, the variant configured with the largest first-stage training (100K samples) and a deeper neural network architecture (42 layers, 5 neurons per layer) achieves the highest KS complement value, surpassing the Gaussian copula and CTGAN by margins of approximately 12

and 17 percentage points, respectively. This suggests that incorporating domain-informed initialization through weight transfer enables more efficient learning even with limited data.

The right plot in Figure 4.6 shifts the focus to how the quantity of synthetic data influences the metric, with the generative adversarial network training data fixed at 1000 samples. Here again, the performance of baseline models stagnates or slightly degrades as synthetic data volume increases beyond 1500 samples, likely due to overfitting or saturation in model learning. On the other hand, the proposed generative schemes maintain strong and consistent performance across all synthetic data sizes. While there is a slight decline in Kolmogorov-Smirnov complement for the largest synthetic size in some configurations, the results still remain substantially better than the baselines. This demonstrates that the proposed models not only utilize training data effectively but also scale well with larger synthetic data generation.

These results suggest that integrating domain knowledge through weight transfer enables the generative network to develop a more stable and generalized understanding of signal behavior, even when training data is limited. Unlike baseline models that tend to overfit or under-utilize available information, the proposed framework effectively bridges the gap between analytical models and data-driven methods. This enhanced capacity to reproduce realistic feature distributions strengthens the credibility and utility of synthetic datasets in downstream wireless modeling tasks. Moreover, the ability to sustain performance across varying synthetic data volumes demonstrates robustness, which is especially critical when deploying such generative methods in real-world settings where data availability and requirements may fluctuate. Overall, these findings demonstrate the practical viability of the proposed approach for enhancing data realism in constrained environments, laying the groundwork for more reliable propagation modeling and network design.

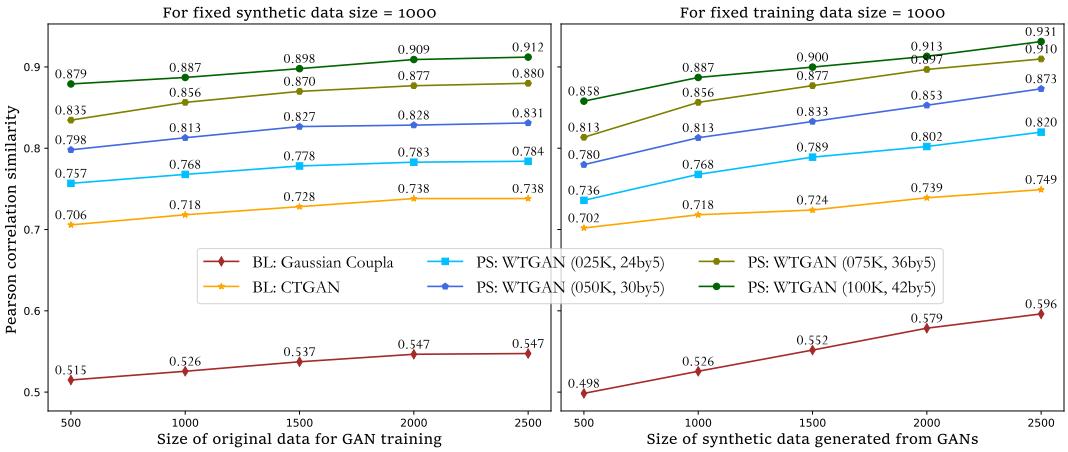


Fig. 4.7: Comparing the Column Pair Trends metric of the baseline (Gaussian Copula, CTGAN) and different variants of the proposed WTGAN scheme, against different data sizes for GAN training and synthetic data generation.

Column Pair Trends

To further evaluate the realism of the generated synthetic data, we examine how well the generative models capture inter-column relationships—an essential aspect for modeling the joint behavior of multiple propagation-related features. This evaluation is performed using the Pearson correlation similarity metric, which quantifies how closely the pairwise relationships in the synthetic dataset resemble those in the original data.

Fig. 4.7a presents the correlation similarity when the number of synthetic samples is held constant, while varying the training data size used for generative model learning. As the size of the training data increases, all models exhibit modest improvement in maintaining column-pair trends. However, the proposed domain-informed weight transfer approach demonstrates clear superiority. Notably, the model variant with pseudo-random training from 100,000 samples and a deeper generator network achieves the highest similarity score. At a training size of 2500 samples, this configuration exceeds the performance of Gaussian copula and Conditional Tabular GAN by margins of 66.5% and 23.6%, respectively. These findings underscore the value of using structured pre-training to better internalize the statistical dependencies

among features.

A similar trend is observed in Fig. 4.7b, where the training data size is fixed while the size of generated synthetic data varies. Although all models exhibit initial improvements with increasing synthetic data, the performance of baseline models saturates or declines slightly, likely due to the limited learning capacity when trained on scarce data. In contrast, the proposed framework continues to yield consistent improvements across the board. At 2500 synthetic samples, the proposed model achieves an improvement of 33.7% over Gaussian copula and 24.3% over Conditional Tabular GAN. This indicates that the pre-trained generator not only captures the marginal distributions effectively but also excels at preserving complex cross-feature dependencies.

These results highlight a significant practical implication: incorporating domain-informed pre-training enables generative models to maintain relational structure even when faced with data scarcity. This capability is crucial in wireless propagation modeling, where accurately capturing interactions between environmental and signal variables is essential for realistic simulation. The ability of the proposed framework to retain such relationships provides valuable consistency in downstream tasks, such as regression modeling, scenario simulation, or network planning, ultimately contributing to more resilient and trustworthy data-driven wireless solutions.

4.4.5 ML Applicability: Model Prediction Performance

This section evaluates the practical utility of different data augmentation strategies by analyzing the predictive performance of machine learning models trained on augmented datasets. Specifically, we aim to assess whether the synthetic data generated by the proposed scheme can effectively support model learning and enhance predictive accuracy. Tree-based regression models including XGBoost, CatBoost, and LightGBM are trained using the PyCaret automation framework [133], and their

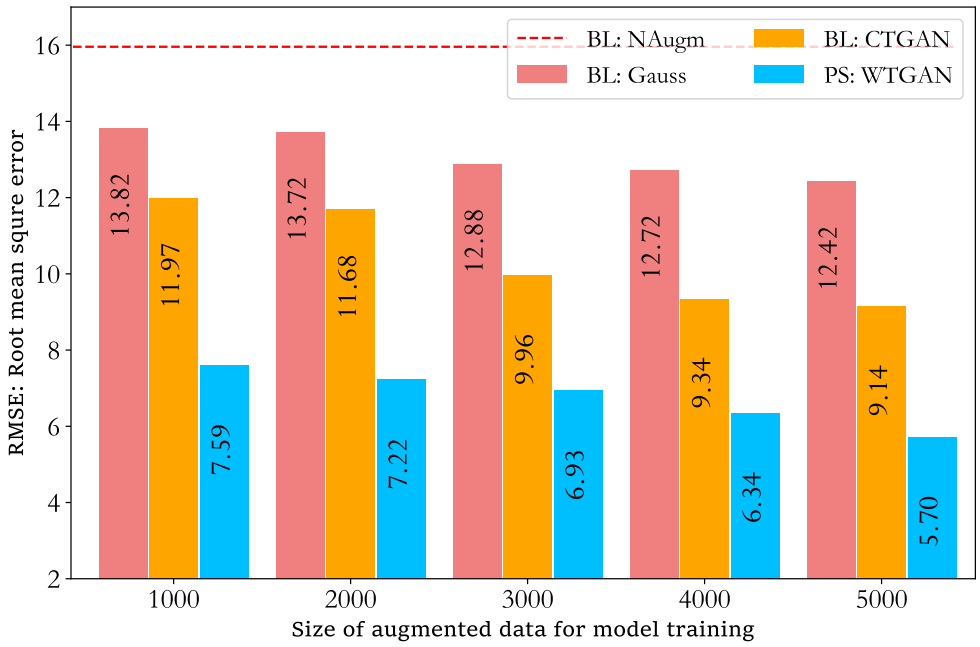


Fig. 4.8: Comparison for the *baseline* (NAugm, CTGAN, Gaussian Copula) and *proposed* (PS: WTGAN) schemes for the root mean square error metric against the increasing augmented data size.

averaged performance on test data is presented in Fig. 4.8 and Fig. 4.9. Fig. 4.8 illustrates the root mean square error values across different augmentation sizes, ranging from 1000 to 5000 synthetic samples. The non-augmented baseline (NAugm) consistently yields the highest RMSE, indicating poor generalization when only limited original data is used. In contrast, all augmentation strategies improve performance to varying degrees. Traditional techniques, such as the Gaussian copula and CTGAN, exhibit gradual reductions in RMSE with increasing augmentation size. However, their improvements are modest and appear to plateau, suggesting limitations in capturing the complex characteristics of data. The proposed weight transfer generative adversarial network, on the other hand, demonstrates a substantially sharper decline in RMSE. For example, when the augmented data size is 5000, WTGAN achieves an RMSE of 5.70, compared to 12.42 for Gaussian copula and 9.14 for CTGAN. This suggests that models trained on WTGAN-augmented data can generalize significantly better due to the realism and diversity embedded

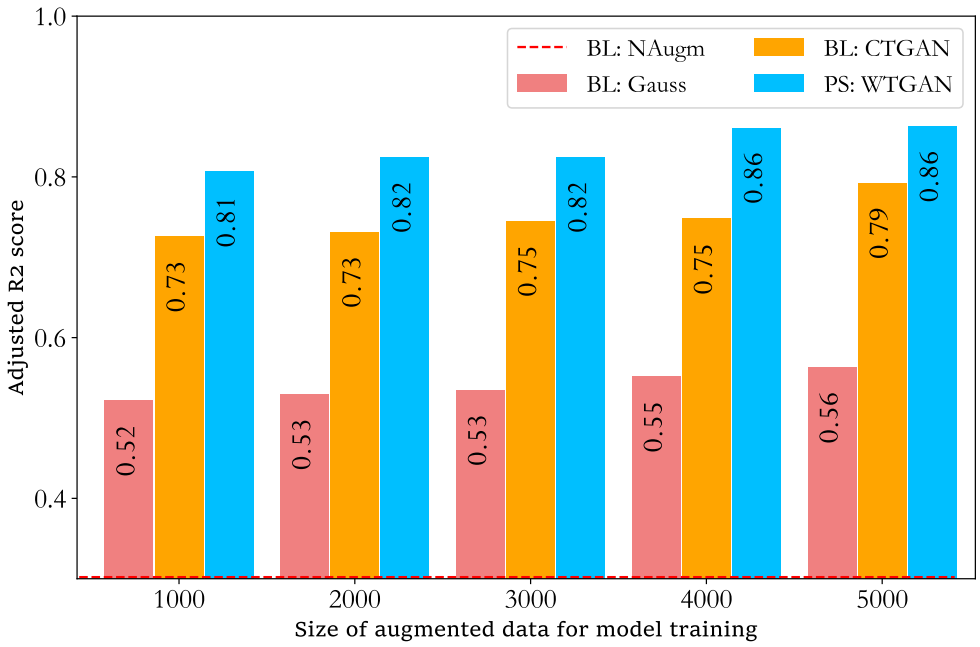


Fig. 4.9: Comparison for the *baseline* (NAugm, CTGAN, Gaussian copula) and *proposed* (PS: WTGAN) schemes for the adjusted R2 square metric against increasing augmented data size.

in the synthetic samples. Fig. 4.9 presents the adjusted coefficient of determination (Adjusted R^2), a metric that evaluates how well the model explains variance in the data while accounting for model complexity. The non-augmented baseline remains consistently low at 0.35, indicating underfitting due to insufficient training data. Gaussian copula and CTGAN again show moderate improvements with increased augmentation. However, their performance remains below that of the WTGAN approach at all data sizes. For instance, at 5000 samples, WTGAN achieves an Adjusted R^2 score of 0.86, compared to 0.56 for Gaussian copula and 0.79 for CTGAN. These results reveal that the WTGAN not only improves model accuracy but also maintains its explanatory power and robustness, which are crucial for real-world deployment.

Together, these findings provide strong evidence of the practical benefits offered by the proposed domain-informed generative model. The consistent improvement in predictive metrics across all data sizes confirms that integrating domain knowl-

edge and weight transfer not only enhances the fidelity of synthetic data but also translates to tangible gains in downstream learning tasks. This underscores WT-GAN's suitability as a reliable augmentation technique in data-constrained wireless propagation modeling environments.

4.5 Conclusion and Transition to Next Chapter

This chapter introduced a domain-informed generative framework to address the persistent challenge of data scarcity in wireless propagation modeling. Conventional data-driven models often require extensive labeled datasets, which are difficult to collect in real-world wireless environments. To overcome this limitation, we propose the weight transfer generative adversarial network. This novel architecture leverages domain knowledge through pre-trained analytical models and transfers their learned weights into a generator based on a generative adversarial network.

The weight transfer generative adversarial network framework was systematically evaluated using varying sizes of training data and different deep neural network configurations. Results show that the weight transfer generative adversarial network significantly improves regression accuracy and synthetic data fidelity in data-scarce conditions. By initializing the generator with domain-informed priors, the model converges faster and produces physically plausible outputs, even with as few as 5000 samples. This underscores the framework's potential in reducing dependency on extensive data collection, while preserving modeling accuracy.

The solution presented in this chapter represents a significant advancement in enhancing the resilience and generalizability of AI-based wireless modeling, particularly under the constraints of sparse training data. However, despite these advancements, generative adversarial network-based synthetic data generation introduces new concerns such as mode collapse, over-fitting to training distributions, and low-

diversity outputs. Addressing these concerns requires not only architectural innovation but also deeper control over the training dynamics.

The next chapter builds directly on these insights by exploring a complementary mechanism to enhance the stability of generative adversarial network training and improve the quality of synthetic data. Specifically, it presents a segmentation-enhanced framework that guides the training process of the generative adversarial network using attention masks derived from domain-informed thresholds. This architecture, known as attention-through-segmentation, enables the generator and discriminator to focus on semantically meaningful regions of the input space. As such, it addresses key shortcomings of standard generative adversarial networks and enhances their applicability in modeling wireless networks under real-world constraints.

CHAPTER 5

Enhancing AI Model Resilience to Distribution Shifts

This chapter presents a comprehensive study on building resilient, machine learning-based propagation models tailored for digital twin-driven cellular networks. Motivated by the need to balance realism, completeness, and computational efficiency, we explore a multi-stage approach that involves feature engineering, data augmentation through generative adversarial networks, and robust model training via attention-through-segmentation. The proposed methodology addresses critical challenges such as distribution shifts and sparse training data, which are common in real-world wireless environments. Through detailed evaluation, we demonstrate how each module contributes to improved model accuracy and generalization, laying the groundwork for reliable digital twin applications in next-generation networks.

5.1 Introduction

In the dynamic and ever-evolving landscape of wireless communication, the concept of Digital Twins (DTs) is rapidly gaining traction as a key tool to accelerate the development of next-generation cellular networks [20]. DTs are essentially real-time digital replicas of physical cellular networks, utilizing a combination of data and sophisticated modeling techniques to create a network simulation platform that is not only physically accurate but also constantly updated [21]. They are instrumental in providing real-time network status and facilitating the continuous prototyping, testing, and optimization of various solutions to improve network operations [20,21,134]. A critical aspect in recognizing the DT of future networks is the development of robust wireless network propagation models, given their pivotal role in enabling var-

ious functionalities. These models must embody essential characteristics, such as realism, completeness, and computational efficiency [135], for seamless integration of digital twins with the actual physical wireless network. These characteristics are vital to ensure that DTs accurately reflect the real network behavior and can be used effectively for network analysis and improvements [102, 103, 136].

Traditional propagation models, which are broadly classified into empirical, deterministic, and stochastic models, often fail to meet the comprehensive requirements essential for the effective implementation of DTs. For example, the aspect of realism in propagation models is typically achieved through ray tracing-based simulation methods [103]; however, these methods tend to be computationally intensive. This computational inefficiency becomes particularly problematic when considering the dynamic nature of wireless systems, which undergo constant changes over time. As a result, integrating such models with DTs based on real-time networks becomes a challenging task due to the significant computational resources required [102]. However, while empirical and stochastic approaches such as the COST-Hata model and ITU-R P.453-15 offer greater computational efficiency, they often lack fidelity to the realistic physical and geographic structure of the environment. This lack of realism leads to a deviation from accurate modeling, which limits their applicability in scenarios aimed at realizing digital twins, where precise network replication is crucial [22].

To address these shortcomings of traditional propagation models, there has been a significant shift towards leveraging data-driven approaches, particularly those based on machine learning and deep neural networks. These modern methodologies are emerging as promising alternatives for network modeling [23] because they aim to amalgamate the three critical characteristics mentioned above. To achieve completeness, these techniques are based on designing a diverse and comprehensive set of features using extensive datasets. These features are developed through an in-

depth analysis of the actual network environment, considering parameters on both the network side and the user side that influence signal propagation, thus achieving realism. Furthermore, modern AI methods capitalize on established practices, such as feature selection and model pruning, which have already proven their efficacy in other relevant domains to achieve computational efficiency [22]. For example, SHapley Additive exPlanations (SHAP) is employed to quantify the importance of different input features in predicting the reference signal received power, a critical performance indicator of signal strength in cellular networks. This approach not only enhances the interpretability of ML models but also provides the flexibility to balance completeness and computational efficiency. By leveraging SHAP's insights, designers can either incorporate a diverse set of features to ensure comprehensive modeling or focus on a subset of the most impactful features to optimize computational resources. The penetration of these advanced models into the field of wireless network propagation modeling represents a significant step toward the realization of more accurate, efficient, and realistic digital twins, which facilitates the advancement of cellular network technologies [24].

5.1.1 Related Work

Within the domain of wireless propagation modeling, extensive research has explored methodologies for accurate pathloss prediction, network planning, and coverage estimation. These works can be categorized into traditional non-machine learning-based approaches, traditional machine learning-based techniques, and advanced machine learning-based methodologies, with evolving solutions to address challenges such as distribution shifts and data scarcity.

Traditional Non-Machine Learning Approaches

Conventional propagation models rely on deterministic and stochastic frameworks, such as the Okumura-Hata [137] and COST231-Hata [138] models, which use empirical equations to predict path loss, reflection, and diffraction. Ray-tracing methods [139] offer greater accuracy by modeling signal propagation in three dimensions. While computationally efficient, these models often make simplifying assumptions that fail to capture the intricacies of real-world environments, particularly in dynamic and heterogeneous systems [140].

Initial Machine Learning Based Approaches

Machine learning brought a data-driven perspective to propagation modeling, enabling models to learn patterns from data. Initial machine learning based studies demonstrated significant improvements in prediction accuracy. For instance, neural networks have been successfully applied to macro-cell scenarios in [141], achieving high accuracy across various terrains. [142] used composite differential evolution algorithms to optimize neural network architectures, further enhancing precision. Similarly, [143] incorporated environmental characteristics into pathloss models, improving adaptability in heterogeneous networks. In the 3D domain, [24] captured the intricate spatial dynamics of wireless networks, while [22] combined artificial intelligence interpretability with 3D modeling for next-generation network coverage prediction. However, these methods are often limited by their reliance on large, diverse datasets for training, which are challenging to obtain in real-world settings.

Advanced Machine Learning Approaches for Complex Scenarios

Recent advancements in machine learning have addressed more complex and large-scale network scenarios. In outdoor cellular networks, [144] used image-to-image

learning paradigms to integrate measured data for cell-level RSRP estimation, improving coverage prediction. Similarly, [104] employed deep convolutional neural networks to map geographic inputs to signal strength distributions, emphasizing robustness and accuracy. For urban planning, [145] incorporated 3D city models and real-world measurements within a deep learning framework.

Indoor environments have also benefited from advancements in machine learning. In [146], RadioUNet was introduced as a high-resolution convolutional model for generating radio field estimates. Similarly, [147] proposed DeepREM for dense radio environment map reconstruction from sparse inputs, while [106] introduced EM DeepRay to enhance realism in indoor modeling. Beyond convolutional approaches, [148] adopted graph neural networks to model spatial relationships, and [149] used generative adversarial network-based augmentation to improve indoor localization accuracy. In the realm of 3D propagation modeling, advanced architectures such as RayProNet [150] and NeRF2 [151] demonstrated exceptional precision in capturing complex diffraction and scattering phenomena using continuous spatial representations. While these methods excel in specific scenarios, they often require large datasets and significant computational resources, limiting their adaptability to rapidly changing environments.

Addressing Distribution Shifts and Data Scarcity

The challenge of distribution shifts, where training and test data distributions differ significantly, has been widely studied across various domains of machine learning. In wireless propagation modeling, this issue is particularly pronounced due to the disparity in data availability between urban and rural areas. Urban environments, being more densely populated, often provide abundant data, leading to models that are biased toward urban scenarios, while their performance deteriorates in underrepresented rural or remote areas [26, 27].

To address these challenges, several studies have explored strategies to mitigate the impact of distribution shifts. For instance, [152] categorized and benchmarked types of shifts across diverse datasets, while [153] proposed techniques for improving generalization under shifting conditions. However, these efforts predominantly focus on image, video, or speech data, leaving a gap in addressing shifts in tabular datasets, which are crucial for modeling wireless networks. The lack of tailored solutions for propagation modeling underscores the need for methodologies that can account for distribution disparities while maintaining predictive accuracy in real-world scenarios.

GAN-Based Approaches for Data Augmentation

Generative adversarial networks have emerged as transformative tools in addressing data scarcity and imbalance, particularly in wireless propagation modeling. GAN-based methods generate synthetic data by learning complex data distributions, offering significant advantages over traditional data augmentation techniques, which often rely on domain-specific knowledge and fail to capture the intricate relationships in tabular datasets [117–119]. This subsection discusses various GAN-based approaches, their applications, and the advancements they bring to wireless networks.

Early implementations of generative adversarial networks for wireless networks focused on generating realistic synthetic data that reflects channel conditions without requiring extensive domain expertise. For example, GAN-based models trained on raw measurement data autonomously captured wireless channel characteristics, simplifying the modeling process [122]. Extensions of these methods incorporated advanced architectures, such as gated recurrent units and long short-term memory networks, to synthesize channel characteristics for the sixth generation communications, achieving improved accuracy and computational efficiency [123, 124].

Specific use cases of generative adversarial networks in wireless networks demonstrate their versatility. Conditional generative adversarial networks have been applied to air-to-ground communication, accurately modeling parameters such as path gain and Doppler frequency based on location and velocity [125]. Similarly, generative adversarial networks have been employed to enhance channel estimation in intelligent reflecting surface-aided systems, significantly outperforming conventional estimation techniques [126, 127]. Path loss generative adversarial networks generate propagation maps from satellite images and terrain data, offering computationally efficient alternatives to traditional ray-tracing methods [128].

Despite these advancements, traditional generative adversarial network architectures often face challenges, including mode collapse and instability during training. To mitigate these issues, domain-informed and conditional generative adversarial network frameworks have been introduced. Conditional tabular generative adversarial network [154], explicitly designed for tabular data, incorporates conditional sampling mechanisms to address imbalances in data distributions effectively. In wireless networks, a conditional tabular generative adversarial network has demonstrated promise by generating balanced datasets for scenarios with significant disparities, such as urban-to-rural data differences [153]. Advanced frameworks, such as tabular transformer generative adversarial network [155], which integrate transfer learning and transformer-based architectures, further enhance the applicability of generative adversarial networks by improving performance under data-scarce conditions.

However, most GAN-based approaches have focused on static datasets or image-based applications, leaving a gap in addressing dynamic distribution shifts and tabular data in wireless propagation modeling. To bridge this gap, this work proposes a domain-informed generative adversarial network framework tailored for tabular data under data-scarce conditions. By integrating feature-specific augmentation

and iterative conditioning, the proposed methodology enhances the quality and representativeness of synthetic data, effectively addressing both data scarcity and distribution shifts.

5.1.2 Problem Statement and Motivation

Despite significant advancements in machine learning and generative adversarial network-based approaches, critical challenges persist in modeling wireless propagation. Data scarcity and imbalance, particularly between urban and rural regions, create biased models that under perform in underrepresented scenarios [25, 26, 156]. Additionally, distribution shifts, where testing data diverge significantly from the training data [27], further degrade model generalizability and robustness. While generative adversarial networks offer potential solutions by augmenting datasets to balance feature distributions, their current implementations in wireless propagation modeling are limited. Most approaches focus on static datasets or single test scenarios, lacking the flexibility required for real-world dynamic environments.

This work addresses these gaps by proposing a robust multistage framework that integrates a conditional tabular generative adversarial network for data augmentation and attention through segmentation, thereby enhancing training. The proposed methodology explicitly targets data imbalances and distribution shifts, enabling the development of more resilient and adaptable machine learning models for wireless networks. The following research questions guide this study:

- How do machine learning models perform under significant distribution shifts between training and testing data?
- What enhancements can improve the resilience of these models to maintain accuracy across diverse and dynamic test scenarios?

To address these questions, we conduct a comprehensive analysis of model resilience and propose novel techniques, including data augmentation based on generative adversarial networks and segmentation-based training. The proposed framework bridges existing gaps, offering robust and scalable solutions for modern wireless networks. A preliminary version of this work was presented in [157], with this manuscript providing substantial extensions and enhancements to address additional aspects of resilient propagation modeling. *A preliminary version of this work was presented in [157]. This manuscript significantly extends the conference paper by incorporating enhanced methodologies, detailed performance analyses, and broader discussions to address additional aspects of resilient propagation modeling in modern wireless networks.* Some initial findings from this proposed AtS approach are accepted in [157]; however, here we perform a comprehensive analysis for various bin sizes, data sizes, and mode complexity.

5.1.3 Contribution Summarized

The main contributions of this work are summarized below:

- **Comprehensive Framework for Resilient Propagation Modeling:** We propose a novel, end-to-end framework for resilient propagation modeling in wireless networks. The framework integrates data-driven methodologies with advanced generative adversarial network-based data augmentation and a segmentation-driven attention mechanism. It addresses the dual challenges of data scarcity and distribution shifts, achieving significant improvements in model robustness and applicability to diverse real-world scenarios.
- **Resilience Analysis of Machine Learning Models:** We systematically investigate the resilience of machine learning based propagation models when the test data distribution diverges from the training data. Our analysis high-

lights a substantial degradation in performance, with root mean square error increasing by over 25% in such cases, emphasizing the critical need for resilience enhancement.

- **Resilience Enhancement through GAN-based Data Augmentation:** To address the observed performance degradation, we introduce a data augmentation approach based on a novel multistage generative adversarial network. Unlike traditional generative adversarial networks, the multistage generative adversarial network leverages pre-trained weights from a deep neural network model, enabling faster convergence (up to a 35% reduction in training iterations) and the generation of high-quality synthetic data. This enhanced data augmentation balances under-represented feature distributions, significantly improving the robustness of machine learning models.

- **Attention through Segmentation based Resilience:** We propose a segmentation based training methodology, termed attention through segmentation, which divides the dataset into localized segments based on essential features. By training multiple specialized models, attention through segmentation captures localized patterns more effectively than single global models. The evaluation shows that attention through segmentation achieves up to 67% improvement in root mean square error compared to the baseline while reducing model complexity and enhancing adaptability to diverse data distributions.

- **Multi-faceted Analysis of the Proposed Framework:** We comprehensively analyze the proposed framework from multiple perspectives, including the quality of synthetic data generation, the applicability of machine learning models trained on augmented datasets, and the computational complexity of attention through segmentation. These evaluations highlight the effectiveness of the proposed methods in striking a balance between performance and

complexity.

- **Broader Impact and Applicability:** This work demonstrates the practical viability of advanced machine learning techniques in tackling real-world challenges in wireless network propagation modeling. The proposed framework applies to various environments, including both urban and rural settings. It provides a blueprint for enhancing machine learning based models in other domains characterized by data scarcity and distributional shifts.

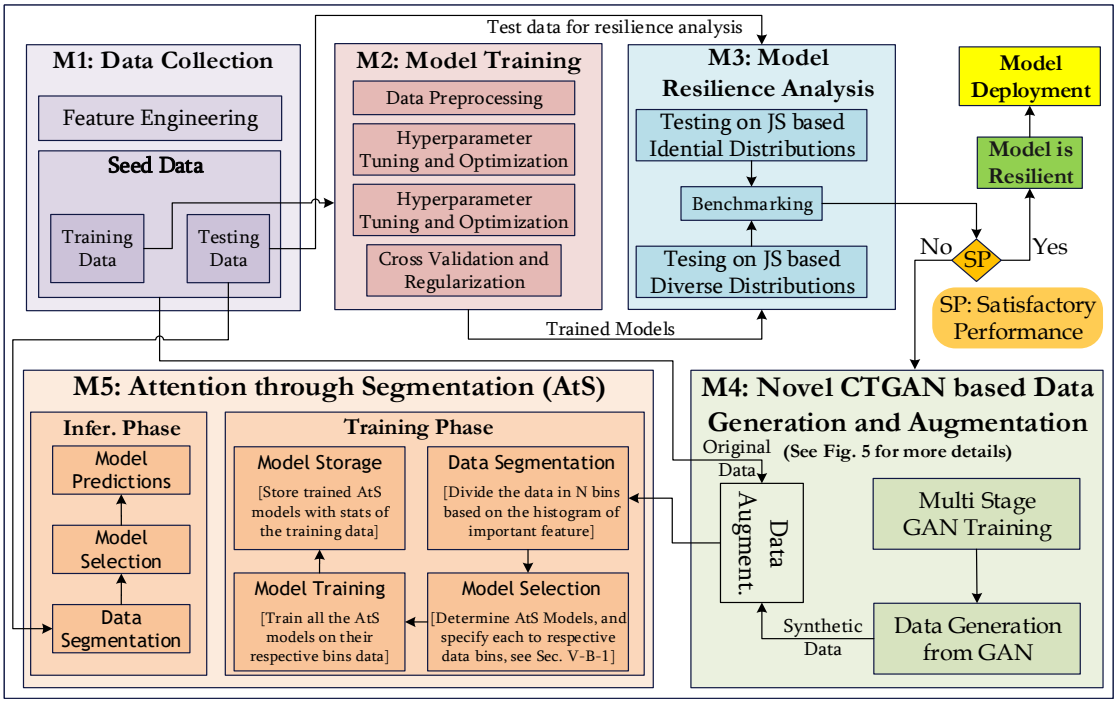


Fig. 5.1: Proposed framework for enhancing resilience in data-driven propagation models through segmented training and GAN-based augmentation. Modules M1–M3 analyze model robustness under distribution shifts, while M4 and M5 improve resilience via synthetic data generation and attention-guided segmentation.

The rest of the paper is organized as follows: Section 5.2 discusses the data collection process, including the system model, raw data collection, and feature engineering, which transforms raw data into the appropriate data for model training. An overview of the proposed framework is presented below. In Section 5.3, we perform resilience analysis of data-driven propagation models by determining the significant

features in model training, analyzing their distributions, and evaluating the models against divergent test data distributions. Section 5.4 presents the model resilience enhancement, including data generation using conventional and proposed two-stage conditional tabular GANs, and attention through segmentation. In Section 5.5, we present the experimental setup and evaluate the performance in terms of data generation quality and RMSE using the AtS approach. Finally, the conclusion and future work are discussed in Section 2.6.

5.2 Data Collection and Framework

This section presents the data collection process, including the system model used to generate raw propagation data and the feature engineering process that transforms it into the appropriate data for training and analyzing machine learning models. However, since these processes are part of the proposed framework, we will first provide a brief overview of the framework in the following section.

5.2.1 Proposed Resilient Propagation Modeling Framework

The proposed framework for resilient propagation modeling is illustrated in Fig. 5.1 and comprises five interconnected modules. The first module (**M1**) focuses on *Data Collection*, where seed data is gathered from network simulations or real-world wireless network deployments. This data is prepared and split into training and testing datasets for subsequent modules. The second module (**M2**) is the *Model Training* module, which performs critical steps such as data preprocessing, hyperparameter optimization, and regularization to develop robust machine learning models tailored to the collected dataset. The trained models are evaluated in the third module.

The **M3** module, *Model Resilience Analysis*, validates the trained models against two types of testing datasets: those with distributions identical to the training data

and those with significantly different distributions to simulate real-world scenarios. If the model's performance drops substantially, as measured by metrics such as root mean squared error, the framework progresses to the enhancement phase. The fourth module (**M4**), *Novel CTGAN-based Data Generation and Augmentation*, addresses the issue of data imbalances. This module utilizes a multi-stage generative adversarial network training approach to generate high-quality synthetic data that balances underrepresented regions of the feature space. The augmented dataset, combining synthetic and original data, is then used in the next module for targeted training.

Finally, the **M5** module, *Attention through Segmentation*, focuses on training and inference using data-segmented models. During training, the dataset is partitioned into localized subsets, and simpler models are trained on these segments to improve adaptability to specific data distributions. For inference, test data is segmented, and the most appropriate model is selected based on the training statistics stored during the segmentation process. This framework addresses key challenges in propagation modeling, including handling data imbalances and distribution shifts, in a unique manner. By integrating **CTGAN** for data augmentation and **AtS** for specialized training, the proposed approach enhances the generalization and resilience of machine learning models. This holistic design enables robust performance across diverse wireless network scenarios, a critical limitation in existing methods [27].

5.2.2 Propagation Related Data Collection (M1 in Fig. 1)

System Model

We deploy a 3GPP-compliant fifth-generation cellular system with N macrocells covering the simulation area of A km^2 in the center of Brussels. Each macrocell has 3 sectors. A realistic commercial radio network planning and optimization tool,

based on ray tracing, is used to create sophisticated network topologies and generate multiple datasets [22,24]. Atoll provides a realistic propagation model by accurately modeling three different aspects: 1) actual antenna heights and Kathrein directional antenna model; 2) geographical information such as ground heights, building heights, and land use maps; and 3) Aster propagation model [158]. Aster employs advanced ray-tracing techniques to compute radio wave propagation phenomena. This includes vertical diffractions on rooftops, horizontal diffractions, ray-launch reflections, atmospheric absorption, rain attenuation, and vegetation losses [158]. This ray-tracing propagation model incorporates detailed environment clutter, ensuring the accurate generation of data for propagation modeling. Once the network is deployed, we use it to generate raw data. Atoll's advanced ray-tracing capabilities enable the generation of realistic data for diverse environments, including urban and rural scenarios. By modeling detailed propagation phenomena such as diffraction, absorption, and vegetation losses [158], Atoll provides robust data critical for training machine learning models resilient to distribution shifts. This distinguishes it from less detailed empirical models [23, 153].

Raw Data Collection

The raw data consists of three essential components: *base station information*, *geographic information*, and *user measurements*. The base station information component contains location coordinates, antenna heights, azimuth angles, tilt angles, transmit powers, frequency bands, and antenna types for all base stations in the observation area. Geographic information components include digital terrain model data for ground altitudes, digital height model data for building heights, and digital land use map data for land cover types within grids. The user measurement component includes the received signal strength, location coordinates, timestamps, and network identification for all users in the observation area.

These three components, gathered using Atoll, collectively form the foundation for our analysis. The resulting dataset is uniquely comprehensive, encompassing base station parameters, geographic characteristics, and user measurements. Unlike studies focused solely on urban or controlled environments [153], this work ensures representational diversity by generating data for urban, suburban, and rural scenarios. Such diversity is crucial for training machine learning models that are resilient to varying distributions, particularly in underrepresented environments.

Feature Engineering: From Raw Data to Right Data

Feature engineering plays a crucial role in machine learning, relying on domain expertise to craft features that effectively describe the target model. In this work, we utilize the feature engineering technique designed in [22] to transform raw base station, geographic, and user measurements into features that better capture the signal propagation environment. These features include distances (both indoor and outdoor), clutter information, the number of building penetrations, diffraction points, and angular separations between the base station and the user equipment. From this process, we identify nine key features, listed on the y-axis of Fig. 5.2, which form the basis of our analysis. Practical feature engineering not only enhances the performance of machine learning models but also ensures the success of the proposed resilience framework. These features enable the conditional tabular generative adversarial network to generate realistic synthetic data by balancing imbalances in underrepresented feature regions, such as those caused by urban-rural disparities. The augmented training set created through this process accurately reflects real-world scenarios, mitigating the distribution shifts often observed in test data. For further details on the considered feature engineering process, interested readers are referred to Section II-C of [22].

5.3 Resilience Analysis: Model Performance against Varying Test Data Distributions

Once the dataset is collected, we train machine learning based propagation models and rigorously evaluate their resilience against alterations in test data distributions. This section outlines the training of machine learning models, the methodology for identifying optimal features and their distributions, and the assessment of model performance under varying test data distributions.

The process begins by training various machine learning models and utilizing the SHAP method to identify essential features. This step is crucial for directing our investigation towards features that are essential for accurate predictions. We then examine the distribution of these key features using histograms with various numbers of bins, a vital step in clearly understanding the distribution and counts of the features. Our study focuses on evaluating how these models perform with test data sampled from various bins of the histograms, whose distribution differs significantly from the training data, thereby emphasizing their adaptability to real-world environments.

5.3.1 ML-based Propagation Model Training (M2 in Fig. 1)

We utilize the nine features identified by feature engineering in sub-section 5.2.2 to train multiple machine learning models to predict the reference signal received power. To streamline the training process, we utilize PyCaret [133], an automated machine learning library recognized for its ability to optimize various steps of machine learning model training, including pre-processing and hyperparameter optimization. Specifically, we train two machine learning regression models, CatBoost and K-nearest neighbor, using this library. Additionally, we incorporate a deep

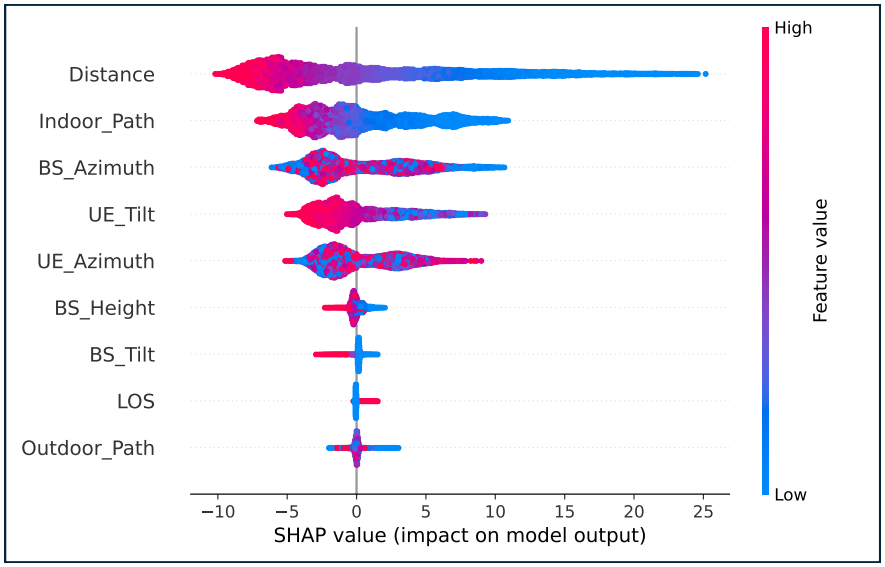


Fig. 5.2: SHAP summary plot identifying the relative impact of key propagation features on model output. Distance and Indoor_Path emerge as the most influential contributors to prediction variability.

neural network model into the analysis to further assess resilience.

High Impact Features

After training the machine learning models, sensitivity analysis techniques such as SHAP [159] are employed to identify high-impact features. Fig. 5.2 illustrates the SHAP summary graph, which ranks the features based on their importance. In this graph, the color of each dot represents the corresponding feature value. At the same time, its position on the *x-axis* indicates whether the feature value positively or negatively correlates with the reference signal's received power. Through this analysis, we identify distance, indoor path, and base station azimuth as the three most significant features for propagation.

Understanding the high-impact features not only provides insights into the key drivers of propagation modeling but also serves as a foundation for evaluating the resilience of the model. By focusing on these features, we can simulate realistic test scenarios that emphasize the most critical aspects of wireless environments,

such as distance variability, indoor attenuation, and base station orientation. This approach builds on established methodologies [23] while introducing a feature-driven evaluation tailored to the dynamic conditions of modern wireless networks.

Distribution of High Impact Features

To explain the resilience analysis of our machine learning models, we focus on the distribution of the three key features identified by the SHAP analysis. The 'Distance' feature exhibits a positive skew, with a high concentration of users located around 900 meters from base stations, as well as notable quantities at larger distances. This variability is crucial for accurate modeling. Similarly, the distribution of 'Indoor Distance' resembles an exponential curve, skewed toward shorter paths. This suggests a higher density of users near indoor entry points or in smaller buildings, highlighting the challenges of achieving uniform network coverage in such varied settings. Finally, the distribution of 'BS Azimuth' is bimodal, reflecting diverse base station orientations with observable gaps that could influence model precision and network planning.

The distributional characteristics of these features directly inform our design of the test scenario. For example, the positive skew in the distance feature highlights the importance of sampling sparsely populated bins to ensure robustness in areas with limited data representation. Likewise, the bimodal distribution of base station azimuth highlights the need to evaluate model performance across a diverse range of base station orientations. This targeted sampling approach aligns with the methodology proposed in [153] and ensures that our resilience analysis captures the full spectrum of real-world variability. Therefore, analyzing resilience over the entire range of these features and selecting test data from specific distribution areas is essential for robust modeling.

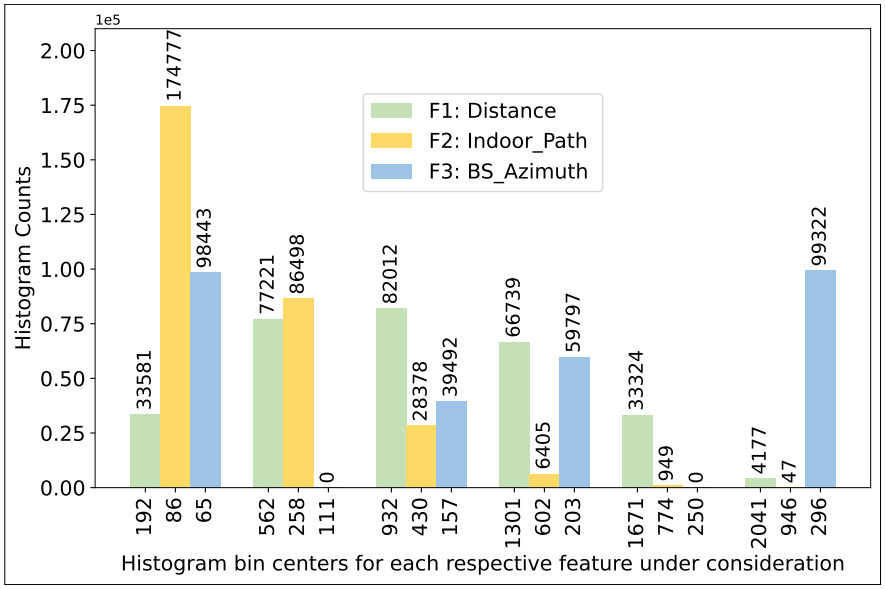


Fig. 5.3: Histogram distributions of Distance, Indoor_Path, and BS_Azimuth across Jensen-Shannon (JS) similarity bins, illustrating feature-wise density variations under low- and high-similarity test scenarios.

5.3.2 Model Evaluation against Test Data Scenarios with Varying JS Similarity (M3 in Fig. 1)

Building on the foundational analysis of high-impact features and their distribution patterns, this subsection examines the resilience of machine learning models to varying test data distributions. To facilitate this resilience analysis, we utilize Jensen-Shannon similarity scores, a symmetric divergence measure that quantifies the similarity between two probability distributions. Unlike other metrics such as Kullback-Leibler divergence, Jensen–Shannon (JS) similarity offers bounded, interpretable scores that make it ideal for comparing test data distributions with the training data [160]. Using these scores, we establish thresholds for low (0.01< JS <0.20), medium (0.04< JS <0.60), and high (0.80< JS<0.99) similarity, shown on the x-axis of Fig. 5.4.

Our selection methodology for the test scenarios is deliberately methodical, utilizing the distribution analysis of key features. Low-similarity scenarios are generated by

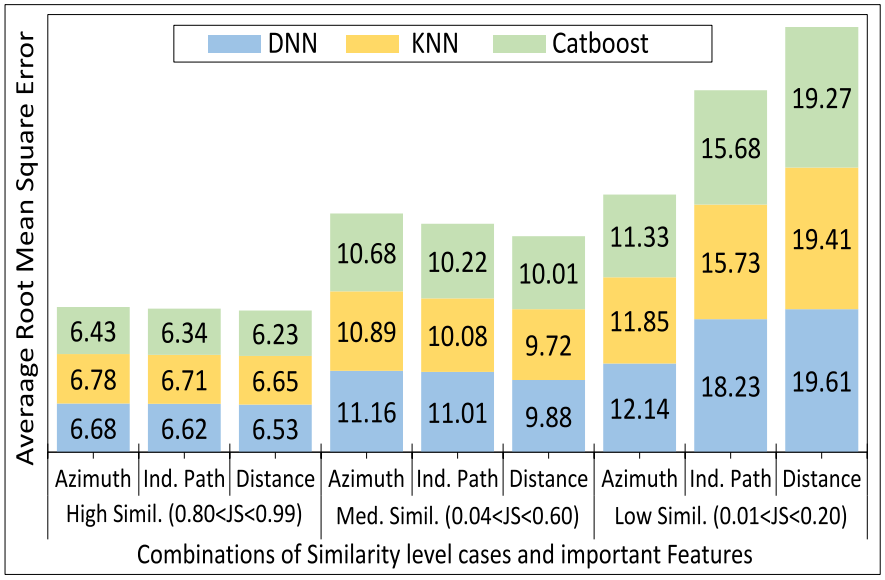


Fig. 5.4: Average RMSE of DNN, KNN, and CatBoost models across test scenarios grouped by high, medium, and low similarity (based on JS divergence) to training data. Results demonstrate degraded performance under greater distribution shifts.

sampling predominantly from the histogram extremes, with fewer data points, while high-similarity scenarios sample from a broader range, especially bins with higher counts. This iterative process continues until we obtain at least 40 test datasets per similarity level, ensuring a comprehensive and systemic evaluation of model performance. By employing multiple similarity scenarios, we aim to transcend anecdotal evidence and gain a more thorough understanding of the model's performance. This approach mitigates the risk of skewed results driven by exceptional test data instances, ensuring that our findings provide a comprehensive depiction of model performance.

The results for three models, deep neural network, K nearest neighbor, and Catboost, measured in terms of average root mean square error over various test scenarios of three similarity categories, are presented in Fig. 5.4. For each similarity category, we separately take 40 different test scenarios by sampling the histograms of the various features under consideration. The averaging of performance metrics across these scenarios serves a dual purpose. First, it allows us to smooth out anomalies and focus on the underlying trends in model performance. Second, it

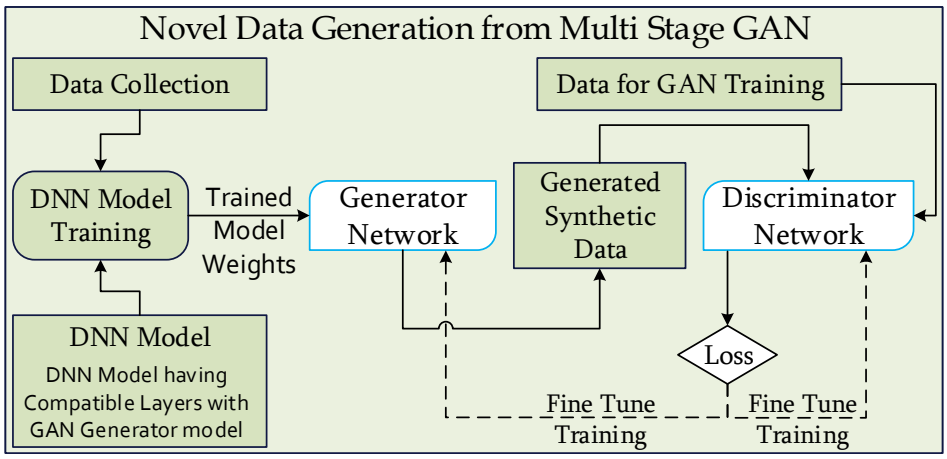


Fig. 5.5: Proposed GAN-based data augmentation framework using multi-stage training and pre-trained deep neural network weight transfer for generator initialization. This design improves training convergence and enhances the quality of generated propagation data under data-scarce conditions.

equips us with a nuanced metric that is more representative of real-world conditions, where data distributions are rarely uniform or predictable.

These results show that for the top-three features, all models retain their performance for test scenarios with high Jensen-Shannon similarity. However, as the similarity level decreases to medium and low, by segmenting data into localized subsets and training specialized models for these segments, the values show a significant increase, particularly for the distance feature. This emphasizes the sensitivity of propagation models to shifts in data distributions, as quantified by Jensen-Shannon scores. The observed performance trends highlight critical challenges in modeling the propagation of wireless networks. For example, the significant increase in root mean square error in low-similarity scenarios underscores the importance of robust training datasets that cover diverse feature distributions. These findings align with real-world deployment scenarios, where models trained predominantly on urban data often fail to generalize to rural or less dense environments. By addressing these gaps, this work lays the groundwork for developing propagation models that can adapt to dynamic and evolving wireless conditions.

5.4 Resilience Enhancement: Data Augmentation and Attention through Segmentation Approach

To address the lack of resilience in machine learning models quantified in the previous section, we propose a bi-pronged approach with two novel modules in our framework (M4 and M5 in Fig. 5.1). These two modules are designed to effectively handle limited data points at the extremes of the distribution.

5.4.1 Synthetic Data Generation Approach (M4 in Fig. 1)

To address data scarcity in under-represented regions of feature distributions, we employ generative adversarial networks based tabular synthetic data generation in the M4 module. Generative adversarial networks have emerged as powerful tools for generating synthetic data by learning underlying data distributions through a generator-discriminator architecture [161]. While traditionally applied to image and text data [162, 163], adapting generative adversarial networks for tabular data presents unique challenges due to the wide variety of feature types, distributions, and inter-dependencies.

Introduction to GANs and CTGANs

Generative adversarial networks are a class of generative models that learn to produce synthetic data resembling a given real dataset [161]. A generative adversarial network consists of two neural networks: a *generator*, which creates synthetic samples, and a *discriminator*, which evaluates how closely these samples match the real data. The generator and discriminator are trained adversarially, iteratively improving until the generator produces data indistinguishable from the real dataset. While generative adversarial networks have shown remarkable success in generating image

and text data [162], their application to tabular data is more complex due to the diverse types and distributions of tabular features.

To address these challenges, a conditional tabular generative adversarial network was introduced as a variant of the generative adversarial network designed explicitly for tabular data [154]. This network incorporates several innovations that make it uniquely suited for this domain. First, it employs *mode-specific normalization* to effectively handle mixed data types, including continuous and categorical variables. Second, it utilizes a *conditional generator*, allowing for targeted data generation based on specific feature conditions. This approach is particularly advantageous for balancing underrepresented regions in tabular data distributions. Additionally, the conditional tabular generative adversarial network employs a *training-by-sampling* method to ensure a balanced representation across discrete categories during training. These features allow the conditional tabular generative adversarial network to overcome many limitations of traditional generative adversarial networks, making it a promising tool for addressing data scarcity and skew in propagation modeling datasets.

Enhancements to the Conditional Tabular Generative Adversarial Network

To address the challenges of convergence time and conditioning complexity, we introduce two key enhancements to the conditional tabular generative adversarial network framework, as depicted in Fig. 5.5. The first enhancement involves initializing the conditional tabular generative adversarial network generator using domain-specific weights derived from a pre-trained deep neural network model. This deep neural network model, trained in *M2: Model Training*, is specifically designed to capture intricate inter-feature correlations and propagation-related patterns present in the training data. The weights of compatible layers between the pre-trained deep

neural network and the conditional tabular generative adversarial network generator are identified and transferred to initialize the generator network.

This weight initialization offers two critical benefits. First, it accelerates the training process of the generative adversarial network by starting with a parameter configuration that already encapsulates domain-relevant knowledge, thereby reducing the number of iterations required for the adversarial training between the generator and discriminator to converge. Second, it provides a robust foundation that mitigates issues such as modal collapse, which often arise during the training of generative adversarial networks, by regularizing the generator's initial outputs and ensuring stability. The second enhancement involves a multi-stage training process for the conditional tabular generative adversarial network framework. After the initial weight transfer, the generator network undergoes fine-tuning on the available training data, as shown in Fig. 5.5. The discriminator is simultaneously fine-tuned to ensure it effectively distinguishes between real and synthetic samples. This iterative fine-tuning process enables the generator to refine its output, ensuring that the generated synthetic data maintains high fidelity and accurately represents the under-represented regions of the data distribution.

These enhancements ensure that the proposed weight transfer generative adversarial network-based framework not only produces high-quality synthetic data but also effectively addresses data imbalances in the original dataset. By leveraging domain-informed initialization and a structured multi-stage training process, the proposed M4 module achieves faster convergence and improved stability, as validated in Section 5.5.2.

Conditional Tabular GAN Implementation with Synthetic Data Vault for Feature Distribution Balancing

The implementation of the conditional tabular generative adversarial network within the synthetic data vault framework is a critical element of the generative adversarial network training and data generation processes depicted in Fig. 5.1. The conditional tabular generative adversarial network employs a *Conditional Generator*, which plays a pivotal role in addressing data imbalances by targeting under-represented regions in the training data distribution. This generator employs a *training-by-sampling* methodology to ensure a balanced representation across all discrete categories or histogram bins [154]. Categories with fewer samples are assigned higher weights during training, prompting the generator to focus more attention on these regions.

The conditional generation process unfolds in three key steps. First, a specific feature is selected as the conditioning variable. Within this feature, a category or range is chosen as the condition. The generator then produces synthetic samples adhering to this condition while maintaining realistic correlations with other features. For example, in propagation modeling, conditioning on the 'Indoor Path' feature ensures that under-represented bins, such as shorter paths, receive targeted synthetic augmentation. Simultaneously, the generator maintains coherence by preserving correlations with other critical features like 'Distance' and 'BS Azimuth'.

To further ensure balanced data generation, the conditional tabular generative adversarial network incorporates an iterative mechanism that calculates the required number of synthetic samples for each under-represented bin. This calculation is guided by the balance threshold $B_t = D_l/N_b$, ensuring that the generated data meets predefined balancing criteria. While the generator conditions on a specific feature, the values for all other features are generated concurrently based on their inherent statistical correlations. This ensures that the augmented dataset remains

Table 5.1: Comparison between original and generated data parameters. NoLfB: Number of Low-frequency Bins, PoLfB: Proportion of Low-frequency Bins values.

Number of Bins of the Histogram	**Data Type**	**F1: Distance**	**F2: Indoor_Path**	**F3: BS_Azimuth**
		NoLfB/PoLfB	**NoLfB/PoLfB**	**NoLfB/PoLfB**
$N_b = 06$	**Orig Data**	3/0.746	04/0.495	2/0.841
	Aug Data	0/0.999	01/0.840	0/1.000
$N_b = 12$	**Orig Data**	5/0.746	08/0.471	5/0.641
	Aug Data	0/0.999	02/0.841	0/1.000
$N_b = 18$	**Orig Data**	8/0.735	11/0.488	5/0.781
	Aug Data	0/0.999	03/0.841	1/0.983

realistic and maintains the integrity of inter-feature relationships.

The integration of this approach within the M4 module enables a conditional tabular generative adversarial network to generate balanced, representative datasets that effectively address data disparities common in wireless network propagation scenarios. By dynamically focusing on under-represented regions while preserving overall feature distributions, the conditional tabular generative adversarial network ensures that the resulting synthetic data supports robust and generalizable machine learning models, as validated in Section 5.5.2.

Data Generation Evaluation of Conditional Tabular Generative Adversarial Network

The efficacy of a conditional tabular generative adversarial network in balancing feature distributions is evaluated using metrics such as *Number of Low-frequency Bins (NoLfB)* and *Proportion of Low-frequency Bin values (PoLfB)*. These metrics quantify the extent of data scarcity and the success of data augmentation in addressing this problem. Table 5.1 provides a comparison between the original and augmented data for the three most important features identified in Section 5.3.1: Distance (F1), Indoor Path (F2), and BS Azimuth (F3).

For example, for the Distance feature (F1) with $N_b = 6$, the original dataset has

three low-frequency bins, with a PoLfB of 0.746, indicating that only 74.6% of the expected data is present in these bins. After augmentation, CTGAN reduces the NoLfB to zero and increases the PoLfB to 0.999, effectively achieving near-complete balancing. Similar results are observed for the BS Azimuth feature (F3). However, for the Indoor Path feature (F2), the starting point of the LfBs is significantly lower, limiting CTGAN's ability to fully balance these bins despite considerable improvement.

These results highlight the strengths and limitations of CTGAN. While it performs well in most scenarios, extreme cases with sparse initial distributions, such as the Indoor Path feature, pose challenges. In these cases, CTGAN generates as many values as possible without compromising the quality of the augmented dataset. The emphasis on metrics such as PoLfB provides a structured approach to measure augmentation success and identify areas where additional interventions may be necessary. The findings underscore the ability of CTGAN to generate balanced, representative datasets, enabling machine learning models to better handle distribution shifts. This capability is critical for propagation modeling, where datasets often reflect diverse real-world scenarios, such as urban-to-rural transitions or network reconfigurations. By addressing data disparities, CTGAN facilitates the development of robust machine learning models that generalize effectively across varying conditions.

5.4.2 AtS: Attention through Segmentation Enhanced Training for the Machine Learning Models (M5 in Fig. 1)

This section focuses on the second aspect of resilience enhancement in the proposed framework: Attention through Segmentation, which segments the data into smaller subsets and trains specialized models for these segments. The section is divided into two subsections. The first subsection provides the **background and motiva-**

tion for the Attention through Segmentation approach, explaining its conceptual foundation and relevance to propagation modeling. The second subsection details the **implementation of Attention through Segmentation in the proposed framework**, describing its integration and operation across the training and inference phases.

Motivation for the Attention through Segmentation approach

While augmenting synthetic data helps balance feature distributions, it does not fully address challenges posed by data imbalances and shifts in real-world applications. Traditional single-model training approaches prioritize high-density data regions, often neglecting sparse or underrepresented areas crucial for robust predictions. To overcome these challenges, attention through segmentation trains multiple specialized models, each focusing on a specific data subset [164].

Attention through segmentation segments the dataset into N bins based on key features. Instead of a single global model, k specialized models are trained, each spanning N/k bins, where k is a user-adjustable parameter. This approach generalizes traditional methods ($k = 1$) and provides flexibility from low attention ($k = 1$) to high attention ($k = N$). By tailoring models to smaller segments, attention through segmentation reduces computational complexity and enhances performance for sparse regions. For instance, urban and rural propagation modeling involves vastly different characteristics; attention through segmentation ensures specialized models address these unique distributions without biases from high-density urban data [164].

A key strength of attention through segmentation lies in combining predictions from specialized models into a unified result. During training, statistical features of data (e.g., range, mean, variance) are stored for each model. In inference, test data statistics are matched with these stored values to dynamically select the most

Table 5.2: Network simulation parameters with their values.

Parameters	**Values**
Network layout	10 Macrocell sites
Number of Users in Simulation Area	10000 users
User distribution	Poisson
Path Loss Model	Aster (Ray Tracing)
Path Loss Matrix Resolution	10m
Geographic Information Resolution	1m
Geographic Models	Digital Terrain
Geographic Building Heights	Digital Height Model
Geographic Land Usage	Digital Land Use Map
Total Clutter Classes	15
eNB Max. Transmit Power	43dBm
eNB Antenna Gain	18.3 dBi
eNB Antenna Horizontal HPBW	63°
eNB Antenna Vertical HPBW	4.7°
eNB Antenna Model	Kathrein Direct. Ant. Model
Total Clutter Classes	15
Frequency Band	2110 (E-UTRA Band 1)
Channel Bandwidth	5 MHz
Size of the simulated data	300 K
Set aside data size for training (testing)	150 K

relevant models. Predictions from multiple models are aggregated to ensure consistency and accuracy. Unlike static ensemble methods, this dynamic selection adapts to distribution shifts, making attention through segmentation particularly effective in diverse scenarios such as urban-to-rural transitions and evolving wireless networks. By addressing these challenges, attention through segmentation significantly improves prediction accuracy and resilience, making it well-suited for advanced machine learning-based propagation modeling.

Implementation of AtS in the Proposed Framework

The attention-through-segmentation methodology is implemented in the M5 module of the proposed framework (Fig. 5.1) to enhance model resilience against distribution shifts. By training specialized models on segmented datasets and dynamically selecting models during inference, attention through segmentation ensures adaptability to diverse and evolving data distributions. The implementation operates in two phases: **Training** and **Inference**, as outlined below.

In the **Training Phase**, the dataset is segmented into smaller chunks based on the histogram bins of critical features, determined by the segmentation parameter k. The *Data Segmentation* block performs this division, preserving dataset diversity while enabling targeted attention to specific data regions. The *Model Selection* block determines appropriate architectures and configurations for each segment, considering feature distributions and computational constraints. These segmented datasets are then used to train simpler models within the *Model Training* block. Upon completion, the trained models and their associated statistics (e.g., feature range, mean, and variance) are stored in the *Model Storage* block for later use.

In the **Inference Phase**, test data is processed through the *Data Segmentation* block to map test instances to their corresponding data bins. Based on the feature statistics, the *Model Selection* block dynamically identifies the most relevant model(s) for each segment. These models generate predictions for their respective data subsets, and predictions from multiple models are aggregated for test data spanning multiple segments, ensuring a unified and coherent output across all segments. This dynamic selection mechanism ensures real-time adaptability, even in the face of significant shifts in distribution.

Attention through segmentation introduces key improvements over traditional approaches. By employing specialized models, it effectively addresses biases and en-

hances performance in sparse and underrepresented regions. Its dynamic model selection ensures robustness across diverse and unseen test scenarios. Moreover, by focusing on critical features identified in Section 5.3.1, attention through segmentation achieves efficient segmentation and precise training, balancing computational complexity with accuracy. These advancements make attention through segmentation implementation a robust solution to challenges such as data imbalances and distribution shifts. Its effectiveness is further evaluated in the next section.

5.5 Simulation Setup & Performance Evaluation

In this section, we first discuss the experimental setup for generating synthetic data, performing data augmentation using a generative adversarial network, and training an attention-through-segmentation based model. Then, the performance evaluation of the generative adversarial network's data generation and convergence is discussed, followed by an assessment of the proposed attention through segmentation methodology.

5.5.1 Experimental Setup

The experimental setup utilizes Atoll to simulate a network environment consisting of an area 1000m $\times$ 1000m, covered by 10 macrocells. The parameters involved in the simulation setup are compiled in Table 5.2. The geographic area is divided into bins, and in each bin, reference signal received power values are computed by multiple users residing in that bin. For every bin, a single reference signal received power value is computed by averaging over the reference signal received power of all users. In general, we deploy 10,000 users in the simulation area, following a Poisson distribution. As discussed in Section 5.2.2, we perform feature engineering to convert raw data to right data in tabular form. As we select the relevant features,

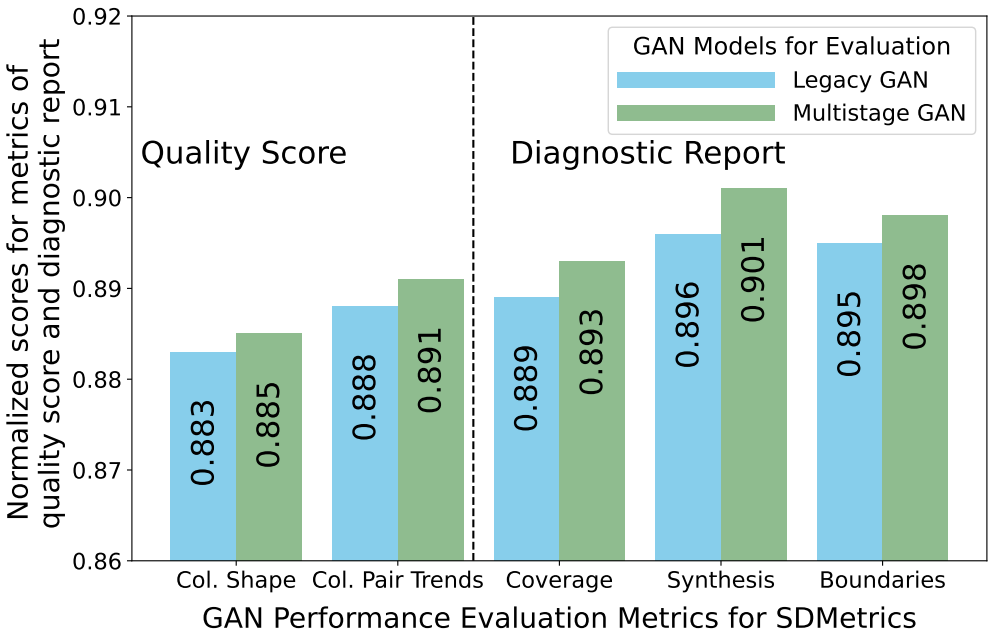


Fig. 5.6: Comparing the quality of GAN-generated synthetic data in terms of *Quality Score* and *Diagnostic Report*, across five key metrics: Column Shape, Column Pair Trends, Coverage, Synthesis, and Boundaries, for the Legacy GAN and proposed Multistage GAN

our dataset consists of 9 features as shown in the Shap summary plot in Fig. 5.2, 1 target variable, the reference signal received power, and the dataset has about $300K$ instances. From this dataset, we set aside approximately $150,000$ values for various testing purposes, such as model evaluation using the classical approach in model resiliency analysis, generative adversarial network data generation quality evaluation, and root mean square error performance evaluation of the proposed attention through segmentation approach. Note that for various testing purposes, different subsets of appropriately sized datasets are taken from this larger set. For example, if a deep neural network model is trained on approximately $120,000$ values with $30,000$ instances used for validation, we use $30,000$ instances as the test dataset from the $150,000$-instance testing dataset. GAN-based model training dataset is similar; however, the size of the generated dataset varies depending on the underlying feature and number of bins.

5.5.2 Evaluation of GANs: Data Quality and Convergence

It is crucial to quantify and compare the ability of generative adversarial networks to generate new data samples for their effective utilization. Therefore, we have evaluated the performance of generative adversarial network data generation by comparing the quality of data generation and the convergence performance. We utilize the data generation *quality score* and *diagnostic report* from the SDMetrics library [165] as two primary groups of metrics for evaluating the data generation capacity of the generative adversarial network. The first group of *Quality Score* encompasses the *Column Shape* and *Column Pair Trends* as metrics. The *Column Shape* evaluates how well the generated columns match the expected shape or structure. The *Column Pair Trends* assess the consistency of relationships between pairs of columns by examining whether the generated data captures the expected patterns or trends between specific column pairs. The second group of *Diagnostic Report* provides a comprehensive evaluation of the generated results, considering multiple dimensions such as *Coverage*, *Synthesis*, and *Boundaries*. *Coverage* measures the extent to which the generated data covers the distribution of the original dataset. In contrast, *Synthesis* assesses the ability of the generator to synthesize new data instances that resemble the original dataset accurately. On the other hand, *Boundaries* evaluate the ability of the generator to generate data points near the boundaries of the original dataset distribution. Fig. 5.6 compares the performance of the legacy generative adversarial network and the proposed multistage generative adversarial network. For *Quality Score*, the multistage generative adversarial network shows slight improvements, with *Column Shape* increasing from 0.883 to 0.885 and *Column Pair Trends* from 0.888 to 0.891. In the *Diagnostic Report*, the multistage generative adversarial network demonstrates better performance across all metrics, with notable gains in *Coverage* (0.893 to 0.901) and *Synthesis* (0.896 to 0.906). While the improvements are incremental, they validate the capability

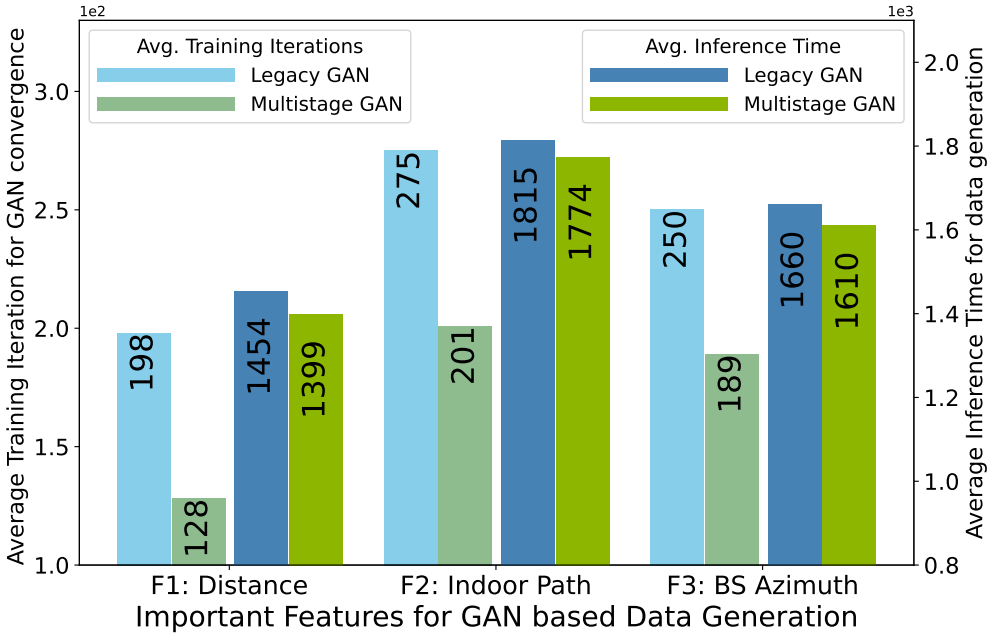


Fig. 5.7: Average training iterations required for GAN convergence (left axis) and average inference time for data generation (right axis) across three important features: Distance, Indoor Path, and Base Station Azimuth, under both Legacy GAN and Multistage GAN models.

of a multistage generative adversarial network. To generate high-quality synthetic data while addressing key aspects of feature representation and boundary coverage. The results indicate that both approaches are effective for data generation, but the multistage generative adversarial network provides enhanced consistency and robustness for diverse propagation scenarios.

However, the evaluation of generative adversarial networks for convergence performance depicted in Fig. 5.7 shows that the multistage generative adversarial network exhibits a significant improvement over the legacy generative adversarial network for data generation conditioned on all features. As evident from the figure, the light colored bars correspond to the left y axis, which represents the *average training iterations* for generative adversarial network convergence in the training phase, whereas the dark colored bars correspond to the right y-axis, which depicts the *average interference time* for data generation in sampling/inference phase. Further, in this comparison, we have evaluated the data generation concerning the distributions of

all three essential features under consideration, as shown on the x-axis of Fig. 5.7. Also, to ensure a fair comparison for this analysis, we have utilized the same computational resources, training, and inference routines for all combinations of both the legacy generative adversarial network and the proposed multistage generative adversarial network.

The proposed approach significantly reduces the number of training iterations for all features, with improvements ranging from 24% to 35%. For example, the required training iterations for the *Distance* (F1) feature decrease from 198 to 128. This acceleration is attributed to the weight initialization strategy employed in the multistage generative adversarial network, which transfers feature correlations learned from the M2 module. The inference time for data generation remains comparable for both generative adversarial networks, with minor improvements observed for all features.

The observed improvements in convergence performance are significant for real-world applications where rapid training and high-quality data generation are critical. The multistage generative adversarial network achieves these gains without compromising the quality of the generated data, as evidenced by the metrics in Fig. 5.6. This balance between efficiency and quality underscores the suitability of the multistage generative adversarial network for propagation modeling, particularly in scenarios that require balanced datasets for accurate and resilient predictions.

In summary, the multistage generative adversarial network outperforms the legacy generative adversarial network by achieving faster convergence and slightly better data quality. These advantages make it a promising tool for generating augmented datasets in dynamic wireless environments. In the next section, we evaluate the proposed attention through segmentation scheme using a generative adversarial network augmented dataset to assess its further impact on the propagation model's

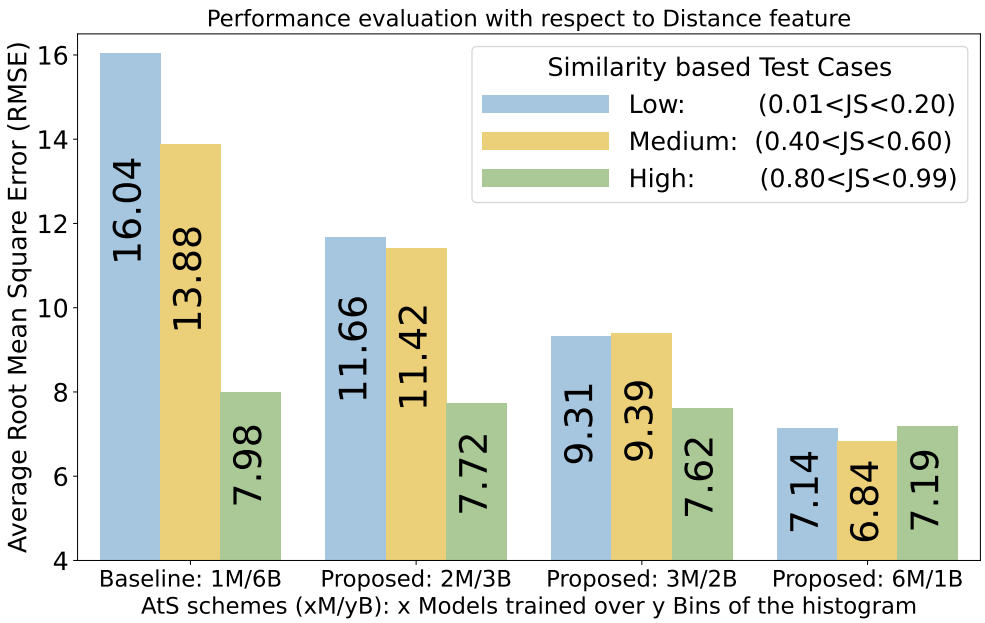


Fig. 5.8: The performance of baseline (1M/6B) and AtS Models (2M/3B, 3M/2B, 6M/1B), in terms of root mean square error for different similarity-based test cases sampled according to the distribution of distance feature.

resilience and accuracy.

5.5.3 Evaluation of Proposed AtS Methodology

In this subsection, we evaluate the model prediction performance, measured as the root mean squared error of the baseline and proposed attention through segmentation methodology, across different levels of attention, data similarity, and sparsity levels, i.e., training data sizes.

RMSE of AtS Approach on Augmented Data

The root mean square error performance of the attention through segmentation approach is shown in Fig. 5.8, Fig. 5.9, and Fig. 5.10, where $N_b = 6$ bins and 4 attention levels are compared under three test cases of JS similarity to the training data. To ensure consistency with *Resilience Analysis*, these test cases, low ($0.01 <$

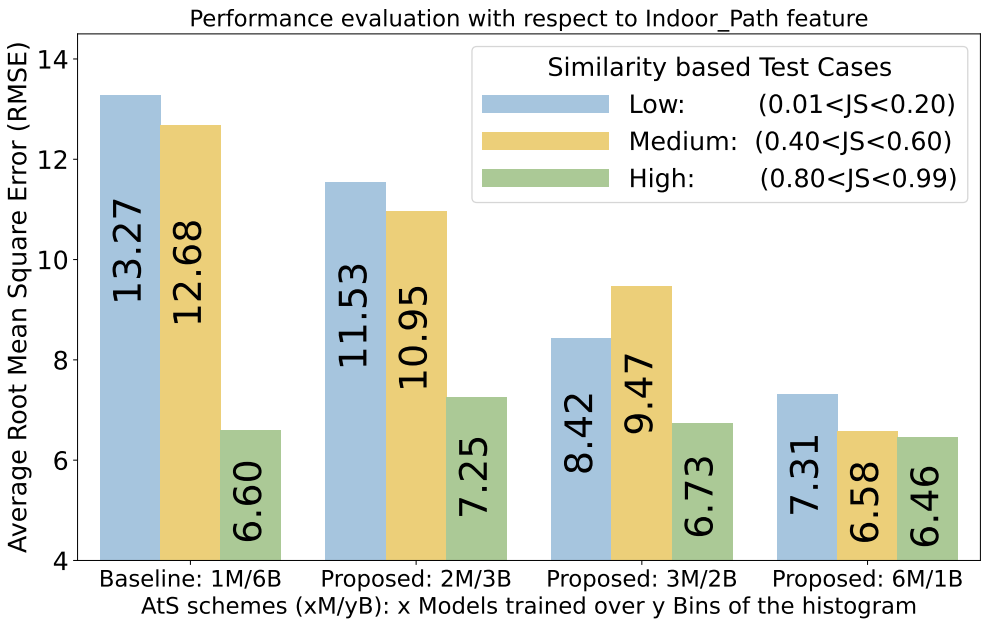


Fig. 5.9: The RMSE performance of baseline (1M/6B) and the proposed attention through segmentation models (2M/3B, 3M/2B, 6M/1B) for different similarity-based test cases sampled according to the distribution of Indoor Path feature.

JS < 0.20), medium ($0.40 <$ JS < 0.60), and high ($0.80 <$ JS < 0.99), were derived from the scenarios detailed in Section 5.3.2.

In order to clearly differentiate the baseline and the attention levels of proposed AtS approach for different number of bins we have adopted a nomenclature of AtS models in Fig. 5.8, Fig. 5.9, and Fig. 5.10 by showing the number of models employed over number of bins as (nM/mB) format. For instance, 'Baseline: 1M/6B' signifies the *Conventional Approach* where a single machine learning model is trained over the entire range of data (all 6 bins of the histogram), while 'Proposed: 2M/3B', 'Proposed: 3M/2B', and 'Proposed: 6M/1B' represent increasingly granular models (2, 3, and 6 models), each trained on specific segments of the data (3, 2, and 1 Bins), respectively. These configurations reflect varying levels of attention to the data range, with a higher level of attention corresponding to a more focused approach that involves more models specified to shorter data ranges. Additionally, it becomes clear from this nomenclature that the baseline approach is a special case of the proposed attention through segmentation method, where we set n=1

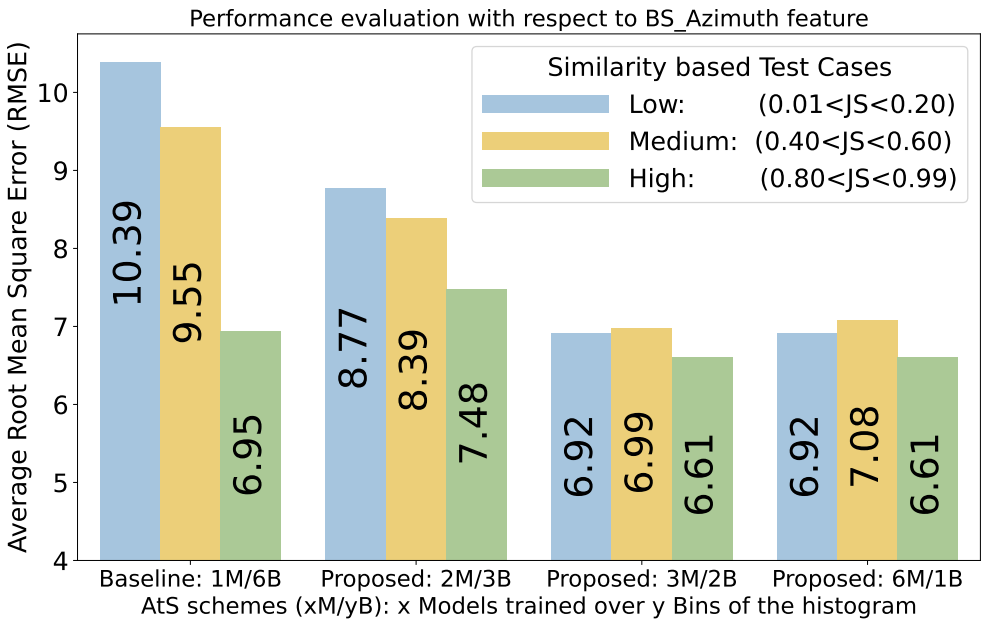


Fig. 5.10: The RMSE performance of baseline (1M/6B) and AtS Models (2M/3B, 3M/2B, 6M/1B) for different similarity-based test cases sampled according to the distribution of BS Azimuth feature.

and m equals the respective number of bins under consideration, i.e., m=6 in this comparison.

A notable trend across all features in Fig. 5.8 is the discernible improvement in RMSE as the model training transitions from the conventional approach 'Baseline: 1M/6B' to the proposed AtS approach with the highest attention level 'Proposed: 6M/1B'. In Fig. 5.8 related to F1: Distance feature, a significant decline in RMSE is observed as we move from the baseline: 1M/6B to the proposed: 6M/1B model, especially at the low similarity level. RMSE drops from 16.04 to 7.14, which translates into a decrease of approximately 56%. At the medium similarity level, the RMSE decreases from 13.88 to 6.84, a 51% reduction, while at the high similarity level, it decreases from 7.98 to 7.19, marking a smaller but notable improvement of 10%.

The F2: Indoor Path feature, shown in Fig. 5.9, also demonstrates marked reductions in RMSE, especially at lower similarity levels. At low similarity, RMSE

reduces by approximately 45%, while at medium similarity, the reduction is slightly higher at 48%. For high similarity, the RMSE decreases marginally, indicating that the benefits of the AtS approach are more pronounced when the test data diverge from the training distribution. Finally, for the F3: BS Azimuth feature depicted in Fig. 5.9, similar trends are observed, albeit with smaller reductions compared to the other features. At low similarity, the RMSE falls by 33%, while at medium similarity, the reduction is 26%. At high similarity, RMSE shows only slight improvements, further supporting the observation that AtS is particularly effective in addressing distribution shifts.

Interestingly, the rate of RMSE reduction decreases as similarity increases, highlighting that the benefits of AtS are more pronounced when test data distributions diverge significantly from the training data. This is expected, as higher similarity inherently leads to better baseline performance, leaving less room for improvement. These results highlight the effectiveness of the AtS approach in enhancing model performance across various propagation features and similarity levels. By tailoring models to specific data ranges, AtS not only enhances resilience under challenging scenarios but also demonstrates scalability across varying attention levels and dataset complexities.

RMSE against Different Training Data Sizes

To assess the resilience of the proposed attention through segmentation approach under varying training data sizes, we evaluate its RMSE performance across three training data density levels (Low: 48k samples, Medium: 96k samples, and High: 144k samples) and two test data similarity conditions (Low and High), as depicted in Fig. 5.11. Similar to previous results, we observe a general improvement in root mean square error with increasing attention levels for both similarity cases and all training data density levels.

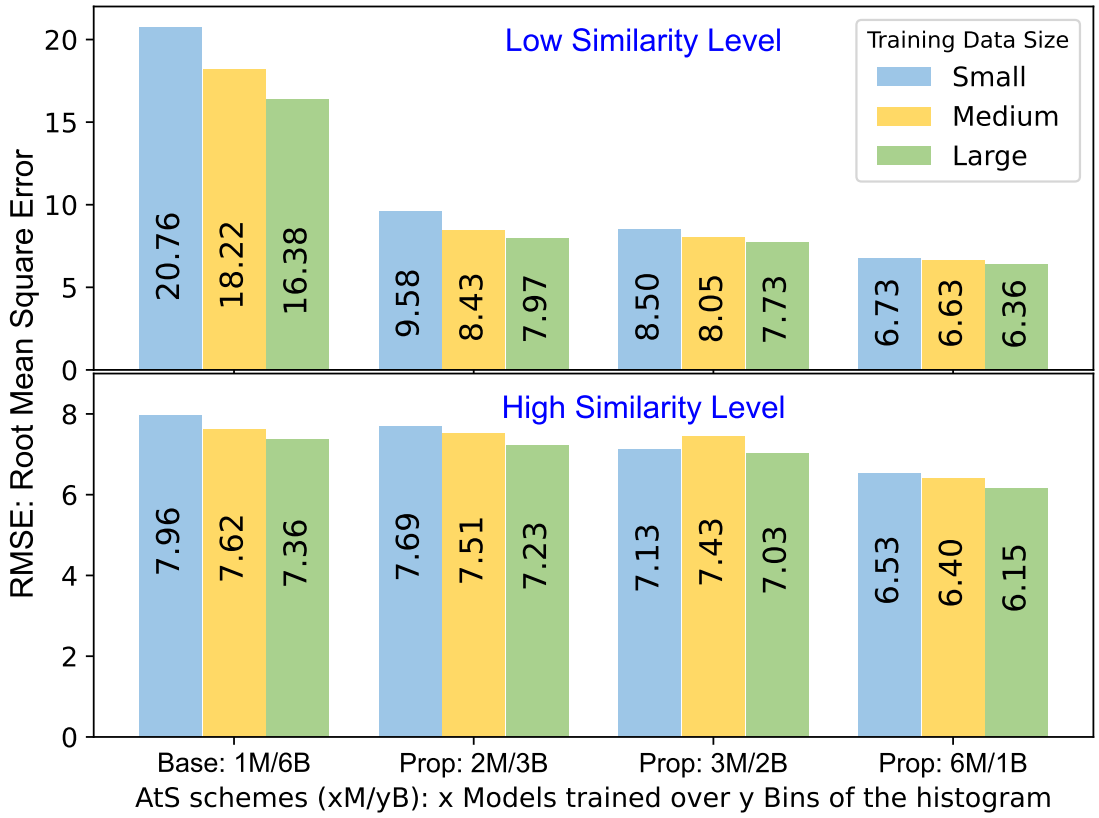


Fig. 5.11: The RMSE performance evaluation of proposed AtS models trained on augmented data for three different training data sizes, and two cases of test data similarity with training data, for $N_b = 06$, and Distance feature.

For low similarity cases (upper subfigure), RMSE decreases consistently with increasing attention levels across all training data sizes. For instance, at low data density, RMSE improves from 20.76 to 9.58 as the attention level shifts from baseline '1M/6B' to the proposed '2M/3B', reflecting a 53.85% reduction. When the attention level reaches '6M/1B', RMSE further drops to 6.73, representing a remarkable total reduction of 67.53%. Similar trends are observed for medium and high data density levels, with significant improvements indicating that attention through segmentation effectively handles sparse training data while maintaining robust performance.

Under high similarity conditions (lower subfigure), RMSE improvements from the baseline scheme are more moderate due to the already low baseline RMSE values.

For example, in the low data density case, RMSE decreases from 7.96 in '1M/6B' to 6.53 in '6M/1B', a reduction of 17.96%. Similar to this comparison, we observe comparable improvements, ranging from 16% to 18%, for other training data sizes. These results underscore that while the attention through segmentation approach is beneficial even in high similarity cases, its advantages are more pronounced in scenarios where the test data distribution diverges significantly from the training data.

Overall, the proposed AtS approach demonstrates exceptional resilience in handling two critical challenges: (1) sparse or limited training data and (2) significant divergences between training and test data distributions. By leveraging segmentation-based training and tailored attention mechanisms, AtS consistently reduces RMSE across both varying similarity conditions and data density levels. Notably, its ability to achieve over 67% reduction in RMSE under low similarity and sparse training data scenarios highlights its robustness against extreme distribution shifts. These results emphasize the scalability and adaptability of AtS, making it an effective solution for real-world applications where data availability is limited or test conditions differ substantially from training environments. The findings underscore AtS's potential to enhance model generalization and reliability in dynamic wireless network settings.

5.5.4 Evaluation of AtS Complexity and Convergence

In the previous comparisons, we established the remarkable RMSE performance of the proposed AtS approach. However, assessing the computational cost of this improvement is crucial for evaluating its practical feasibility. Therefore, in Fig. 5.12, we compare model complexity, represented by the number of trainable parameters, and convergence performance, indicated by average iterations required during training, for all three features under consideration with $N_b = 6$. Furthermore, for a

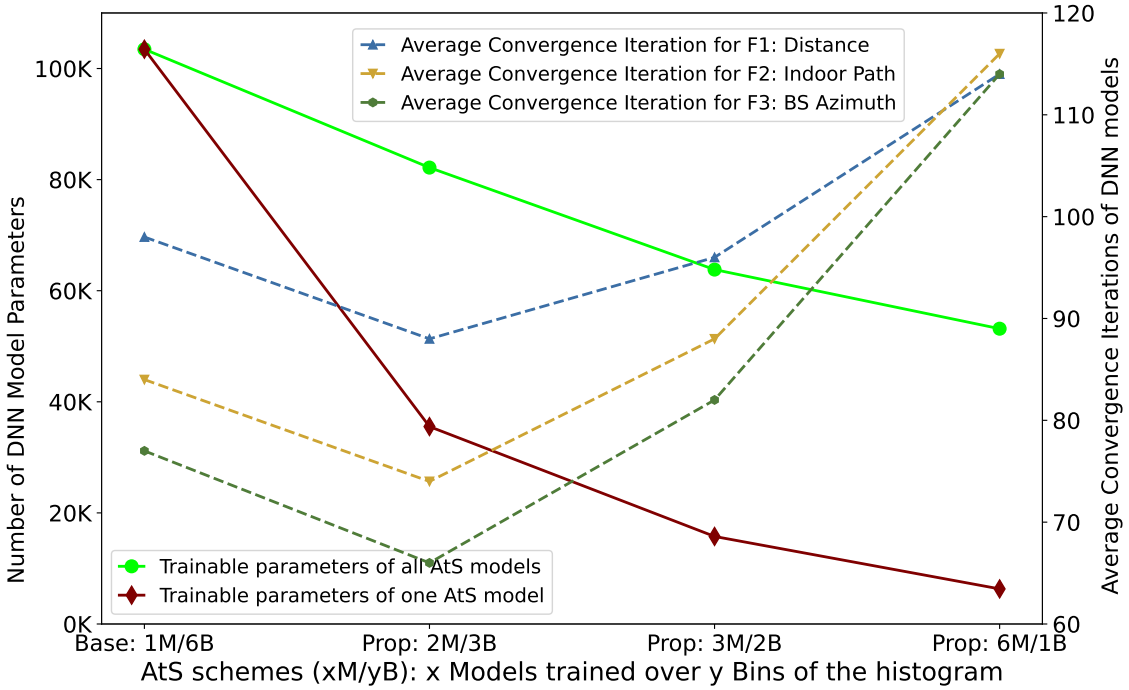


Fig. 5.12: Comparing the AtS model complexity manifested as the number of parameters and average convergence iterations for three features under consideration for $N_b = 06$ bins.

specific attention level, we employ the same deep neural network model architecture for all features under analysis; hence, the complexity of the deep neural network model, as measured by the number of trainable parameters (left y-axis), is represented by a single line for all features. The falling brown curve shows the parameters of one model at an attention level; however, for a fair and clear comparison with the baseline approach, we also depict the total parameters of all models at certain attention levels by the green curve, which otherwise is the sum of parameters of all models at the given attention level. To compare the model complexity, it is worth noting that the number of parameters for '1M/6B' is considered the benchmark. Hence, any value less than this is taken as the improvement in model complexity.

A key observation from this result is the substantial reduction in the complexity of the AtS models (brown curve) as the attention level increases from '1M/6B' to '6M/1B'. Hence, the total trainable parameters for all AtS models at any given attention level remain consistently below the baseline benchmark. For instance,

at the '6M/1B' attention level, the total parameters are approximately 45% lower than the baseline, despite utilizing multiple models. This trend highlights the efficiency of the AtS scheme, where improved RMSE performance is achieved without adding to the overall model complexity. By leveraging smaller, specialized models, the proposed approach not only avoids additional computational burden but also enhances resilience and performance.

The convergence patterns of the AtS models (right y-axis) reveal a nuanced trade-off between model complexity and the size of the training data available at higher attention levels. Initially, as the attention level increases from '1M/6B' to '3M/2B', we observe a notable decrease in convergence iterations due to the reduced complexity of the individual models. For example, for the Distance feature, the average number of convergence iterations drops from approximately 110 to 75, highlighting the efficiency gains achieved through segmentation and simpler models. However, as the attention level further increases to '6M/1B', convergence iterations rise again, reaching approximately 90. This shift reflects the impact of smaller training data sizes associated with higher attention levels, which limits the number of examples available for each model to learn from.

This pattern is intuitive: simpler models trained on smaller datasets require more iterations to learn meaningful patterns from limited examples. However, the overall increase in iterations remains manageable, particularly given the inherent parallelizability of the AtS approach. By design, AtS enables multiple models to be trained concurrently, leveraging modern parallel processing techniques to offset the computational cost associated with additional iterations. This capability is especially relevant in practical deployments, where distributed and parallel computing resources are often available. In summary, the AtS framework achieves a favorable balance between reduced overall model complexity, enhanced RMSE performance, and a manageable increase in convergence iterations. This trade-off demonstrates

the practicality and robustness of the AtS approach for real-world ML-based propagation modeling in dynamic wireless networks. The ability to adapt to diverse data distributions, while efficiently managing computational demands, positions AtS as a promising solution for future wireless network applications.

5.6 Conclusion and Transition to Next Chapter

This chapter presented a resilient modeling framework that directly addresses the core challenges of data scarcity and distribution shifts in wireless propagation modeling. These challenges, common in realistic deployment scenarios—such as urban-to-rural transitions or sparsely monitored areas—limit the generalization and robustness of machine learning models when tested under non-identical distributions.

To overcome these limitations, we introduced a dual-pronged strategy. First, a multistage conditional tabular generative adversarial network was proposed, where the generator was initialized with domain-specific weights from a pre-trained deep neural network to accelerate convergence and improve synthetic data quality. Empirical evaluations showed that this multistage GAN not only reduced training iterations by up to 35% but also produced balanced synthetic datasets that significantly mitigated data imbalances in critical feature regions.

Second, we proposed a novel attention-through-segmentation approach, which replaces the traditional single-model paradigm with multiple localized models trained on segmented feature spaces. This design was shown to improve performance, particularly under low-similarity test scenarios, dramatically. The attention-through-segmentation approach achieved a reduction of up to 67% in root mean square error, while maintaining lower model complexity and enabling faster convergence compared to the baseline.

The proposed framework was rigorously validated across multiple test scenarios and

training configurations, including variation in attention levels, feature distribution similarity, and training data sparsity. Furthermore, an in-depth analysis of attention through segmentation model complexity revealed that despite employing multiple specialized models, the total number of trainable parameters was reduced compared to a single baseline model, demonstrating both efficiency and scalability. Overall, the framework introduced in this chapter provides a scalable, data-efficient, and generalizable solution for robust wireless propagation modeling. It paves the way for real-world deployment in scenarios where training data is sparse, imbalanced, or non-representative of future operational conditions.

In the next chapter, we conclude this dissertation by synthesizing the key insights from all proposed frameworks, highlighting their collective contribution to resilient and accurate AI-driven propagation modeling. We also discuss future research directions to expand the applicability of these techniques to next-generation wireless networks, including real-time modeling, federated learning integration, and edge-deployment scenarios.

CHAPTER 6

Conclusion and Future Research Directions

This chapter brings together the core contributions of this dissertation, discusses their significance for the advancement of wireless networks, and outlines promising avenues for future research.

6.1 Contributions and Conclusions of Each Chapter

This dissertation consists of four core chapters, each addressing a distinct but interconnected challenge in the design and deployment of intelligent wireless networks.

Chapter 2 has presented a unified, two-phase artificial intelligence-driven framework for outage management in ultra-dense cellular networks. The first phase has utilized an improved extreme gradient boosting model, termed Impv-XGBoost, to reliably detect outages even under challenging shadowing and measurement-scarce conditions. The second phase has proposed a fairness-aware outage compensation mechanism based on actor-critic reinforcement learning. The reinforcement learning agent has dynamically adjusted key radio parameters, such as antenna tilt and transmission power, to restore service while maintaining fairness across affected and served users. The results have demonstrated that this two-phase detection and compensation architecture successfully improves detection accuracy, accelerates mean time to compensate, and supports balanced service recovery across ultra-dense wireless networks.

Chapter 3 has investigated the underexplored issue of positional errors in user-

centric ultra-dense networks. These networks depend heavily on accurate position estimates of both user equipment and distributed nodes for service zone formation and resource allocation. This chapter has first quantified the performance losses introduced by typical positioning errors, showing that even modest inaccuracies can result in overlapping service zones, misaligned coverage, and substantial interference. To counter these effects, two complementary solutions have been developed. The first solution has applied time-series forecasting techniques to predict optimal radio configurations under positional uncertainty. The second solution has introduced a data-driven optimization and error compensation framework that learned residual patterns between ideal and erroneous configurations. Experimental evaluations on a 3GPP-compliant simulator have confirmed that this framework restores degraded spectral and energy efficiency, demonstrating that data-driven error compensation can preserve user-centric network performance in dynamic, dense deployments.

Chapter 4 has tackled the challenge of model brittleness under data imbalance and distribution shifts for wireless propagation modeling. A comprehensive machine learning framework has been introduced that fuses a conditional tabular generative adversarial network with a segmentation-based training methodology. Domain-relevant features, such as carrier frequency and propagation environment, have been used to partition the data into coherent sub-regions. Within each segment, lightweight local models have been trained with attention to under-represented classes and rare environments. This segmentation-based attention mechanism has increased predictive accuracy and reduced the root mean square error by up to 67%, while improving generalization to previously unseen distributions. The findings have demonstrated that data augmentation combined with feature-aware segmentation can significantly bolster the resilience and scalability of wireless propagation models under real-world, nonstationary conditions.

Chapter 5 has focused on mitigating extreme data scarcity in tabular wireless datasets by proposing a domain-informed generative modeling approach. The work has introduced a novel weight transfer generative adversarial network, which first trains a generator on analytically simulated pseudo-random data derived from wireless propagation equations, then fine-tunes this model on limited measured data. This transfer of knowledge has enabled stable training under data-scarce conditions, accelerated convergence, and yielded synthetic datasets with high statistical fidelity. Evaluations have demonstrated that training downstream machine learning models with weight transfer generative adversarial network-augmented data reduces the predictive error by up to 50% compared to conventional generative baselines. This chapter has established that incorporating domain knowledge into generative frameworks is an effective and practical strategy for scalable and transferable propagation modeling when measurement campaigns are limited.

6.2 Implications for Emerging Wireless Networks

Taken together, these contributions highlight the value of merging domain expertise with data-driven learning techniques to enable self-sustaining, resilient, and adaptable wireless networks. The unified detection–compensation framework in Chapter 2 shows that zero-touch automation can be enhanced with fairness-aware optimization and real-time adaptation, making it feasible to deploy in dense fifth- and sixth-generation networks. The error compensation and residual learning solutions in Chapter 3 offer a practical path to mitigating positioning inaccuracies that degrade network performance in user-centric and mobile-centric designs. The segmentation- and generative-based propagation modeling techniques of Chapters 4 and 5 underscore the potential of intelligent data augmentation and model specialization to ensure robust performance under unpredictable variations and data scarcity. Collectively, these advances establish a strong foundation for applying ar-

tificial intelligence and domain-informed techniques to modern wireless networks. They enable networks to adapt rapidly to diverse operating conditions, scale efficiently as deployments grow denser, and achieve fairer, more consistent service for all users.

6.3 Future Research Directions

While this dissertation has established a strong foundation, there remain several promising directions that can further enhance resilience, adaptability, and trust in next-generation wireless networks. Five key avenues for future research are outlined here:

1. **Adapting to Emerging Network Paradigms:** Future work can explore the application of these outage management, error-compensation, and generative modeling techniques to next-generation architectures such as non-terrestrial networks, reconfigurable intelligent surfaces, and cell-free massive multiple-input multiple-output systems. These architectures introduce new propagation behaviors, mobility patterns, and scalability challenges, requiring refined AI-driven solutions.

2. **Developing Continuous Digital Twin Feedback Loops:** Real-time integration of data-driven frameworks into live digital twin environments would enable continuous calibration of models against network observations. Research can focus on co-simulation approaches that leverage on-the-fly updates of outage and compensation policies, allowing networks to anticipate and counteract faults before they impact end users.

3. **Designing Privacy-Preserving and Distributed Learning Protocols:** Scalable wireless networks will increasingly require collaborative, distributed

model updates without sharing raw data. Combining federated learning with domain-informed augmentation and reinforcement learning can support privacy-preserving model training and local customization across geographically distributed nodes, especially under strict data security requirements.

4. **Enhancing Explainable and Trustworthy Artificial Intelligence Techniques:** Future research can integrate explainable artificial intelligence into outage detection, resource allocation, and generative augmentation pipelines. Techniques such as attention visualizations, counterfactual analyses, and human-readable policy summaries will help operators understand and verify the decisions of automated systems, accelerating acceptance and standardization.

5. **Validating Performance in Large-Scale Experimental Testbeds and Early Deployments:** Finally, moving beyond simulated validation to real-world testing is a critical next step. Future research can leverage experimental platforms such as OpenAirInterface, Colosseum, and industry trials to measure practical performance under dynamic loads, user mobility, and complex interference. These pilot deployments will help reveal practical bottlenecks and inform standardization for autonomous wireless operations in commercial 6G networks.

Closing Remarks

This dissertation has demonstrated that integrating domain-informed learning techniques with artificial intelligence and machine learning algorithms can significantly enhance the resilience, adaptability, and accuracy of wireless network management. The proposed solutions, including unified outage handling, error-compensated optimization, and generative modeling under data-scarce and shifting distributions, have established practical paths for realizing self-sustaining and resilient wireless

networks that maintain fair and robust service in complex, dynamic environments. Going forward, these contributions provide a strong foundation for continued innovation, ensuring that future wireless networks can rise to the increasing demands of connectivity, scalability, and intelligence.

Funding Acknowledgments

The projects undertaken in this dissertation are based upon work supported by the National Science Foundation under Grant Numbers 1923669 and 1730650. Any opinions, findings, and conclusions or recommendations expressed in this material are those of the author(s) and do not necessarily reflect the views of the National Science Foundation. For more inquiries about these works, please visit www.AI4networks.com.

Bibliography

[1] M. Latva-aho and K. Leppänen, "Key drivers and research challenges for 6g ubiquitous wireless intelligence," *6G Research Visions, White Paper*, vol. 1, pp. 1–36, 2020. [Online]. Available: https://www.6gchannel.com/wp-content/uploads/2020/06/6G-White-Paper-2020.pdf

[2] S. Dang, O. Amin, B. Shihada, and M.-S. Alouini, "What should 6G be?" *Nature Electronics*, vol. 3, no. 1, pp. 20–29, 2020.

[3] F. Khoramnejad and E. Hossain, "Generative AI for the Optimization of Next-Generation Wireless Networks: Basics, State-of-the-Art, and Open Challenges," *IEEE Communications Surveys & Tutorials*, pp. 1–1, 2025.

[4] M. Giordani, M. Polese, A. Roy, M. Mezzavilla, and M. Zorzi, "Toward 6g networks: Use cases and technologies," *IEEE Communications Magazine*, vol. 58, no. 3, pp. 55–61, 2020.

[5] A. Tavakoli, A. Garcia-Rodriguez, N. Maturo, G. Giambene, M. Kader, and O. Kodheli, "6g and non-terrestrial networks: The sky is not the limit," *IEEE Communications Standards Magazine*, vol. 5, no. 4, pp. 46–52, 2021.

[6] A. Imran, A. Zoha, and A. Abu-Dayya, "Challenges in 5G: How to Empower SON with Big Data for Enabling 5G," *IEEE Network*, vol. 28, no. 6, pp. 27–33, 2014.

[7] P. Semasinghe, E. Hossain, and K. Zhu, "An Evolutionary Game for Distributed Resource Allocation in Self-Organizing Small Cells," *IEEE Transactions on Mobile Computing*, vol. 14, no. 2, pp. 274–287, 2015.

[8] W. Saad, M. Bennis, and M. Chen, "A Vision of 6G Wireless Systems: Applications, Trends, Technologies, and Open Research Problems," *IEEE Network*, vol. 34, no. 3, pp. 134–142, 2020.

[9] E. Hossain, F. Goudarzi, and Y. Abdelmoula, "Artificial intelligence-enabled wireless networks for 6g: Challenges, opportunities, and research directions," *IEEE Communications Magazine*, vol. 60, no. 1, pp. 74–80, 2022.

[10] A. Asghar, H. Farooq, and A. Imran, "Self-Healing in Emerging Cellular Networks: Review, Challenges, and Research Directions," *IEEE Communications Surveys & Tutorials*, vol. 20, no. 3, pp. 1682–1709, 2018.

[11] Y. Al-Eryani and E. Hossain, "Self-organizing mmwave mimo cell-free networks with hybrid beamforming: A hierarchical drl-based design," *IEEE Transactions on Communications*, vol. 70, no. 5, pp. 3169–3185, 2022.

[12] T. Reshmi and M. Azath, "Improved Self-Healing Technique for 5G Networks using Predictive Analysis," *Peer-to-Peer Networking and Applications*, vol. 14, no. 1, pp. 375–391, 2021.

[13] B. Hussain, Q. Du, A. Imran, and M. A. Imran, "Artificial Intelligence-Powered Mobile Edge Computing-Based Anomaly Detection in Cellular Networks," *IEEE Transactions on Industrial Informatics*, vol. 16, no. 8, pp. 4986–4996, 2020.

[14] S. Chen, F. Qin, B. Hu, X. Li, and Z. Chen, "User-centric ultra-dense networks for 5g: Challenges, methodologies, and directions," *IEEE Wireless Communications*, vol. 23, no. 2, pp. 78–85, 2016.

[15] U. S. Hashmi, S. A. R. Zaidi, and A. Imran, "User-centric cloud ran: An analytical framework for optimizing area spectral and energy efficiency," *IEEE Access*, vol. 6, pp. 19 859–19 875, 2018.

[16] I. Akbari, O. Onireti, M. A. Imran, A. Imran, and R. Tafazolli, "Effect of inaccurate position estimation on self-organizing coverage estimation in cellular networks," in *2014 20th European Wireless Conference*, 2014, pp. 176–180.

[17] I. Akbari, O. Onireti, A. Imran, M. A. Imran, and R. Tafazolli, "How reliable is mdt-based autonomous coverage estimation in the presence of user and bs positioning error?" *IEEE Wireless Communications Letters*, vol. 5, no. 2, pp. 196–199, 2016.

[18] H. N. Qureshi and A. Imran, "Optimal bin width for autonomous coverage estimation using mdt reports in the presence of user positioning error," *IEEE Communications Letters*, vol. 23, no. 4, pp. 716–719, 2019.

[19] A. Zappone, M. D. Renzo, and M. Debbah, "Wireless networks design in the era of deep learning: Model-based, ai-based, or both?" *IEEE Transactions on Communications*, vol. 67, no. 10, pp. 7331–7376, 2019.

[20] H. X. Nguyen, R. Trestian, D. To, and M. Tatipamula, "Digital Twin for 5G and Beyond," *IEEE Communications Magazine*, vol. 59, no. 2, pp. 10–15, 2021.

[21] Z. Liu, W. Liu, X. Liu, and X. Zhang, "Digital Twin-Enabled 6G: Vision and Key Design Requirements," *IEEE Communications Magazine*, vol. 60, no. 12, pp. 30–36, 2022.

[22] U. Masood, H. Farooq, A. Imran, and A. Abu-Dayya, "Interpretable AI-Based Large-Scale 3D Pathloss Prediction Model for Enabling Emerging Self-Driving Networks," *IEEE Transactions on Mobile Computing*, vol. 22, no. 7, pp. 3967–3984, 2023.

[23] S. Sun and S. Mao, "DeepProp: A Deep Learning Framework for Wireless Propagation Modeling Using Ray Tracing Data," *IEEE Transactions on Wireless Communications*, vol. 19, no. 9, p. 6156–6170, 2020.

[24] U. Masood, H. Farooq, and A. Imran, "A Machine Learning Based 3D Propagation Model for Intelligent Future Cellular Networks," in *2019 IEEE Global Communications Conference (GLOBECOM)*. IEEE, 2019, p. 1–6.

[25] H. N. Qureshi, U. Masood, M. Manalastas, S. M. A. Zaidi, H. Farooq, J. Forgeat, M. Bouton, S. Bothe, P. Karlsson, A. Rizwan *et al.*, "Towards Addressing Training Data Scarcity Challenge in Emerging Radio Access Networks: A Survey and Framework," *IEEE Communications Surveys & Tutorials*, 2023.

[26] V. P. Rekkas, S. Sotiroudis, P. Sarigiannidis, S. Wan, G. K. Karagiannidis, and S. K. Goudos, "Machine Learning in Beyond 5G/6G Networks—State-of-the-Art and Future Trends," *Electronics*, vol. 10, p. 2786, 2021.

[27] M. Zhang, "Adaptation Based Approaches to Distribution Shift Problems," Ph.D. dissertation, EECS Department, University of California, Berkeley, Dec 2021. [Online]. Available: http://www2.eecs.berkeley.edu/Pubs/TechRpts/2021/EECS-2021-262.html

[28] Y. Wei, M.-M. Zhao, and M.-J. Zhao, "Channel Distribution Learning: Model-Driven GAN-Based Channel Modeling for IRS-Aided Wireless Communication," *IEEE Transactions on Communications*, vol. 70, no. 7, pp. 4482–4497, 2022.

[29] C. Huang, R. He, B. Ai, A. Molisch, B. Lau, K. Haneda, B. Liu, C. Wang, M. Yang, C. Oestges, and Z. Zhong, "Artificial Intelligence Enabled Radio Propagation for Communications—Part II: Scenario Identification and Channel Modeling," *IEEE Transactions on Antennas and Propagation*, vol. 70, pp. 3955–3969, 2021.

[30] 3rd Generation Partnership Project, "TR36.814 v9.0.0: Further Advancements for E-UTRA Physical Layers Aspects (Release 9)," 3GPP, Sophia Antipolis, France, Technical Report TR36.814 v9.0.0, March 2010.

[31] W. Raza, S. B. A. Zaidi, M. U. B. Farooq, H. N. Qureshi, and A. Imran, "Refining Wireless Propagation Models using Domain-Informed GANs amid Data Scarcity," in *2024 IEEE 100th Vehicular Technology Conference (VTC2024-Fall)*, 2024, pp. 1–6.

[32] T. Zhang, K. Zhu, and E. Hossain, "Data-Driven Machine Learning Techniques for Self-Healing in Cellular Wireless Networks: Challenges and Solutions," *Intelligent Computing*, vol. 2022, 2022. [Online]. Available: https://spj.science.org/doi/abs/10.34133/2022/9758169

[33] N. Bhushan, J. Li, D. Malladi, R. Gilmore, D. Brenner, A. Damnjanovic, R. T. Sukhavasi, C. Patel, and S. Geirhofer, "Network Densification: The Dominant Theme for Wireless Evolution into 5G," *IEEE Communications Magazine*, vol. 52, no. 2, pp. 82–89, 2014.

[34] J. Johansson, W. A. Hapsari, S. Kelley, and G. Bodog, "Minimization of Drive Tests in 3GPP Release 11," *IEEE Communications Magazine*, vol. 50, no. 11, pp. 36–43, 2012.

[35] O. Onireti, A. Zoha, J. Moysen, A. Imran, L. Giupponi, M. Ali Imran, and A. Abu-Dayya, "A Cell Outage Management Framework for Dense Heterogeneous Networks," *IEEE Transactions on Vehicular Technology*, vol. 65, no. 4, pp. 2097–2113, 2016.

[36] M. Qin, Q. Yang, N. Cheng, H. Zhou, R. R. Rao, and X. Shen, "Machine Learning aided Context-Aware Self-Healing Management for Ultra Dense Networks with QoS Provisions," *IEEE Transactions on Vehicular Technology*, vol. 67, no. 12, pp. 12 339–12 351, 2018.

[37] C. M. Mueller, M. Kaschub, C. Blankenhorn, and S. Wanke, "A Cell Outage Detection Algorithm Using Neighbor Cell List Reports," in *Self-Organizing Systems*. Springer, 2008, pp. 218–229.

[38] I. de-la Bandera, R. Barco, P. Muñoz, and I. Serrano, "Cell Outage Detection

Based on Handover Statistics," *IEEE Communications Letters*, vol. 19, no. 7, pp. 1189–1192, 2015.

[39] M. Alias, N. Saxena, and A. Roy, "Efficient Cell Outage Detection in 5G HetNets Using Hidden Markov Model," *IEEE Communications Letters*, vol. 20, no. 3, pp. 562–565, 2016.

[40] A. Asghar, H. Farooq, and A. Imran, "Outage Detection for Millimeter Wave Ultra-Dense HetNets in High Fading Environments," in *IEEE International Conference on Communications (ICC)*, 2019, pp. 1–6.

[41] A. Zoha, A. Saeed, A. Imran, M. A. Imran, and A. Abu-Dayya, "Data-Driven Analytics for Automated Cell Outage Detection in Self-Organizing Networks," in *11th International Conference on the Design of Reliable Communication Networks (DRCN)*, 2015, pp. 203–210.

[42] W. Feng, Y. Teng, Y. Man, and M. Song, "Cell Outage Detection based on Improved BP Neural Network in LTE System," in *11th International Conference on Wireless Communications, Networking and Mobile Computing (WiCOM 2015)*, 2015, pp. 1–5.

[43] P.-C. Lin, "Large-Scale and High-Dimensional Cell Outage Detection in 5G Self-Organizing Networks," in *2019 Asia-Pacific Signal and Information Processing Association Annual Summit and Conference (APSIPA ASC)*, 2019, pp. 8–12.

[44] Y.-H. Ping and P.-C. Lin, "Cell Outage Detection using Deep Convolutional Autoencoder in Mobile Communication Networks," in *Asia-Pacific Signal and Information Processing Association Annual Summit and Conference (APSIPA ASC)*, 2020, pp. 1557–1560.

[45] U. Masood, A. Asghar, A. Imran, and A. N. Mian, "Deep Learning Based Detection of Sleeping Cells in Next Generation Cellular Networks," in *IEEE Global Communications Conference (GLOBECOM)*, 2018, pp. 206–212.

[46] T. Zhang, K. Zhu, and D. Niyato, "A Generative Adversarial Learning-Based Approach for Cell Outage Detection in Self-Organizing Cellular Networks," *IEEE Wireless Communications Letters*, vol. 9, no. 2, pp. 171–174, 2020.

[47] Z. Ma, Z. Pan, and N. Liu, "A sparse autoencoder-based approach for cell outage detection in wireless networks," *Science China Information Sciences*, vol. 64, no. 8, p. 189302, 2021.

[48] L. Wenjing, Y. Peng, J. Zhengxin, and L. Zifan, "Centralized Management Mechanism for Cell Outage Compensation in LTE Networks," *International Journal of Distributed Sensor Networks*, vol. 8, no. 11, p. 170589, 2012. [Online]. Available: https://doi.org/10.1155/2012/170589

[49] M. O. Osifeko, O. I. Sanusi, O. Folorunsho, and R. O. Abolade, "A Genetic Algorithm-based Approach for Cell Outage Compensation in Self-Healing Networks," *Journal of Information Science, Systems and Technology*, vol. 1, no. 2, pp. 1–10, 2017.

[50] F.-q. Li, X.-s. Qiu, L.-m. Meng, H. Zhang, and W. Gu, "Achieving Cell Outage Compensation in Radio Access Network with Automatic Network Man-

agement," in *2011 IEEE GLOBECOM Workshops (GC Wkshps)*, 2011, pp. 673–677.

[51] L. Kayili and E. Sousa, "Cell Outage Compensation for Irregular Cellular Networks," in *2014 IEEE Wireless Communications and Networking Conference (WCNC)*, 2014, pp. 1850–1855.

[52] E. Vaezpour, L. Majzoobi, M. Akbari, S. Parsaeefard, and H. Yanikomeroglu, "A Deep Learning-Based Approach for Cell Outage Compensation in NOMA Networks," *IEEE Open Journal of Vehicular Technology*, vol. 3, pp. 149–166, 2022.

[53] I. de la Bandera, P. Muñoz, I. Serrano, and R. Barco, "Adaptive Cell Outage Compensation in Self-Organizing Networks," *IEEE Transactions on Vehicular Technology*, vol. 67, no. 6, pp. 5231–5244, 2018.

[54] S. Adel, K. Muhammed, A. Abdallah, M. Rida, A. Morsy, G. Nasser, A. Khattab, A. Taha, and H. El-Akel, "Cell Outage Compensation Using Q-learning for Self-Organizing Networks," in *2021 International Conference on Microelectronics (ICM)*, 2021, pp. 102–105.

[55] J. Moysen and L. Giupponi, "A Reinforcement Learning Based Solution for Self-Healing in LTE Networks," in *2014 IEEE 80th Vehicular Technology Conference (VTC2014-Fall)*, 2014, pp. 1–6.

[56] X. Yang, P. Yu, L. Feng, F. Zhou, W. Li, and X. Qiu, "A Deep Reinforcement Learning based Mechanism for Cell Outage Compensation in 5G UDN," in *IFIP/IEEE Symposium on Integrated Network and Service Management (IM)*, 2019, pp. 476–481.

[57] J. Guo, Z. Wang, X. Shi, X. Yang, P. Yu, L. Feng, and W. Li, "A Deep Reinforcement Learning based Mechanism for Cell Outage Compensation in Massive IoT Environments," in *15th International Wireless Communications & Mobile Computing Conference (IWCMC)*, 2019, pp. 284–289.

[58] W. Xue, H. Zhang, Y. Li, D. Liang, and M. Peng, "Cell Outage Detection and Compensation in Two-Tier Heterogeneous Networks," *International Journal of Antennas and Propagation*, vol. 2014, no. 1, p. 624858, 2014. [Online]. Available: https://onlinelibrary.wiley.com/doi/abs/10.1155/2014/624858

[59] A. Zoha, A. Saeed, A. Imran, M. A. Imran, and A. Abu-Dayya, "A Learning-based Approach for Autonomous Outage Detection and Coverage Optimization," *Transactions on Emerging Telecommunications Technologies*, vol. 27, no. 3, pp. 439–450, 2016.

[60] P. Yu, X. Yang, F. Zhou, H. Li, L. Feng, W. Li, and X. Qiu, "Deep Reinforcement Learning aided Cell Outage Compensation Framework in 5G Cloud Radio Access Networks," *Mobile Networks and Applications*, vol. 25, pp. 1644–1654, 2020.

[61] T. Omar, T. Ketseoglou, and I. Naffaa, "A novel self-healing model using precoding & big-data based approach for 5G networks," *Pervasive and Mobile Computing*, vol. 73, p. 101365, 2021. [Online]. Available: https://www.sciencedirect.com/science/article/pii/S1574119221000353

[62] S. Fortes, C. Baena, J. Villegas, E. Baena, M. Z. Asghar, and R. Barco, "Location-Awareness for Failure Management in Cellular Networks: An Integrated Approach," *Sensors*, vol. 21, no. 4, 2021. [Online]. Available: https://www.mdpi.com/1424-8220/21/4/1501

[63] G. Stamatelatos, A. Sgora, and N. Alonistioti, "Intelligent SON Coordination in the 5G-and-beyond era," in *2022 Global Information Infrastructure and Networking Symposium (GIIS)*, 2022, pp. 99–103.

[64] S. M. A. Zaidi, M. Manalastas, H. Farooq, and A. Imran, "SyntheticNET: A 3GPP Compliant Simulator for AI Enabled 5G and Beyond," *IEEE Access*, vol. 8, pp. 82 938–82 950, 2020.

[65] G. Wanying, K. Jahwan, S. I. Farah, Q. N. M. Faseeh, and S. D. Ryeol, "QoS-Aware Energy-Efficient Microbase Station Deployment for 5G-Enabled HetNets," *Journal of King Saud University-Computer and Information Sciences*, vol. 35, no. 4, p. 101517, 2023.

[66] J. G. Andrews, F. Baccelli, and R. K. Ganti, "A Tractable Approach to Coverage and Rate in Cellular Networks," *IEEE Transactions on Communications*, vol. 59, no. 11, pp. 3122–3134, 2011.

[67] S. Sun, T. S. Rappaport, S. Rangan, T. A. Thomas, A. Ghosh, I. Z. Kovacs, I. Rodriguez, O. Koymen, A. Partyka, and J. Jarvelainen, "Investigation of Prediction Accuracy, Sensitivity, and Parameter Stability of Large-Scale Propagation Path Loss Models for 5G Wireless Communications," *IEEE Transactions on Vehicular Technology*, vol. 65, no. 5, pp. 2843–2860, 2016.

[68] S. Khurram, K. M. Noor, and J. Ahmed, "Performance Analysis of Coverage-Centric Heterogeneous Cellular Networks using Dual-Slope Path Loss Model," *Computer Networks*, 2021.

[69] H.-S. Jo, C. Park, E. Lee, H. K. Choi, and J. Park, "Path Loss Prediction Based on Machine Learning Techniques: Principal Component Analysis, Artificial Neural Network, and Gaussian Process," *Sensors*, vol. 20, no. 7, 2020.

[70] M.-T. Nguyen, S. Kwon, and Y. H. Cho, "Estimation of Measurement Errors in 3GPP Filtering Models," in *2020 International Conference on Information Networking (ICOIN)*, 2020, pp. 510–512.

[71] W. Li, P. Yu, M. Yin, L. Feng, and X. song Qiu, "Automated cell outage compensation mechanism based on downtilt adjustments in cellular networks," *2016 16th International Symposium on Communications and Information Technologies (ISCIT)*, pp. 1–6, 2016. [Online]. Available: https://api.semanticscholar.org/CorpusID:17494367

[72] Y. Mengjun, F. Lei, L. Wenjing, Y. Peng, and Q. Xuesong, "Cell outage compensation based on CoMP and optimization of tilt," *The Journal of China Universities of Posts and Telecommunications*, vol. 22, no. 5, pp. 71–79, 2015. [Online]. Available: https://www.sciencedirect.com/science/article/pii/S1005888515606835

[73] N. Jiang, Y. Deng, A. Nallanathan, X. Kang, and T. Q. Quek, "Overview on Interference Management Technology for Ultra-Dense Network," *IEEE*

Access, vol. 6, pp. 70 604–70 620, 2018.

[74] M. Ding, P. Wang, D. López-Pérez, G. Mao, and Z. Lin, "Performance Impact of LoS and NLoS Transmissions in Dense Cellular Networks," *IEEE Transactions on Wireless Communications*, vol. 15, no. 3, pp. 2365–2380, 2016.

[75] 3GPP, "LTE; Evolved Universal Terrestrial Radio Access (E-UTRA); Radio Resource Control (RRC); Protocol specification for Radio Measurement Collection for Minimization of Drive Tests (MDT)," ETSI, TS 137.320, 2013.

[76] C. Zhou and R. C. Paffenroth, "Anomaly Detection with Robust Deep Autoencoders," in *Proceedings of the 23rd ACM SIGKDD International Conference on Knowledge Discovery and Data Mining*, 2017, pp. 665–674.

[77] S. Zhang, X. Li, M. Zong, X. Zhu, and R. Wang, "Efficient kNN Classification With Different Numbers of Nearest Neighbors," *IEEE Transactions on Neural Networks and Learning Systems*, vol. 29, no. 5, pp. 1774–1785, 2018.

[78] J. Feng, Y. Yu, and Z.-H. Zhou, "Multi-Layered Gradient Boosting Decision Trees," in *Advances in Neural Information Processing Systems*, 2018, pp. 3551–3561.

[79] T. Chen and C. Guestrin, "XGBoost: A Scalable Tree Boosting System," in *Proceedings of the 22nd ACM SIGKDD International Conference on Knowledge Discovery and Data Mining*, 2016, pp. 785–794.

[80] R. S. Sutton and A. G. Barto, *Reinforcement Learning: An Introduction*. MIT Press, 1998.

[81] A. B. Sediq, R. H. Gohary, and H. Yanikomeroglu, "Optimal Tradeoff between Efficiency and Jain's Fairness Index in Resource Allocation," in *IEEE 23rd International Symposium on Personal, Indoor and Mobile Radio Communications - (PIMRC)*, 2012, pp. 577–583.

[82] P. Trivedi and N. Hemachandra, "Multi-Agent Natural Actor-Critic Reinforcement Learning Algorithms," *Dynamic Games and Applications*, vol. 13, pp. 25–55, 2023.

[83] L. Canese, G. C. Cardarilli, L. Di Nunzio, R. Fazzolari, D. Giardino, M. Re, and S. Spanò, "Multi-Agent Reinforcement Learning: A Review of Challenges and Applications," *Applied Sciences*, vol. 11, no. 11, p. 4948, 2021.

[84] R. Lowe, Y. I. Wu, A. Tamar, J. Harb, O. P. Abbeel, and I. Mordatch, "Multi-Agent Actor-Critic for Mixed Cooperative-Competitive Environments," *Advances in neural information processing systems*, vol. 30, 2017.

[85] W. Li, B. Jin, X. Wang, J. Yan, and H. Zha, "F2A2: Flexible Fully-decentralized Approximate Actor-critic for Cooperative Multi-agent Reinforcement Learning," *Journal of Machine Learning Research*, vol. 24, no. 178, pp. 1–75, 2023.

[86] O. Yilmaz, S. Hamalainen, and J. Hamalainen, "Comparison of remote electrical and mechanical antenna downtilt performance for 3GPP LTE," in *2009 IEEE Vehicular Technology Conference*, 2009.

[87] M. Mohri, A. Rostamizadeh, and A. Talwalkar, *Foundations of Machine*

Learning. MIT Press, 2012.

[88] Y. Zhang and Y. J. Zhang, "User-centric virtual cell design for cloud radio access networks," in *2014 IEEE 15th International Workshop on Signal Processing Advances in Wireless Communications (SPAWC)*, 2014, pp. 249–253.

[89] C. Pan, M. Elkashlan, J. Wang, J. Yuan, and L. Hanzo, "User-centric c-ran architecture for ultra-dense 5g networks: Challenges and methodologies," *IEEE Communications Magazine*, vol. 56, no. 6, pp. 14–20, 2018.

[90] J. Huang, C.-X. Wang, L. Bai, J. Sun, Y. Yang, J. Li, O. Tirkkonen, and M.-T. Zhou, "A Big Data Enabled Channel Model for 5G Wireless Communication Systems," *IEEE Transactions on Big Data*, vol. 6, no. 2, pp. 211–222, 2020.

[91] K. Chen, Q. Kong, Y. Dai, Y. Xu, F. Yin, L. Xu, and S. Cui, "Recent Advances in Data-Driven Wireless Communication Using Gaussian Processes: A Comprehensive Survey," *China Communications*, vol. 19, no. 1, pp. 218–237, 2022.

[92] S. K. Kasi, U. S. Hashmi, S. Ekin, A. Abu-Dayya, and A. Imran, "D-ran: A drl-based demand-driven elastic user-centric ran optimization for 6g & beyond," *IEEE Transactions on Cognitive Communications and Networking*, vol. 9, no. 1, pp. 130–145, 2023.

[93] L. Yu, H. Zhang, L. Zhang, L. Song, Z. Han, and P. Fan, "Hypergraph-based scma codebook allocation in user-centric ultra-dense networks with machine learning," in *2019 11th International Conference on Wireless Communications and Signal Processing (WCSP)*, 2019, pp. 1–6.

[94] B. Shang and L. Liu, "Machine learning meets point process: Spatial spectrum sensing in user-centric networks," *IEEE Wireless Communications Letters*, vol. 9, no. 1, pp. 34–37, 2020.

[95] O. Onireti, A. Imran, M. A. Imran, and R. Tafazolli, "Impact of positioning error on achievable spectral efficiency in database-aided networks," in *2016 IEEE International Conference on Communications (ICC)*, 2016, pp. 1–6.

[96] G. Auer, V. Giannini, C. Desset, I. Godor, P. Skillermark, M. Olsson, M. A. Imran, D. Sabella, M. J. Gonzalez, O. Blume, and A. Fehske, "How much energy is needed to run a wireless network?" *IEEE Wireless Communications*, vol. 18, no. 5, pp. 40–49, 2011.

[97] U. S. Hashmi, S. A. R. Zaidi, A. Imran, and A. Abu-Dayya, "Enhancing downlink qos and energy efficiency through a user-centric stienen cell architecture for mmwave networks," *IEEE Transactions on Green Communications and Networking*, vol. 4, no. 2, pp. 387–403, 2020.

[98] Y. He, L. Dai, and H. Zhang, "Multi-branch deep residual learning for clustering and beamforming in user-centric network," *IEEE Communications Letters*, vol. 24, no. 10, pp. 2221–2225, 2020.

[99] W. Raza, U. S. Hashmi, A. Imran, and S. Ekin, "Towards positioning error impact characterization and minimization in user-centric ran," in *2022 IEEE Wireless Communications and Networking Conference (WCNC)*, 2022, pp. 734–739.

[100] H. A. H. Alobaidy, M. Jit Singh, M. Behjati, R. Nordin, and N. F. Abdullah, "Wireless transmissions, propagation and channel modelling for iot technologies: Applications and challenges," *IEEE Access*, vol. 10, pp. 24 095–24 131, 2022.

[101] M. Takai, R. Bagrodia, K. Tang, and M. Gerla, "Efficient wireless network simulations with detailed propagation models," *Wireless Networks*, vol. 7, pp. 297–305, 2001.

[102] F. Lara, R. Lara-Cueva, M. Castillo, J. F. Arellano, and L. Top'on, "Modeling Wireless Propagation Channel: A Traditional Versus Machine Learning Approach," in *Emerging Research in Intelligent Systems*. Springer, 2022, p. 281–297.

[103] D. F. S. Fernandes, A. Raimundo, F. Cercas, P. J. A. Sebasti ao, R. Dinis, and L. S. Ferreira, "Comparison of Artificial Intelligence and Semi-Empirical Methodologies for Estimation of Coverage in Mobile Networks," *IEEE Access*, vol. 8, p. 139803–139812, 2020.

[104] X. Zhang, X. Shu, B. Zhang, J. Ren, L. Zhou, and X. Chen, "Cellular Network Radio Propagation Modeling with Deep Convolutional Neural Networks," in *Proceedings of the 26th ACM SIGKDD International Conference on Knowledge Discovery & Data Mining*, 2020, p. 2378–2386.

[105] T. Sarkar, Z. Ji, K. Kim, A. Medour, and M. Salazar-Palma, "A survey of various propagation models for mobile communication," *IEEE Antennas and Propagation Magazine*, vol. 45, pp. 51–82, 2003.

[106] S. Bakirtzis, J. Chen, K. Qiu, J. Zhang, and I. J. Wassell, "EM DeepRay: An Expedient, Generalizable, and Realistic Data-Driven Indoor Propagation Model," *IEEE Transactions on Antennas and Propagation*, vol. 70, no. 6, pp. 4140–4154, 2022.

[107] S. Zhang, A. Wijesinghe, and Z. Ding, "RME-GAN: A Learning Framework for Radio Map Estimation Based on Conditional Generative Adversarial Network," *IEEE Internet of Things Journal*, vol. 10, no. 20, pp. 18 016–18 027, 2023.

[108] Y.-S. Feng, L.-X. Guo, P. Wang, and Z.-Y. Liu, "Efficient Ray-Tracing Model for Propagation Prediction for Microcellular Wireless Communication Systems," in *ISAPE2012*, 2012, pp. 432–435.

[109] G. M. Galván-Tejada and J. Aguilar-Torrentera, "Analysis of propagation for wireless sensor networks in outdoors," *Progress In Electromagnetics Research B*, 2019.

[110] D. Fernandes, G. Soares, D. Clemente, R. Cortesao, P. Sebastiao, F. Cercas, R. Dinis, and L. S. Ferreira, "Combining Measurements and Propagation Models for Estimation of Coverage in Wireless Networks," *2019 IEEE 90th Vehicular Technology Conference (VTC2019-Fall)*, pp. 1–5, 2019.

[111] X. Zhou, W. Liu, J. D. Parsons, and A. G. Goicoechea, "A Hybrid Ray-Tracing Vector Parabolic Equation Method for Propagation Modeling in Train Communication Channels," *IEEE Transactions on Antennas and Propaga-*

tion, vol. 55, no. 12, pp. 3586–3594, 2007.

[112] S. Sesia, I. Toufik, and M. Baker, *LTE-the UMTS long term evolution: from theory to practice*. Wiley, 2011.

[113] A. Seretis and C. Sarris, "An Overview of Machine Learning Techniques for Radiowave Propagation Modeling," *IEEE Transactions on Antennas and Propagation*, vol. 70, pp. 3970–3985, 2021.

[114] Y. L. Yang, G. Wan, and M. Tong, "A Novel Wireless Propagation Model Based on Bi-LSTM Algorithm," *IEEE Access*, vol. 10, pp. 43 837–43 847, 2022.

[115] H. Zhang, J. Dong, X. Liu, J. Liu, and X. Zhang, "An artificial intelligence radio propagation model based on geographical information," *IEEE Transactions on Antennas and Propagation*, vol. 70, pp. 12 049–12 060, 2022.

[116] A. C. Vanleer and C. Anderson, "Improving Propagation Model Predictions via Machine Learning with Engineered Features," *MILCOM 2021 - 2021 IEEE Military Communications Conference (MILCOM)*, pp. 420–425, 2021.

[117] L. Perez and J. Wang, "The effectiveness of data augmentation in image classification using deep learning," *arXiv preprint arXiv:1712.04621*, 2017.

[118] S. Yang, W. Bian, X. Jiang, J. Xie, Y. Gao, and Y. Ding, "Image data augmentation for deep learning: A survey," *arXiv preprint arXiv:2204.08610*, 2022.

[119] J. Wei and K. Zou, "EDA: Easy data augmentation techniques for boosting performance on text classification tasks," in *Proceedings of the 2019 Conference on Empirical Methods in Natural Language Processing and the 9th International Joint Conference on Natural Language Processing (EMNLP-IJCNLP)*. Hong Kong, China: Association for Computational Linguistics, November 2019, pp. 6382–6388. [Online]. Available: https://aclanthology.org/D19-1670

[120] X. Xu, L. Huang, W. Pan, Y. Zhang, L. Qian, N. Gao, and Y. Wu, "Mixing signals: Data augmentation approach for deep learning based modulation recognition," *arXiv preprint arXiv:2204.03737*, 2022.

[121] L. Huang, W. Pan, Y. Zhang, L. Qian, N. Gao, and Y. Wu, "Data augmentation for deep learning-based radio modulation classification," *IEEE Access*, vol. 8, pp. 1498–1506, 2020.

[122] Y. Yang, Y. Li, W. Zhang, F. Qin, P. Zhu, and C. Wang, "Generative-Adversarial-Network-Based Wireless Channel Modeling: Challenges and Opportunities," *IEEE Communications Magazine*, vol. 57, pp. 22–27, 2019.

[123] Z. Li, C. Wang, C.-Y. Huang, J. Huang, J. Li, W. Zhou, and Y. Chen, "A GAN-GRU Based Space-Time Predictive Channel Model for 6G Wireless Communications," *IEEE Transactions on Vehicular Technology*, vol. 73, pp. 9370–9386, 2024.

[124] C.-Y. Huang, C. Wang, Z. Li, Z. Qian, J. Li, and Y. Miao, "A Frequency Domain Predictive Channel Model for 6G Wireless MIMO Communications Based on Deep Learning," *IEEE Transactions on Communications*, vol. 72, pp. 4887–4902, 2024.

[125] Y. Tian, H. Li, Q. Zhu, K. Mao, F. Ali, X. Chen, and W. Zhong, "Generative Network-Based Channel Modeling and Generation for Air-to-Ground Communication Scenarios," *IEEE Communications Letters*, vol. 28, pp. 892–896, 2024.

[126] M. Haider, I. Ahmed, A. Rubaai, C. Pu, and D. B. Rawat, "GAN-Based Channel Estimation for IRS-Aided Communication Systems," *IEEE Transactions on Vehicular Technology*, vol. 73, pp. 6012–6017, 2024.

[127] Y. Wei, M.-M. Zhao, and M. Zhao, "Channel Distribution Learning: Model-Driven GAN-Based Channel Modeling for IRS-Aided Wireless Communication," *IEEE Transactions on Communications*, vol. 70, pp. 4482–4497, 2022.

[128] A. Marey, M. Bal, H. F. Ates, and B. K. Gunturk, "PL-GAN: Path Loss Prediction Using Generative Adversarial Networks," *IEEE Access*, vol. 10, pp. 90 474–90 480, 2022.

[129] T. Dash, S. Chitlangia, A. Ahuja, and A. Srinivasan, "A review of some techniques for inclusion of domain-knowledge into deep neural networks," *Scientific Reports*, vol. 12, no. 1, pp. 1–23, 2022.

[130] C. She, C. Sun, Z. Gu, Y. Li, C. Yang, H. V. Poor, and B. Vucetic, "A tutorial on ultrareliable and low-latency communications in 6g: Integrating domain knowledge into deep learning," *Proceedings of the IEEE*, vol. 109, no. 11, pp. 1952–1984, 2021.

[131] N. Muralidhar, M. R. Islam, M. Marwaha, A. Karpatne, and N. Ramakrishnan, "Incorporating prior domain knowledge into deep neural networks," in *2018 IEEE International Conference on Big Data (Big Data)*. IEEE, 2018, pp. 1526–1535.

[132] T.-H. Teng, A.-H. Tan, and J. M. Zurada, "Self-organizing neural networks integrating domain knowledge and reinforcement learning," *IEEE Transactions on Neural Networks and Learning Systems*, vol. 26, no. 9, pp. 1936–1948, 2015.

[133] M. Ali, "PyCaret: An open source, low-code machine learning library in Python," April 2020, pyCaret version 1.0.0. [Online]. Available: [PyCaretDocumentation](https://www.pycaret.org)

[134] M. Shu, w. sun, j. zhang, x. duan, and m. ai, "Digital-Twin-Enabled 6G Network Autonomy and Generative Intelligence: Architecture, Technologies and Applications," *Digital Twin*, vol. 2, no. 16, 2022.

[135] M. Manalastas, M. U. bin Farooq, S. M. Asad Zaidi, and A. Imran, "Toward the Development of 6G System Level Simulators: Addressing the Computational Complexity Challenge," *IEEE Wireless Communications*, vol. 30, no. 6, pp. 160–168, 2023.

[136] M. U. Bin Farooq, M. Manalastas, H. Qureshi, Y. Liu, A. Imran, and M. O. Al Kalaa, "MDT-based Intelligent Route Selection for 5G-Enabled Connected Ambulances," in *2022 IEEE International Conference on E-health Networking, Application & Services (HealthCom)*, 2022, pp. 81–87.

[137] T. Mahmood, H. K. AL-Qaysi, and A. Hameed, "The Effect of Antenna

Height on the Performance of the Okumura/Hata Model Under Different Environments Propagation," *2021 International Conference on Intelligent Technologies (CONIT)*, pp. 1–4, 2021.

[138] S. A. Siddiqui, N. Fatima, and A. Ahmad, "Comparative Analysis Of Propagation Path Loss Models In LTE Networks," in *2019 International Conference on Power Electronics, Control and Automation (ICPECA)*, 2019, pp. 1–3.

[139] Z. Yun and M. Iskander, "Ray Tracing for Radio Propagation Modeling: Principles and Applications," *IEEE Access*, vol. 3, pp. 1089–1100, 2015.

[140] T. Sarkar, Z. Ji, K. Kim, A. Medouri, and M. Salazar-Palma, "A survey of various propagation models for mobile communication," *IEEE Antennas and Propagation Magazine*, vol. 45, no. 3, pp. 51–82, 2003.

[141] M. Ribero, R. W. Heath, H. Vikalo, D. Chizhik, and R. A. Valenzuela, "Deep Learning Propagation Models over Irregular Rerrain," in *ICASSP 2019-2019 IEEE International Conference on Acoustics, Speech and Signal Processing (ICASSP)*. IEEE, 2019, pp. 4519–4523.

[142] S. P. Sotiroudis, S. K. Goudos, K. A. Gotsis, K. Siakavara, and J. N. Sahalos, "Application of a Composite Differential Evolution Algorithm in Optimal Neural Network Design for Propagation Path-Loss Prediction in Mobile Communication Systems," *IEEE Antennas and Wireless Propagation Letters*, vol. 12, pp. 364–367, 2013.

[143] S. I. Popoola, E. Adetiba, A. A. Atayero, N. Faruk, and C. T. Calafate, "Optimal Model for Path Loss Predictions using Feed-Forward Neural Networks," *Cogent Engineering*, vol. 5, no. 1, p. 1444345, 2018.

[144] Y. Zheng, J. Wang, X. Li, J. Li, and S. Liu, "Cell-Level RSRP Estimation With the Image-to-Image Wireless Propagation Model Based on Measured Data," *IEEE Transactions on Cognitive Communications and Networking*, vol. 9, no. 6, pp. 1412–1423, 2023.

[145] L. Eller, P. Svoboda, and M. Rupp, "A Deep Learning Network Planner: Propagation Modeling Using Real-World Measurements and a 3D City Model," *IEEE Access*, vol. 10, pp. 122 182–122 196, 2022.

[146] R. Levie, Ç. Yapar, G. Kutyniok, and G. Caire, "RadioUNet: Fast Radio Map Estimation With Convolutional Neural Networks," *IEEE Transactions on Wireless Communications*, vol. 20, no. 6, pp. 4001–4015, 2021.

[147] A. Chaves-Villota and C. A. Viteri-Mera, "DeepREM: Deep-Learning-Based Radio Environment Map Estimation from Sparse Measurements," *IEEE Access*, vol. 11, pp. 48 697–48 714, 2023.

[148] S. Liu, T. Onishi, M. Sasaki, and S. Watanabe, "A Generalizable Indoor Propagation Model Based on Graph Neural Networks," *IEEE Transactions on Antennas and Propagation*, vol. 71, no. 7, pp. 6098–6110, 2023.

[149] W. Njima, I. Ahriz, R. Zayani, M. Terre, and R. Bouallegue, "Indoor Localization Using Data Augmentation via Selective Generative Adversarial Networks," *IEEE Access*, vol. 9, pp. 98 337–98 347, 2021.

[150] G. Cao and Z. Peng, "RayProNet: A Neural Point Field Framework for Radio

Propagation Modeling in 3D Environments," *IEEE Journal on Multiscale and Multiphysics Computational Techniques*, vol. 9, pp. 330–340, 2024.

[151] X. Zhao, J. An, J. Huang, and C. Jiang, "NeRF2: Neural Radio-Frequency Radiance Fields," in *Proceedings of the 29th Annual International Conference on Mobile Computing and Networking*. ACM, 2023, pp. 393–407.

[152] "awesome-distribution-shift," accessed: February 29, 2024. [Online]. Available: https://github.com/weitianxin/awesome-distribution-shift#learning-strategy

[153] S.-W. Huang, C.-T. Lin, S.-P. Chen, Y.-Y. Wu, P.-H. Hsu, and S.-H. Lai, "AugGAN: Cross Domain Adaptation with GAN-Based Data Augmentation," in *European Conference on Computer Vision*. Springer, 2018, pp. 731–744.

[154] L. Xu, M. Skoularidou, A. Cuesta-Infante, and K. Veeramachaneni, "Modeling Tabular data using Conditional GAN," *arXiv preprint arXiv:1907.00503*, 2019.

[155] Z. Hu, Y. Li, and C. Han, "Transfer Learning enabled Transformer-based Generative Adversarial Networks for Modeling and Generating Terahertz Channels," *Communications Engineering*, vol. 3, p. 153, 2024.

[156] M. Chen, Y.-C. Liang, and H.-H. Chen, "Machine Learning for Wireless Networks with Artificial Intelligence: A Comprehensive Survey," *IEEE Access*, vol. 6, pp. 36 114–36 134, 2018.

[157] W. Raza, F. A. Khan, H. N. Qureshi, U. Masood, and A. Imran, "An AI-Driven Framework for Enhancing Resilience in Propagation Models to Enable Digital Twin," in *Proceedings of the IEEE International Symposium on Personal, Indoor and Mobile Radio Communications (PIMRC)*. IEEE, 2024. [Online]. Available: https://www.ai4networks.com/files/conferences/c-24-2.pdf

[158] "Atoll," [Online]. Available: https://www.forsk.com/atoll-overview.

[159] S. M. Lundberg and S.-I. Lee, "A unified approach to interpreting model predictions," *Advances in neural information processing systems*, vol. 30, 2017.

[160] A. Levy, B. R. Shalom, and M. Chalamish, "A Guide to Similarity Measures," 2024.

[161] I. Goodfellow, J. Pouget-Abadie, M. Mirza, B. Xu, D. Warde-Farley, S. Ozair, A. Courville, and Y. Bengio, "Generative Adversarial Nets," *Advances in neural information processing systems*, p. 2672–2680, 2014.

[162] T. Salimans, I. Goodfellow, W. Zaremba, V. Cheung, A. Radford, and X. Chen, "Improved Techniques for Training GANs," in *Advances in Neural Information Processing Systems*, 2016, pp. 2234–2242.

[163] M. Lucic, K. Kurach, M. Michalski, S. Gelly, and O. Bousquet, "Are GANs Created Equal? A Large-Scale Study," in *Advances in Neural Information Processing Systems*, 2018, pp. 700–709.

[164] C. Zhang, S. Dang, B. Shihada, and M.-S. Alouini, "Dual Attention-Based

Federated Learning for Wireless Traffic Prediction," in *IEEE INFOCOM 2021 - IEEE Conference on Computer Communications*, 2021, pp. 1–10.

[165] "SDMetrics: Synthetic Data Metrics," accessed: February 29, 2024. [Online]. Available: https://docs.sdv.dev/sdmetrics/